

NOSC TD 352 Vol 1

AD A 0 9 1 6 1 9

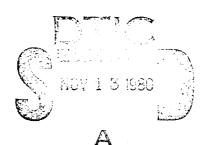
Technical Document 352

NOSC TD 352 Vol 1

STRATEGIC LASER COMMUNICATIONS PROGRAM

Volume 1 — Proceedings of the Navy/DARPA Fourth Technical Interchange Meeting, 25-27 March 1980

Reproduced From Best Available Copy



31 July 1980

Prepared for PME 117 NAVELEX 310 ONR 220 DARPA DEO

COPY

Approved for public release; distribution unlimited

FILE

NAVAL OCEAN SYSTEMS CENTER SAN DIEGO, CALIFORNIA 92152

33

80 11 13 026



NAVAL OCEAN SYSTEMS CENTER, SAN DIEGO, CA 92152

AN ACTIVITY OF THE NAVAL MATERIAL COMMAND

SL GUILLE, CAPT, USN

Commander

HL BLOOD

Technical Director

ADMINISTRATIVE INFORMATION

The 25-27 March 1980 Navy/DARPA Technical Interchange Meeting on the Strategic Laser Communications Program was arranged under NOSC Work Unit CM06 by members of the Strategic Laser Communications Program Office (Code 8105) for PME 117, NAVELEX 310, ONR 220, and DARPA DEO. This document is a compilation of the unclassified papers presented at the meeting and was approved for publication 31 July 1980.

Released by CA Nelson, Head Long Range Plans and Policy Office Under authority of HD Smith, Head Communications Systems and Technology Department

DD 1 JAN 73 1473

EDITION OF 1 NOV 65 IS OBSOLETE S/N 0102-LF-014-6601

UNCLASSIFIED

SECURITY CLASSIFICATION OF THIS PAGE (When Date Sprong)

FOREWORD

This document is a compilation of material presented at the Fourth Technical Interchange Meeting (TIM IV) of the Strategic Laser Communications (SLC) Program held at NOSC 25-27 March 1980. The meeting was sponsored by the Naval Electronic Systems Command, the Defense Advanced Research Projects Agency, Directed Energy Office, and the Office of Naval Research. The SLC Program addresses the practicality and suitability of an optical solution for transmitting strategic information to submerged submarines. The purpose of the meeting was to assemble present and potential program contributors to exchange information on recent progress in each of the following areas:

System engineering

Space-based laser concept

Earth-based laser concept
Single-bounce approach
Double-bounce approach

Threat definition/System vulnerability

Channel characterization

Propagation characteristics

Climatology and oceanic property statistics

Subsystem technology

Lasers (eg XeCl, HgBr)

Downconversion techniques

Filters

Many of the illustrations are inferior copies of Vugraphs and photographs, but they were the only copies available at the time of printing.

The NOSC point of contact for the Strategic Laser Communications Program is LB Stotts, Code 8105, telephone (714) 225-7245 (commercial) or 933-7245 (Autovon).

CONTENTS (In order of conference presentation)

INTRODUCTI	ION A STATE OF THE
i P	rogram overview, by LB Stotts (NOSC) page 5
SYSTEM ENG	INEERING SESSION
	SCAR spaceborne system: phase IB; by TE Flom, PJ Titterton GTE Sylvania) 29
3 C	ontained in vol 2
4 C	ontained in vol 2
-SUBSYSTEM	TECHNOLOGY SESSION
	esium atomic resonance filter studies, by R Burnham, Wexler (Naval Research Laboratory) 59
	irefringent blue-green filters, by AM Title, WJ Rosenberg Lockheed Palo Alto Research Laboratory) 69
	o-index electro-optic filters recent experimental results, y JF Lotspeich, DM Henderson (Hughes Research Laboratories)83
	hristiansen-Bragg filters,-by P Yeh, J Tracy (Rockwell sternational Science Center) 99
	hermal control for hole-burning filter, by R Rochat, JE Jackson McDonnell Douglas Astronautics) 113
	on linear optical phase conjugation for SLC uplink; by R Giuliano (Hughes Research Laboratories) 145
SPACE-BASEI	D LASER SESSION A STATE OF THE SESSION AND ADDRESS OF THE SESSION AND ADDRESS OF THE SESSION ADDRESS OF THE SESS
	tatus of blue-green discharge laser work at NRL, by Caracham (Naval Research Laboratory) 171
jo	fficient Raman conversion of XeCl laser into the blue-green region, y H Komine, EA Stappaerts, WH Long Jr (Northrop Research and echnology Center, Northrop Corporation) 183
	ead vapor conversion of an X-ray preionized XeCl laser, by Levatter, SC Lin (University of California, San Diego) 201
	xeimer laser engineering development at LASL, by PN Mace Los Alamos Scientific Laboratory of the University of California) 213
	TRC blue-green laser research, by RT Brown, WL Nighan (United echnologies Research Center) 249
	ercury bromide laser scaling approaches, by JJ Ewing, C Fisher, Moody, A Pindroh, D Quimby (Mathematical Sciences Northwest) 275
17 - Pa	arameterization studies of HgBr lasers, by CS Liu (Westinghouse

18 HgBr₂/HgBr dissociation laser, by EJ Schimitschek (NOSC) . . . 309

R&D Center) . . . 295

CONTENTS (Continued)

- 19 'Efficient conversion of XeF* radiation to the blue-green through SRS, by R Heinrichs, H Hyman, I Itzkan, D Trainor (AVCO Everett Research Laboratory, Inc)...323
- Scaling studies of efficient Raman converters, by EA Stappaerts, H Komine, JB West, WH Long Jr (Northrop Research and Technology Center, Northrop Corporation) . . . 343
- 21 Ground based XeC1-Pb blue-green source, by N Djeu (Naval Research Laboratory) . . . 359
- Tunable blue-green laser development, by WK Bischel, G Black, DJ Eckstrom, DL Huestis, DC Lorents, HH Nakano, KY Tang, RA Tilton, HC Walker Jr (SRI International) . . . 377
- 23 Contained in vol 2
- 24 XeC1 lasers for blue-green conversion, by J Asmus (Maxwell Labs) . . . 415
- 25 Electron beam excited blue-green XeF, by JD Campbell, CH Fisher, RE Center, AL Pindroh (Mathematical Sciences Northwest) . . . 431
- The current status of copper laser development, by RE Grove (Lawrence Livermore Laboratory) . . . 445

CHANNEL CHARACTERIZATION SESSION

- 27 Downlink laser cloud propagation experiments, by GR Hostetter (GTE Sylvania) . . . 459
- 28 The temporal and spatial smearing of blue-green pulses in clouds, 2000 by GC Mooradian, M Geller (NOSC)...509
- 29 Kauai cloud experiment measurements: 02 absorption techniques, by HS Stewart, DF Hansen (HSS Inc) . . . 529
- 30 Uplink propagation and adaptive optics, by DP Greenwood (MIT Lincoln Lab) . . . 557
- 31 Quasi-inherent characteristics of the diffuse attenuation coefficient for irradiance, by KS Baker, RC Smith (Scripps Institution of Oceanography Visibility Laboratory, University of California, San Diego) . . . 601
- 32 Assessment of the diffuse attenuation coefficient from remote sensed (CZCS) radiance, by RW Austin (Scripps Institution of Oceanography Visibility Laboratory, University of California, San Diego) . . . 605
- 33 An analytic model for cloud propagation, by AP Ciervo (Pacific Sierra Research)...633

INTRODUCTION

PROGRAM OVERVIEW

by

LB Stotts NOSC

The same

NAVY/DARPA

STRATEGIC BLUE-GREEN OPTICAL COMMUNICATIONS PROGRAM TECHNICAL INTERCHANGE MEETING

STRATEGIC BLUE/GREEN OPTICAL **COMMUNICATIONS PROGRAM**

Sponsors: PME 117, NAVELEX 310, ONR 220, DARPA STO

Technical Advisor: NOSC

Objective: Determine practicality and suitability of an optical solution to strategic communications to submerged submarines

Approach:

Assess their projected performance levels relative to operational Define various communication system concepts to be pursued Determine and/or develop realistic component capabilities Define strategic submarine operational requirements Resolve uncertainties in the transmission channel requirements

Operational requirements and threat definition analysis Major program task areas to reduce uncertainty: Systems demonstrations and experiments Communications systems engineering Channel characterization Subsystem technology

SUMMARY OF CRITICAL ISSUES

Components

Laser TX

- Energy per pulse a
 - Efficiency
- Lifetime <u>ပ</u>
 - Color ð

Receiver 6

S

- Fifter narrow bandwidth, wide field of view (a)
- sion efficiency, area Cptics-transmis-<u>e</u>
- Detector-sensitivity, gain, area, quantum efficiency, norse factor <u>ပ</u>
- 3. HEL Space mirror and adaptive optics

Modeling

Bulk loss **(**2) <u>a</u>

Cloud

- spreading Spatial
- Time dispersion <u>(</u>ပ
- Water loss off zenith તાં
- dispersive channel in Optimum detection angular/ temporal of photons in an the presence of background ო

Propagation Availability

- Water loss worldwide
- Cloud losses/ occurrences d
- **Biolumines**cence (a)

Noise variations

က

- Short term variation loss
- Turbulence worldwide statistics 4

BLUE-GREEN LASER PROGRAM NAVY/DARPA

SPACE-BASED LASER

Power-200-1000 watts (100-300 pps) Demonstrate laser performance by 1985 System efficiency > 1% Run time-1010 shots **Objective**

Phase III—200-1000 watt brassboard—FY85 Phases I & II -- 200 watt breadboard for two Three-phase main program thrust candidates—FY82 Technology program Approach



Xeci frequency shifted Laser

• Status

Wavelength—308 nm ramar shifted to 455—Pb vapor

499—H₂

Single pulse energy—5 j (x-ray pre-ionized)--UCSD Efficiency (capacitor store) XeCI--1.4%--ÚCSD Converter—50% Pb at 25 mJ—NPL Repped pulse—55 W at 600 pps—LLL Bandwidth—XeCl:Pb < 0.05A—NRL

Current programs
 XeCl kinetics—NRL

Molecular conversion—NRTC

X-ray pre-ionization—UCSD

Pb conversion at 1-2J—NRL/UCSD Repped pulse—100 pps/.1J—NRL

HgBr LASER

• Status

Single pulse energy—100 mJ (UV preionized)—NOSC Efficiency (capacitor store)-1% (at 60 mJ)-110SC Repped pulse—1 pps, 10's of seconds—NOSC Bandwidth—1A (low efficiency)—NOSC Wavelength—439-502 nm

Current programs

Pre-ionization techniques---MSNW, Westinghouse E-beam sustained discharges--UTRC Modeling-NRL, UTRC, Kansas State Rep-rate testing—NOSC

GROUND-BASED BLUE-GREEN LASERCANDIDATES

Molecular freq. shifted XeCl or XeF via H₂/D₂ — 450-500 nm

XeF-20% at 20 mj

Resonantly pumped Tm:YLF (XeF)—453 nm

Photolytically pumped Xe₂Cl— funable 470-520 nm

Photolytically pumped XeF(C-A)—tunable 460-

Atomic freq. shifted XeCI via Pb-459 nm 20% at 1;

3

STRATEGIC BLUE-GREEN OPTICAL DOWNLINK EXPERIMENT COMMUNICATIONS

ALTITUDE)-TO-SUBSURFACE COMMUNICATIONS EXPERIMENT OBJECTIVE: DEVELOP AND CONDUCT AN AIRCRAFT-(MEDIUM COMMUNICATIONS IN AN OPERATIONAL ENVIRONMENT. DESIGNED TO SIMULATE STRATEGIC SUBMARINE

KEY ISSUES TO BE ADDRESSED:

- BACKGROUND, DISPERSIVE TRANSMISSION CHANNEL PERFORMANCE OF ASYNCHRONOUS PIM IN A HIGH
- ASSESSMENT OF CRITICAL SIGNAL DEGRADATION EFFECTS BY THECHANNEL
- PERFORMANCE OF CLOUD SENSING DEVICES IN SIMULATED **ADAPTIVE SCAN MODE.**

BIREFRINGENT (LYOT) FILTER (LOCKHEED)

Objective

- Develop large aperture, narrowband, wide FOV, blue-green filter for
- Program goal: 30 cm diameter, 6.1 nm, \pm 30 $^{\circ}$

Background

- Given material characteristics, performance predictable with high Lyot filter technology well developed Fiown on Spacelab 1 accuracy
- Crystal birefringent materials not suitable for large aperture, 0.1 nm
- Must develop large plastic birefringent components Small tunable all-plastic filter already produced

- Large area, 100-sheet lamination techniques developed Foster-Grant PVA identified as 10" filter material
- Extend technology to Mylar in FY80 Highly birefringent Sub-angstrom bandwidths possible



NARROWBAND FILTER/RECEIVER DEVELOPMENT (MDAC)

Objective

Develop wide FOV, sub-angstrom bandwidth blue-green filter technology

Approaches

- Atomic resonance absorption and fluorescence filter Potentially scalable to large aperture Bandwidth .01-.001 nm
- Transmission wavelength and bandwidth controliable Basic physical process not fully understood Spectral hole burning filter

- Cs device → 31% effective transmission, 32 µsec pulse stretching Materials, coatings, reasonable configuration identified Preliminary atomic resonance filter design completed @ 455 nm
- 7 kw, 1300 kg refrigerator/container required for liquid helium temp. Hole burning filter cryogenics requirements roughly defined

LIGHT PROPAGATION THROUGH CLOUDS (SYLVANIA)

Objective

 Experimentally characterize optical attentuation and pulse stretching produced by thick clouds

Approach

Project diverging pulsed laser beam from aircraft at 40,000 ft.

Spot diameter = 6km

Simulates satellite transmitter

Cloud altitude = 3km

Detect and analyze using 6-inch-diameter pm on ground

Determine cloud optical thickness via

Knollenberg on second aircraft 530 nm irradiance measurements on ground

- Experiment completed
- 18 flights, 325 passes, 30 data points/pass
- 22 usec pulse stretching observed
- Double exponential decay observed; not understood
- Finite area cloud model needed

LOW LIGHT LEVEL TELERADIOMETER (HSS)

Objective

- Providesimple means for ineasuring cloud optical thickness
- Relate measured optical thickness to observed laser pulse stretching

Approach

- Design, fabricate, deliver two channel low light level teleradiometer
- Measure moonlight, through cloud, at wavelengths in and outside 0, absorption band
- Determine optical path length from relative attenuation, known path absorption characteristics

Staius

- Successfully participated in Kauai experiment
 - Data reduction underway
- Moon-light and laser-light received through different clouds Good qualitative agreement with laser measurements
 - Model refinement and deployable instrument design in FY80



BLUE-GREEN PULSE PROPAGATION THROUGH FOGS/CLOUDS (NOSC)

Objective

- Experimentally determine effect of medium-dense clouds on pulsed optical propagation
- Compare results to theory
- Analyze impact upon satellite-to-sub optical communication

Approach

- Measure laser beam attenuation through coastal fog over 1-2.4 km
- Characterize fog through Knollenberg measurements
- Perform low-medium density cloud measurements on Kauai

Status

- Measurements made for fog paths of medium optical density Losses 20 cB smaller than predicted by diffusion theory Knollenberg data taken; reduction underway Pulse stretching less than few hundred nsec Scattering predominately less than 2°
- Analysis of Kauai data underway

Ţ

Ţ

OPTICAL CHANNEL MODELING (PSR)

Objective

 Develop analytic model for optical propagation from satellite through clouds, to sea surface

Ray directions at cloud bottom Attenuation Pulse stretching Compare model predictions with experimental results

- Model completed
- Comparison with cloud propagation experimental results in



OPTICAL CLIMATOLOGY (MDAC)

Objective

- Provide global data base of cloud optical thickness occurrence statistics
- Allow accurate optical link availability estimates for strategically important locations

Approach

- Obtain cloud statistics from 3D NEPH tapes
- Use existing model/code to estimate statistics of optical/physical thickness

Progress

- Data generated for 50 locations uniformly spaced over op area
- Data accurately represented by polynomial curves
- Variations with latitude, longitude, and season established

Plans

- Refine temporal and spacial resolution
- Establish spacial correlation statistics
- Expand model to treat clouds of finite lateral extent

Ĭ

1

OCEAN OPTICAL PROPERTIES (SIO)

Objective

 Develop data base and model for optical properties of large ocean areas

Approach

- Develop Technique for determining surface K from NIMBUS G CZCS
- Develop model to calculate depth dependence of K from surface value
 - Develop required instrumentation and perform ground-truth measurements
- Establish worldwide ocean optical property data bank

- Surface K algorithm developed; to depth extrapolation initiated
 - Four ground-truth cruises completed
- Comparison of algorithm predictions with ground-truth underway 20 entry comparison table due end of February 20% accuracy anticipated
 - Data storage/retrieval system development initiated

l



MEW FY80 STARTS

Diffuse optical propagation

Determine angle/dept! dependence of signal beam Objective:

diffusion

Background: Degree diff. → receiver FOV, Eff. water range

Measure solar radiance Vrs. depth using digital camera Approach:

XeCI laser/Cs filter system

Establish compatibility Pb-XeCHaser/Cs filter Objective:

Background Pb-XeCllaser leading space-based candidate

Cs filter -* 31% Eff. Trans., Sub-Ang. bandwidth

Tune/frequency-narrow laser to match filter Approach:

Pressurize filter Gas to broaden pass band, reduce purse

stretching



BACKGROUND BIOLUMINESCENCE

Characterize SLC background bioluminescence noise Objective:

Biolum, can dominate at night; stimulated by sub. motion Background:

Femporal char., occurrence statistics unknown

Approach Literature survey, laboratory exps., ??

Workshop Feb 25-29

RECEIVER STUDY

Address system aspects of sub. receiver Objective:

PMT's for blue-green detection available Background:

Filter technology dev. underway

Study transmitter system concepts and SSBN environment Approach:

Design receiver system; state-of-the-art technology

Exper. verify untested concepts/subsystem designs



Cloud propagation data analysis

Obtain max. info. from Kauai cloud prop. experiment Objective:

Five simultaneous experiments; three organizations Background:

Careful data correlation necessary

Compare with navy model predictions Collect/analyze all data Approach:

Expand model if necessary

Nonclassical noise

Characterize underwater optical fluctuation noise Objective: Shot-noise on D.C. optical background considered so Background:

far

Variable cloud cover, surface waves, etc →

fluctuations

Measure background fluctuation spectrum with fast Approach:

irradiance receiver

SUBMARINE BACKGROUND MEASUREMENT

Objective: Characterize optical noise under sub.

operational conditions

Approach: Irradiance detector on submarine

Scope problems Design detection system

Fabricate and test sensor

1



APPROACH TO AN AIR-TO-SUBSURFACE COMMUNICATION EXPERIMENT

• OBTAIN A 0.5-1.0 JOULE/PULSE, 100 PPS AIRBORNE TRANSMITTER - OPTIONS: (a) USC ODACS LASER/AIRPLANE

(b) DEVELOP A DOWN-CONVERTED XeCI HgBr

LASER/AIRBORNE PLATFORM

(c) TBD

 DEVELOP AN UNDERWATER NARROWBAND, ASYNCHRONOUS PIM RECEIVER AND INTEGRATE INTO A TACTICAL/RESEARCH SUBMARINE DEVELOP TEST PLAN AROUND ABOVE TO MEET EXPERIMENTAL OBJECTIVE

 FIELD WITH NECESSARY SUPPORT AND CHANNEL CHARACTERIZATION EQUIPMENT

GEOMETRY OF A STRATEGIC BLUE-GREEN OPTICAL COMMUNICATIONS



-0.5-2.0 JOULE/PULSE LASER TRANSMITTER:

- 100 PPS

- DEADTIME ≤ 5 MS

- REPRESENTATION OF MESSAGE:

A TYPICAL OPERATIONAL MESSAGE

> - DIFFUSIVE CLOUD LAYER IN ATMOSPHERE TRANSMISSION CHANNEL:

27

- JERLGV II/III WATER WITH BIOLUMINESCENCE

- DIFFERENTIAL PIM CODING SUBMARINE RECEIVER: -- 1-3 Å, ± 25° FOV

—≥30 CM DIAMETER APERTURE

SYSTEM ENGINEERING SESSION

Papers 3 and 4 are contained in volume 2.

OSCAR SPACEBORNE SYSTEM: PHASE IB

T. E. FLOM AND P. J. TITTERTON

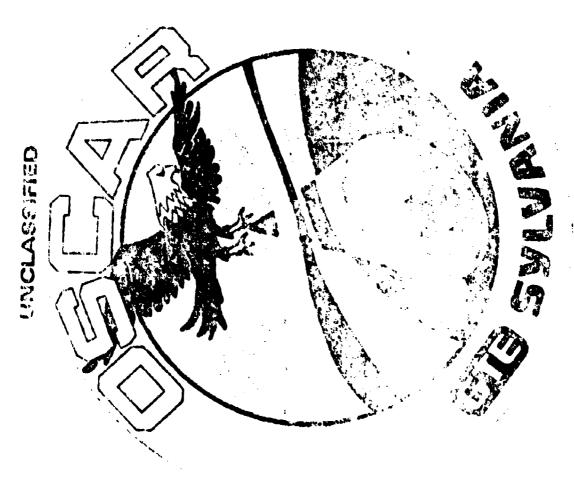
GTE SYLVANIA

Phase IB of the Optical Submarine Communications by Aerospace Relay (OSCAR) has initially concentrated on two main tasks: test case evaluation and experiment definition.

16 environmental test cases provided by NOSC were used as inputs to the propagation and system models developed in Phase IA, and a system design which met the full system requirements for these 16 cases was developed. The driving factors and sensitivity of the results for these test cases has also been explored.

All critical sub-system, sub-system interfaces, sets, set interfaces and units were identified; and critical experiments were identified and defined.

GTE Sylvania PO Box 188 Mountain View CA 94042



Optical Submarine Communications by Aerospace Relay Sponsor- Naval Electronics System Command (U)

UNCLASSIFIED

The state of the s

TEST CASE EVALUATION

DATE IA SCOLL 3

THE STATE STATE OF THE CONTROL OF THE

C TECHFORM - 1600 GENTE (SEPTIENT) (STIME COUNTE) | BECHWEP OF ALS TRANSMISSION | CEPTIENT (SEPTIENT) N (THE CALL ALTER BY NOFASS)

ς (1 γ

OF THE CHEEK AND ANDERS THEN BOARD OF INTERHER

UNCLASSIFICD

UNCLASSIFIED

TEST CASE EVALUATION CHANGES FROM PHASE IA TO IB TEST CASES





CHANGE IN DACKGROUND MODELS:

(THE INCREASE SOLAR AND FUNAR RADIANCE AT DEPTH BY X #

(2) INCREASE BLUE SKY RADIANCE AT DEPTH BY X 2.5

DATA BASFS

CLOUDS:

MORE, AND MUCH THICKER CLOUDS PRESENT

WATER:

THERMOCLINE AT 50m

DIFFUSE ATTENUATION COFFFICIENT BELOW 59m IS SFT TO 2/3 OF ITS VALUE ABOVE 50m

BIOLUMINESCENCE:

ALWAYS PRESENT

UNCLASSIFIED

e Welter Killand

1

SUN AND MOON LOCATIONS AND

UNCLASSIFIED

CLOUD PROPERTIES FOR 16 TEST CASES (U)

s,i		! <u></u>		ż	*****	
	•	1000 100	:			
		3 . 1 3 3 3 4 3 4 4 4 4 4 4 4 4 4 4 4 4 4 4	Heart man	4.17	1011	6.1
	_	•		:	•	
	_	1-1	<u>.</u>	2	ş	
	. " . ne"		2			3.
		٧.			c	
		•			÷	
	 -	1-4	06.	c	Đ.	
			=			29.6
					٠.	
	sa:	V	ş	E C	2113	28.5
	_	, V	9	-3	:	28.6
	2.	A-8	273	53	e.) () ()
	-	<<		c	Đ _A ,	 .r
	<u>=</u>	F. <<	00	c	W.	- -
	=	41,			za.	<u>.</u> .
	<u> </u>	5	2.3		ŝ	Ţ.
	=	*Z	; F		ž	:- :: :: ::
	<u>.</u>	···				
	- - £	Α-3	<u>.</u>		£.	••
		t ar,	-	12		
	· :		-	1		

UNCLASSIFIED

DOWNLINK AVALABILITY OF OSCAR SYSTEM IN TEST SCENARIOS

8	£ .	699	1.0	998	9046	.9867	6 6.	985	86	55.	0.5	\$1361	Ť:	9	367	5
AVADEACTER ANDARTE		\$33	e.	:9:6:	: 096°	e.	. 364	v96·	e. -	ن ن ن	e	. <u>.</u>	* 956*	9	XC 4.	386
PACIFIC N	967	£89.	c -	0.	97	970	215	766.	63:	167	9.1	£,	e:-	<u>c</u>	. 16.7	- 5448.
\$0411300 \$0411300		U	<u>-</u>	2	Ð	2	<u>~</u>	2	21	ç		ت	<u> 2</u> 5	c	_	2:
10:11:V1		ζ.;	9		£7 #.	73.5	23.5	<u>د</u> ۳			S		23.5			
11 TO 115501	: ! ¥ !	5 .		0/	e .	96	<u>.</u>	1976		ç	2	7.0	<u></u>	₽	<u>.</u>	ETT Thu
Lingsoca Clerks	A-1			•	. v	y-6	A-7	8:			νυ	A-',	y			Α.,
		~						3.	-	\$		<u> </u>		<u>-</u> 	<u></u>	<u>.</u>
		i Nga sa														

		_			_
PACIFIC	'	-		_	;
ATLANT 10			~	_	-
"MILLITT POLITION"					
'ATE:: 17;	c	•	<u>'</u>	<u>c</u>	ز

UNCLASSIFIED

SYSTEM EFFECTIVENESS

ნ. 999 GROUND STATION.

0 9990

MILIUM

SATELLITE

0, 787

0.9229

DOWNLINK

65.0

SUBNIARINE

0.901

SYSTEM

UNCLASSIFIED



DISCUSSION OF DOWNLINK RESULTS





Systems

ENVIRONMENTAL EFFECTS

TIME-OF-DAY DEPENDENCE AND DOMINANT BACKGROUNDS

TEMPORAL ASPECTS

BEAM DIVERGENCE

ALTERNATIVE WIDE PULSE / NARROW SLOT COMPENSATION TECHNIQUE

MASTER CHART



- 1

UNITED STATES

The course of the same section of the course of the course

Systems

AVAILABILITY

. 656

660

ORDERING	ERTY NO.			er e'n e'n in make', e'n 'n en	THE LIBERT PARTY AND ADDRESS OF THE PARTY AND					marindo miss community in the community of the community	and the second of the second o				
TEST CASES: C	CLOUD PROPERTY NO.	A-2	A-2	N-1	A-7	N-7	A-1	5- V	ý-V	8-V	A-8	A-6	A-A	N. A.	A-6
150	NO.														
	CASE NO.	15	2	16	2	10	p.m.i.	12	5	6	တ	9	4	13	part)
	্টুনা ক		Link												

37

.9615

<u>S)</u>

.87 .9165

9026

. 9867

. 985

. 86

. 995

366

1.0

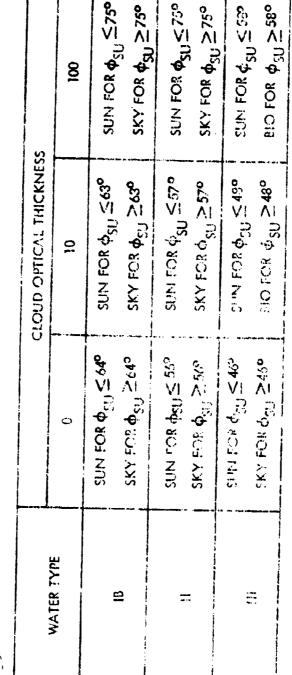
1-3

Sylvente Systems Group Western Division

UNCLASSINED

DAYTIME DOMINANT BACKGROUND NOISE SOURCES (TIE)

Systems



♦SU = COLAS ZENITY ANGLE

A TEST CASE RESULTS

NIGHT TIME:

100% BIOLUMINEDCENCE LIMITED

DAWN/DUSK:

61.4% BIOLUMIN'ESCENCE LIMITED

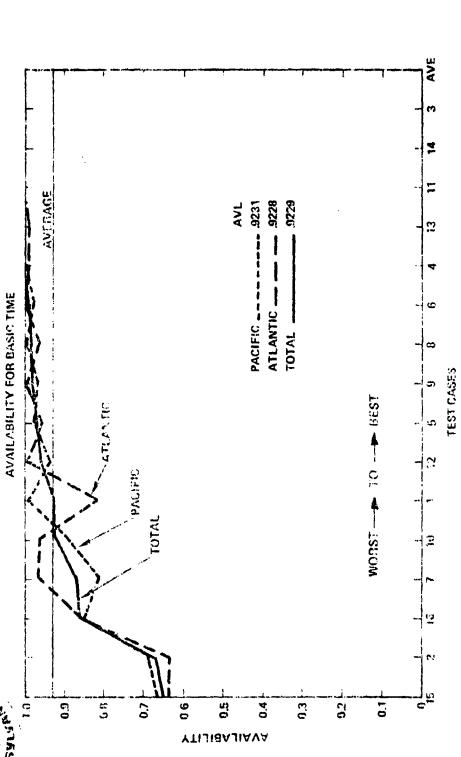
DAY TUAE

14% BIOLUMINESCENCE LIMITED

これに 本 コンボラのはのなる

TEMPORAL EFFECTS

Dysteral party



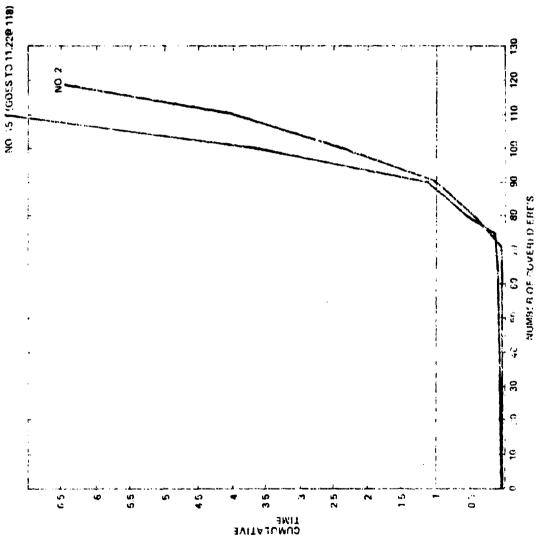
NECLECTING 15 ARDING 2 (\$\frac{1}{2}\) AVI, PL 10,9601

THE VALIDITY OF THE DATA BASES FOR THE WORST OF OUD CASES ARE OF PRIMARY EMPORTANCE.

Sylvania Systems Group Wast in Daision

TEMPORAL EFFECTS CONTINUED

Systems





Sylvania Systems Group Western Division

TEMPORAL PRECTS CONTINUED

Systems

NO. 13 NO. 4 100 119 120 129 - 8 NUMBER OF COVERED ERES 0.3 CUMULATIVE

CURLIE LA LIVE TIME TO COVER TRES PACIFICATASES 13, 4.

UNCLASSIFIED

TEMPORAL CONCLUSIONS

Systems

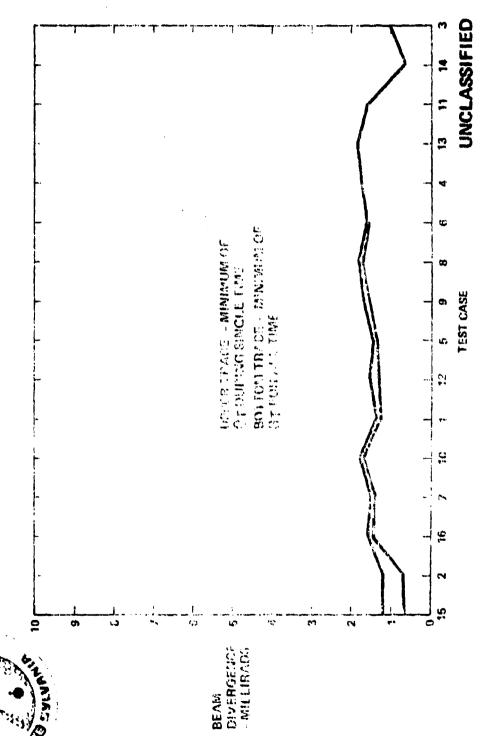
	TOTAL ERE'S COVERED IN PEQUIRED TIME	% COVERED IN. 1/3 OF REQUIRED TIME, OR LESS
ATLANTIC		
# 2/15	48/48	775/17% (37)
# 7/10	73/73	82 32% (60)
# 4/13	3676	875/265 (66, 65)
PACIFIC	· ii ·	
# 2/15	60,87	(77) 2691 ETS
# 7/10	911/901	777./89% (82, 103)
# 4/13	120/130	100% IN 10% OF REQUIPED TIME



BEAM DIVERGENCE







SYSTEM ONLY NEEDS A BEAM DIVERGENCE CAPABILITY ATMILLIRACIONS FROM MOLINYA ORBIT

MINIMUM BEAM PIVERGENCE FOR THE TEST CASES

Sylvania Systems Group Western Division





- 3 SATELLITES FOR FULL COVERAGE
- MOST OF BROADCAST AREA CAN BE COVERED IN A FRACTION OF THE REQUIRED DELIVERY TIME 6)
- S CLOUD DISTRIBUTION OF IN THE DOMINANT AVAILABLE ITY DRIVER
- RELATIVE DAY VERSUS MICHT PORORMANCE COMPANISONS CANNOT BE MADE FROM THEST CASES e
- SINCE BIOLUMINESCENCE IS THE DOMINANT BACKGROUND SOURCE, A CHANGE IN IT WOULD HAVE THE LARGEST IMPACT OF ANY MODEL CHANGES
- SINCE THE SYSTEM DESIGN IS DRIVEN BY THE WORST CLOUD CASES, THE VALIDITY OF THE WORST CASE CLOUD DISTRIBUTIONS IS OF PRIME IMPORTANCE
- THESE RESULTS CANNOT BE EXTRAPOLATED TO OTHER TEST CASES
- PROPAGATION MODELS AND DATA BASES

ŧ

Ţ

I

I

A STREET

Sylvaeia Systems Greep Western Division

.

- i

TECHNOLOGY SCALING OF EACH TEST CASE

Systems

FIGURE 23 FACH OF 16 TEST GASE RESULTS

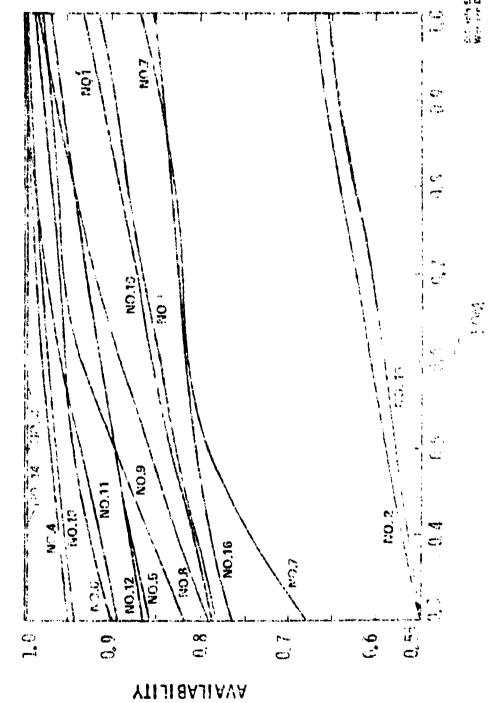
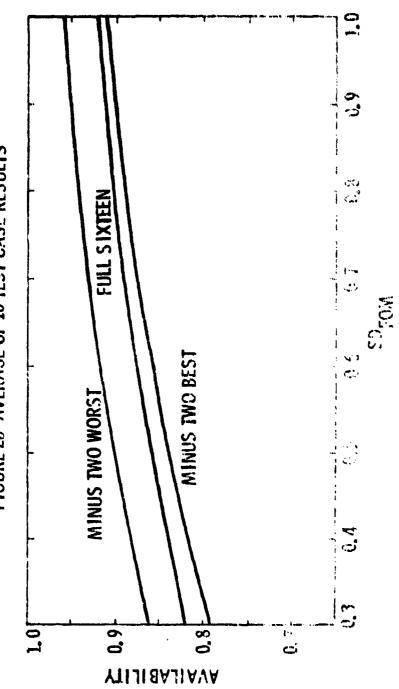


FIGURE 26 AVERAGE OF 16 TEST CASE RESULTS



1



I

EXPERIMENT DEFINITION



- IDENTIFY THOSE AREAS WITH ISSUES REQUIRING EXPERIMENTAL RESOLUTION
- METHOD EXAMINE OSCAR DESIGN AT SYSTEM, SUB-SYSTEM, SET, SET INTERFACE AND UNIT LEVEL, FOR HIGH RISK/UNCERTAINTY AREAS. (ALSO CONSIDER CHANNEL CHARACTERIZATION.)



DEFINITION OF RISK CATAGORIES

CATEGORY

DESCRIPTION

- OFF THE SHELF (PRODUCTION COMPONENTS).
- STRAIGHTFORWARD DESIGN USING EXISTING TECHNOLOGY.
- IS FEASIBLE, BUT REQUIRES ADVANCES NOT YET ACHIEVED.
- IS POSSIBLE, BUT REQUIRES SOME FEASIBILITY DEVELOPMENT.
- IS POSSIBLE IN PRINCIPLE, ALTHOUGH THERE ARE MANY FEASIBILITY ISSUES.
- 6. MAY BE POSSIBLE.

UNCLASSIFIED

1

٠,٠

OSCAR EXPERIMENTS



- 1. POWER, THERMAL, LASER
- 2. POINTING, SCANNING, AND BEAM SHAPING
- 3. MODULATION, DEMODULATION, AND SYNCHRONIZATION
 - 4. OPTICAL RECEIVER
- 5. DOWNLINE COMMINICATIONS
- 6. SATELLIJE REMOTE SENSOR
- 7. SUBMARINE REMOTE SENSOR
- 8. CHANNEL CHARACTERIZATION

INCLASSIFIED

- OBJECTIVE OF EXPERIMENT
- REQUIREMENTS AND SPECIFICATIONS
- IDENTIFICATION OF YEY 1950ES
- C APPROACHE, TO ATT THIS REQUEREMENTS
- TRADE-07FS ANY APPROACH SELECTION
- RECOMMENDED WORK



A STATE OF THE STA

]

SPACEBORNE LASER EXPERIMENT





≥ 1% EFFICIENCY

RAMAN SHIFTER

- 1-15 JOULES/PULSE
- 50-100 PULSE PÉR SECOND
- < 1 ANSTROM LINEWIDTH
- S 5 YEAR LIFE
- GAS CLEAN-UP
- ELECTRODES AND PREIONIZER
- POWER AND SWITCHING

RAIL CAP

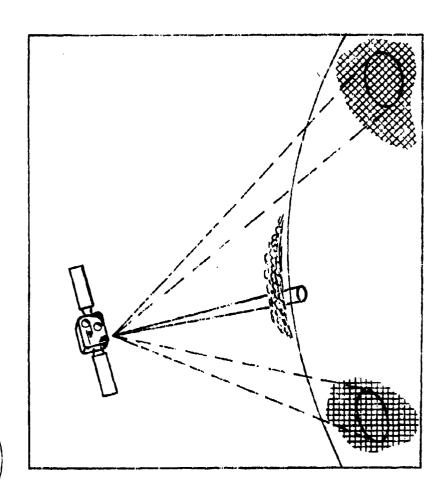




UNCLASSIFIED POINTING, SCANNING AND BEAM SHAPING EXPERIMENT



- SCAN SPEED
- ADAPT TO PATH LOSSES

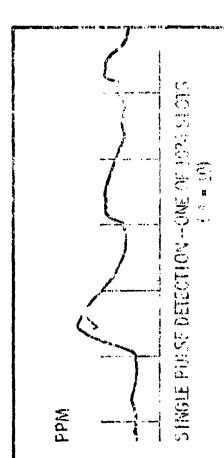




こう とう のはのを関いているのでは、これののでは、これの

MODULATION, DEMODULATION AND SYNCHRONIZATION

: ::



MESSACE -- YX FRAMES

March Street, Spirit	- AP 16-
	-3

	.]
	٠
	inni.
	4
	1
	-
	_
	−
	TETT
M.A	100
	-4
	1
	- 1
	-
	===
•	
```	<b>=</b> 1
•	$\supset$
	_
	=
	$\bar{\Xi}$
	$\frac{1}{2}$
	unim
	mulma
	ساسيا
	undund
	mhamha
	mhanhin
	mhanhm
	lmulaadmi
	ساسطساد
	ulmulanim
	ակապարտ
	milmetalim
	հոտկոսևումում
	ահատկապետանու
	<u>udandandanda</u>
	ահակապա
	ահակապա
	ահակապա
	անահատկապետվում
	ահակապա

MESSAGE IDENTIFICATION—ONE OF ≈ 2,000 MESSAGE WINDOWS

SINGLE PULSE DETECTION

- PULSE WIDTH/SLOT WIDTH RATIO
- INTEGRATION OR MATCHEL FILTER
- MISRECISTRATION SENSITIVITY

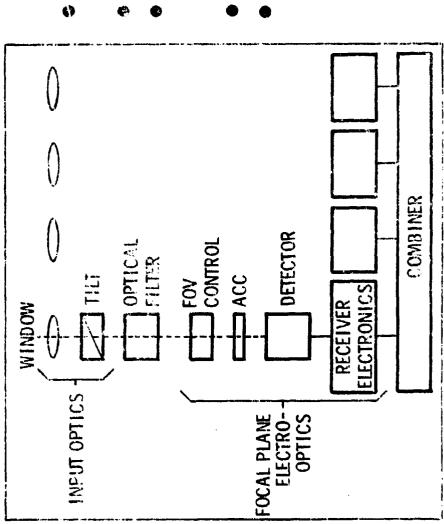
MESSAGE 10

 SIGNATURE PULSES ADDED, OR PEAK VALUE SCORING

## OPTICAL RECEIVER EXPERIMENT

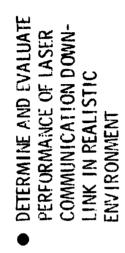


- # #30" FIELD -OF-VIEW
- I METER EFFECTIVE APERTURE (SIZE AND LOCATION OF MODULES)
- **▶** POINTING
- DETECTOR ACCEPTANCE ANGLE AND PACKING DENSITY



CHILLICUY COM

# DOWNLINK COMMUNICATION EXPERIMENT



• CLOUDS

OPTICAL

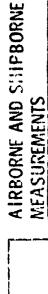
路

- WATER
- SUN
- BLUE SKY
- **BIOLUMINESCENCE**

UNCLASSIFIED

8





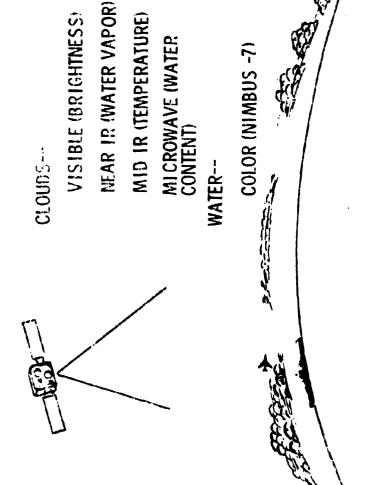
Sylves O

• CLOUDS

THICKNESS ~10-30% EXTINCTION COEFF ~20-80%

WATER

ATTENUATION COEFF ~5-20% LAYER THICKNESS ~5-20% BIOLUMINESCENCE ~ 50-200%



UNCLASSIFIED

#### 

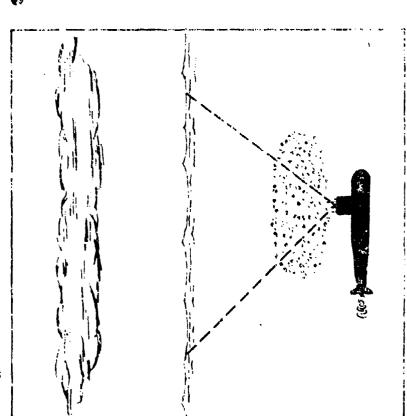
#### UNCLASSIFIED

これの あるとなるといれるといれるというない

# SUBMARINE REMOTE SENSOR EXPERIMENT







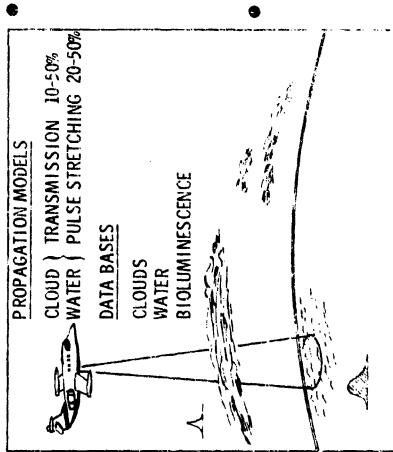
WHAT CAN BE LEARNED FROM PREVIOUS DOWNLINK MESSAGES?

- SHAPE OF PREVIOUS PULSES
- CONTENT -- SATELLITE PREDICTS FUTURE CONDITIONS

WHAT IS THE PENALTY FOR NO REMOTE SENSING?

# CHANNEL CLARACTERIZATION EXPERIMENTS





▶ PROFAGATION MODELS— CLOUDS-

SIG PULSE SHAPE & TRANSMISSION

FOV AND POINT: NG SIG PULSE SHAPE & TRANSMISSION

WATER--

COMPLETE PATH-- SUPERPOSTITON WATER EFFECTS OF CLOUD AND

• DATA BASES ..-

CLO! IDS....

DATA, AND GROUND TRUTH MEASUPENENTS USE OF RAW 3-D NEPH

WATER-

FIMEUS-7 ?

DIGITAL NESCENCE—FIELD

SINGMENTS

#### UNCLASSIFIED

#### SUBSYSTEM TECHNOLOGY SESSION

#### CESIUM ATOMIC RESONANCE FILTER STUDIES

R. Burnham and B. Wexler Naval Research Laboratory Washington, D. C. 20375

#### SUMMARY

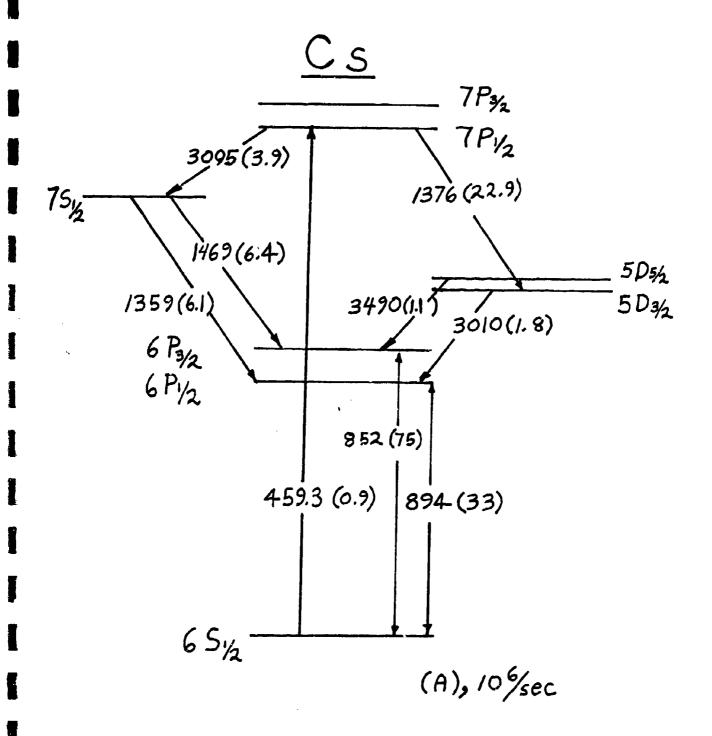
Several aspects of the atomic cesium resonance filter are being studied experimentally to determine its usefulness for strategic blue-green communications. First, the temporal response of the filter is being investigated as a function of pressure broadening on the 459 and 894 nm resonance lines. Calculations indicate that the resonance trapping time on the 894 nm line can be reduced to ~ 1 usec at reasonable buffer gas pressures. Second, the effect of broadening on the actual filter linewidth is also being measured. Finally, the tunability of the XeCl laser downshifted in Pb vapor is being studied to determine if efficient extraction from this laser can be obtained at the frequency of the 459 nm Cs filter.

# NRL-Cs Atomic Resonance Filter Studies

- Filter Wavelength @ 459.3nm
- 0.01 < 4 × ≤ 0.1 Å
- FOV \$ 180°

#### Issues:

- XeCI-Pb Laser Matching Filter to
- Filter Response Time Vs. Linewidth



# Schematic of Cs Filter

4593nm + Solar Backround

Filter-Pass Blue

Dieck Yeddonm

Cs + Buffer

50-100°C

# FIIter - Pass >800 nm Slock <700nm

Output 8524 894 nm

Large Aperture Defector

#### Radiation Trapping on Cs 894 nm line

Assume:  $k_0 l = 3$  on 459 nm line then  $k_1 l = 800$  at 894 nm  $t' = \frac{1}{GA}$  where  $G = \frac{1.9}{k_0 l \sqrt{\pi k_0 l/2}} = 5 \times 10^{-4}$ 

T'= 56 MSEC (DOPPLER ONLY)

For VoigT PROFILE:

 $a = \frac{\Delta y_n}{\Delta y_D} \sqrt{2} = \begin{cases} 1.4 \times 10^{-4} & (459) \\ 0.01 & (894) \end{cases}$ 

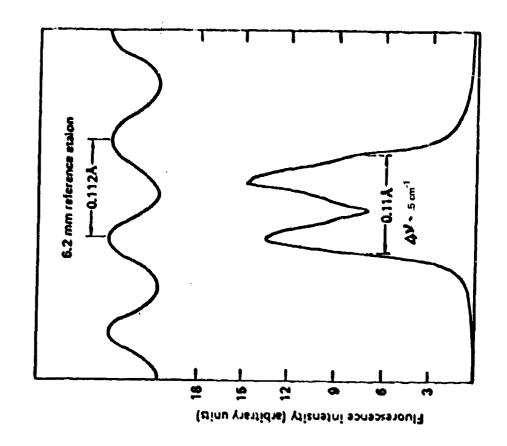
From SISUN CALCULATION:

t'= 13.5 Msec (VOIGT)

IF  $\alpha' > 0.1$  USE LORENTZIAN LINESHAPE  $\gamma' = \frac{1}{GA} WHERE G = \frac{1.1}{\sqrt{\pi k' l'}}$ 

FOR BROADENING OF 1.5 x 109/sec @ 100T

J'= 14500 (PRESSURE BROADENED)



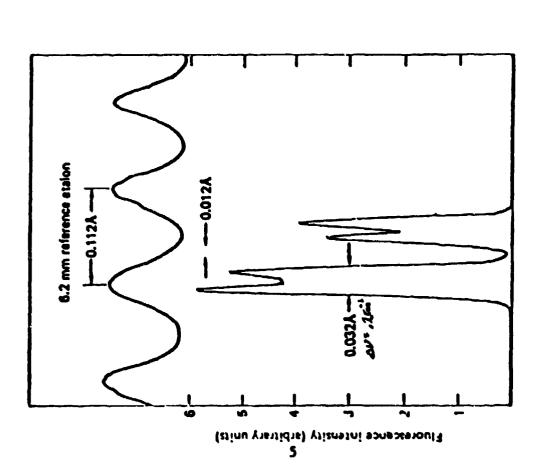


FIGURE 3 - Hyperfine structure of the 459 nm line of cestum.

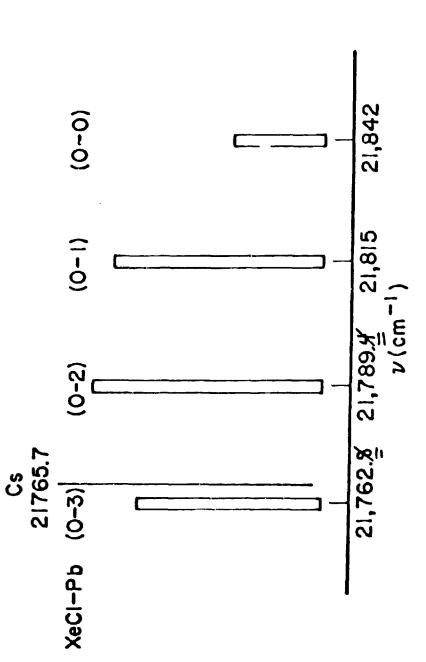
a) at low temperature (45°C) and b) at 140°C. (Fro

Ref. 1)

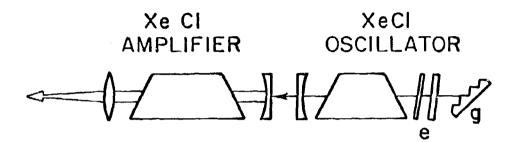
•

The state of the s

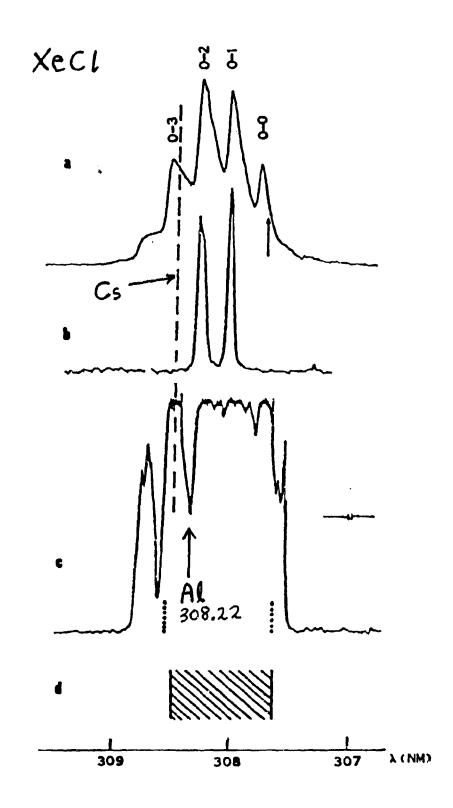
64



vapor. The height of each laser line is proportional Vibrational transition. The position of the Cs FIGURE 1 - Spectrum of the XeCl laser downshifted in lead to the Franck-Condon factor for the particular



e-INTRACAVITY ETALONS g-ETCHELLE GRATING



#### BIREFRINGENT BLUE-GREEN FILTERS March 25, 1980

Alan M. Title William J. Rosenberg

#### **ABSTRACT**

The status of plastic film elements is reviewed. Poly vinyl alcohol can be laminated to make 30 cm elements or waveplates while polyesters still have too many non-uniformities. For elements smaller than 30 cm, quartz mosaic filters and Michelson interferometer elements are attractive. An actual Michelson analog birefringent element is discussed with a candidate configuration for a narrow band (<|A|) filter of such elements.

A new, highly efficient Solc filter design is presented. This design, using only 16 elements and 3 polarizers, results in a finesse of 240 with an integrated out-of-band transmission below  $<10^{-3}$ . In band transmission of 80-90% in polarized light should be possible.

At the present time it is practical to build a quartz filter with a 30 cm x 30 cm aperture, 2R FWHM, and a  $19^{\circ}$  half angle field of view. It is suggested that construction of such a filter be started for near term experimentation.

Lockheed Palo Alto Research Laboratory 3251 Hanover St Palo Alto CA 94304

# BIREFRINGENT BLUE-GREEN FILTERS



PROGRAM REVIEW

MARCH 25, 1980

LOCKHEED RESEARCH LABS. WILLIAM J. ROSENBERG PALO ALTO, CA 94304 3251 HANOVER STREET (415) 493-4411ALAN M. TITLE

# BIREFRINGENT BLUE-GREEN FILTERS



- * PLASTIC FILM TECHNOLOGY
- * OTHER MATERIAL/TECHNOLOGY
- * FILTER DESIGNS
- * FUTURE DIRECTION

## PLASTIC FILM TECHNOLOGY



### PVA LAMINATION

- * CAN PRODUCE LARGE ELEMENTS
- * ESSENTIAL FOR LARGE APERTURE WAVEPLATES
- * WELL ESTABLISHED

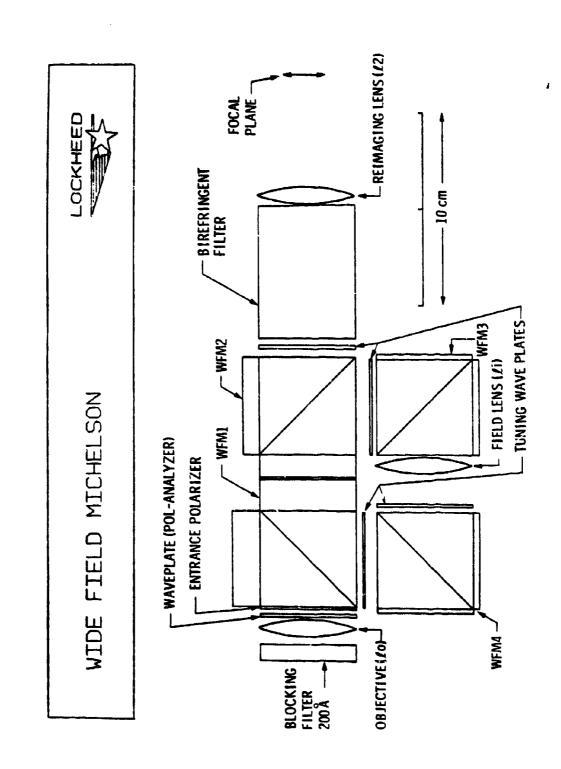
## POLYESTER NONUNIFORMITIES

- * INHERENT IN THE ORIENTATION PROCESS
- * MAY BE ABLE TO POLISH OR COMPENSATE
- * STILL QUESTIONABLE

## OTHER MATERIALS/TECHNOLOGY



- * QUARTZ MOSAIC
- QUARTZ KDP TYPE II ELEMENTS <del>*</del>
- WIDE FIELD MICHELSON ANALOG ELEMENTS *
- * HIGH TRANSMISSION POLARIZERS



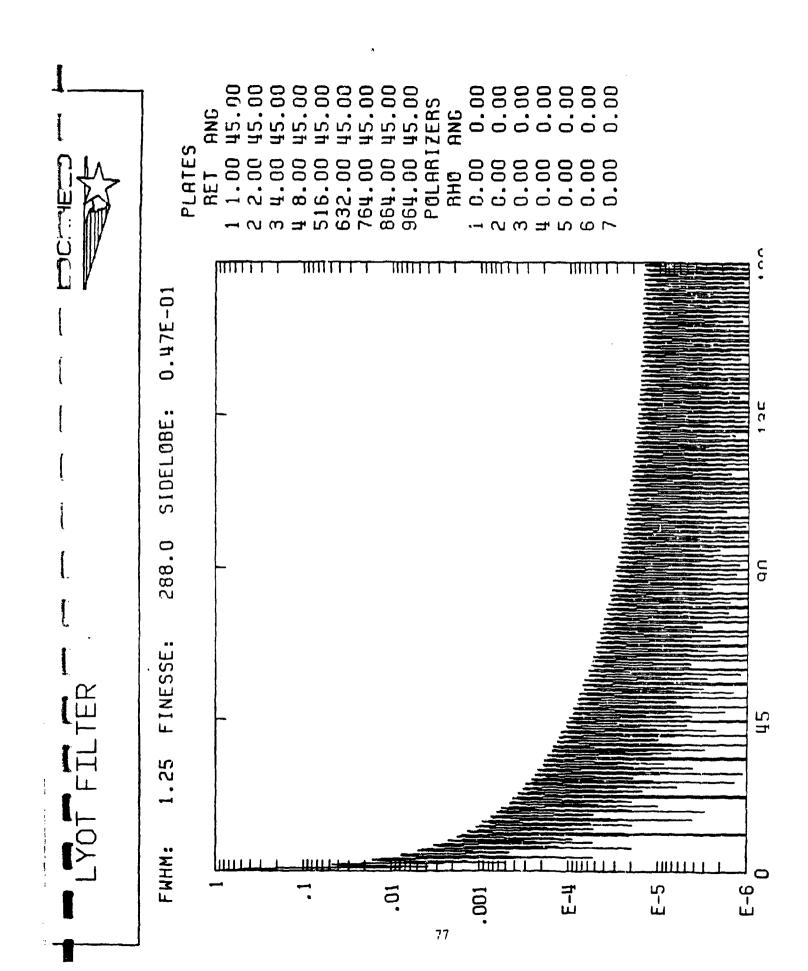
LOCKHEED WIDE FIELD MICHELSON 75

# SOLC FILTER DESIGNS

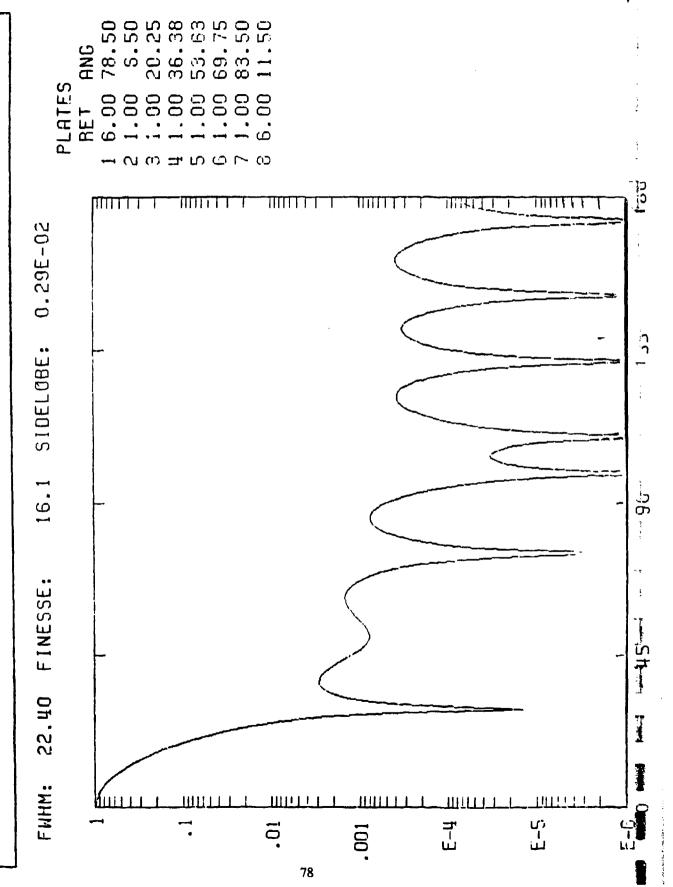


- * COLLAPSABLE (DEGENERATE) SOLUTIONS
- * WAVEPLATE ROTATORS
- ANALYSIS-SYNTHESIS CALIBRATION <del>*</del>
- HYBRID DESIGNS HAVE HIGH FINESSE/PLATE *
- TRANSMISSION 85-90% (POLARIZED) *
- * WIDEFIELD ANALYSIS APPLICABLE

I







#### PLATES 2 1.00 3 1.00 4 1.00 5 1.00 6 1.00 7 1.00 8 6.00 984.00 တ 180 0.75E-02 135 SIDELOBE: 224.8 90 FINESSE: HYBRID SOLC .60 FWHM: E-5 E-6 E-4 .01 .001

## BIREFRINGENT FILTERS



APERTURE	10-15 CM OR MOSAIC	15-30 CM	SAME AS
HALF ANGLE	19. 25.	. 69. 20.	13.
BANDWIDTH	1.0 3.E	9.5 1.0 3.0	1.0
MATERIAL	QUARTZ	KDP	QUARTZ

15-30 CM

9.0

8.5 1.9

MYLAR

QUARTZ

25.

3.0

### MICHELSON FILTERS

LOCKHEED	
----------	--

HALF ANGLE	
BANDWIDTH	
TYPE	

APERTURE

12.	15.

19.

ø.2 ø.5 1.0

WIDE FIELD

DYSON

#### NEXT PHASE



2.0 A	2.0 A
QUARTZ	OUARTZ
HYBRID SOLC FILTER	HYBRID SOLC MOSAIC

10 CM DIAM

22 X 30 CM

ΑM
OGR.
PR
F
E E
ÆL(
OE/

- PRACTICAL TODAY	- NO MAJOR PROBLEMS	- UNIFORMITY
10 CM SOUARE	10 CM SQUARE	30 CM DIAM.
WIDE FIELD MICHELSON	DYSON MICHELSON	MYLAR ELEMENTS

#### ISO-INDEX ELECTRO-OPTIC FILTER: RECENT EXPERIMENTAL RESULTS

- J. F. Lotspeich
- D. M. Henderson

Hughes Research Laboratories 3011 Malibu Canyon Road Malibu, CA 90265

#### **ABSTRACT**

Recent high-resolution measurements of  $AgGaS_2$  iso-index filter samples have confirmed earlier theoretical predictions first presented in 1979. We have observed a filter pass-band of less than  $1.0\text{\AA}$  at  $4970\text{\AA}$  in a sample 3mm thick and have achieved electro-optic control of transmission efficiency up to a maximum of 60% for polarized light with about 1000V. These results translate to filter passbands of less than  $0.3\text{\AA}$  in a 1-cm sample with comparable voltage requirements and with negligible electric power dissipation. The filter response for off-normal light beams indicates a field-of-view capability in excess of  $45^\circ$  half angle (f/0.5) with less than 20% increase in passband over the narrow field condition. Temperature tuning of the pass wavelength has also been observed, with a tuning rate of  $0.25\text{\AA}/^\circ\text{C}$ . A larger tuning range, for matching

a particular laser transmitter wavelength, is possible by variation of chemical composition.

The presence of optical activity in AgGaS₂ was confirmed. Its effect on transmittance at zero voltage and on passband characteristics for various crystal orientations is currently being addressed.

A theoretical model for characterizing iso-index materials has been developed, based on the classical dispersion theory of doubly-resonant damped harmonic oscillators (band edge splitting). The analysis indicated that the best candidate materials should exhibit (a) a large non-resonant birefringence, (b) a short wavelength band edge, and (c) a small band splitting.

HUGHESTAIRCRAFT COMPANY

HUGHES

. . . Novel

8691-3

#### ISO-INDEX ELECTRO-OPTIC FILTER RECENT EXPERIMENTAL RESULTS ΒY

JAMES F. LOTSPEICH

# ISO-INDEX COUPLED-WAVE FILTER

HUGHES

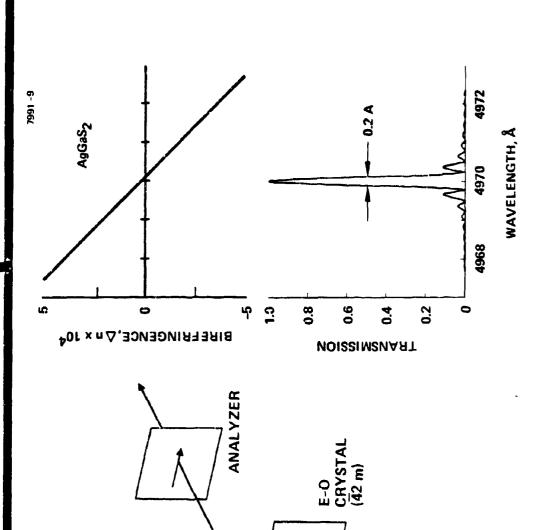
HUGHES AIRCRAFT COMPANY RESEARCH LABORATORIES

### **OPERATING CHARACTERISTICS**

- REQUIRES A BIREFRINGENT MATERIAL
- OPERATES BY POLARIZATION COUPLING
- OPERATES BETWEEN CROSSED POLARIZERS
- RESONANCE OCCURS AT ZERO CROSSING OF BIREFRINGENCE
- COUPLING MAY BE INDUCED BY
- (1) ELECTRIC FIELD
- (2) STRESS/STRAIN FIELD
- 3) MAGNETIC FIELD
- FILTER CAN BE TUNED BY
- (1) TEMPERATURE VARIATION
- (2) COMPOSITION VARIATION
- (3) PERIODIC PERTURBATION

## ISO-INDEX ELECTRO-OFTIC FILTER





POLARIZER

(110) "0"

 $\langle 001 \rangle$ ,  $n_{\rm e}$ 

RESEARCH LABORATORIE

PRINCIPAL DIRECTIONS OF INDEX EIGENVECTORS

The me PRINCIPAL DIRECTIONS OF INDE

$$\tan 2\alpha = \frac{2 n_0^2 n_e^2 r_{41} E_1}{n_0^2 - n_e^2}$$

3

* n-1/2 n3 r41 E1

#### MAY 1979

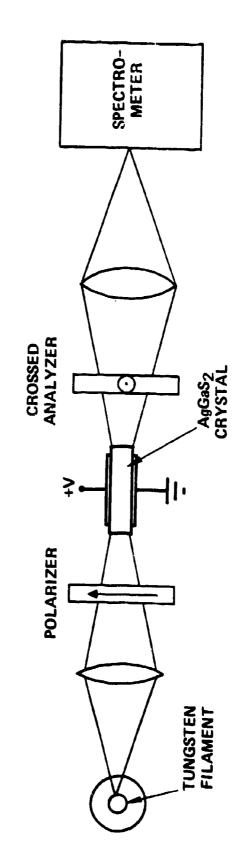
## ISO-INDEX E-O FILTER EXPERIMENTAL SET-UP

17 19 日本日本の 1 大学の日本の

HUGHES

HUGHES AIRCRAFT COMPANY NESEARCH LABORATORIES

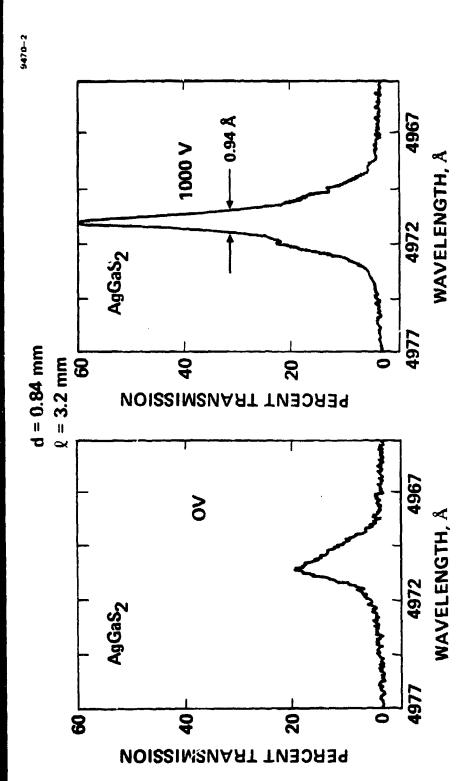
8691-5

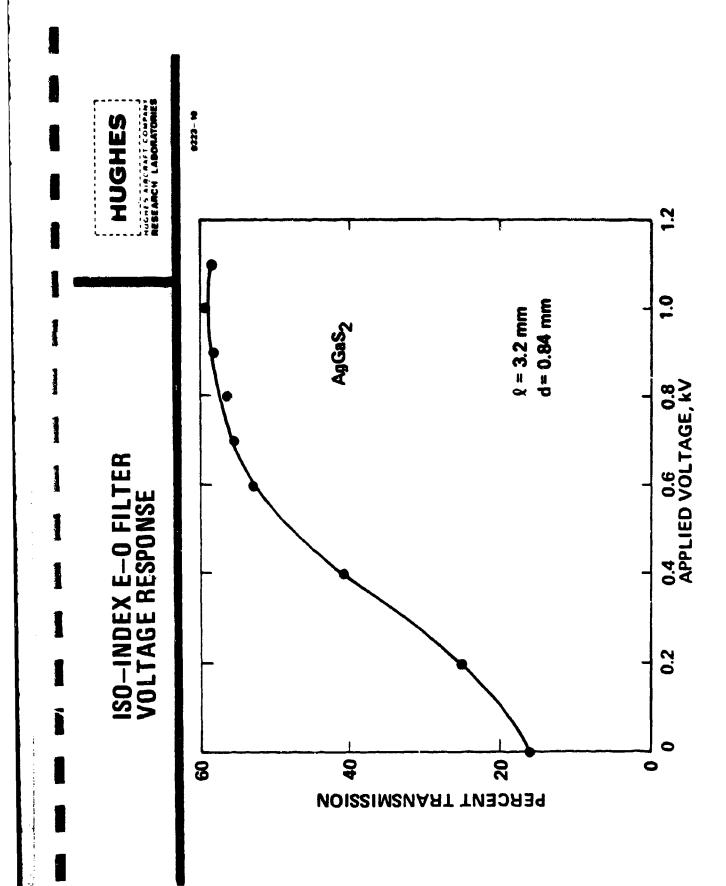


#### ISO-INDEX E-O FILTER VOLTAGE SENSITIVITY

HUGHES AIRCRAFT COMPANY

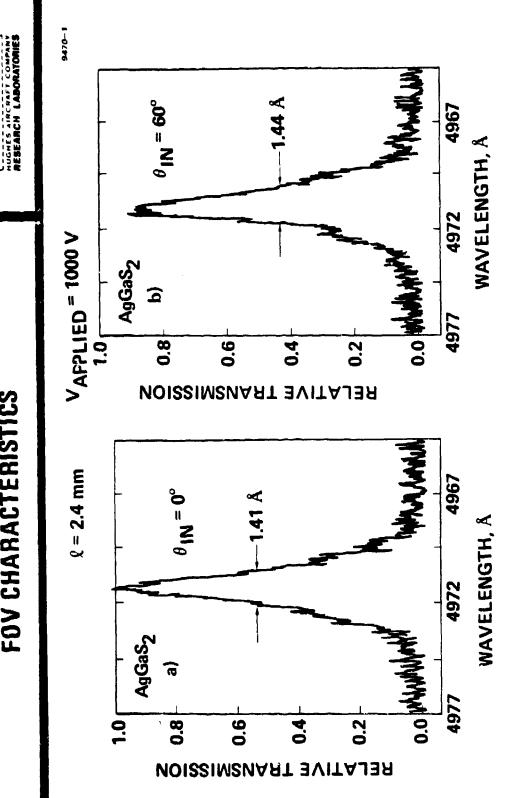
HUGHES

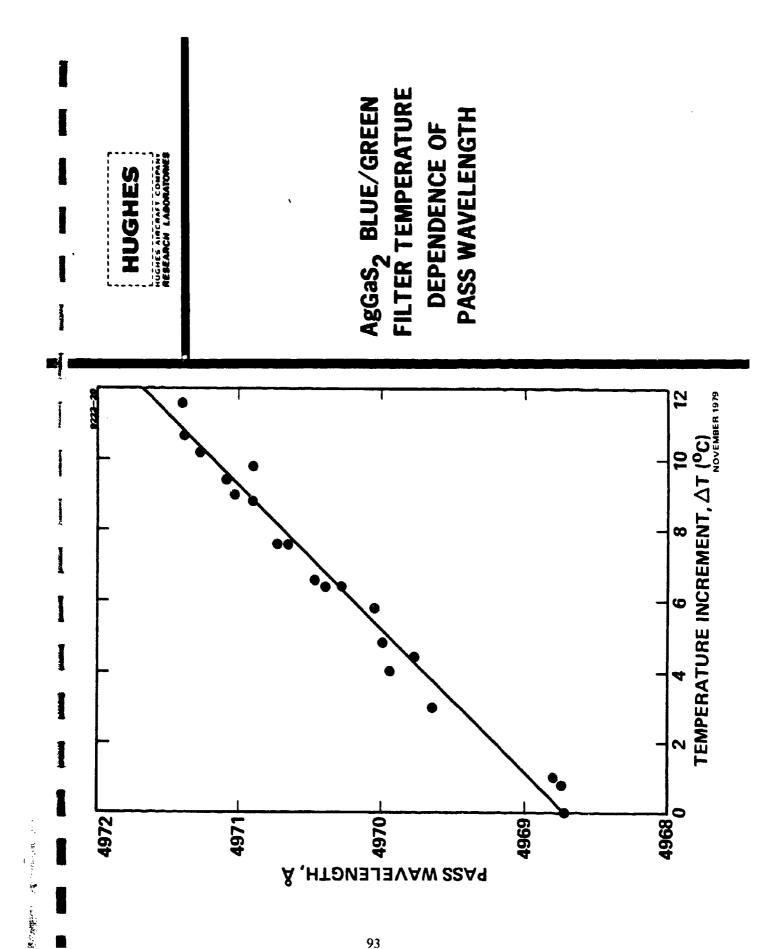




ISO-INDEX E-O FILTER FOV CHARACTERISTICS

HUGHES





### ISO-INDEX ELECTRO-OPTICAL FILTER THEORETICAL MODEL

HUGHES

HUGHES AIRCRAFT COMPANY RESEARCH LAGORATORIES

629 - 2

### **RESULTS OF ANALYSIS**

- GOOD AGREEMENT BETWEEN MEASUREMENTS AND CALCULATION OF ISO-INDEX POINT AND SLOPE OF BIREFRINGENCE FOR KNOWN ISO-INDEX CRYSTALS.
- **BEST CANDIDATE CRYSTALS HAVE:**
- LARGE BIREFRINGENCE
- SHORT WAVELENGTH BANDGAP
- SMALL BANDGAP SPLITTING

•

]

1

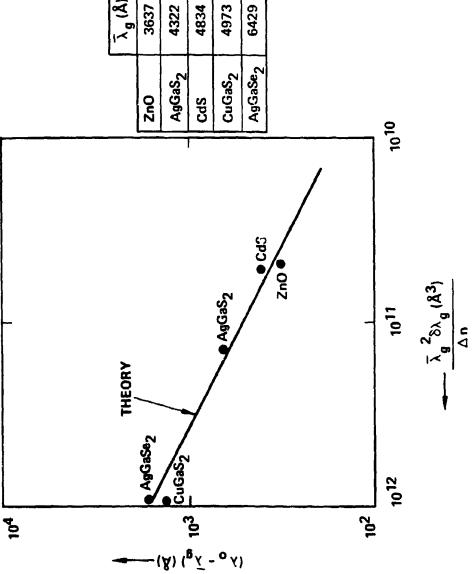
## MEASURED OFFSET OF ISO-INDEX POINT FROM BAND EDGE AS FUNCTION OF MATERIAL PARAMETERS

HUGHES AIRCRAFT COMPANY HUGHES

9223-26

 $(\lambda_0 - \lambda_g A)$ 323 648 411 1341 1607 0.013 0.055 0.006 0.017 ٦ 0.03 82g (A) 48 240 422 38 λg (A) 3637 4973 4322 4834

989

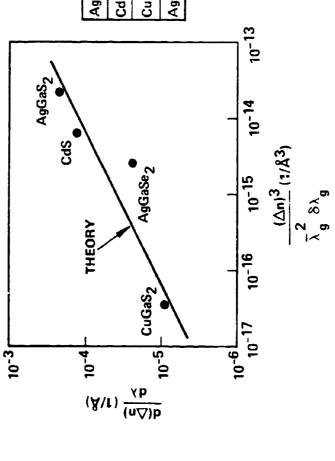


### AS FUNCTION OF MATERIAL PARAMETERS MEASURED SLOPE AT ISO-INDEX POINT

HUGHES AIRCRAFT COMPANY HUGHES

9223-25

	-λ _g (Å)	δλ _g (Å)	Δn	<b>∀</b> ₽/(υ∇)₽	æ
AgGaS ₂	4322	422	930.0	1.9 x 10 ⁻⁴	0.26
CdS	4834	38	0.017	$0.017   1.2 \times 10^{-4}$	0.44
CuGaS ₂	4973	240	900'0	$8.0 \times 10^{-6}$	7.9
AgGaSe ₂ 6429	6429	989	0:030	$1.9 \times 10^{-5}$	4.2



#### BLUE/GREEN CANDIDATE MATERIALS

HUGHES

BEARCH LABORATORIE

9593-6

| - N

CdS - ZnO

CdS - ZnS

1 - III - VI

CuAIS₂ - AgGaS₂ CuAIS₂ - CuAISe₂ CuAIS₂ - CuGaS₂

# ISO-INDEX ELECTRO-OPTIC FILTER:

HUGHES

HUGHES ANCRAFT COMPANY RESEARCH LABORATORIES

#### CONCLUSION

8691-6R1

#### • RESULTS

- NARROW BANDWIDTH: ~ 0.3Å IN 1-CM SAMPLE
- WIDE FIELD OF VIEW:  $\sim f/0.3~(\pm~60^\circ)$
- TUNABLE (TEMPERATURE, COMPOSITION)
- THROUGHPUT IS CONTROLLABLE ELECTRICALLY
- WORKABLE THEORETICAL MODEL
- AREAS OF FURTHER INVESTIGATION
  - PASSBAND SELECTIVITY
- OPTICAL ACTIVITY
- MATERIALS STUDIES
- MATERIALS PRODUCTION (SCALE UP)

.

1

7

#### CHRISTIANSEN-BRAGG FILTERS P Yeh and J Tracy

#### Summary

A new type of narrowband wide field-of-view filter is proposed and analyzed. This filter is made of a periodic layered structure which consists of alternating layers of two dielectric materials such that the dispersion curves of these two media intersect at a desired wavelength  $\lambda_{\rm C}$ . This layered structure is optically homogeneous only to the radiation of wavelength  $\lambda_{\rm C}$ . Other radiation will be reflected provided the thicknesses of the layers are properly chosen. In particular, if the layered structure is made of a chirped quarter-wave stack, this forms a broadband reflector for all wavelengths except those near  $\lambda_{\rm C}$ . A broadband Bragg reflector generally has a wide angular rejection cone. In addition, the transmission of light at  $\lambda_{\rm C}$  is a material property of the layered structure which is independent of the angle of incidence. Therefore a chirped Christiansen-Bragg filter can be a narrowband transmission filter with a large field-of-view. The field-cf-view can, in principle, be as large as  $2\pi$  steradians.

Rockwell International 1049 Camino Dos Rios, PO Box 1085, MS A20 Thousand Oaks CA 91360

#### Rockwell International Science Center

frame brown

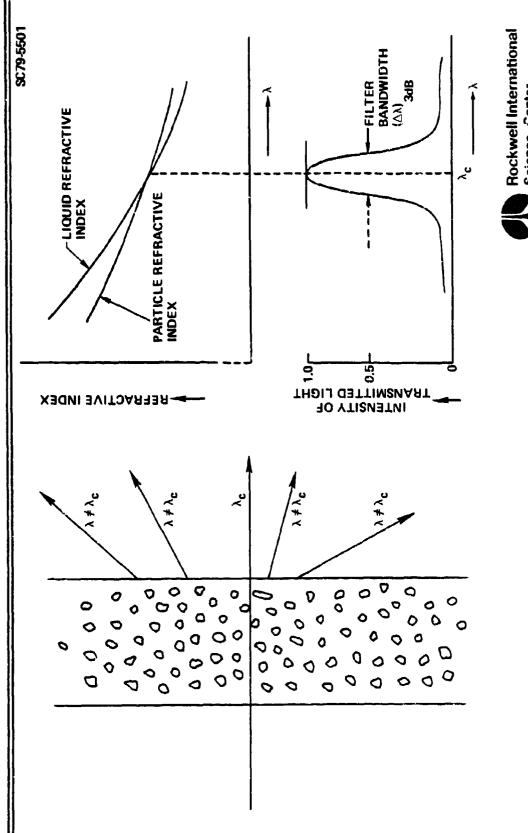
1

I

## **CHRISTIANSEN-BRAGG FILTERS**

- 1. INTRODUCTION
- 2. CHRISTIANSEN FILTERS
- 3. BROADBAND BRAGG REFLECTORS
- 4. CHRISTIANSEN-BRAGG FILTERS
- 5. MATERIALS AND DISCUSSIONS

### CHRISTIANSEN EFFECT





## **BANDWIDTH OF A CHRISTIANSEN FILTER**

Δλ_{0.5}/λ_c OF A CHRISTIANSEN FILTER:

$$T = \exp\left[-KcLa(\Delta n')^2 \left(\frac{\Delta \lambda}{\lambda_c}\right)^2\right]$$
$$\frac{\Delta \lambda_{0.5}}{\lambda_c} = \left(\frac{2.77}{K}\right)^{1/2} \frac{1}{(cLa)^{1/2}} \Delta n'$$

WHERE c = PARTICLE VOLUME PER UNIT VOLUME

 $n_0$  = REFRACTIVE INDEX OF LIQUID

" REFRACTIVE INDEXES OF PARTICLES

L = LENGTH OF CELL

a = AVERAGE PARTICLE SIZE

 $\Delta n' = \frac{d}{d\lambda} (n_0 - n_p)$ 

 $\lambda_c = WAVELENGTH AT WHICH n_0 = n_o$ 

 $\Delta\lambda$  = SHIFT IN WAVELENGTH AWAY FROM  $\lambda_c$ 

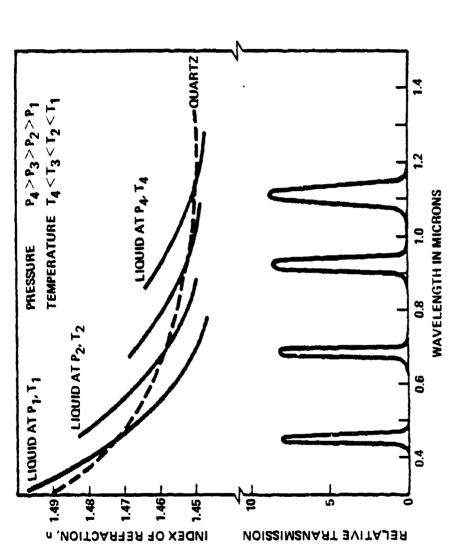
THE CONSTANT K MAY ASSUME A VALUE BETWEEN 8 AND 49, DEPENDING ON THE PARTICULAR MECHANISM FOR SCATTERING ASSUMED.



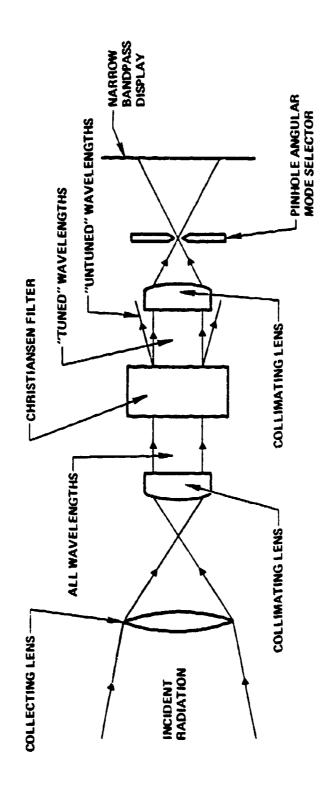
j

# TRANSMISSION CHARACTERISTICS AND SPECTRAL TUNING OF CHRISTIANSEN FILTER

SC 79-5504









•

*

## A BROADBAND BRAGG REFLECTOR

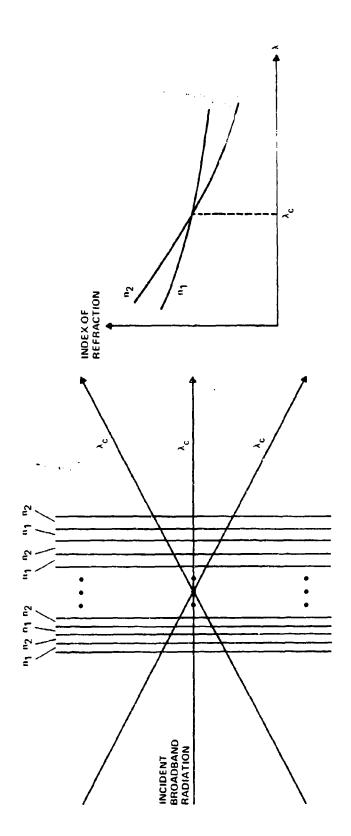
SC78-2000A		
	2 u	λ ₂ 4η ₂
	e [[]	4n ₁
[		•
		•
	<u> </u>	
	2"	
	u u	
	2 _u	A1 4n2
	u ^l	1 1 1 4 1 4 1 1 1 1 1 1 1 1 1 1 1 1 1 1



5.00 REFLECTIVITY OF A BROADBAND BRAGG REFLECTOR SC78-1998A 4.75 4.50 IMIANTEI ENL'TLI INI LINITE DE AALCDAN AIAs/GaAs STACK ~ 100 LAYERS 4.25 4.00 3.50 3.23 3.00 0.9 0.8 0.4 0.7 0.3 0.2 0.1 REFLECTIVITY

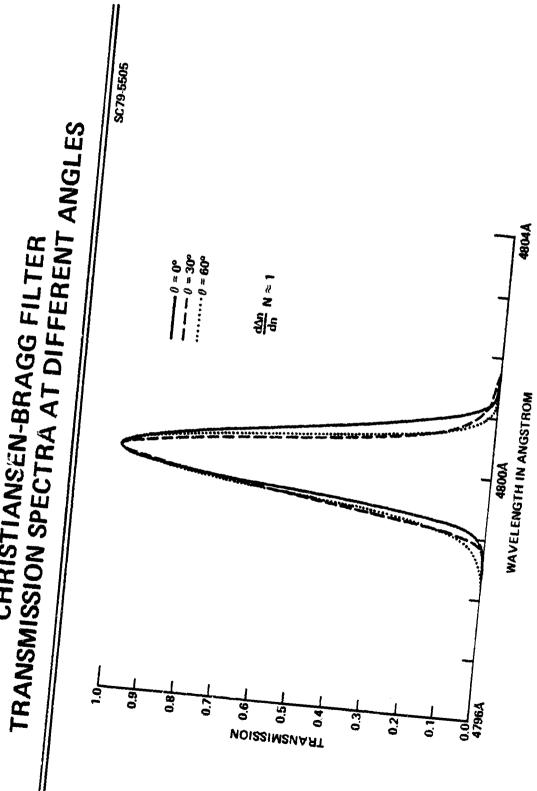
# CHRISTIANSEN-BRAGG FILTER STRUCTURE

SC79-5242





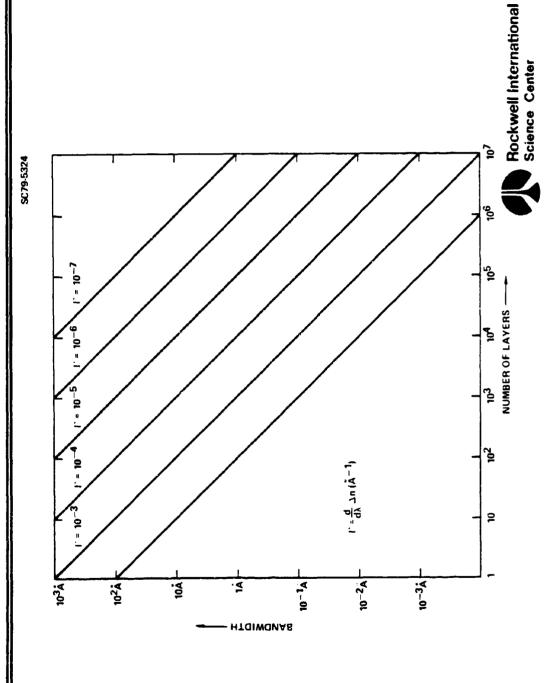
CHRISTIANSEN-BRAGG FILTER



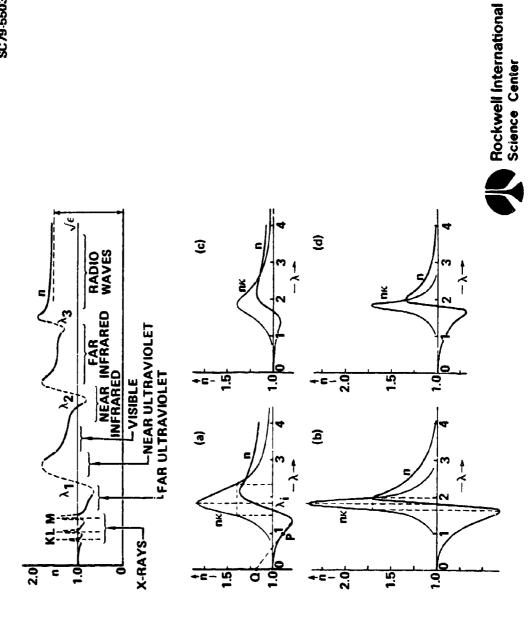


. ...

# BANDWIDTH OF CHRISTIANSEN-BRAGG FILTER



### MATERIAL DISPERSION

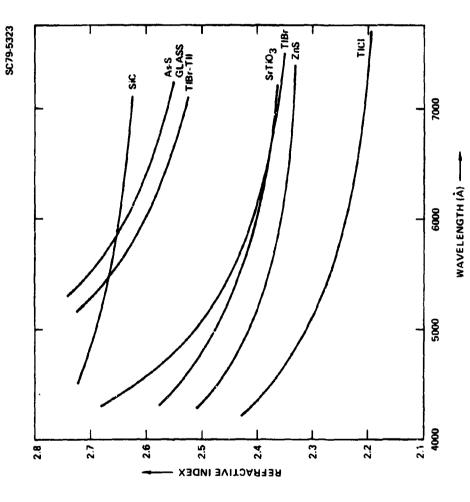


7

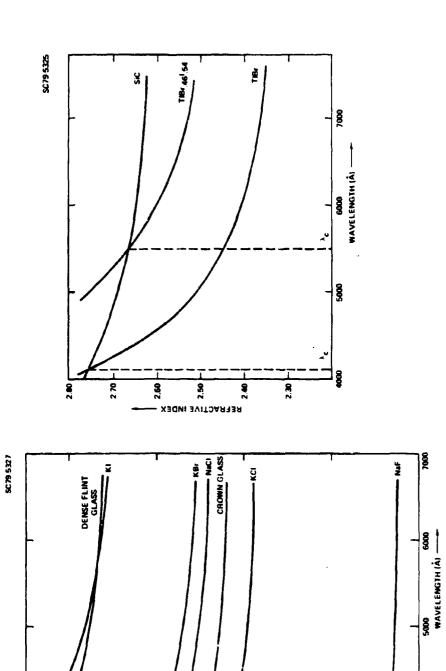
1

### Rockwell International Science Center

### **MEASURED DISPERSION**



### **MEASURED DISPERSION**





1

]

흏

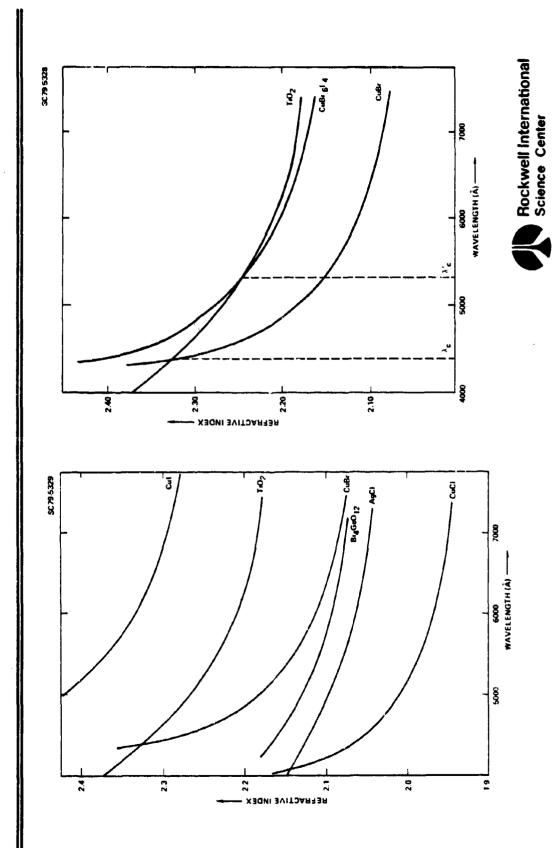
1.6

1.7

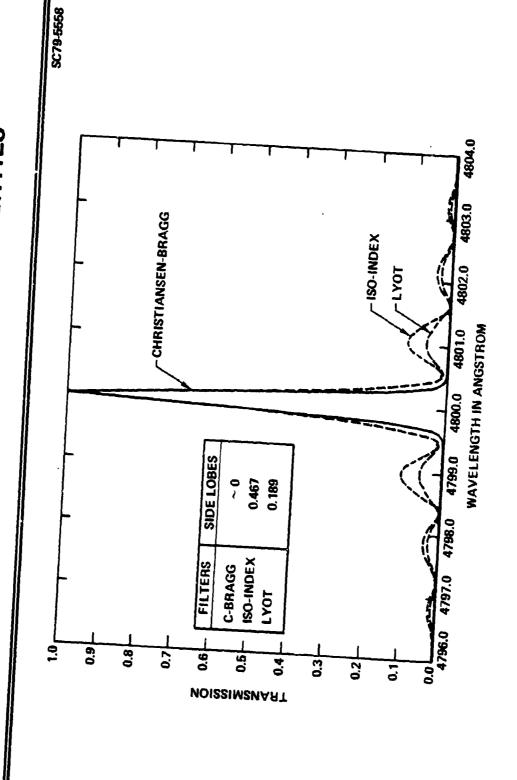
- XERNACTIVE INDEX -

•

### **MEASURED DISPERSION**



# COMPARISON OF OUT-OF-BAND PROPERTIES





1

]

Summary: Thermal Control For Hole-Burning Filter

by R. Rochat and J. E. Jackson

This paper describes the hole-burning filter concept. At this point in time, it is only a concept since no research has been directed to develop material systems exhibiting the required filtering characteristics for the blue-green laser receiver. Conceptually the hole burning-filter possesses most of the characteristics sought for in this application: very narrow bandwidth, hemispherical field of view, unlimited aperture size, potentially high transmission, selectable center bandpass, and high out of band rejection. Conceptually a receiver employing the hole-burning filter would require about 10 dB less laser power than a receiver employing any of the other filter concepts. The research in hole-burning has been directed to memory devices and studies of fundamental material properties at cryogenic temperatures. There are two types of hole-burning: photochemical hole-burning (PHB) and nonphotochemical hole-burning (NPHB). Most all glasses and polymers exhibit NPHB but only about twenty glasses and crystallines have been observed to date that exhibit PHB. PHB is the preferred since a more stable and higher transmission filter could be fabricated. Examples of both NPHB and PHB material systems are given.

A small study has been done to determine the size, weight, and power of the cryogenic system required for the hole-burning filter. The results of this study are included.

McDonnell Douglas Astronautics Corp PO Box 516 St Louis MO 63166

### CRYOGENIC COOLING FEASIBILITY STUDY HOLE BURNING FILTER

R.D. ROCHAT

712000000

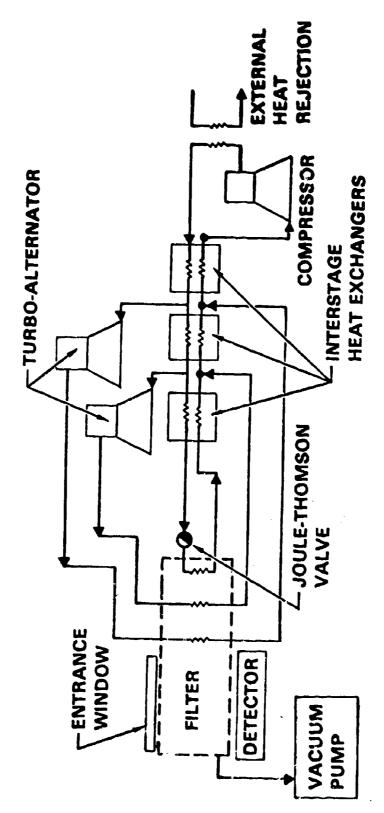
### DESIGN CONDITIONS/CONSTRAINTS

TEMPERATURE = 20°C PRESSURE = 1 ATM LOADS = 6.3 AYES	SIZE = 1 METER DIA.  TRANSMISSION = 50% AT 0.5 $\mu$ m  HEAT LOAD = 0 W (ONLY HEAT LEAV)
	# E

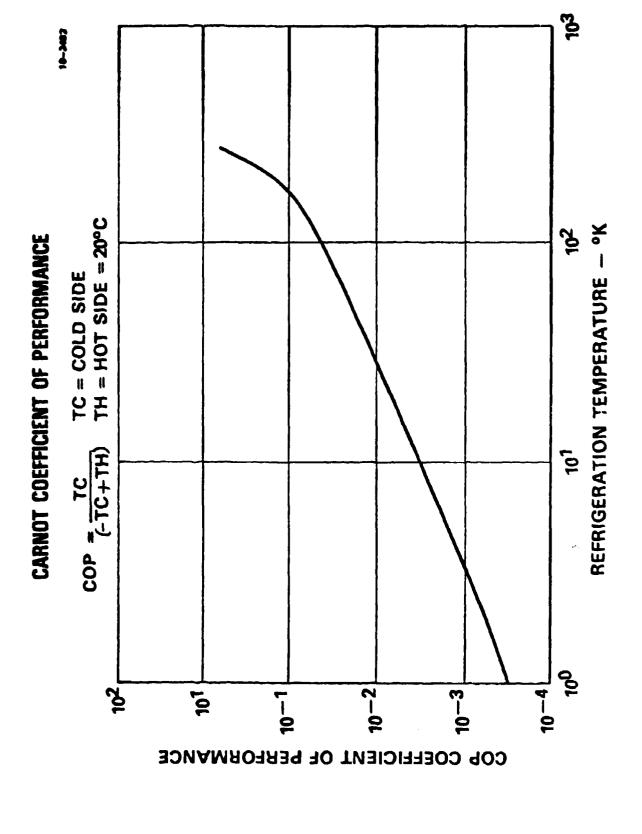
### REFRIGERATION SYSTEM CONCEPT

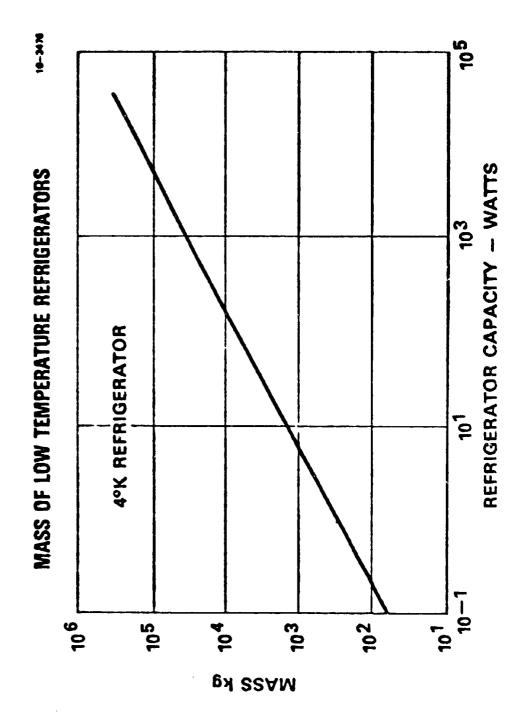
į

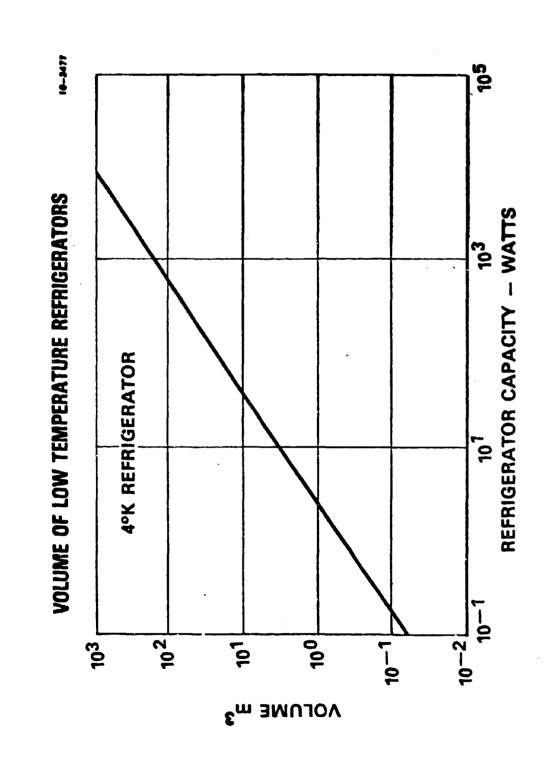
 HELIUM WORKING FLUID • 3 STAGE CLAUDE CYCLE



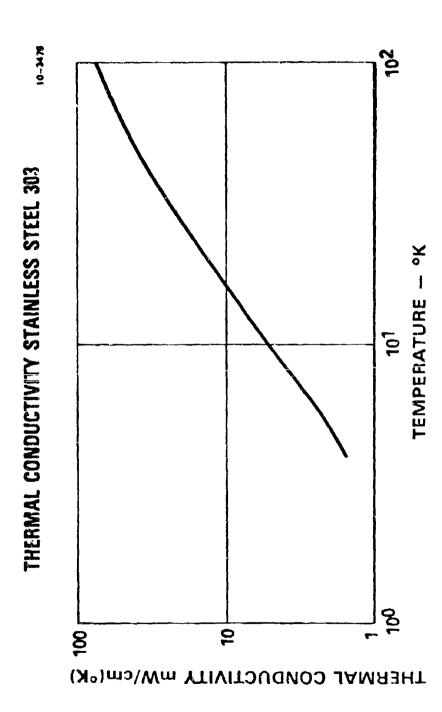
Ī

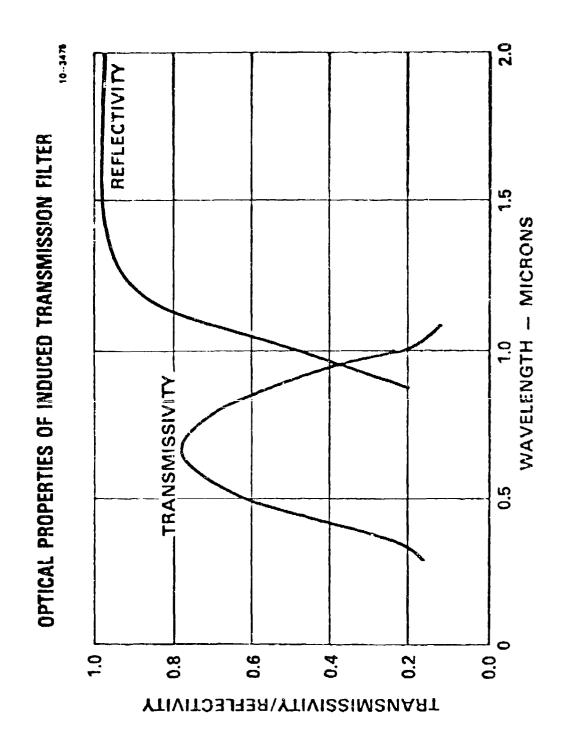


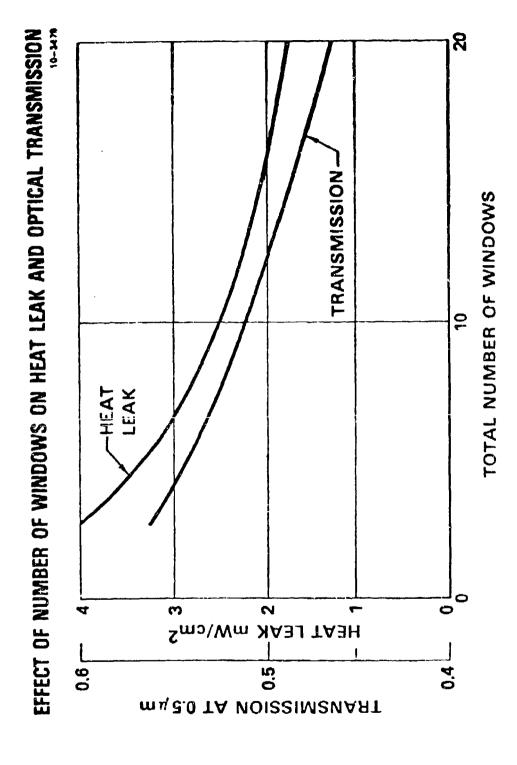




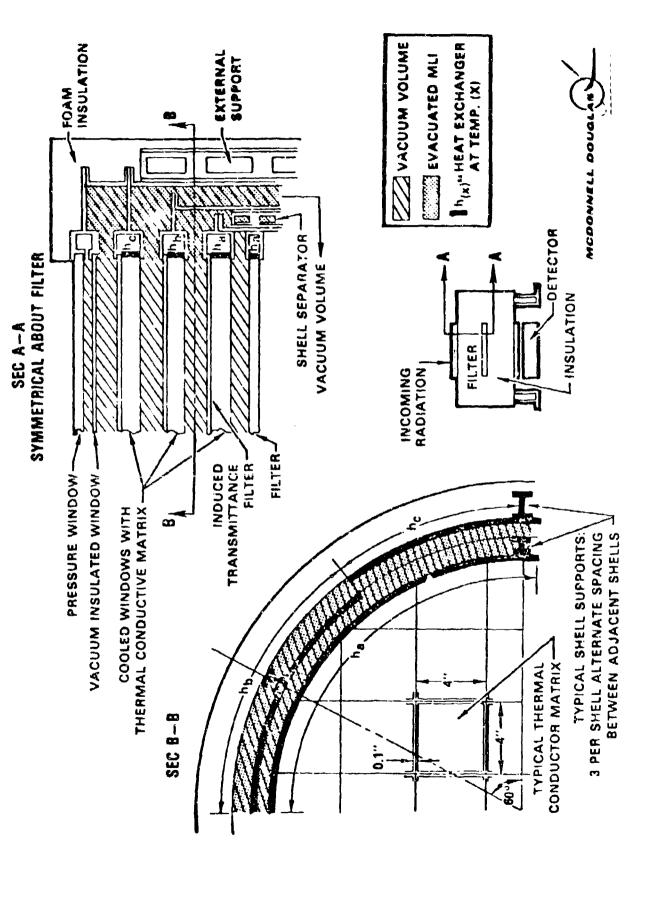
EFFICIENCY OF LOW TEMPERATURE REFRIGERATORS REFRIGERATOR CAPACITY - WATTS 101 102, 100 101 PERCENT CARNOT







### FILTER CONTAINMENT



## FILTER CONTAINMENT THERMAL MODEL

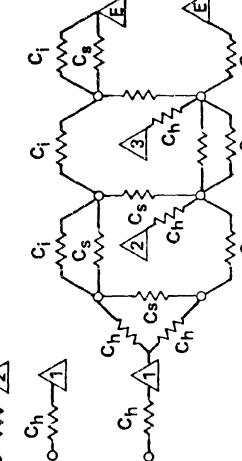
į

### THERMAL NODES



C_k

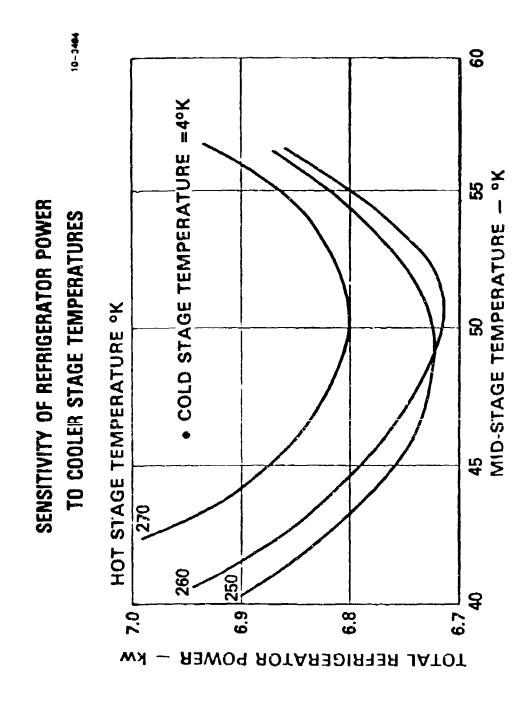
C_v = CONVECTION
C_s = STRUCTURE
C_i = INSULATION
C_i = HEAT EXCHANGER



MCDONNELL BBUBLÁB)

œ Œ œ Ě æ

127

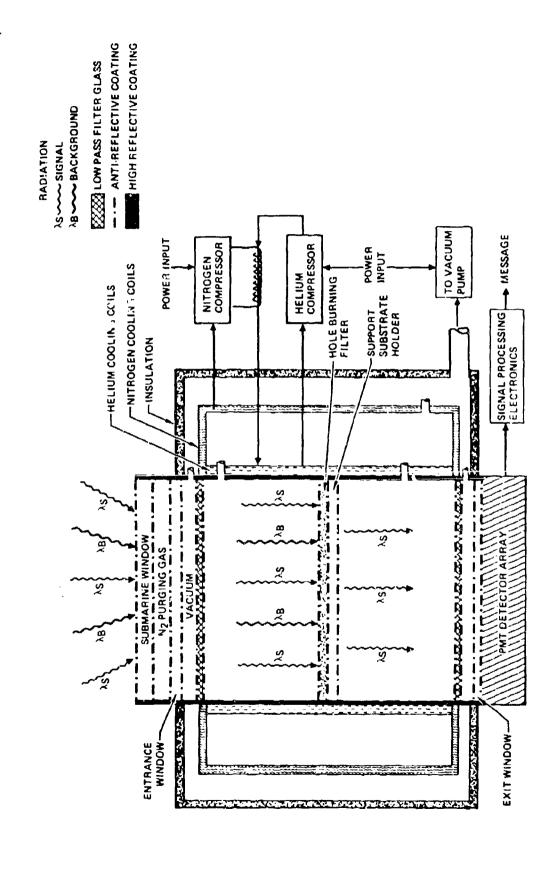


## FILTER CONTAINMENT SUMMARY

HEAT LEAK/POWER SUMMARY

	HEAT LEAK	REFRIGERATOR POWER	<b>ର</b>	CONFIGURATION SUMMARY	SUMMARY	. •	
HEAT SINK	HATTS	MATTS					
Containment Shells				REFRIGERATOR	TOR	CONTAINMENT	ENT.
Cold Stage, 4°K	0.7	950	Power	8x 7.8		•	
Mid Stage, 51°K	22.0	2090	Size	), 4 m ³	~~·	0.8 83	~ <u>.</u>
Hot Stage, 260°K	74.0	155	Weight	860 kg		450 kg	rg C
Optical Windows				•			
Cold Stage, 4°K	2.2	3010	!		WE IGHT	WEIGHT & TRIDERT WEIGHT	X TRIDEIT SAIL WEIGHT
Hid Stage, 260°K	2.0	S	Hole Burning Filter Refrigerator and	19 Filter or and	1310	₹0.,	5.2
TOTAL	106.1	6700	Containment				
			Birefringement	Birefringement Filter	320	4,003	1,3

## HOLE BURNING FILTER RECEIVER CONCEPT



## HOLE BURNING FILTER CHARACTERISTICS

- VERY NARROW BANDWIDTH (CUSTOMIZING) < 10⁻³ Å POSSIBLE
- ANGLE OF INCIDENCE INDEPENDENCE
- NOT APERTURE SIZE LIMITED
- TRANSMISSION
- SHOULD IN PRINCIPLE BE VERY HIGH
- HAVE OBSERVED UP TO 50% IN SOME SAMPLES
- CENTER BANDPASS IS SELECTABLE

131

- NO TIME DISPERSION
- HIGH OUT-OF-BAND REJECTION
- LIFETIME
- MAY REUIRE IN SITU RENEWING DUE TO BLEACHING
- NOISE MECHANISMS
  - FLUORESCENCE
- OTHERS

UNCLASSIFIED

MCDONNELL DOUGLAS ASTRONAUTICS COMPANY-ST. LOUIS DIVISION

FILTER-RECEIVER CONCEPT COMPARISONS

10-3519

	Į
	Ì
	1
	ı
	١
	ı
	1
	1
	ı
	ł
!	
:	
,	
:	İ
) i	ļ
i	
)	

PERFORMANCE	AR	ARAF	BIREFRINGENT	GENT	HOLE BURNING FILTER	#ING
WAVELENGTH (A)	4255	ŧ	5183.6	<b>9</b> 9	5183.6	88
TRANSMISSION WINDOW. WATER INTERFACE TO PMT ARRAY (%)	31.8	-2.49	25.2*	-2.99	35	-2.28
FIELD OF VIEW IN WATER (DEGREES)	6 <b>V</b> 7	O	±1.64"	-12.96	449	o
TIME SPREAD (JSEC)	32.1	-0.136	G	0	0	0
PMT QUANTUM EFFICIENCY (%)	7.8	-5.54	15.7	-4.02	15.7	-4.02
RELATIVE TYPE 111 WATER TRANSMISSION (%/m)	87.83	-2.70	83	0	68	0
RELATIVE SOURCE IRRADIANCE (WATTS .m-2 .u-1)	1046.7	-5.43	(.07)*1200 (FRAUNHOFER)	0	(.07)*1200 (FRAUNHOFER)	0
BACKGROUND BANDPASS (A)	90.0	6.11	0.1•	5.00	0.1	10
SIGNAL BANDPASS (A)	G.006	0	0.1*	0	0.01	0
OUT OF BAND REJECTION RADIO	9-01	Ú	.9-01	0	9-0-	a
FILTER RELATED NOISE	10-4	0	1	0	_	0
RELATIVE TOTAL SIGNAL POWER DIFFERENCES (48)		-9.41		-13.67		0

* DR. A TITLE OF LOCKHEED (PRIVATE COMMUNICATIONS) ESTIMATE OF EXPECTED PERFORMANCE.

### HISTORY: HOLE BURNING FILTER

- FIRST PROPOSED BY RUSSIANS OPT. SPECTROSC. VOL 39 PAGE 140, AUGUST 1975
- ullet U. S. BEGAN HOLE BURNING RESEARCH  $\sim$  1976
- 1BM
- EASTMAN
- -- AMES LABORATORY, IOWA STATE UNIVERSITY

MCDONNELL DOUGLAS ASTRONAUTICS COMPANY-ST. LOUIS DIVISION

### UNCLASSIFIED

### HOLE BURNING FILTER TYPES

PHOTOCHEMICAL

- IBM

**EASTMAN KODAK** 

MEMORY DEVICE RESEARCH

(PHOTO PHYSICAL)

NONPHOTOCHEMICAL

- AMES LABORATORY: STUDIES OF MATERIAL PROPERTIES AT CRYOGENIC TEMPERATURES

## MATERIAL SYSTEMS UNDERGOING NPHB AND PHB

10-4362

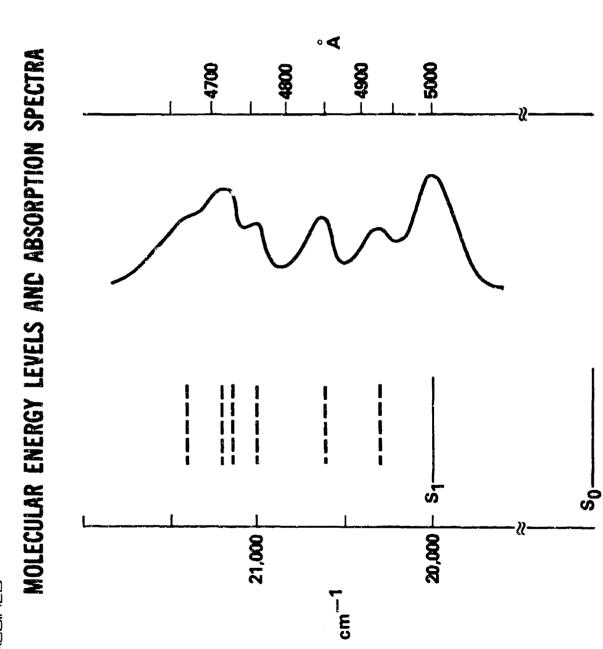
### NPHB

- INORGANIC GLASSES
- ORGANIC GLASSES
- POLYMERS

### PHB

- LESS THAN 20 HAVE BEEN INVESTIGATED
- GLASSES
- CRYSTALLINES

10-4279

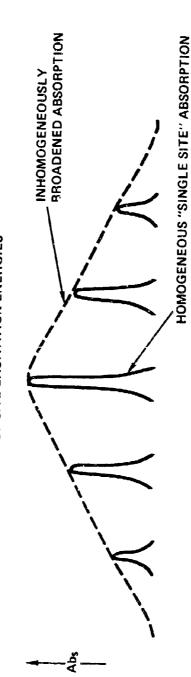


a) HOMOGENEOUS:

LIFETIME  $< 10^{-1}\,\mathrm{cm}^{-1}$ 

b) INHOMOGENEOUS:

AMORPHOUS STRUCTURE YIELDS STATISTICAL VERY LARGE (~ 200 cm-1) DISTRIBUTION DISTRIBUTION OF IMPURITY SITES WITH OF SITE EXCITATION ENERGIES



NARROWBAND SOURCES (LASERS) CAN PROBE "SINGLE SITE" PROCESSES AT LOW TEMPERATURES (<10K) WHERE SITE INTERCHANGE IS SLOW,

A, + h, -- A*

"SINGLE SITE" ABSORPTION

 $A_{\nu}^{*}$   $\longrightarrow$   $A_{\nu} + h_{\nu}$ 

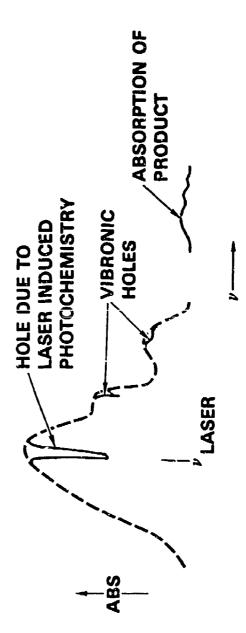
"SINGLE SITE" FLUORESCENCE

BROADENED ABSORPTION AT THE FREQUENCY, v., I.E., A HOLE IF, DURING THE LIFETIME OF THE STATE A*, THERE IS SOME PROCESS WHICH PREVENTS RETURN OF A* TO THE STATE A_ν, THEN A GAP WILL APPEAR IN THE INHÖMOGENEOUSLY WILL BE BURNT AT ».

### PHOTOCHEMICAL HOLE BURNING

10-4374

SINGLE SITE ABSORPTION B* PHOTO REARRANGEMENT ► B_p' PRODUCT FLUORESCENCE ·B* SOLVENT ADDITION Ry + hr - A" S A* + ## | | *****^ OR



## NON-PHOTOCHEMICAL HOLE BURNING

10-4372

 $A_v + h^v - A_v^*$ 

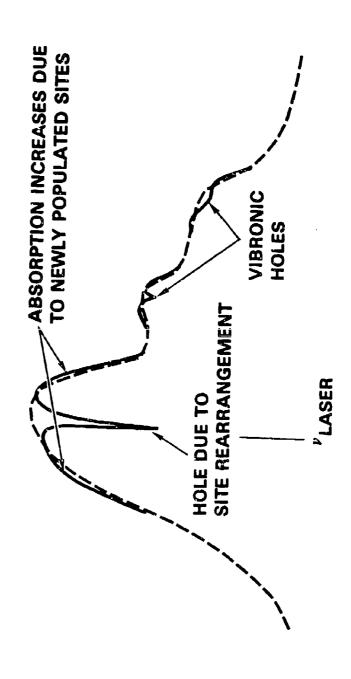
SINGLE SITE ABSORPTION

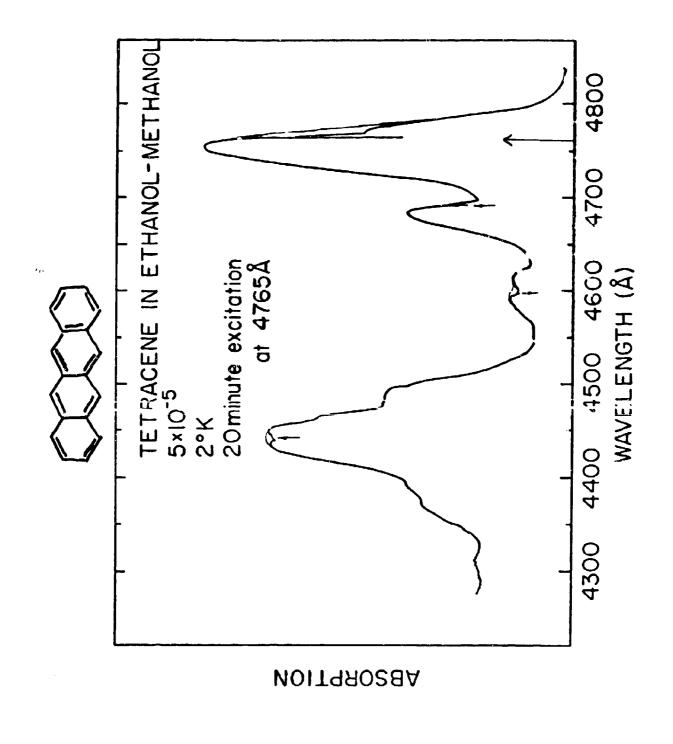
A" A".

SITE REARRANGEMENT

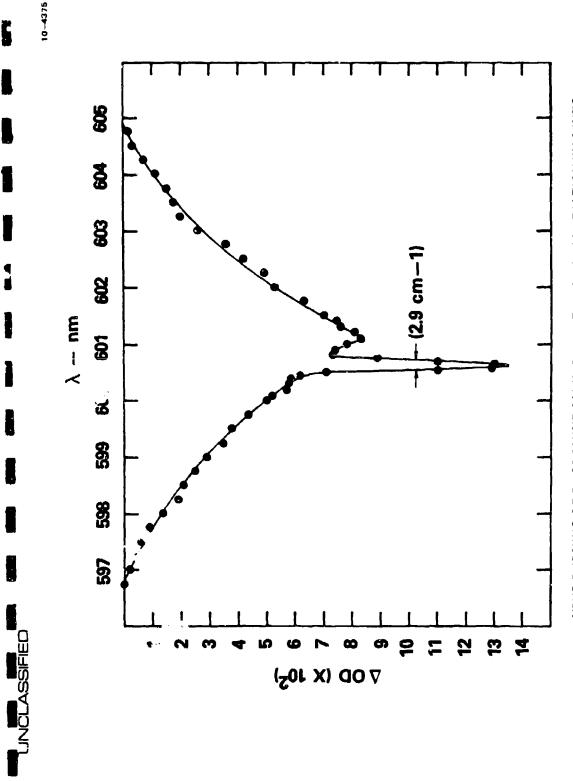
A* + h, + h,

NEW SITE FLUORESCENCE





MCDOWNELL DOUGLAS ASTRONAUTICS COMPANY-ST.LOUIS DIVISION



COINCIDENT WITH  $\nu_B$ .  $\Delta OD$  DENOTES THE CHANGE IN OPTICAL DENSITY PRODUCED BY BURNING. 0-0 BAND OF R640'S ABSORPTION SPECTRUM. THE SHARP DIP (2 9 cm-1 WIDE) IS NPHB BURNING OF RHODAMINE 640 IN FMMA, TB = 4.2K. IRRADIATION WAS INTO

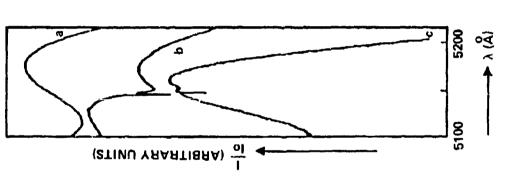
PHONON STATES OF THE GLASS. IB > REPRESENTS AN INTERMEDIATE STATE IN THE PHOTOCHEMICAL REACTION SCHEME.  $\delta_0$  AND  $\delta_1$  ARE REACTION BARRIERS THE ENERGY LEVEL SCHEME FOR QUINIZARIN (R) AND ITS PHOTOPRODUCT (P). SUPERIMPOSED ON THE ELECTRONIC AND VIBRATIONAL STATES (
u) ARE THE IN THE GROUND AND EXCITED STATE ENERGY SURFACE.

UNCLASSIFIED

MCDONNELL DOUGLAS ASTRONAUTICS COMPANY-ST. LOUIS DIVISION

. 4

]





GLASS (3:1). B) AFTER 20 MINUTE EXPOSURE TO THE RADIATION OF AN Ar ION LASER C) AFTER 5 MINUTE EXPOSURE TO THE RADIATION OF A X+HIGH PRESSURE LAMP

(75W, TRACE c iS ON & DIFFERENT SCALE).

UNCLASSIFIED

DOUGLAS ASTRONAUTICS COMPANY-ST. LOLIS DIVISION

3:1 MIXTURE OF ETOH AND MEOH (2°K), PRODUCED BY 15 MINUTE IRRADIATION, WITH PHOTOCHEMICAL HOLE IN THE FIRST SINGLET ABSORPTION OF QUINIZARIN IN A AN Ar ION LASER (3mW). THE BANDPASS OF THE SPECTROMETER WAS 0.66 cm-1.

UNCLASSIFIED

DATE

HUGHES AIRCRAFT COMPANY RESEARCH LABORATORIES

# NON LINEAR OPTICAL PHASE CONJUGATION FOR SLC UPLINK

#### C R GIULIANO

Hughes Research Laboratory 3011 Malibu Canyon Road Malibu CA 90265

REGEARCH LABORATORIES

# **ELEMENTS OF PRESENTATION**

## WHAT IS PHASE CONJUGATION?

- HOW CAN IT BE USED?
- HOW DO WE MAKE CONJUGATORS?
- WHERE DO WE STAND?
- WHAT'S LEFT TO BE DONE

### BACKGROUND

HUGHES AIRCOAFT COMPANY RESEARCH LABORATORIES HUGHES

	USA	USSR
		AREAS OF ACTIVITY
	72	RAPIDLY EXPANDING ACTIVITY OVER 100 PUBLICATIONS SINCE 1972
(1979)		AFOSR SUPPORT
(1978)		DOE/LASL SUPPORT
(1977)		DARPA/ONR SUPPORT
(1976)	I HRL	EXPERIMENTAL DEMONSTRATION AT HRL
(1974)	REAL-TIME HOLOGRAPHIC CONJUGATION AT HRL	CONCEPT FOR REAL-TIME HOLOGRAF
(1974)	OF CONCEPT FOR LASER APPLICATIONS AT HRL	DEVELOPMENT OF CONCEPT FOR LAS
9473-3 (1972)	t al; STEPANOV, et al.)	EARLY SOVIET WORK (ZELDOVICH, et al; STEPANOV, et al.)

AFWL/U. ARIZONA

BELL LABS

INSTITUTE FOR RADIOPHYSICS **USSR ACADEMY OF SCIENCES** 

- 大学学生の大学学生

MOSCOW UNIVERSITY LEBEDEV INSTITUTE

**UKRANIAN SSR** 

nsc

LASL

CAL TECH HUGHES

UNCLASSIFIED

HUGHES PRESENTATION ----

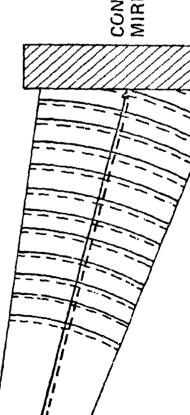
HUGHES

8703-5

RESEARCH LABORATORIES

ORDINARY MIRROR

ORDINARY MIRROR AND CONJUGATE MIRROR



CONJUGATE

HUGHES THEST

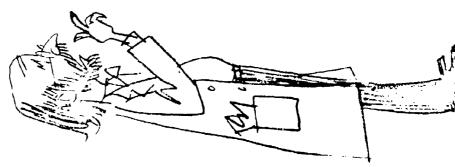
HUGHES AIRCHAFT COMPANY REQUESTER ORIGINATOR

HUGHES AIRCRAFT COMPANY RESEARCH LABORATORIES

HUGHES

CONJUGATOR, CONJUGATOR, ON THE WALL....





UNCLASSIFIED

PRESENTATION

HUGHES

MUGHES AIRCRAFT COMPANY REQUESIER ORIGINATOR _____

DATE

## WHAT DO YOU SEE IN A CONJUGATE MIRROR?

HUGHES

HUGHES

HUGHES

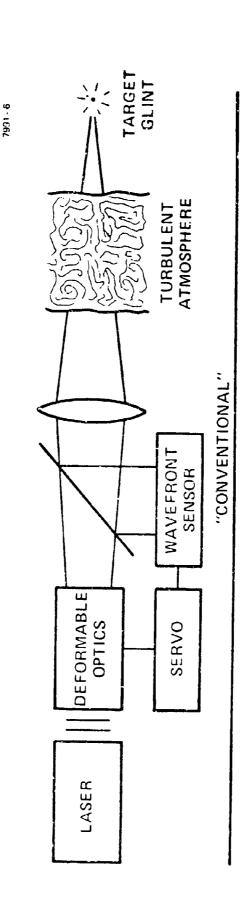
HESERRCH LABORATORIES

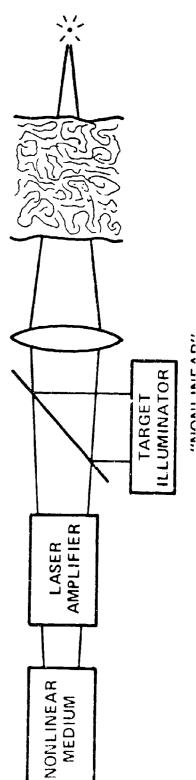
686-23

- A. YOUR IMAGE
- B. YOUR IMAGE, INVERTED
- YOUR IMAGE, TIME-REVERSED (i.e., YOUNGER) ပ
- D. YOUR IMAGE, ABERRATION-FREE
- E. THE BACK OF YOUR HEAD
- F. YOUR INNER SELF
- G. TOTAL BLACKNESS
- H. NONE OF THE ABOVE

PRESENTATION

HUGHES AIRCRAFT COMPANY REQUESTER/ORIGINATOR





WRICALI IAIF A DV

HULHES A HET TOWN TO THE OUESTER ORIGINATOR ...

۷۵ -----

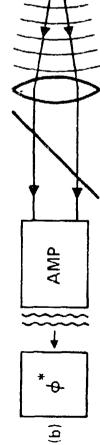
HUGHES

7162 . 2R1

RESEARCH LABORATORIES

BASIC NONLINEAR PHASE CONJUGATION SCHEME

ILLUMINATOR CONJUGATOR AMPLIFIER ILLUMINATION AMP



REFLECTED DISTORTED WAVEFRONT



(C)







PRESENTATION ...

HUGHES AIRCRAFT COMPANY REQUESTER ORIGINATOR

- DATE

LASER UPLINK USING PHASE CONJUGATION

HUGHES

HUGHES AIRCRAFT COMPANY

9630-1

* ILLUMINATOR AMP CONJUGATOR PHA.SE **ATMOSPHERE** AMP BEACON

**ORBITING RETRO** 

ORBITING BEACON

DATE

HUGHES

HUGHES AIRCRAFT COMPANY

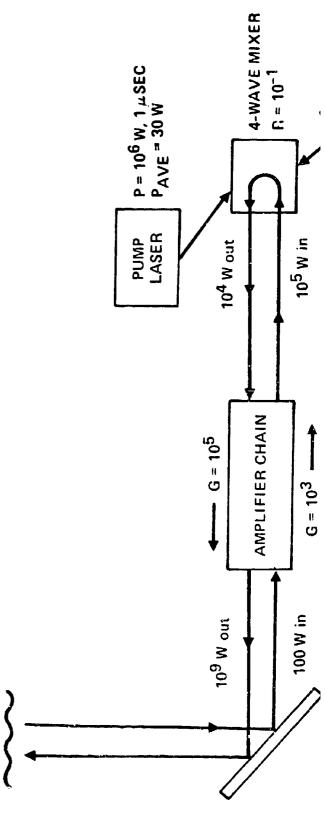
9473-1

# CANDIDATE UPLINK SYSTEM CONCEPT

 $5 \text{ kW } 1 \mu \text{ SEC PULSES}$  (PAVE = 150 mW)

ORBITING LASER BEACON

PATH EFFICIENCY (0.02)



MUCHES ANGENTITY COMPANY REQUESTER ORIGINATOR _______

( !

## NONLINEAR vs CONVENTIONAL ADAPTIVE OPTICS

#### HUGHES

HUGHES AIRCRAFT COMPANY RESEARCH LABORATORIES

#### **ADVANTAGES**

SIMPLICITY (NO MOVING PARTS, NO ACTUATORS, NO WAVEFRONT SENSORS, NO SERVOS)

SUPERIOR CORRECTION OF HIGH SPATIAL FREQUENCIES (SUBAPERTURE ORDER OF WAVELENGTH)

HIGH SPEED OF RESPONSE

MULTIPLE WAVELENGTH OPERATION

### CONSTRAINTS

- NEED BRIGHT REFERENCE AND/OR HIGH GAIN AMPLIFIERS
- NEED TO OVERRIDE CONJUGATOR IF POINTING (OR FOCUS) ADJUSTMENT IS REQUIRED
- MAY NEED TO PROVIDE SEPARATE LASER PUMPS
- MAY NEED TO COMPENSATE FOR DOPPLER SHIFTS
- NOT YET DEMONSTRATED AT HIGH AVERAGE POWER

PRESPONDED

# CANDIDATE NONLINEAR PHENOMENA

MUCHES AIRCRAFF COMPANY HUGHES

9473-4

STIMULATED BRILLOUIN SCATTERING, SBS

DEGENERATE FOUR-WAVE MIXING, DFWM

***

DATE ___

## STIMULATED BRILLOUIN SCATTERING-SBS

HUGHES

HUGHES AIRCRAFT COMPANY RESEARCH LABORATORIES

9392-66

INCIDENT WAVE BACKSCATTERS INTO STOKES WAVE

• PROCESS

INPUT WAVE  $\omega_1$ ,  $k_1$  (PHOTON)

ω_s, k_s (PHONON)

 $\omega_2$ ,  $k_2$  (PHOTON)

OUTPUT WAVE ←

 $\omega_2 + \omega_s = \omega_1$ 

k2+k3=k1

ACOUSTIC WAVE

FOR COLLINEAR GEOMETRY

 $|k_1| = |k_2| = 1/2 |k_s|$ 

 $\frac{\omega_s}{\omega_1} = \frac{\omega_1 - \omega_2}{\omega_1} = \frac{V_s}{c} \sim 10^{-5} \text{ (TYPICALLY)}$ 

SBS MEDIUM AUTOMATICALLY ACTS AS A PHASE CONJUGATE REFLECTOR BULK MATERIALS, CAN BE MUCH LESS IN WAVEGUIDE CONFIGURATIONS) WHEN SBS THRESHOLD IS EXCEEDED (THRESHOLD  $\sim$  10 - 500 Mw/cm² IN

OVER 90% OF BACKSCATTERED WAVE IS THE CONJUGATE OF THE INPUT WAVE

JANUARY 1980

President National Contra

6282-4 R1

DISTORTING

INCIDENT

HUGHES

PHASE CONJUGATION VIA SBS

ORDINARY MIRROR

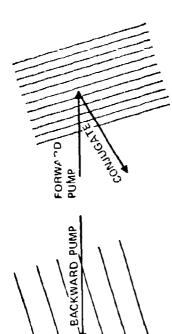
SBS MIRROR SOUND

REFLECTED WAVES

MUGHEST AND COMPANY REQUESTER ORIGINATOR

FORMATION BACKWARD PUMP

READOUT



CONTUCATE

GRATING SPACING D =  $\lambda$  /2 SIN  $\theta$ /2

FEBRUARY 1980

HUGHES

HUGHES AIRCRAFT COMPANY RESEARCH LABORATORIES FOUR-WAVE MIXING/ DUAL GRATING PICTURE

FORWARD PUMP

PACIFIE .

13 A T E

I

Y STORY AND A

# INDUCED POLARIZATION FOR 4 WAVE MIXING

#### HUGHES

HUGHES AIRCHART COMPANY RESEARCH LABORATORIES

8703-6

 $\vec{P} = A(\theta) [\vec{E}_f \cdot \vec{E}_p^*] \vec{E}_b + A(\pi - \theta) [\vec{E}_b \cdot \vec{E}_p^*] \cdot \vec{E}_f$ 

 $+B[\bar{E}_{f}\cdot\bar{E}_{b}]\bar{E}_{p}^{*}$ 

 $\theta$  = ANGLE BETWEEN PUMP AND PROBE  $\overline{E_f}$  = FORWARD PUMP FIELD

 $\vec{E}_{\mathbf{b}} = \mathsf{BACKWARD} \; \mathsf{PUMP} \; \mathsf{FIELD}$   $\vec{E}_{\mathbf{p}} = \mathsf{PROBE} \; \mathsf{FIELD}$ 

TOGALS THE COUNTY REQUESTER ORIGINATION

DATE

# COMPARISON OF NONLINEAR EFFECTS FOR PHASE CONJUGATION

HUGHES

HUSHES ANGRAFT CONFAY

8703-2

#### **SBS AND SRS**

### HIGH EFFICIENCY POSSIBLE (UP TO 99%)

161

## THRESHOLD REQUIREMENT

## NO SEPARATE PUMPS REQUIRED

## OCCURS WITH FREQUENCY SHIFT

## **GENERATES RETRO BEAM ONLY**

### INPUT AND OUTPUT POLARIZATIONS **ARE THE SAME**

### FOUR-WAVE MIXING

### GREATER THAN UNITY EFFICIENCY WITH RESONANT ENHANCEMENT

### NO THRESHOLD

## REQUIRES SEPARATE PUMPS

## BEAM ANGLE MAY BE VARIED ABOUT RETRO DIRECTION

#### **OUTPUT POLARIZATION CAN BE VARIED** RELATIVE TO INPUT BY PROPER CHOICE **OF PARAMETERS**

## ONGOING HRL ACTIVITIES

HUGHES

HUGHES AIRCRAFT COMPANY RESEARCH LABGRATORIES

#### DARPA/ONR

SBS AND FOUR-WAVE MIXING IN THE VISIBLE (BLUE-GREEN, RUBY)

MULTIFREQUENCY PHASE CONJUGATION

EXPERIMENT, THEORY, SYSTEMS APPLICATIONS

#### DOE/LASL

lacktriangle FOUR-WAVE MIXING AT 10.6  $\mu$  m

▶ RESONANT ENHANCEMENT, MULTI-LINE CONJUGATION

#### -R&L

HIGH EFFICIENCY CONJUGATORS (VISIBLE, 1.06  $\mu$ m, 10.6  $\mu$ m)

THEORY OF RESONATORS WITH CONJUGATE "MIRRORS"

PICOSECOND PHASE CONJUGATION

NEW APPLICATIONS CONCEPTS

#### AFOSR

PHASE CONJUGATE OPTICAL RESONATORS

EXPERIMENTAL DEMO OF LOW POWER PULSED PHASE CONJUGATE RESONATOR

FOUR-WAVE MIXING IN SODIUM VAPOR

DYE AMPLIFIER

# **ISSUES ADDRESSED ON THIS PROGRAM**

#### HUGHES

HUGHES AIRCRAFT COMPANY

392-100

- WHAT SORT OF CONJUGATE EFFICIENCIES CAN WE GET?
- NEW MATERIALS, RESONANT ENHANCEMENT, FURTHER THEORETICAL DEVELOPMENT, EXPERIMENTAL OPTIMIZATION
- HOW GOOD IS THE CONJUGATION CORRECTION?

DETAILED FAR-FIELD MEASUREMENTS

- WHAT ARE THE CONSTRAINTS ON THE PROCESS?
- ANGULAR MISALIGNMENT, FREQUENCY SHIFTS, PUMP ABERRATIONS, COHERENCE EFFECTS
- HOW CAN WE EXPLOIT THE CONSTRAINTS?
- POINT AHEAD, DOPPLER COMPENSATION, FOCUS OVERRIDE, POLARIZATION ROTATION
- HOW DOES IT APPLY TO DARPA NEEDS?
- UPLINK SYSTEM CONCEPTS, BEACON VS RETRO REFERENCE, GAIN AND EFFICIENCY REQUIREMENTS

PRESENTATION .....

MUGHES ANGERST COMPANY REQUESTER ORIGINATOR

HUGHES

HUGHES AIRCRAFT COMPANY

9392-12

### DFWM PHASE CONJUGATION-FAR FIELD PHOTOGRAPHS

ABERRATED INPUT SIGNAL

CORRECTED SIGNAL

LASER SIGNAL INPUT

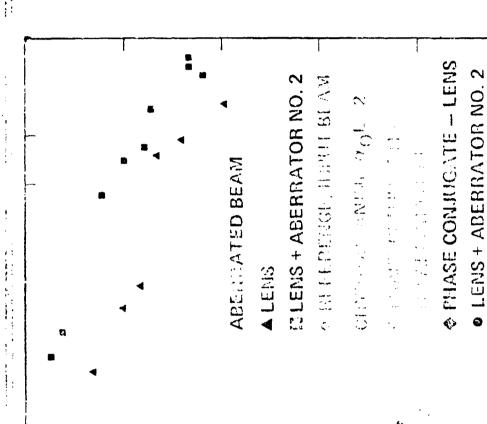
164

### HUGHES PRESENTATION

REQUESTED OBIGINATOR

## INTERSTA PROFILES





10-3

10.5

10-4

10-5

INTENSITY, ARBITARY UNITS

 $10^{-1}$ 

PRESENTATION

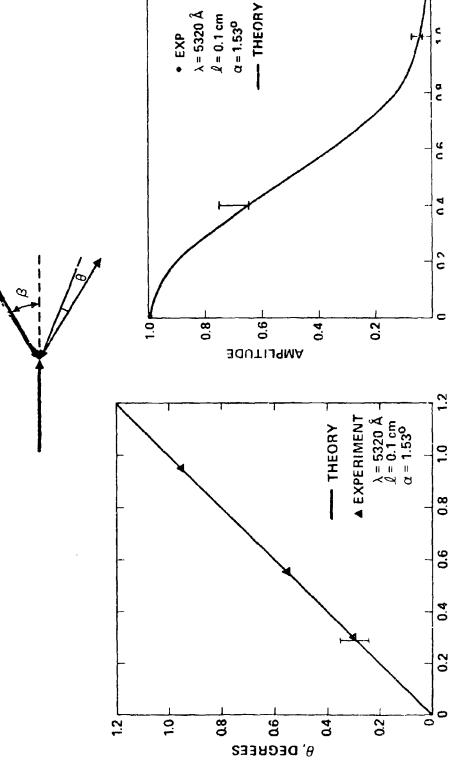
HUGHES AINTERNIT COMPANY REQUESTER ORIGINATION

- DATE

# POINT AHEAD CAPABILITY WITH DFWM

HUGHES AIRCRAFT COMMANDRIES

NONCOLLINEAR PUMP GEOMETRY CAN PROVIDE MODERATE POINT AHEAD



DATE

HUGHES

PRESENTATION -

HUGHES AIRCRAFT COMPANY REQUESTER ORIGINATOR

SEPARATE CONTROL OF THE CONJUGATE WAVE THE USE OF POLARIZATION IN D4WM FOR

HUGHES
HUGHES ARCHATT CONTANT
RESEARCH LABORATORIES

8686-21

(REFERENCE) CONJUGATE PROBE CONTROL FOCUS CONTROL 4-WAVE MIXER anna

HUGHES AINCRAFT COMPANY RESEARCH LABORATORIES

9392-71

WHAT'S BEEN DONE

WAVELENGTH	LASER	PULSED OR CW	NONLINEAR INTERACTION	NONLINEAR MEDIUM	COMMENTS
10 km	200	PULSED	DFWM DFWM DFWM DFWM	SF6* HgcdTe* CO2 (INVERTED) Ge NH3*	37%, 200 kW/cm ² , 2 cm 10%, 100 kW/cm ² , 0.5 mm 0.5% 25%, 10 MW/cm ² , 15 cm ~1% (PRELIM)
3.8µm	DF	PULSED	DFWM	Ge Ge	
1.06µm	Nd: YAG	PULSED	DFWM SBS DFWM 3 WM	Sı* CS <b>2</b> , CH4* Nd: YAĞ Li FORMATE	180%, 1 mm, 6 MW/cm ² 10 - 90% ~0.5% POOR CORRECTION
0.69 µm	RUBY	PULSED	SBS SBS DFWM DFWM DFWM	CS2* CH4 CRYPTOCYANINE* CdS CdSe GLASS* CS2	10 - 90% 30% (PRELIM) ~ 5% >100%, 40 cm
5890Å	DVE	CW PULSED	DFWM DFWM	Na* Na	17%, NARROW BAND 10 ⁴ %, NARROW BAND
5320Å	DOUBLED Nd: YAG	PULSED	DFWM DFWM DFWM DFWM	CdS, CdSe GLASSES* IODINE VAPOR* RHODAMINE 6G* RHODAMINE B*	~30% ~0.1% (PRELIM) >100%, 1 nnm ~10% (PRELIM) (ALSO 5650Å)
5100Å	DYE	PULSED	DFWM	CdS, CdSe GLASS*	~1% (PRELIM)
4880Å, 5145Å	Ārၞ	ω	DEWM OFWM DEWM	RUBY BSO BaTiO ₃ LIQUID CRYSTALS*	~ 0.2% ~ 1% SLOW ~ 25% SLOW ~ 0.1% SLOW

HRI TK

HIGHES ATH THE COMPANY REQUESTER ORIGINATOR ....

DATE

## PERFORMANCE OF PHASE CONJUGATE RESONATOR MODEL FOR DIFFERENT FRESNEL NUMBERS

HUGHES

HUGHES AIRCRAFT COMPANY RESEARCH LABORATORIES

9392-55 R1

OUTPUT CONJUGATOR MIRROR

OUTPUT WAVE PHASE

N = 15/7

N = 15/7

N = 15/7

DISTANCE

3.2 ABERRATOR PHASE

3.2
0
0
-1.6 -0.8 0 0.8 1.6
DISTANCE

MIRROR QUALITY - NOT ON INTRACAVITY DISTORTIONS PHASE OF OUTPUT WAVE DEPENDS ONLY ON OUTPUT **KEY RESULT:** 

HUGHES AINCHAIL COMPANY REQUESTER ORIGINATOR

## REMAINING ISSUES

HUGHES

HUGHES AIRCRAFT COMFANY

### TECHNOLOGICAL

# CHOICE OF MATERIAL FOR SPECIFIC APPLICATION

- SPECIFIC WAVELENGTH(S) OF OPERATION
- **TEMPORAL AND SPECTRAL BANDWIDTH**
- EFFICIENCY (CONJUGATE WAVE REFLECTIVITY)
- POWER HANDLING CAPABILITIES/PHYSICAL SIZE
- COMPETING NONLINEAR EFFECTS AT HIGH AVERAGE/PEAK POWER

#### SYSTEMS

- MOPA OR INTRACAVITY
- **BEACON OR RETRO-REFERENCE**
- AMPLIFIER GAIN REQUIREMENTS
- POINT AHEAD
- DOPPLER

8

#### SPACE-BASED LASER SESSION

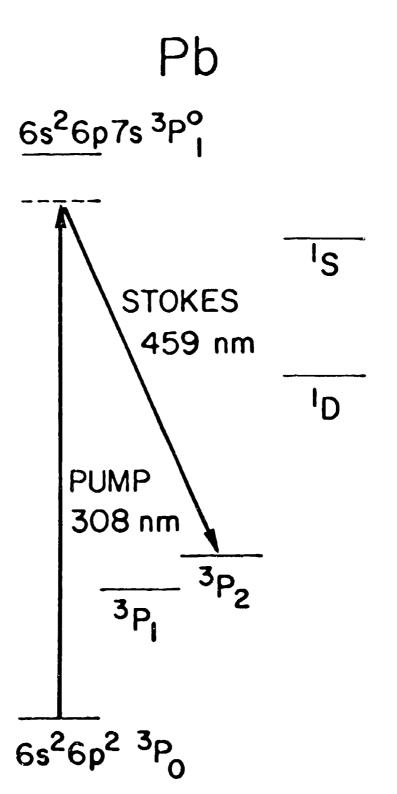
Paper 23 is contained in volume 2.

#### STATUS OF BLUE-GREEN DISCHARGE LASER WORK AT NRL

R. Burnham Naval Research Laboratory Washington, D. C. 20375

#### SUMMARY

Experiments designed to demonstrate the feasibility of a 1 J/pulse 100 pps blue-green laser using XeCl, Raman shifted to 459 nm in lead vapor are being carried out. In initial experients we have obtained ~ 30% energy conversion from 308 nm to 459 nm using an x-ray preionized discharge laser with an output of > 1.0 J in a 100 nsec pulse. The principal limitation to conversion efficiency appears to be the quality of the pump laser beam which contained considerable superfluorescence. Injection locking experiments are being carried out to correct this limitation. We have also investigated problems concerning high-repetition-rate downconversion using a 100 Hz XeCl laser. Preliminary results indicate that there is no fundamental problem with inter-pulse relaxation at repetition rates up to 100 Hz.



RAMAN CONVERSION OF XECI LASER TO BLUEGREEN

ВА	474.5, 475.0	20%	31%	SCATTERING IN MEDIUM RESONANCE ABSORPTION
PB	458.4, 458.8	<b>2</b> 5h	<b>57</b> %	\$10% SCATTERING IN PRESENT EXPERIMENTS
MATERIAL	MAVELENGTH (NM)	ENERGY CONVERSION EFFICIENCY	PHOTON CONVERSION EFFICIENCY	LIMITATIONS

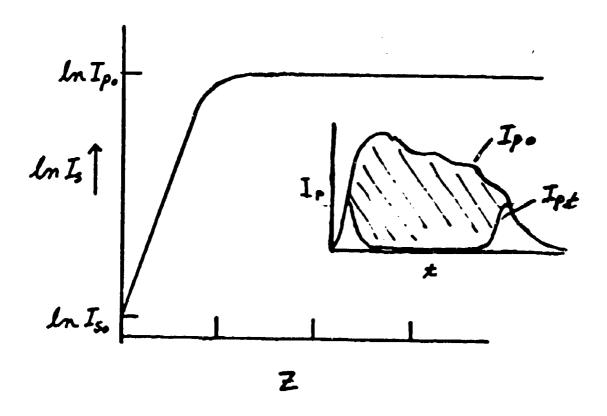
#### FORWARD SRS WITH PUMP DEPLETION

$$\frac{dI_s}{dz} = g_0 I_p I_s N ; I_p = (I_{po} - \lambda \nu_{f \nu_p} I_s)$$

$$\frac{dI_s}{dz} = g_0 N(I_s I_{po} - \lambda \nu_{f \nu_p} I_s^2)$$

Solution:

$$I_s(z) = \frac{I_{po}}{(I_{po}/I_{so} - L\nu_{f/L\nu_s})exp(-g.NI_{po}z) + L\nu_{f/L\nu_s}}$$



#### RAMAN LASER SCALING

#### FOR COLLIMATED PUMP BEAM

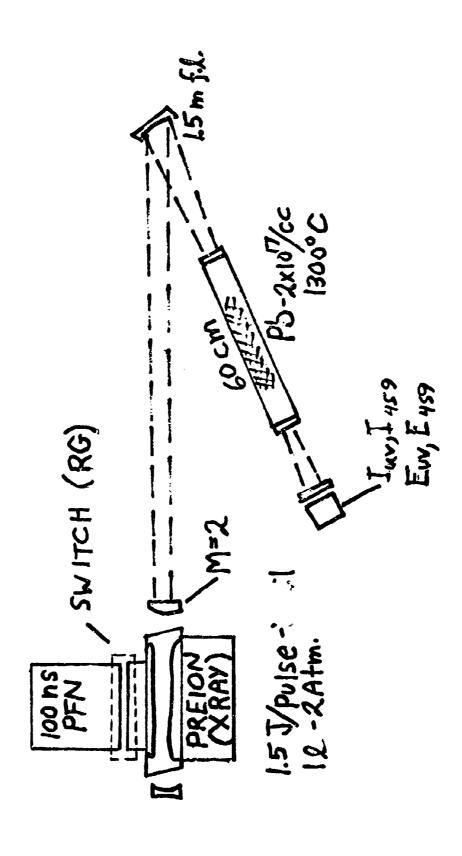
SOLVING FOR & GIVES:

FOR N= 2x1017:cm-3; g= 2x10-25 cm//w.

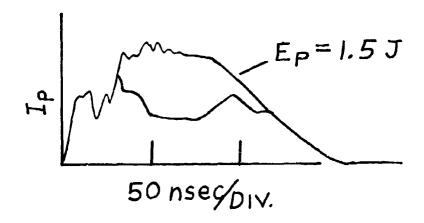
$$L = 1.4 \times 10^{2} \left( \Delta t (year) \right)^{1/2} cm$$

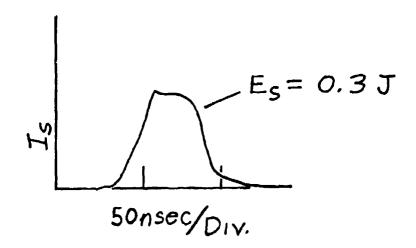
$$E_{P/A} = 6.4 \times 10^{2} L J/cm^{2}$$

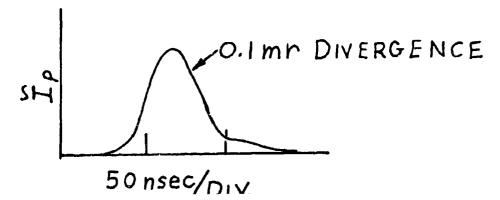
Dt	0.01	0.1	1.0 yse
L cm	14	44	140
A cm ²	1.1	.35	0.1
Eg/A Jam	1	2.9	10



### 1 JOULE XeCI-Pb DOWN-CONVERSION







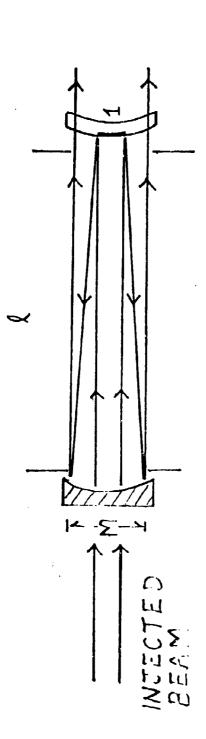
# Xecl-Pb Raman Down-Conversion

Conversion Experiments

100 Hz DOWN-CONVERSION

## RES. CAVITY BUILDUP TIME WITH UNSTABLE

-



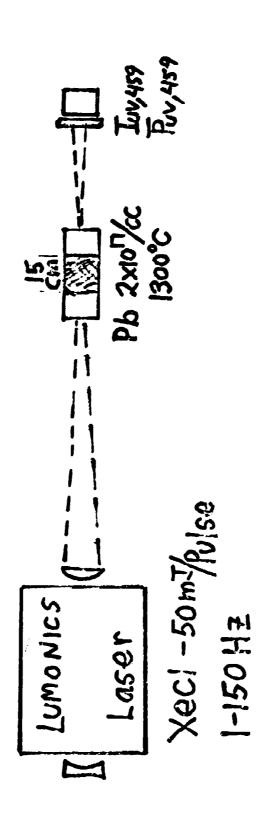
to n=400, M=2, 1/c= 3 msec

WITH INJECTED BEAM WITH DIAM. 1 I's = 2-3 & 4 lonsec.

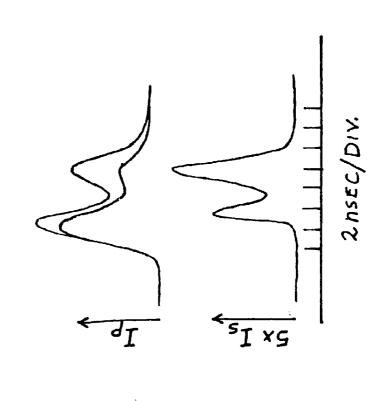
**** 

 $\mathbf{y}$ 

## Downconversion 100 Hz XeCI-Ph



DOWN-CONVERSION 100 Hz XeCI - Pb



No Change in RR-10-100 HE PRF



USING THALLIUM DATA: 02 = 100 Å2 022 5 A2

T_a= 10⁻⁷sec. T_b = 10⁻²sec. (1cm.)

- MEASURE SELF-QUENCHING & DIFFUSION IN Pb VAPOR
- O INVESTIGATE PROPAGATION OF ACOUSTIC DISTURBANCES W/INTERFEROMETER

### EFFICIENT RAMAN CONVERSION OF XeC1 LASER INTO THE BLUE-GREEN REGION

H. Komine, E. A. Stappaerts, W. H. Long, Jr.
Northrop Corporation
Northrop Research and Technology Center
One Research Park
Palos Verdes Peninsula, California 90274

March 1980

### ABSTRACT

An efficient, blue-green laser source is urgently needed for the Navy submarine communication system. The rare-gas halide excimer lasers developed over the last few years appear to meet the requirements on efficiency and scalability, but the wavelength of their near-uv emission is too short for direct use. Recently, Raman shifting of the excimer laser wavelengths has been investigated using atomic metal vapor and molecular gases as conversion media. During the past year, under a Navy-sponsored program, Northrop Research and Technology Center (NRTC) has demonstrated the feasibility of a novel conversion scheme, based on higher order Raman scattering, for efficiently shifting the uv wavelengths of these excimer lasers to the blue-green region.

The technique uses an oscillator-amplifier combination, and the Raman medium is typically a gas such as hydrogen or deuterium at a pressure of a few atmospheres. In preliminary experiments with a frequency-tripled Nd:YAG laser (355 nm), energy conversion efficiencies as high as 35 percent was obtained for the second Stokes order, in good agreement with computer simulations. The laser pulse length in these initial experiments was very short (6 ns), which limits the amplifier efficiency because of reduced Raman gain at the leading and trailing edges of the pulse. For longer, nearly-rectangular pulses, and flat-topped beam profiles as obtained with large Fresnel number unstable resonators, conversion efficiencies approaching the quantum limit should be possible for second and third order converters.

During the experimental investigation of the new scheme, the pump laser bandwidth was found to have a major effect on the amplifier gain. A comprehensive analytical model has been developed which explains these observations in terms of the interference between the various longitudinal modes of the pump and Stokes waves. In addition, a gain enhancement technique, which increases broadband gains to the value observed for monochromatic pumping, has been proposed and demonstrated. This new technique eliminates the necessity for injection-locking the pump laser in those cases where a narrow bandwidth is not necessary for other reasons. For the Navy application, injection-locking will probably be necessary in order to maximize the signal-to-noise ratio of the receiver. Experiments with an injection-locked, spectrally narrowed XeCl laser are in progress.

## **EFFICIENT RAMAN CONVERSION OF XeCI LASER**

### INTO THE BLUE-GREEN REGION

March 1980

H. Komine E. A. Stappaerts W. H. Long, Jr. Northrop Corporation
Northrop Research and Technology Center
One Research Park
Palos Verdes Peninsula, California 90274

]

7

1

### **OUTLINE**

RAMAN OSCILLATOR-AMPLIFIER SCHEME

SUMMARY OF Nd: YAG THIRD HARMONIC PUMPING EXPERIMENTS

**BROADBAND PUMPING ANALYSIS** 

**GAIN ENHANCEMENT TECHNIQUE** 

Xeci Laser Injection-locking

Committee a prince a constitute of

1

4-1

il

### XeCI / RAMAN CONVERSION MEDIA

ATOMIC METAL VAPOR:

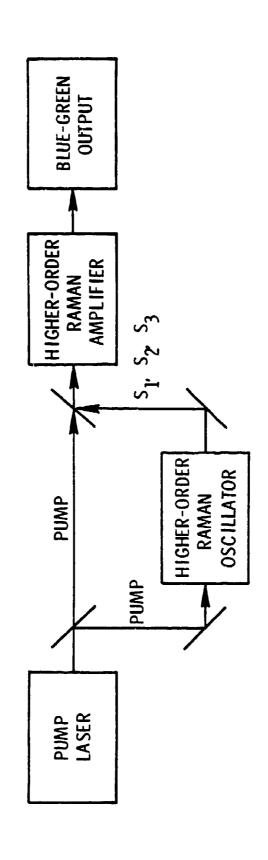
Pb(459 nm)

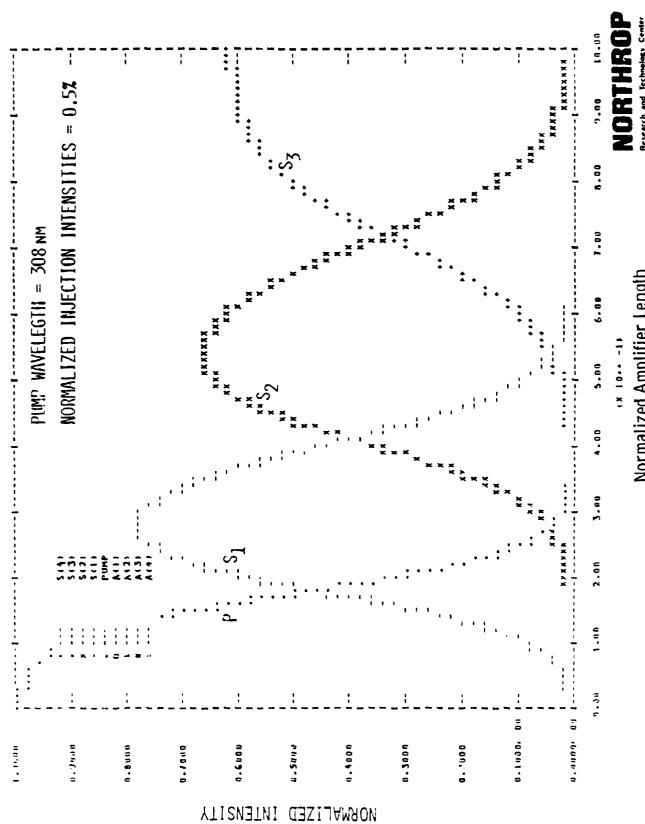
MOLECULAR GAS:

 $H_2$  (500 nm)

 $H_2/D_2$  (472 nm)

# HIGHER-ORDER RAMAN SHIFTING OSCILLATOR/AMPLIFIER SCHEME

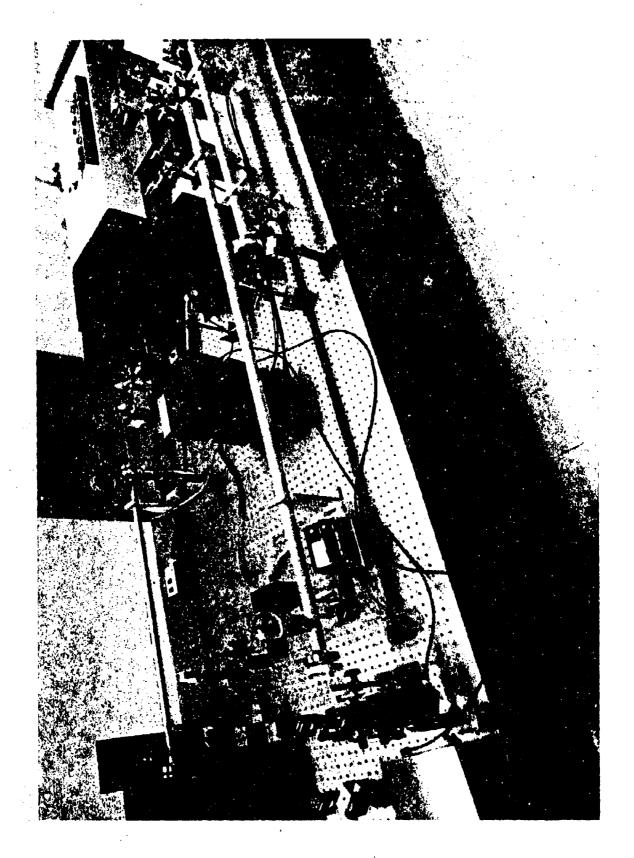




Normalized Amplifier Length

三十二年 大山山海水 神事中

-



## Nd: YAG THIRD HARMONIC (355 nm) PUMP ING EXPERIMENT

### SUMMARY

### RAMAN OSCILLATOR:

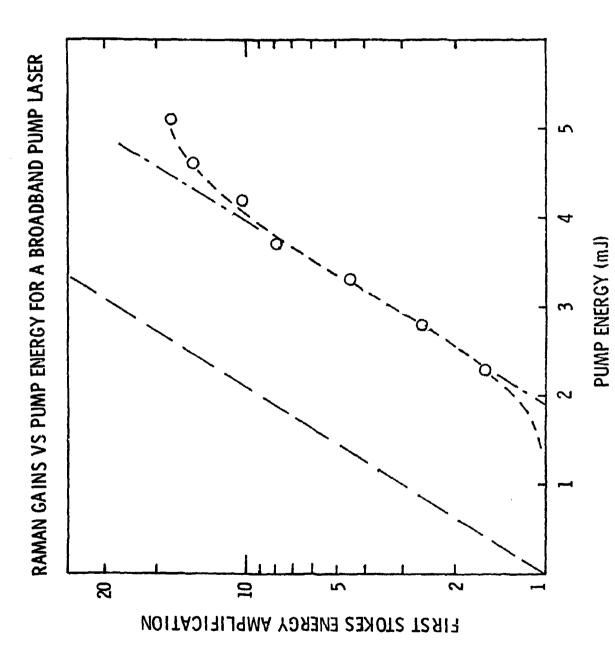
- MULTIPLE-STOKES-ORDER OUTPUT (S $_1$ , S $_2$ , S $_3$ , etc.)
- NEAR DIFFRACTION-LIMITED BEAM
- ~90% PUMP DEPLETION

### RAMAN AMPLIFIER:

- ~35% ENERGY CONVERSION (~50% PHOTON EFFICIENCY) INTO 503 nm (S₂)
- SUPPRESSION OF FOUR-WAVE MIXING
- NON-EXPONENTIAL RAMAN AMPLIFICATION (PUMP LASER **BANDWIDTH EFFECT)**

ŧ





### STIMULATED RAMAN SCATTERING OF A NONMONOCHROMATIC PUMP

$$\frac{\partial v_j}{\partial z} = \frac{g}{2} \sum_{n=1}^{\infty} \sum_{k=1}^{\infty} \frac{v_k u_{k-n}^* u_{j-n}}{1 + i \frac{2n\gamma}{n}} \exp \left[i(k - j)\gamma vz\right]$$

$$\frac{\partial u_{j}}{\partial z} = -\frac{9}{2} \frac{\omega_{L}}{\omega_{S}} \sum_{n} \sum_{k} \frac{u_{k} v_{k-n}^{*} v_{j-n}}{1 + i \frac{2n\gamma}{\Gamma}} \exp\left[i(j - k)\gamma v_{L}\right]$$

- ui, vi AMPLITUDES OF PUMP AND STOKES COMPONENTS
  - q MONOCHROMATIC GAIN COEFFICIENT
  - T HOMOGENEOUSLY BROADENED MOLECULAR LINEWIDTH
  - Y MODE SPACING
  - **U** DISPERSION PARAMETER



### INCREMENTAL FORWARD GAIN

$$G_{f} = \frac{g}{\sum_{j} |v_{j}|^{2}} \sum_{n} \frac{\left|\sum_{j} u_{j-n}^{*} v_{j}\right|^{2}}{1 + i \frac{2n\gamma}{\Gamma}}$$

### INCREMENTAL BACKWARD GAIN

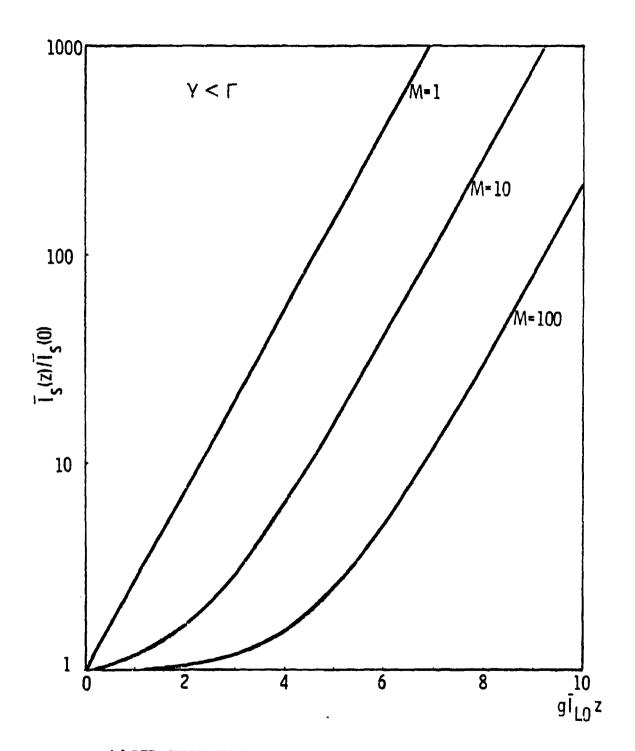
$$G_b = \frac{g}{\sum_{j} |v_j|^2} \sum_{n} \frac{\sum_{j} |u_{j-n}|^2 |v_j|^2}{1 + i \frac{2n\gamma}{\Gamma}}$$

### MONOCHROMATIC GAIN

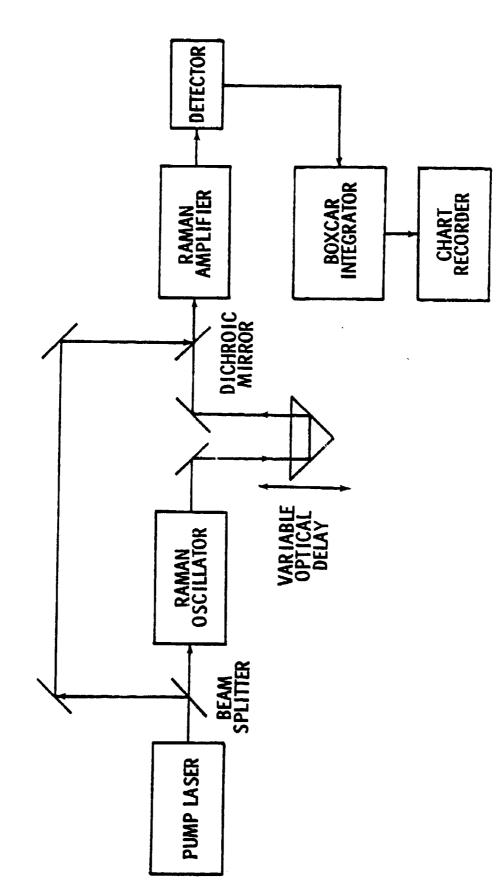
WHERE 
$$I_{L0} = \sum_{j} |u_{j}|^2$$

IS THE AVERAGE INCIDENT PUMP INTENSITY

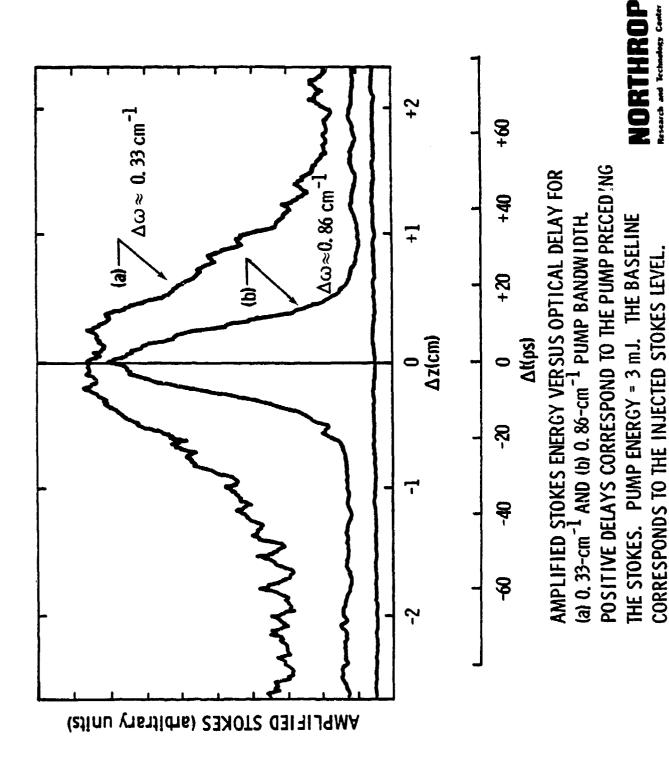




LASER-BANDWIDTH DEPENDENCE OF FORWARD GAIN IN A RAMAN AMPLIFIER WITH UNCORRELATED INJECTED PHASES.

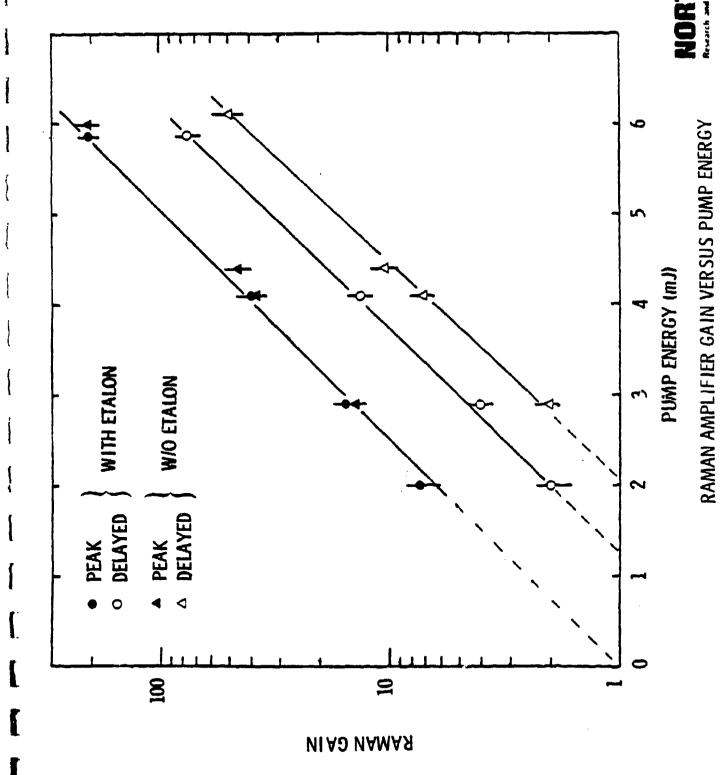


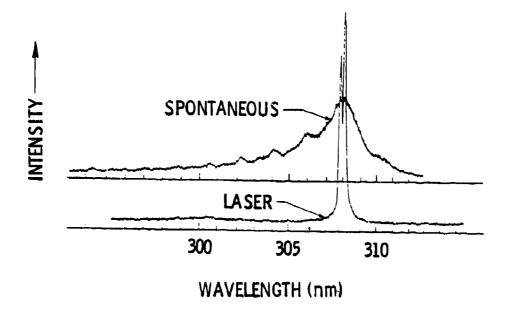
SCHEMATIC OF THE EXPERIMENTAL SETUP



]

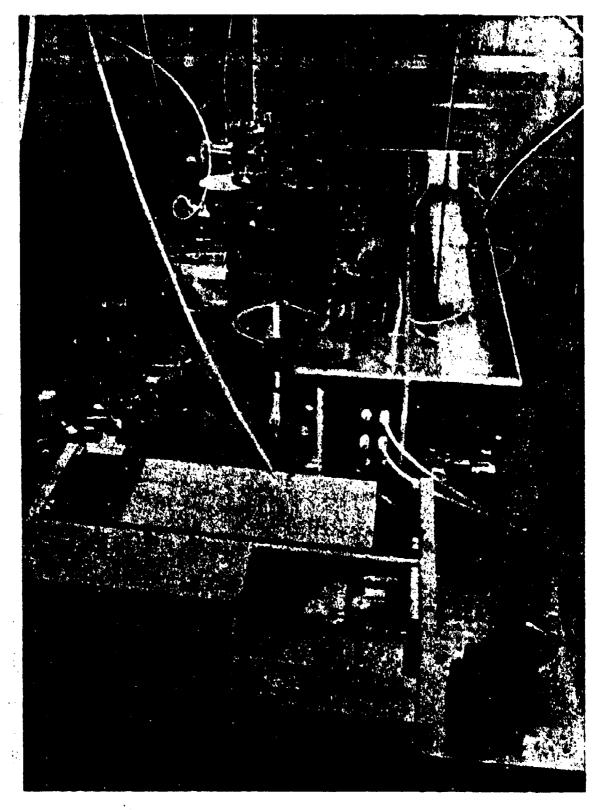






XeCI FLUORESCENCE AND LASER SPECTRA





Tunable Narrow Bandwidth Injection-Locking Source

### LEAD VAPOR CONVERSION OF AN X-RAY PREIONIZED XeCI LASER

J.I. LEVATTER & S.O. LIN UCSD

I. NEW AVALANCHE DISCHARGE FORMATION MODEL

II. X-RAY PREIONIZED LASER SYSTEM

III. RAMAN DOWN CONVERSION IN PL VAPOR

University of California San Diego CA 92093

### DISCHARGE FORMATION MODEL

(J. Appl. Phys. 51, 210, 1980)

### NECESSARY CONDITIONS:

- I. MINIMUM PREIONIZATION DENSITY, neo (min)
- II. Neo (min) MUST BE VOLUMETRICALLY UNIFORM
- III. È MUST BE UNIFORM
- IV. MINIMUM  $\frac{d(E/n)}{dt}$  (ie, VOLTAGE RISETIM.  $t_f$ ) ALLOWABLE

FUNCTIONAL DEPENDENCE OF CONDITIONS

I.  $\propto$  GAS MIXTURE,  $\frac{d(E/h)}{dt}$ , & PRESSUE.

IV. & GAS MIXTURE, & PRESSURE

### SATISFACTORY OPERATING CONDITIONS FOR TYPICAL RARE GAS HALIDE LASERS

EXAMPLE 1: XeF (He:Xe: F2=94.5:5:0.5)

Pressure - 1 atm.

$$n_{eo} (min) = 2 \times 10^5 cm^3$$

$$t_r = 16 \text{ nsec}$$

EXAMPLE 2: XeF (He:Xe:F= 94.5:5:0.5)
Pressure - 6 atm.

$$n_{eo} (min) \ge 3 \times 10^6 cm^3$$
  
 $T_r \le 6 \, nsec$ 

### CONCLUSION OF THEORETICAL MODEL-

PROVIDED THE DISCHARGE IS PROPERLY
INITIATED (i.e., CONDITIONS I - IV ARE
SATISFIED) THERE IS NO INTRINSIC LIN
TO THE VOLUME OR TEMPORAL SCALABILIS
OF RARE GAS HALIDE AVALANCHE
DISCHARGES

RECENT EXPERIMENTAL VERIFICATION:

(APPL. PHYS. LETT. 34, 505, 1979)

XEF, KrF, & XeCI DISCHARGES AT > 1

PRESSURE IN A 2.5 LITER VOLUME HA

BEEN PRODUCED WITH NO ARCING OF

STREAMER FORMATION FOR A DURATION OF 100 nsec

XeCI

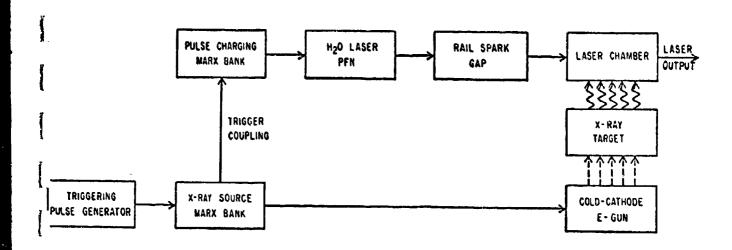
BURN

DISCHARGE

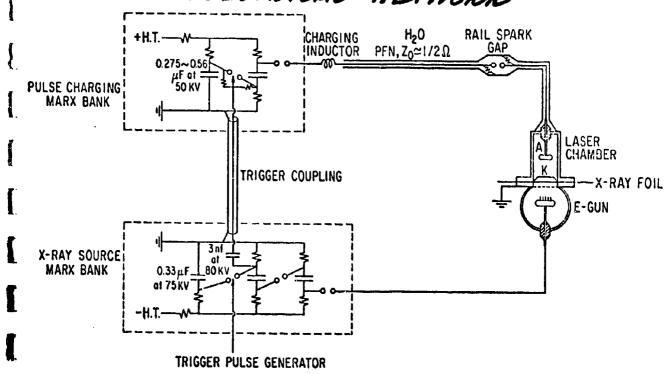
PATTERN

LUMINOSITY

### X-RAY PREIONIZED LASER SYSTEM BLOCK DIAGRAM



### ELECTRICAL NETWORK



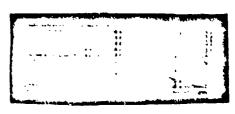
### TYPICAL LASER PERFORMANCE - XeCI

1. LITER DISCHARGE VOLUME: 2.5 JOULE 2.5 LITER DISCHARGE VOLUME: > 5 JOULE

DISCHARGE VOLTAGE 35 kV/cm 50 nsec/cm



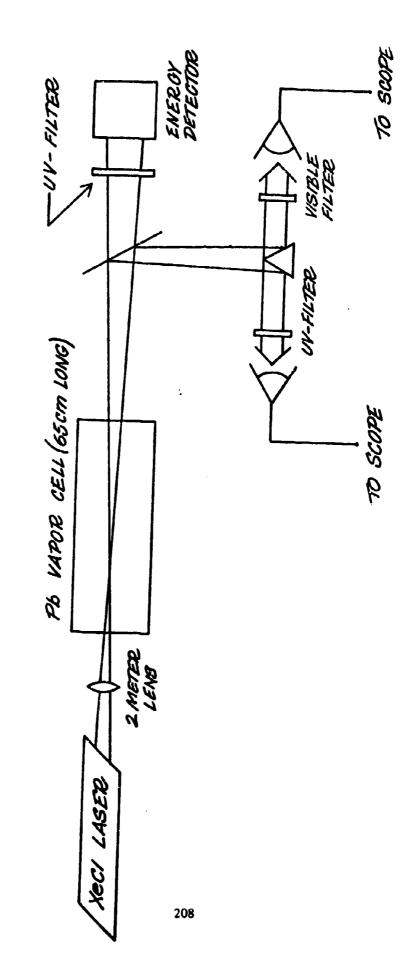
XeCl OUTPUT 20 nsec/cm 18 Mw/cm



### RAMAN DOWN CONVERSION

- · REQUIRES GOOD BEAM QUALITY.
- · REQUIRES HIGH OPTICAL DENSITY.
- HOT SPOTS IN OPTICAL BEAM CAN EASILY DAMAGE OPTICS AT THE MULTI-JOULE LEVEL.

# EXPERIMENTAL ARRANGEMENT



ŀ

### XeCI BEAM QUALITY (1 LITER DISCHARGE)

UNSTABLE RESONATOR USED (M=1.4)

NEAR FIELD

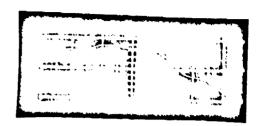
ENERGY ~ 1.5-2.5 J

FOCUS OF 2 METER LENS

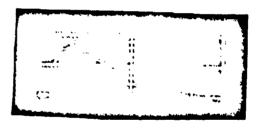


USABLE ENERGY 0.86 TO 1.5 T

INPUT-UV E=0.86 J 20 nsec/cm



0VTPVT-459 nm E=0.132 J 20 nsec/cm



DEPLETED UV 20 nsec/cm (~40% REMAINING)



### CONCLUSION

- · CAN GENERATE MULTI-JOULE UV OUTPUT.
- EFFICIENT FREQUENCY CONVERSION

  REQUIRES HOMOGENEOUS DISCHARGE

  TO AVOID BEAM PARASITICS & HOT SPOTS

  WHICH CAN DAMAGE OPTICS •
- RESONATOR OPTICS SHOULD BE DESIGNED SO THAT THE LASER MODE STRUCTURE
   IS IN STEADY STATE
- 50% ENERGY CONVERSION SEEMS
  POSSIBLE PROVIDED THE OPTICAL BEAM
  QUALITY IS SUFFICIENT TO ALLOW THE
  PROPAGATION OF A COLLIMATED INDUT
  BEAM.

### LA-UR 80-445

TITLE:

EXCIMER LASER ENGINEERING DEVELOPMENT AT LASL

AUTHOR(S):

Phillip N. Mace, AP-1

SUBMITTED TO:

Blue-Green Technical Interchange Meeting, NOSC, San Diego, CA

By acceptance of this article for publication, the publisher recognizes the Government's (license) rights in any copyright and the Government and its authorized representatives have unrestricted right to reproduce in whole or in part said article under any copyright secured by the publisher.

The Los Alamos Scientific Laboratory requests that the publisher identify this article as work performed under the auspices of the USERDA.

los alamos scientific laboratory

of the University of California LOS ALAMOS, NEW MEXICO 87545

An Affirmative Action/Equal Opportunity Employer

Form No. 8 to St. No. 2629 1775 UNITED STATES ENERGY RESEARCH AND DEVELOPMENT ADMINISTRATION CONTRACT W-7405-ENG. 36

### EXCIMER LASER ENGINEERING DEVELOPMENT AT LASL

Phillip N. Mace, AP-1
Los Alamos Scientific Laboratory, University of California
Los Alamos, New Mexico 87545

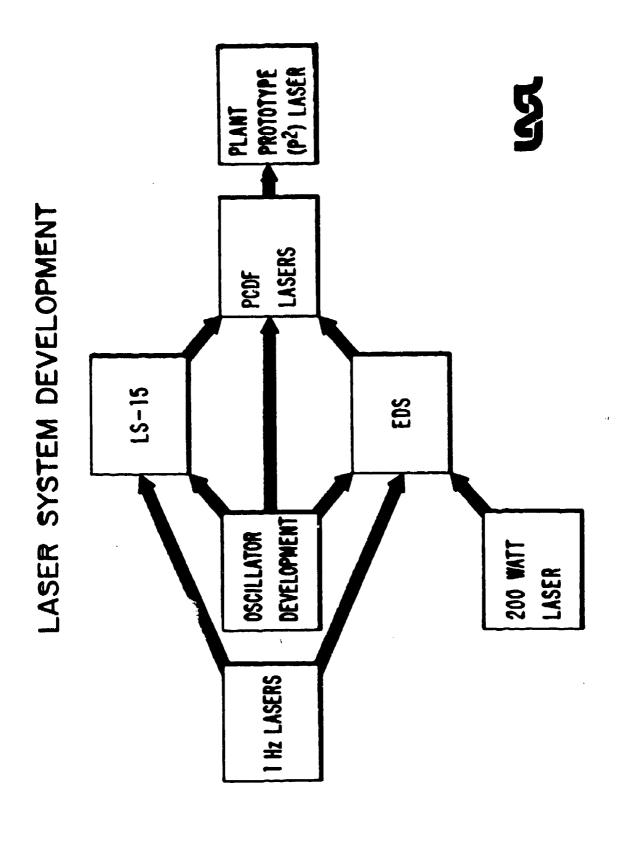
The Molecular Laser Isotope Separation program under development in AP-Division, Los Alamos Scientific Laboratory, requires development of XeCl laser systems having specifications which differ from those required for the Blue-Green Strategic Communications Program satellite based laser only in energy/pulse and pulse repetition rate. There is thus clearly a high degree of overlap in the critical technology issues which must be addressed in order to be able to design efficient, long-life laser systems. Two areas are presented in this discussion; development of cleanup systems for XeCl closed loop lasers and predictions of future clean-up system requirements, and work underway to develop reliable, long-life pulse power components meeting voltage, peak current, and dI/dt requirements of discharge pumped excimer lasers. Other key technology issues which will be mentioned but not discussed in detail include flow system and acoustic attenuator design, discharge electrodynamics, laser kinetics and PFN design, preionization techniques, optical system design, optical damage, and advanced component concepts.

## **EXCIMER LASER ENGINEERING AT LASL**

### AREAS OF DEVELOPMENT

- PREIONIZATION
- KILOHERTZ SYSTEM STUDIES
- **EFFICIENCY, ENERGY SCALING**
- CHEMISTRY
- PULSE POWER COMPONENT DEVELOPMENT
- OPTICAL DAMAGE



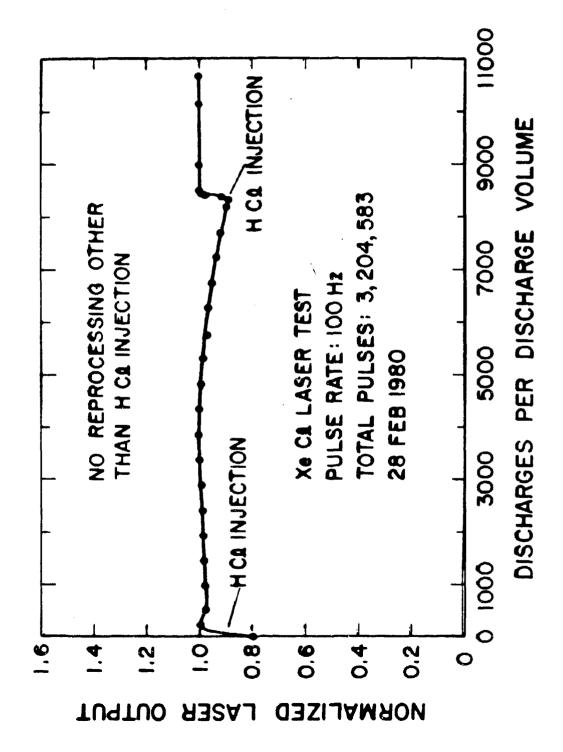


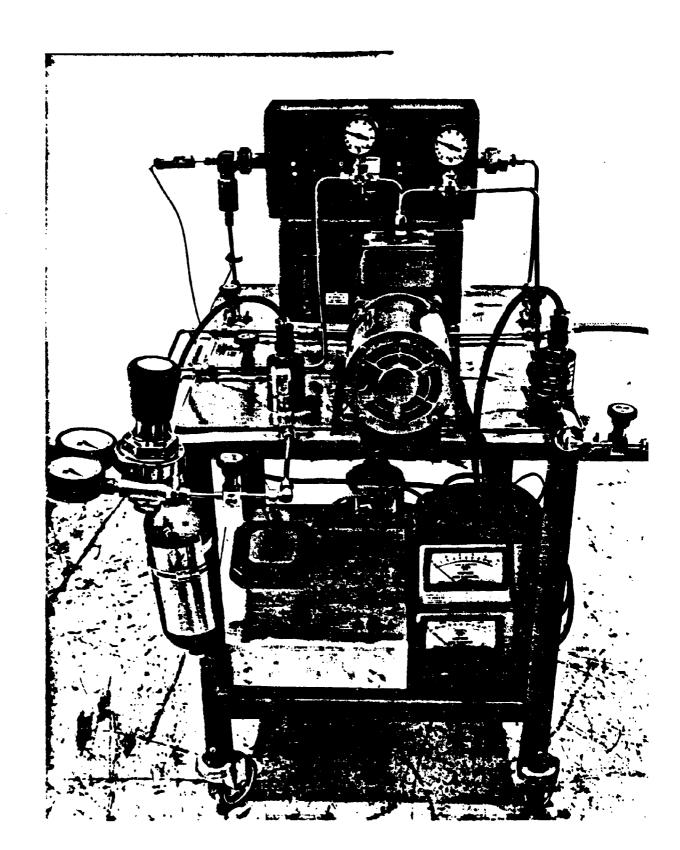


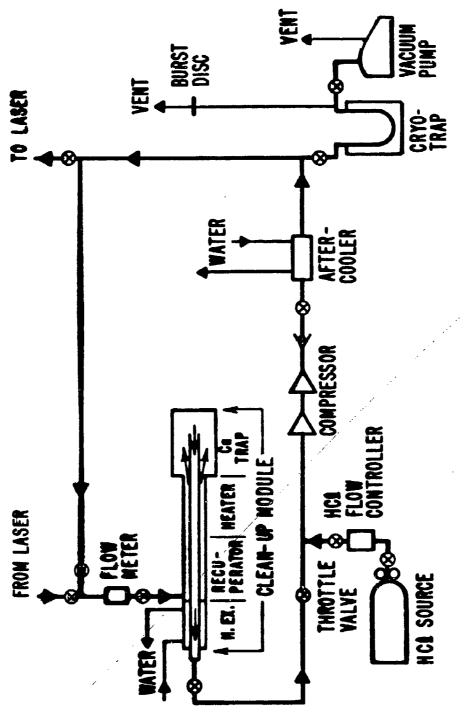
### LASER GAS CHEMISTRY

- CLEAN-UP SYSTEMS HAVE BEEN DEVELOPED CAPABLE OF MAINTAINING INITIAL OUTPUT FOR LONG TIMES
- XeCR AT LEAST 200X LONGER LIFE THAN KIF
- NO PROBLEMS ANTICIPATED FOR 1984









LS-15 GAS CLEAN-UP SCHEMATIC





### XeCI CLEAN-UP SYSTEM

REPROCESSING RATE:

GETTER TRAP TEMPERATURE: 650°C (TITANIUM)

HCM INJECTION RATE: ~0.3 SCCM

ESTIMATED SYSTEM LIFETIME: 1010 PULSES @ 100 Hz (~3.2 YEARS)

OVEN POWER CONSUMPTION: ~120 WATTS WITHOUT RECUPERATOR

AMOUNT OF TITANIUM REQUIRED: ~1 LITER

3

### LASL

### TECHNOLOGY DEVELOPMENT ADVANCED PULSE POWER



### COMPONENT DEVELOPMENT

IS THE KEY TO EFFICIENCY

AND SYSTEM RELIABILITY

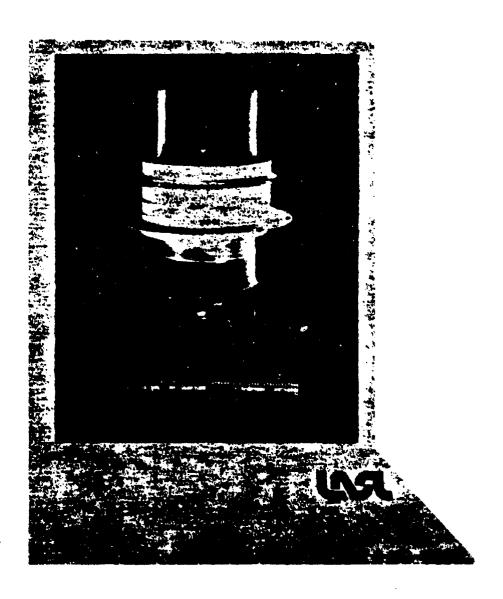


### THYRATRON DEVELOPMENT

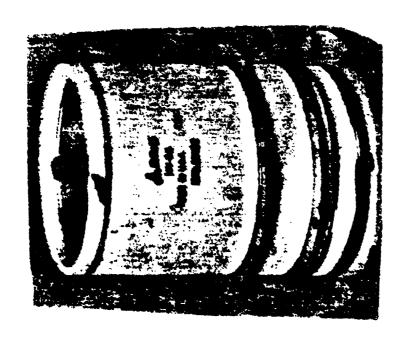
- PRIME CONTRACTOR EG&G
- MAJOR PROGRAM GOALS:
- INCREASE TOTAL CURRENT CAPABILITY
- INCREASE dI/dt CAPABILITY
- **DEMONSTRATE SUB-NANOSECOND JITTER**
- FOR PARALLEL OPERATION
- INVESTIGATE TUBE HEATING DURING
- LEADING EDGE
- 5. INVESTIGATE TUBE RECOVERY
  - TIME REQUIRED
- REVERSE VOLTAGE PROTECTION

### RECENT PROGRESS IN THYRATRON DEVELOPMENT

- KEY SPECIFICATIONS ACHIEVED IN ONE TUBE
  - 50 kV OPERATING VOLTAGE
  - 20 kA PEAK CURRENT
  - ->10¹² A/s DI/DT
- NO FUNDAMENTAL PHYSICS DISCOVERED WHICH WILL LIMIT ULTIMATELY REACHING LIFE OF >10,000 HOURS

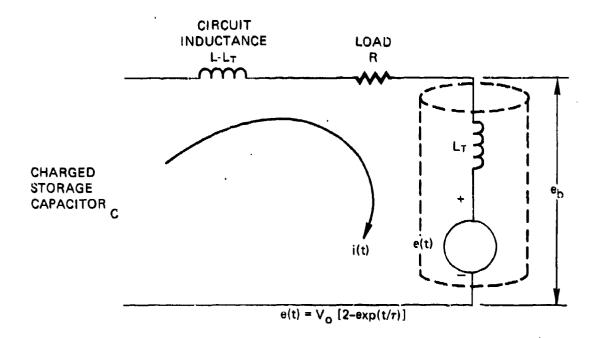


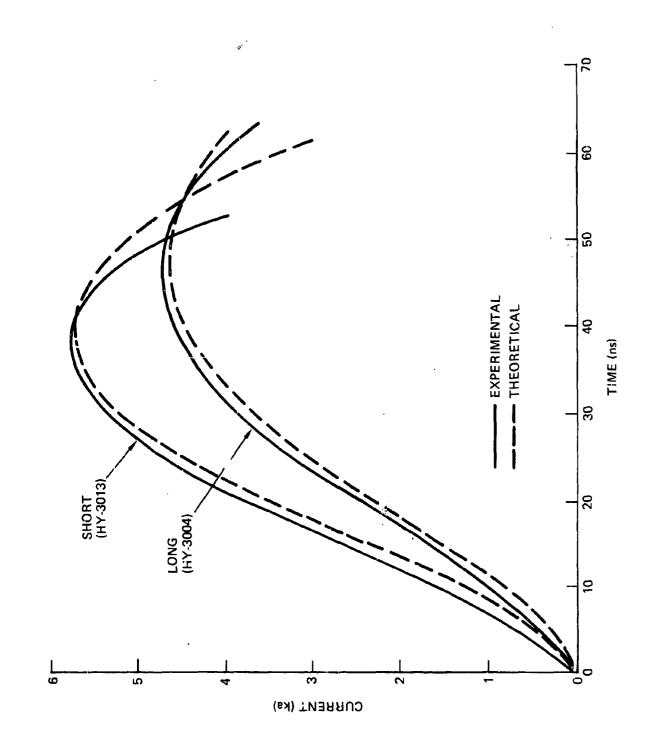


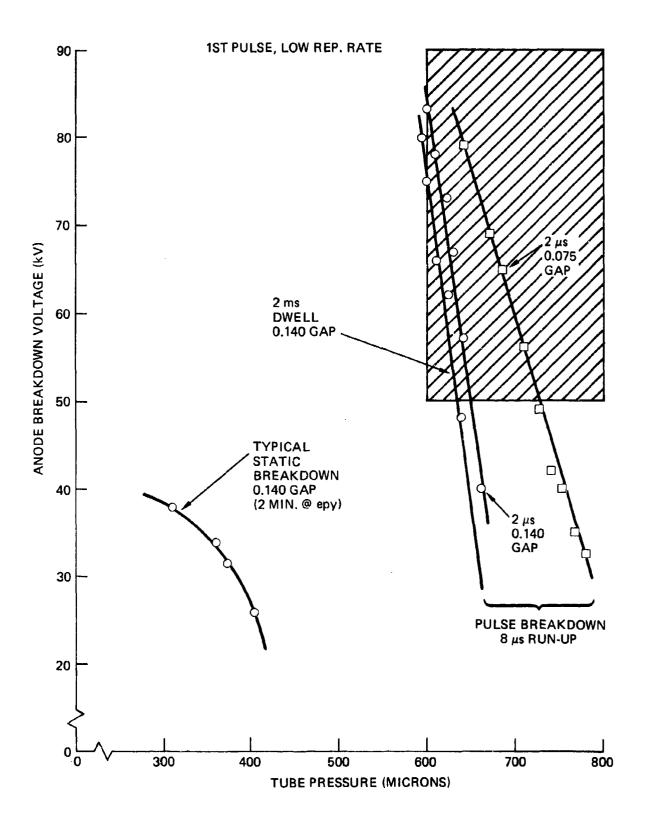


### THYRATRON LIFE

- CATHODE THERMAL EVAPORATION RATE OF CATHODE COATING
- RESERVOIR GAS CLEANUP RATE
- MECHANICAL SEAL FAILURE (OFTEN ACCIDENTAL)









### THYRATRON DEVELOPMENT

### REMAINING TECHNOLOGY ISSUES:

- INCREASE PEAK CURRENT CAPABILITY **TO 50 KA**
- DEVELOP INVERSE VOLTAGE CAPABILITY
- DEMONSTRATE FULL POWER OPERATION UNDER DESIGN THERMAL LOAD



### CAPACITOR DEVELOPMENT

1 KHZ TEST FACILITY COMPLETE AND IN USE.

### FEATURES:

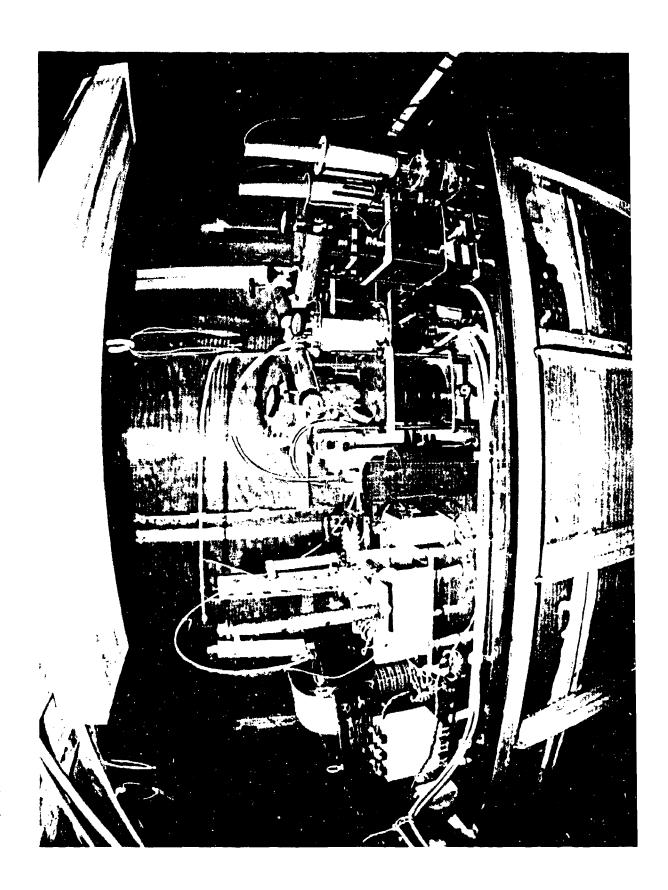
- OPERATING VOLTAGE UP TO 80 kV. Į
- AVERAGE POWER DURING TESTS OF 20 kW,

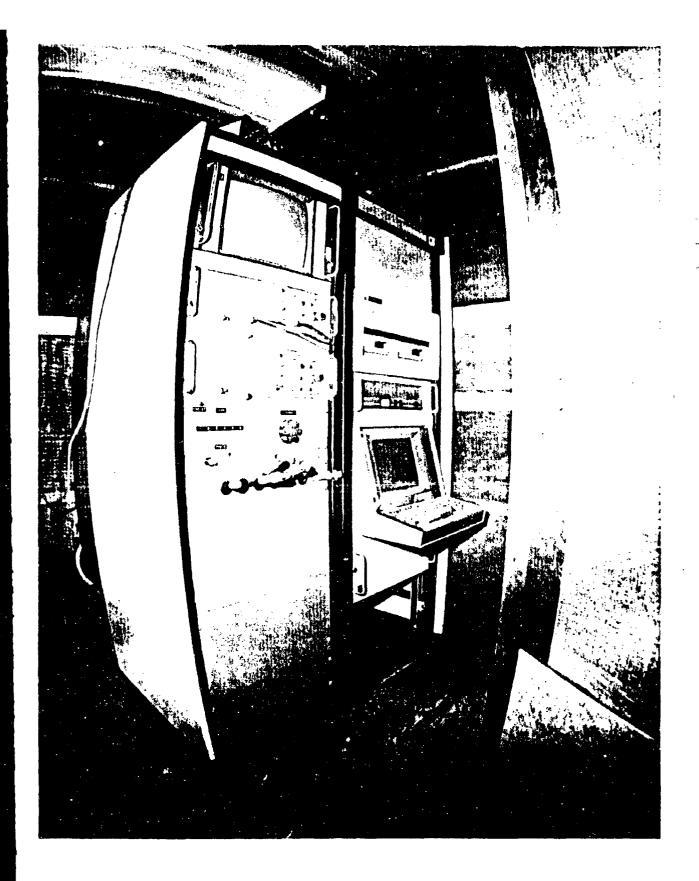
TO BE UPGRADED TO 300 kW.

COMPLETE DATA ACQUISITION AND DATA

REDUCTION SYSTEM.

- THIS IS THE ONLY MULTIKILOWATT HIGH REP RATE COMPONENT TEST SYSTEM IN EXISTENCE.
- THE LASL HIGH PULSE RATE PULSED POWER DEVELOP-MENT PROGRAM IS UNIQUE IN THE NATION







### CAPACITOR DEVELOPMENT

- TESTING SIMULTANEOUSLY ASSESSES
- CAPACITORS
- SWITCHES
- CHARGING TECHNIQUES
- ADVANCED MODULATOR COMPONENTS į
- FOR LIFETIME, RELIABILITY AND MAINTAINABILITY.

### CAPACITUR DEVELOPMENT

### MLIS REQUIREMENTS:

- 1-2 kHz PRF
- PEAK SYSTEM CURRENT >100 kA
- PEAK dI/dT > 1 MEGAMPERE/MICROSECOND
- LIFE >1010, PREFERABLY >1012 SHOTS
- TOTAL ENERGY STORED ~100 J
- OPERATING VOLTAGE 50-100 kV





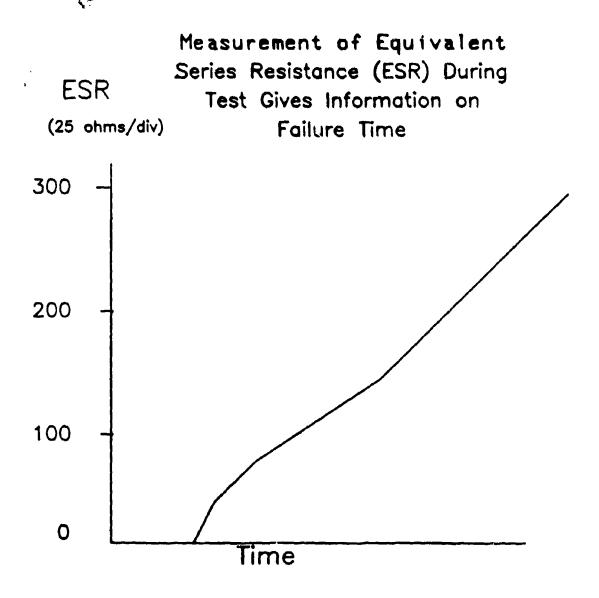
THE PROPERTY OF A CHARLEST AND COMMENTS

### CAPACITOR DEVELOPMENT

### TWO PRIMARY APPROACHES:

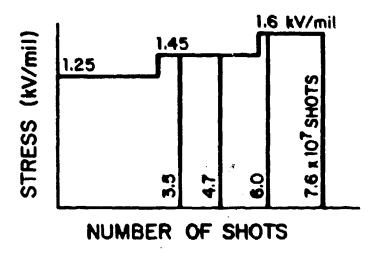
- RECONSTITUTED MICA, REDESIGNED FOR HIGH PEAK CURRENT, RMS CURRENT, & DI/dT
- PLASTIC FILM/LIQUID IMPREGNANT UNWICKED

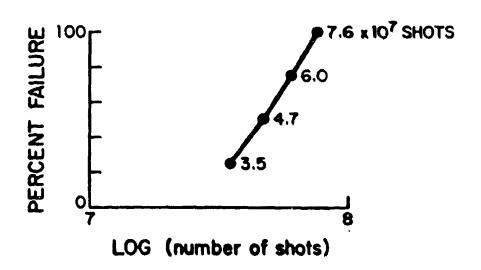
### Capacitor Tests Include Development of New Diagnostic Aids



### RECENT RESULTS FROM CAPACITOR TESTS

### FAILURE RELATIONSHIP TO VOLTAGE STRESS GIVES A PREDICTIVE CAPABILITY OF TIME-TO-FAILURE







### AP - 1 - VG - 5201

### UV OPTICAL DAMAGE TESTS

### LASER

• XeCl 308 nm

• 7 J/cm²

• 100 Hz

700 W/cm²

### RESULTS

 $MgF_2$ 

(E

CaF₂

2

SURFACE GLOW FROM POLISHING COMPOUND

NO DAMAGE IN 105 SHOTS

FLUORESCENCE FROM BULK MATERIAL BUT

NO PERMANENT DAMAGE

RED FLUORESCENCE BUT NO BULK DAMAGE SUPRASIL II

AT 300 W/cm²

VERY RAPID SURFACE DAMAGE

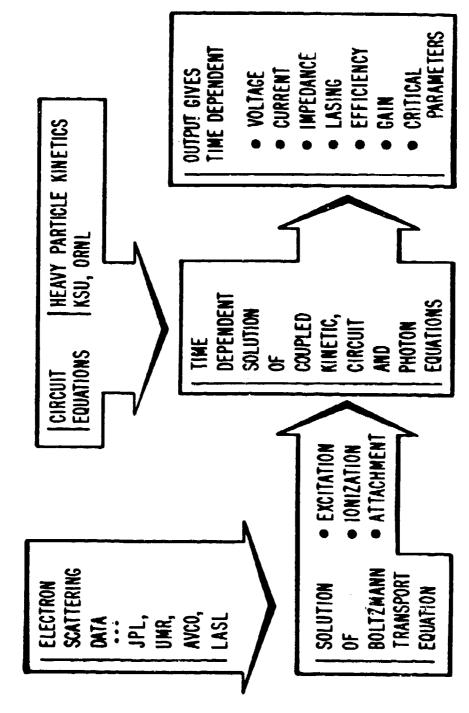
(4)  $AI_2O_3$ 

PRELIMINARY CONCLUSION IS 308 IS MUCH BETTER ON OPTICS THAN 248.

10° shots at 100 Mg

			<b>.</b>						r & -1		<b>4.</b>		
	<b>5</b> -2	-	-				اعيت					<b>+</b>	
								l					
		7 A -					=		T		"		
	-	}-U==		_1	_	: :		-	T	=			
				<u></u>			==		ł		-		
		= -		-	- 1			7 7 2	1	# - 12 T			
			-			==			1			•==:	
		-	<u> </u>		1				1				, ,
		-==	====					·- ÷	t:		7.	N	
					-				H		<u> </u>		
									1			1	1
	= =1	-		+=1		F			13				
				<b>5</b> 7	1								
	-			-				- E	1				
			-	-	=	Ш			ł.				-
									Ŀ				
			# <b>7</b> -		=	Ξ			Ŀ				
			-	-1		- 3			Ħ				
					ਦੁ				H				
					Ξ				L				
			1	L	<b>_</b>				1				
					7				1	后喜			
			-	·f					t	-		7	
								<u> </u>					
	= :-:		<u> </u>			-			L			=-:	1 1
					1.1	111		lin H					
		33							t			-	
		====		-					H				
					Ĩ.	= :	-		L	- ا	11	4-14-7	
			T <u>#</u> ]	<b>⊦.</b> }	Ħ			===	•		i i i i i i i i i i i i i i i i i i i	<u></u>	1
												-	
			<del>`</del> -						Н				
			<del></del>	1					Ļ			: <u> </u>	
		- <u>-</u>		• •	#				. =				-===
		1.3			7.	1	1						
					₹				Н				3
				-	III				H			-	
		7.3					7		Ħ				
			<u> </u>	<u>.</u>	$\equiv$	=3	=		=				
									$\equiv$				
				-}-					H				
				7				= ::	Ę				
					$\equiv$				,				
					٩İ				11:			t <del>_</del>	
			===						3				
					=		==	= :	Η				
				14					녑				
					3			<u> ==</u>	4				l=== þ
				は	==				1				
								-:=					
				1					E				
			<b>+</b>	1   2				==:	اللا				-===
					Ħ				-				
									H				
									Ï				
			E						1				
				==					1				
				苣					Ħ				
									7				
					=				:				20
	F 6	13	<b>₽</b>						1				
					=		=		Lil				
			24						Ξ				
是 4 4 4 4 5 1 5 1 5 1 5 1 5 1 5 1 5 1 5 1		ZJ,	تتوو		Ξ.	= 5							
			<i>F</i> :	1 - 1	==				=				
									•	****		<u> </u>	

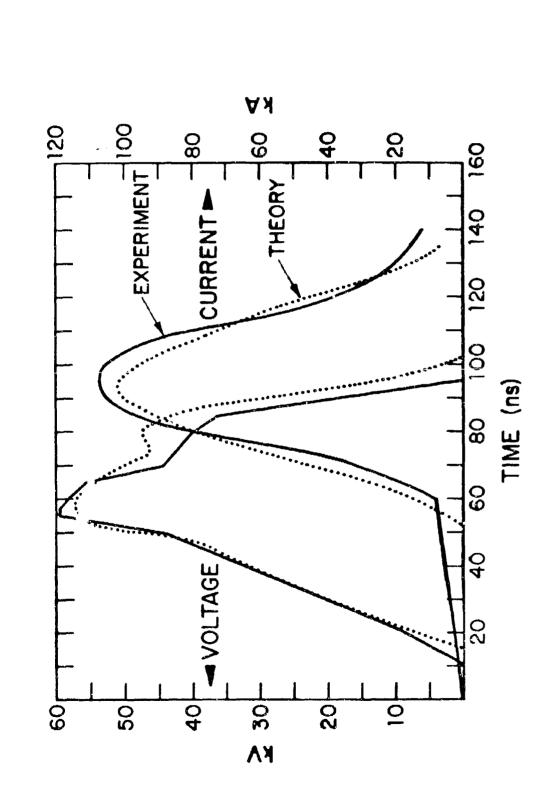
## RARE GAS HALOGEN LASER MODEL

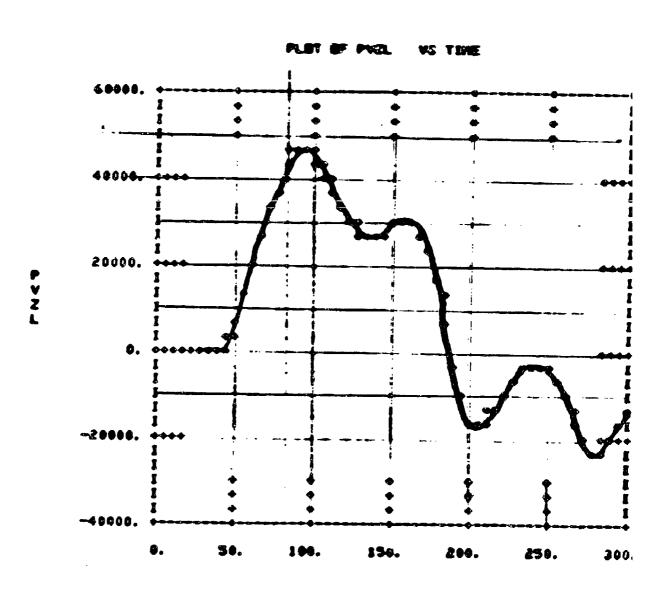


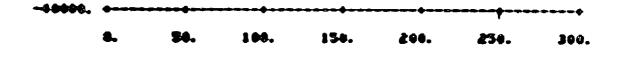


-

1

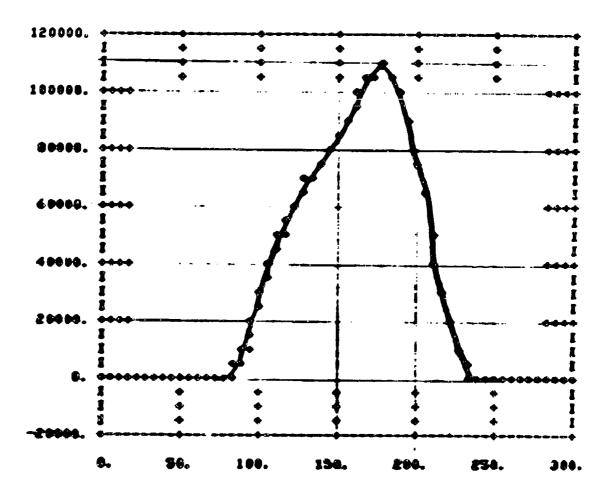




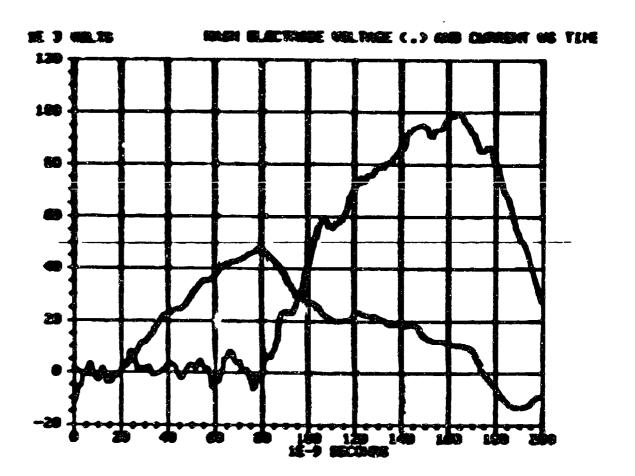


TINE 1

PLOT OF IAL VS TIME



### Shot # 51



### Strategic Blue-Green Optical Communications Program

### Annual Technical Interchange Meeting 25-27 March 1980

### Abstract For

UTRC Blue/Green Laser Research*

R. T. Brown and W. L. Nighan

Over the past two years UTRC has been carrying out a theoretical and experimental investigation of e-beam assisted XeCl(B) laser discharges¹. Primary attention in this investigation has been focused in two areas: (1) development of techniques to enhance discharge stability, and (2) identification and evaluation of conditions compatible with high discharge: e-beam energy enhancement. The principal results of this study relevant to e-beam discharge excitation of the XeCl(B+X) laser will be presented.

Theoretical and experimental investigations of the  ${\rm HgBr}({\rm B})/{\rm HgBr}_2$  dissociation laser are also underway, with particular attention directed toward e-beam controlled discharge excitation². Basic kinetic processes related to  ${\rm HgBr}({\rm B})$  formation in this laser will be discussed.

^{*} Supported in part by NOSC under Contract N00014-78-C-0830 and by ONR under Contract N00014-76-C-0847.

¹ W. L. Nighan and R. T. Brown, Appl. Phys. Lett. (April 1, 1980).

² W. L. Nighan, Appl. Phys. Lett., 36, 173 (1980).

# UTRC BLUE/GREEN LASER RESEARCH

E-beam controlled discharge excitation

XeCI(B)

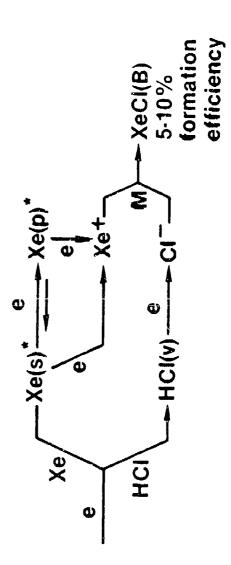
HgBr(B)/HgBr₂

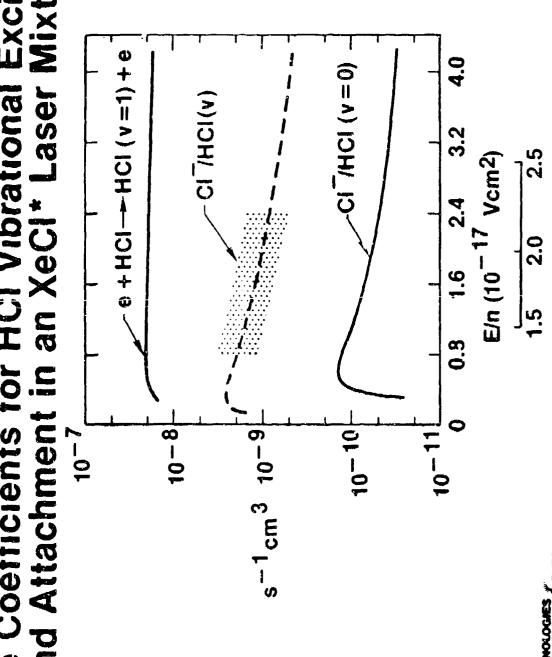
R.T. Brown — XeCl results

W.L. Nighan — HgBr(B)/HgBr₂ results

#### UNITED TECHNOLOGIES 🚁

# XeCI(B) FORMATION SEQUENCE IN DISCHARGE EXCITED MIXTURES

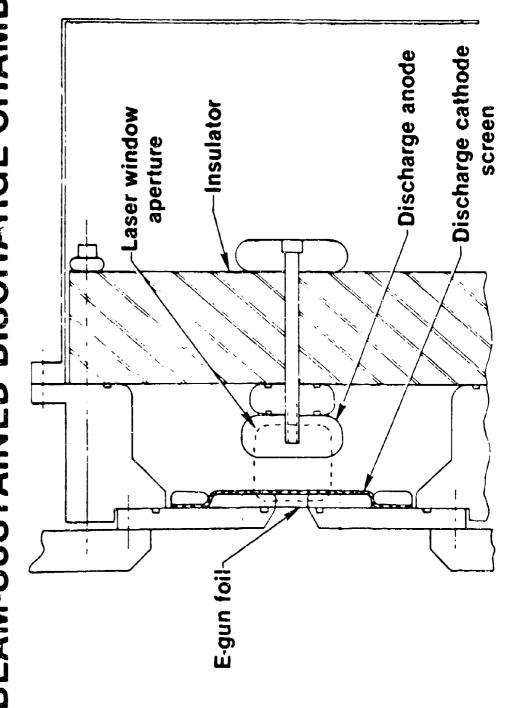




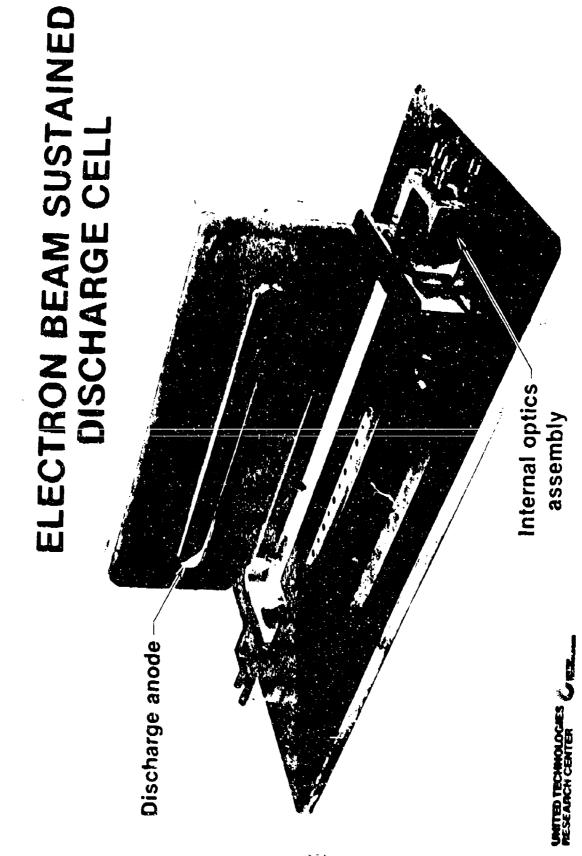
Mean electron energy, eV

252

# E-BEAM-SUSTAINED DISCHARGE CHAMBER

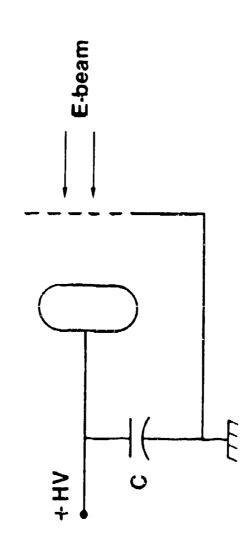


UNITED TECHNOLOGIES CHES.



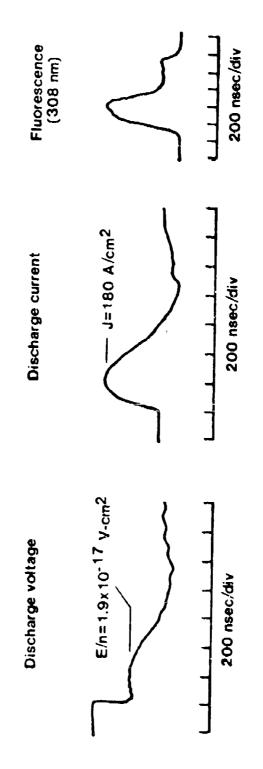


## DISCHARGE DRIVING CIRCUIT



# Measured XeCI* Discharge Characteristics

Ne/Xe/HCL: 0.99/0.01/0.0007; p=3.0 atm; S=50 + 2.5x107 t sec-1

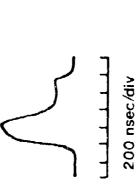


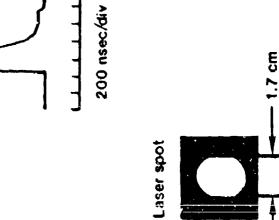
Energy enhancement factor = 6

## Measured XeCi* Laser Characteristics

Ne/Xe/HCI: 0.99/0.01/0.000/7; p=3.0 atm; S=50+2.5x10 7 t sec-1

Fluorescence Laser intensity
R1=0.99; R2=0.50

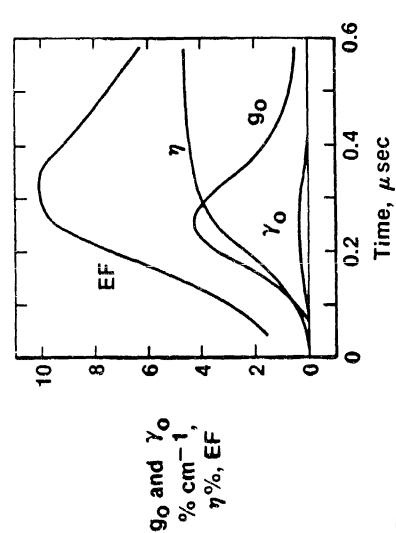






### COMPUTED XeCI(B) MEDIUM PROPERTIES IN AN E-BEAM ASSISTED DISCHARGE

Ne/Xe/HCI = 0.989/0.01/0.001 P = 3 atm



### E-BEAM ASSISTED XeCI LASER DISCHARGE MEASURED CHARACTERISTICS IN AN

Ne/Xe/HCI = 0.989/0.01/0.001

p = 3 atm

 $j_e = 0.8 \text{ A/cm}^2$ 

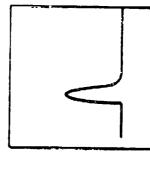
J = 150A/cm²

Discharge

current

Etched screen cathode

Fluorescence





E/n = 2.0 x $10 - 17 \text{ V-cm}^2$ 

Discharge

voltage



 $0.2~\mu\,\mathrm{sec}/\mathrm{div}$ 

0.2 µ sec/div

3 91 -3

NESEARCH CENTER

### MEASURED Xeci* Intrinsic Laser Properties

Ne/Xe/HCI = 0.989/0.01/0.001
Gas mixture

3.0 atm
ressure

**Temperature** 

Pulse fength

### MAJOR ACCOMPLISHMENTS

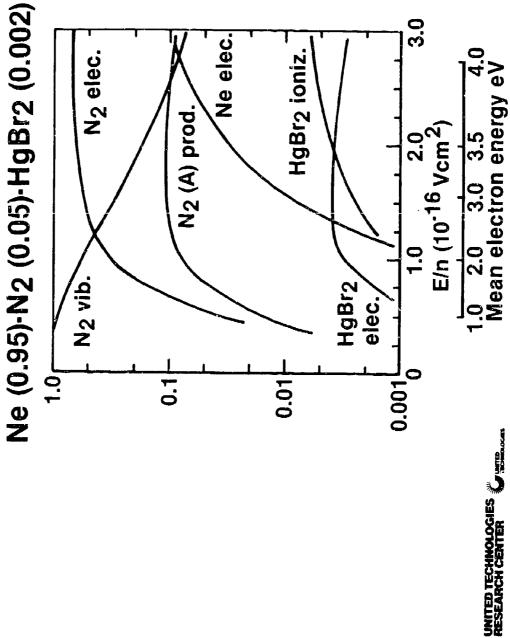
- Identification of vibrational excitation of HCI as a fundamental process in the XeCI(B) formation sequence
- process in discharge excited XeCl lasers recombination as the XeCI(B) formation Identification of Xe⁺ - CI⁻
- discharge design permitting attainment of large volume, long duration, diffuse XeCl discharges having properties compatible Development of an E-beam assisted with Navy requirements

#### 489-505 nm HgBr(B)/HgBr₂ DISSOCIATION LASER

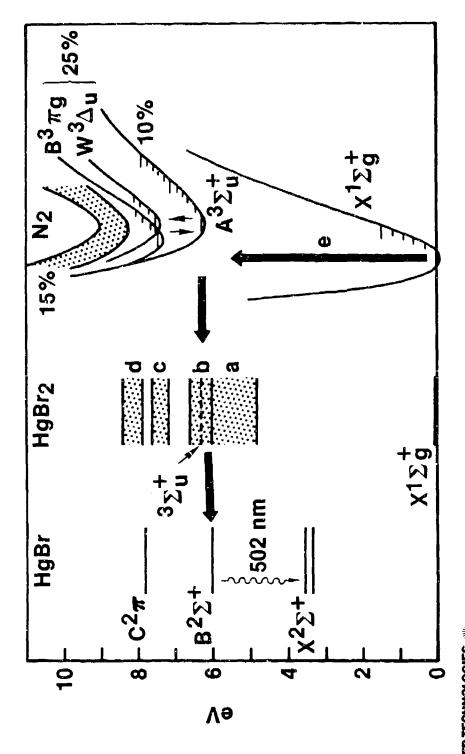
- Status
- Discharge excitation of N₂/HgBr₂ mixtures
- Electrical-optical conversion efficiency, 0.5-1.0%
- ullet Laser pulse energy,  $\sim$  1 joule/liter
- **Potential**
- Conversion efficiency, 2-10%
- Pulse energy, 2-10 joules/liter
- Other mixtures, e.g., Xe/HgBr₂

RITED TECHNOLOGIES

# Fractional Electron Power Transfer



## Schematic Energy Level Diagram



UNITED TECHNOLOGIES

#### ,

# N2* -- HgBr2 EXCITATION TRANSFER

$$N_2(A^3\Sigma_u^{+}) + HgBr_2 \longrightarrow HgBr_2(^3\Sigma_u^{+}) \longrightarrow HgBr(B^2\Sigma^{+})$$
 1/3 --- HgBr( $A^2\pi, X^2\Sigma^{+}$ ) 2/3

$$N_2(B^3m_g)^+$$
 HgBr $_2$  — HgBr $_2(^3m_g)$  — HgBr $(C^2m)$  — HgBr $(A^2m, B^2\Sigma_+^+, X^2\Sigma_+^+)$ 

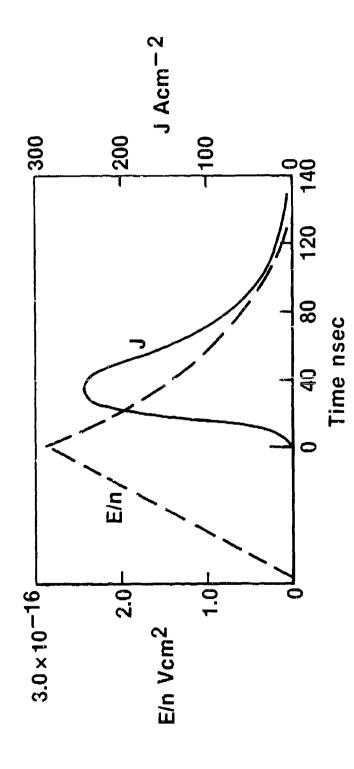
$$N_2(W^3\Delta_U) + HgBr_2 \longrightarrow HgBr_2(^3\Delta_U) \longrightarrow HgBr(A^2\pi, C^2\pi)$$

 $N_2^*$  energy utilization efficiency  $\sim 5-10\%$ 

#### NITED TECHNOLOGIES

### CURRENT DENSITY AND E/n VARIATION FOR FAST-PULSE DISCHARGE CONDITIONS

 $N_e(0.95) - N_2(0.05) - HgBr_2(0.002)$ ; 2 atm, 155°C

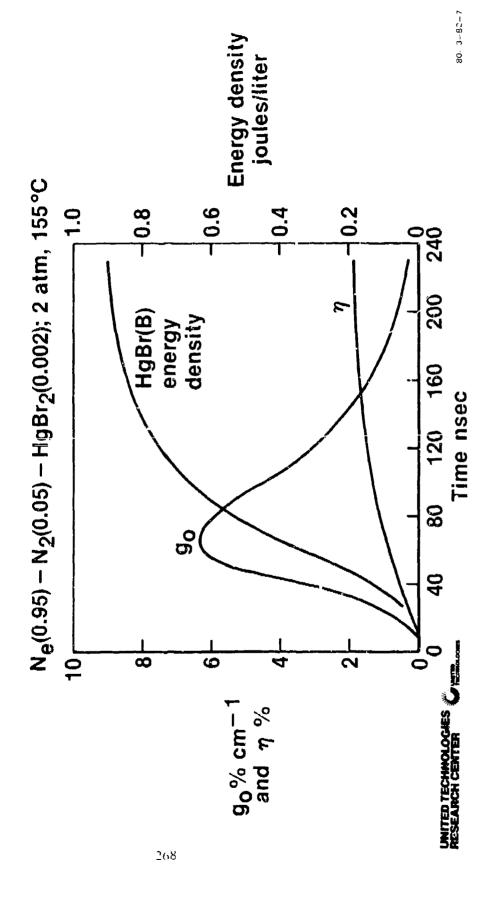


267

UNITED TECHNOLOGIES

3 82

### GAIN, HGBr(B) FORMATION EFFICIENCY AND ENERGY DENSITY FOR FAST-PULSE DISCHARGE CONDITIONS

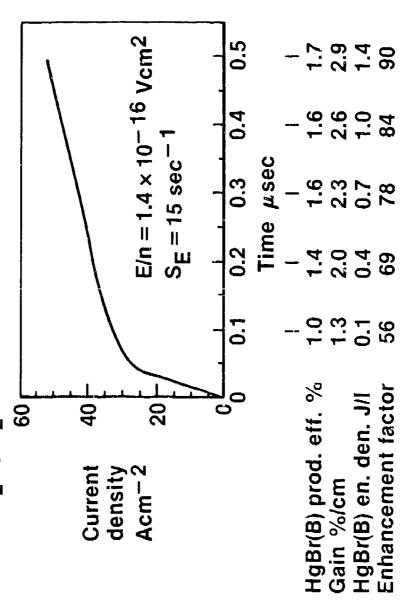


1

#### 80 3 82-5

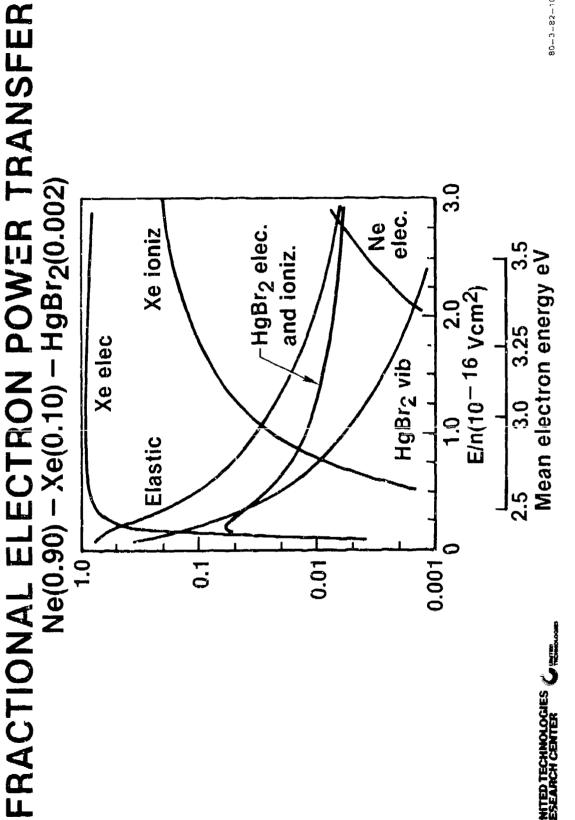
### DISCHARGE AND LASER PROPERTIES IN AN ELECTRON-BEAM CONTROLLED HgBr(B-X) LASER DISCHARGE: N2 MIXTURE

Ne/N₂HgBr₂ = 0.95/0.05/0.0025; P = 2.0 atm, T = 163 °C



UNITED TECHNOLOGIES WHENCOWN

- 100 日本の大山地の山



I

# Xe* - HgBr2 EXCITATION TRANSFER

$$e + Xe \longrightarrow Xe(^{3}P_{2}) + e$$

$$Xe(^3P_2) + HgBr_2 \longrightarrow HgBr_2(^3\Sigma_{u}^{+}, ^3\pi_{u}) \longrightarrow HgBr(B^2\Sigma^{+}) = 5/6$$

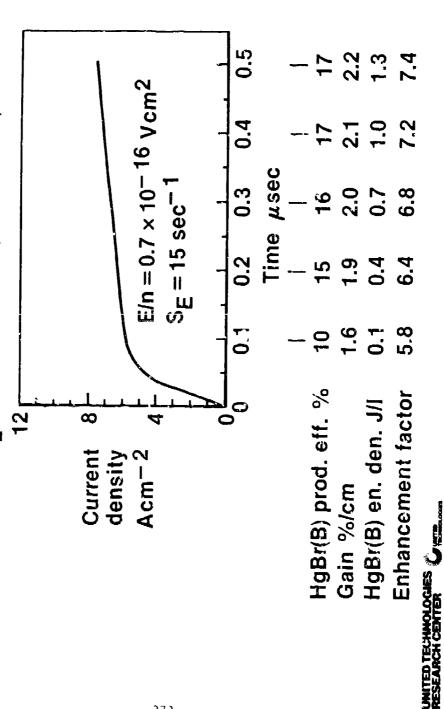
Xe* energy utilization efficiency ~ 85 %

MITED TECHNOLOGIES

#### A . CO C DO

### DISCHARGE AND LASER PROPERTIES IN AN ELECTRON-BEAM CONTROLLED HgBr(B-X) LASER DISCHARGE: Xe MIXTURE

Ne/Xe/HgBr₂ = 0.90/0.10/0.0025; P = 2.0 atm, T = 163°C



#### SUMMARY

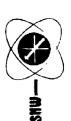
- HgBr(B)/HgBr2 laser has the potential to meet the requirements of the Navy application
- Data base not yet complete
- Electronic energy utilization efficiency (N2) and discharge stability (Xe) are key issues

### MERCURY BROMIDE LASER SCALING APPROACHES

J.J. EWING, C. FISHER, S. MOODY, A. PINDROH, D. QUIMBY

WORK SUPPORTED BY NOSC/ONR AND MSNW IR&D

Mathematical Sciences Northwest PO Box 1887 Bellevue WA 98009



- - -

### DISCHARGE EXCITED HGBR LASER SCALING

OBJECTIVE: EVALUATE METHODS FOR SCALING HgBr

- LENGTH : GAIN/LOSS

- APERTURE : PREIONIZATION METHOD

UV OR X-RAY

- ENERGY DENSITY : PR

PRESSURE ALTERNATE MIXTURES

HgBr₂ DENSITY

### MSNW MERCURY BROMIDE KINETICS CODE

- PREDICT HgBr PERFORMANCE AND SCALING

- OVERALL EFFICIENCY - HIGH ENERGY OUTPUT

- BOLTZMANN ELECTRON KINETICS

- HEAVY BODY KINETICS

- LASER BUILDUP

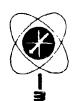
- TEMPORAL E/N, GAIN

- CIRCUIT EQUATIONS

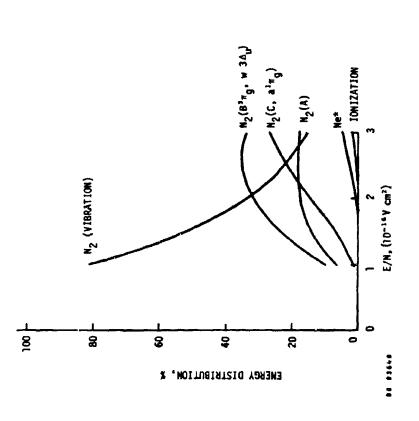
LASING TRANSITION COLL IS IONAL QUENCHING ENERGY FLOW IN THE DISCHARGE EXCITATION OF NE/N2/HGBR2 MIXTURES MIXING HgBr (X,22) HqBr(X,0) PREDISSOCIATING STATES HgBr(B) HgBr(C) ENERGY TRANSFER HgBr₂  $^{\rm HgBr}_{2}$ N2 GROUND STATE **K**,(C) N2(B.W) (V)2N N, (A) ¥• Ke* ¥.

278

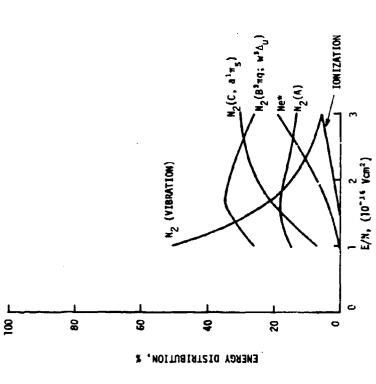
I



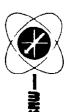
BOLTZMANN CODE PREDICTIONS FOR 10 PERCENT N2, 90 PERCENT NE



BOLTZMANN CODE PREDICTIONS FOR 5 PERCENT N2, 95 PERCENT NE

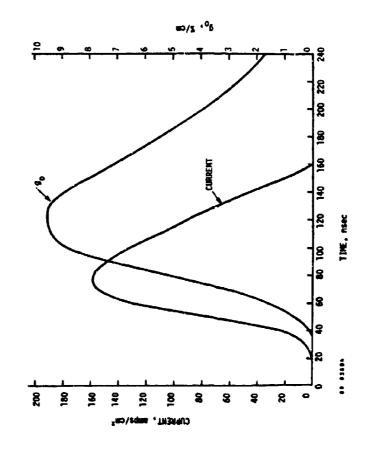


280

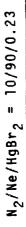


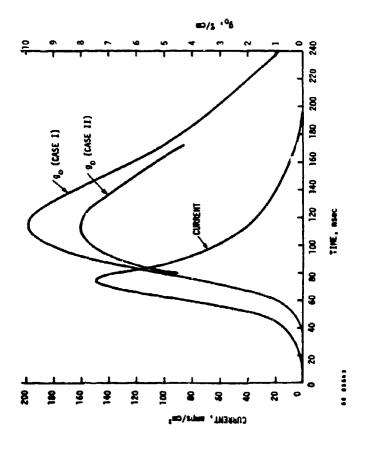
CALCULATION OF GAIN AND CURRENT FOR HGBR LASER, USING THE PUBLISHED E/N PROFILE

Ne/N₂/HgBr₂ = 95/5/0.23



MSNW MODEL PREDICTIONS OF HGBR(B+X) SMALL SIGNAL GAIN





CASE I; HEAVY BODY MIXING OF HgBr C  $\stackrel{\neq}{\leftarrow}$  B NEGLECTED CASE II: HEAVY BOPY AND ELECTRON MIXING OF HgBr C  $\stackrel{\neq}{\leftarrow}$  B NEGLECTED, AND N₂(A) + HgBr + HgBr(B) + N₂ NEGLECTED.

The state of

1

Ī

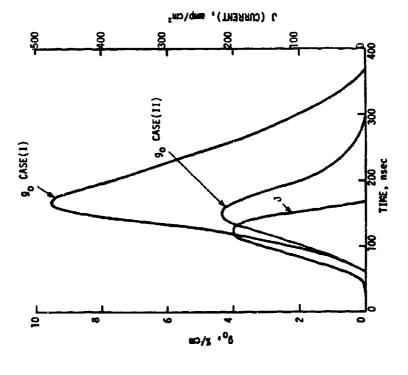
- MSHE

282



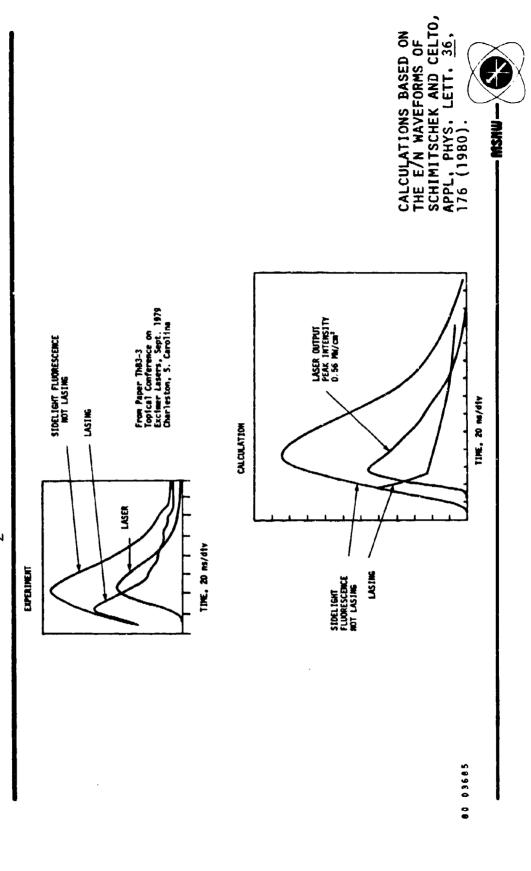
MSNW MODEL PREDICTIONS GF HGBR(B+X) SMALL SIGNAL GAIN

 $Ne/HgBr_2 = 100/0.23$ 



ELECTRON UP PUMPING RATE CONSTANT BH9Br(x) + e  $\Rightarrow$  HgBr(B) + e, K = 10⁻⁸ cm³/sec k = 10⁻¹⁰ cm³/sec CASE II: CASE 1:

#### FOR 10 PERCENT N2 HGBR LASER WITH 50 PERCENT FEEDBACK CALCULATED LASER OUTPUT AND SIDELIGHT FLUORESCENCE



**

•

İ

1



### APERTURE SCALING DEPENDENT ON PREIONIZATION

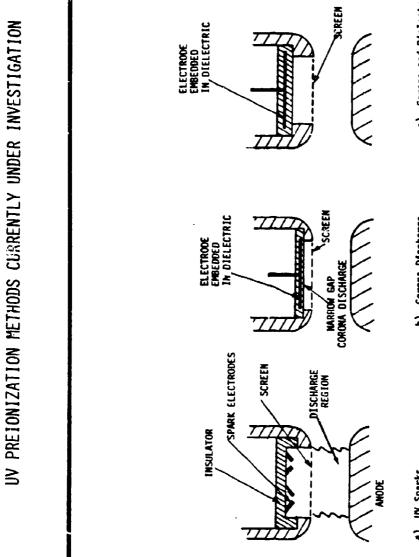
SIMPLE, PENETRATION DEPTH?	SPARKER SURVIVABILITY
ÀΛ	

- X-RAY MINIMUM STOPPING - UNIFORM MINIMIZE E-BEAM CURRENT MORE COMPLEX

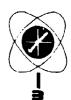
- E-BEAM HIGH ELECTRON DENSITY POSSIBLE FOIL SURVIVABILITY



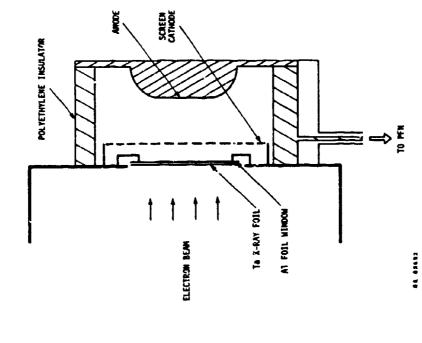
-



c) Corona and Dielectric Surface Discharge b) Corona Discharge d) UV Sparks *******

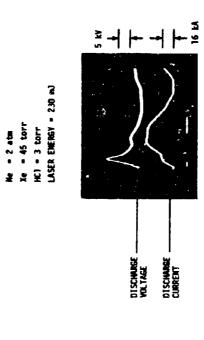


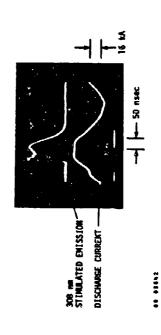
## SCHEMATIC DIAGRAM OF MSNW X-RAY PREIONIZED XECL DISCHARGE LASER





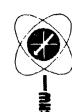
## DIAGNOSTIC TRACES OF MSNW X-RAY PREIONIZED XECL DISCHARGE LASER





### ENERGY DENSITY SCALING

- UTILIZE MIXTURES THAT HAVE HIGHER BRANCHING RATIOS
- $Xe^* + HgBr_2 + HgBr^* + Xe + Br$
- DOESN'T WORK WELL WITH UV
- X-RAY
- E-BEAM
- PRESSURE SCALE



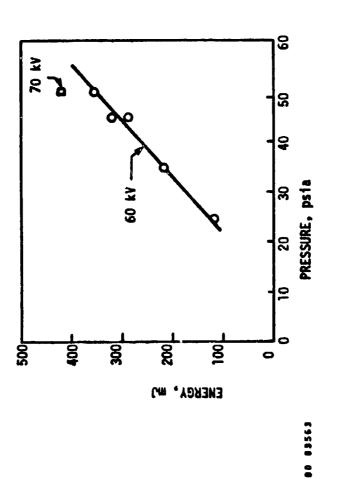
# COMPARISON OF HGBR GAIN/LOSS MEASUREMENTS TO MSNW CODE PREDICTIONS

	Experiment 1	Model	
Mixture	900 torr Ne 100 torr N ₂ 2.3 torr HgBr ₂	900 torr Ne 100 torr N ₂ 2.3 torr HgBr ₂	1800 torr Ne 200 torr N ₂ 4.6 torr HgBr ₂
E/N(V-cm ² )	1.5 x 10 ⁻¹⁶	1.5 x 10 ⁻¹⁶	1.5 x 10 ⁻¹⁶
Current Density (A/cm²)	150*	150	150
Small Signal Gain (%cm ⁻¹ )	9-9-9	ω	16

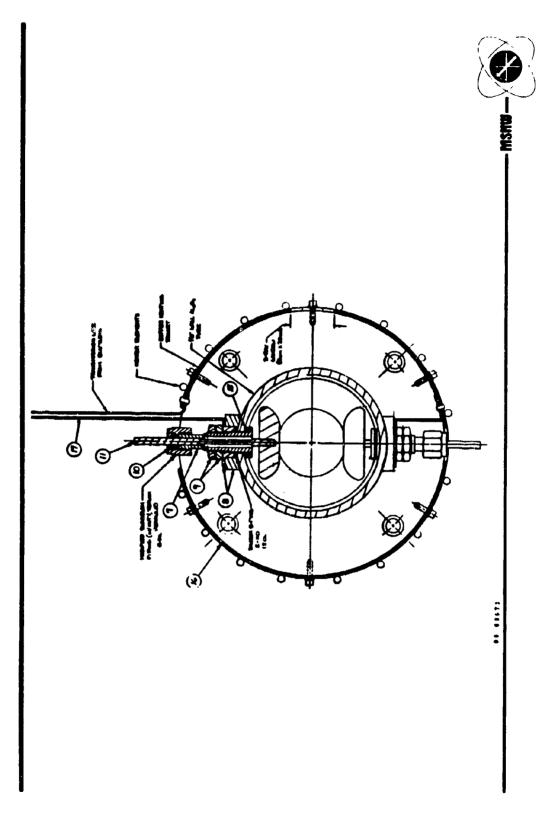
bischarge current in fringe of laser active volume assumed to be 50 percent of total.

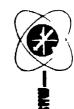


## MSNW UV PREICNIZED XECL LASER PERFORMANCE



Ne + 3% Xe + 0.2% HCl; C = 25 nF; ELECTRODE GAP = 3 cm.





### HGBR LASER SCALING STATUS

- CODE UNDER DEVELOPMENT
- REASONABLE AGREEMENT
- FABRICATED HIGH PRESSURE HgBr LASER
- DEMONSTRATED X-RAY PREIONIZED HgBr LASER
- OPTIMIZATION IN PROGRESS

TITLE: PARAMETERIZATION STUDIES OF HGBR LASERS
CS LIU

SPONSOR: NOSC (MONITORED BY UNR)

CONTRACT PERIOD: MARCH 1980 - OCTOBER 1980 (8-MONTHS)

Westinghouse R&D Center 1310 Beulah Road Pittsburgh PA 15235

### PARAMETERIZATION STUDIES OF HGBR LASERS

During the past several years, mercury bromide has shown great promise as a high efficiency, high energy tunable laser in the bluegreen region of the spectrum. Lasing in this medium has been demonstrated using a number of excitation techniques; optical pumping, theam, theam sustained discharge, and self-sustained discharge. The most promising technique thus far seems to be a UV-preionized self-sustained discharge, which has demonstrated energies of \$100 mJ, and efficiencies of \$1 percent.

Although there has been some speculation about the details of the excitation and lasing kinetics, optimization of this laser system still depends on empirical parameterizations. Optimization studies made to date were limited by the apparatus available. A number of important questions remain: for example, the independent effect of temperature and of HgBr₂ density, and the effect of buffer gas density on laser kinetics and discharge characteristics.

Attempts to establish parameters for a number of variables in the mercury bromide system have been severely limited in range. Buffer gas pressures have extended up to \$1 amagat, with temperatures up to \$200\cappa^3\textsc{C}\$ and \$\text{HgBr}_2\$ densities to \$5 \times 10^{16}/cm^3\$. This range of parameters has been determined basically by the type of apparatus used: that is, \$0-ring seals, simple Pyrex structures, and stainless steel electrode materials. The density of \$\text{HgBr}_2\$ has been adjusted by varying the \$\text{temperature}\$ of the laser tube; thus the gas temperature and the \$\text{HgBr}_2\$ density were not independent variables. Both the temperature and pressure affect the laser kinetics, through the collision rates, for instance. In addition, the buffer gas density affects the discharge characteristics by changing both the E/N and the glow voltage. As the length of the discharge region is increased to produce larger volumes, the discharge impedance decreases; it would be advantageous to increase the impedance by \$\text{ncreasing}\$ the buffer gas density.

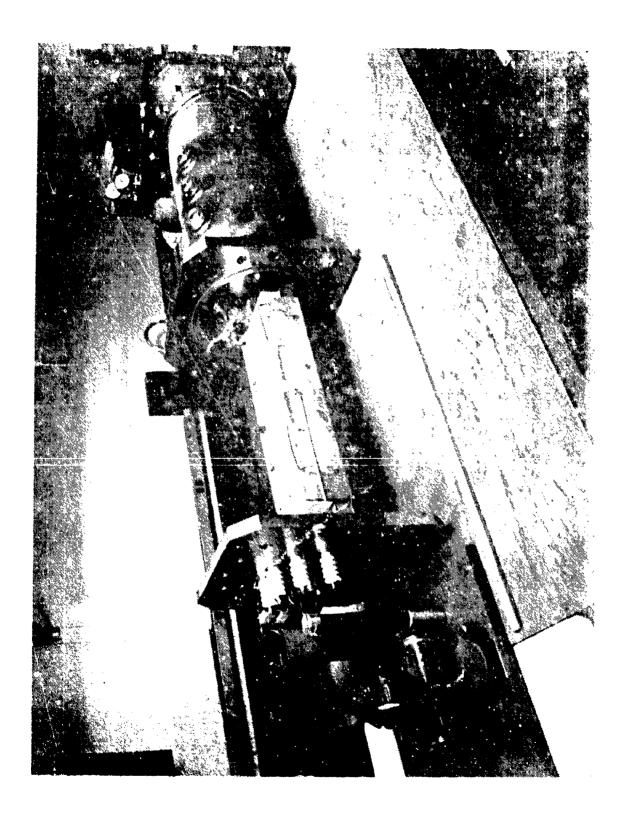
Ideally, the buffer gas density, temperature, and energy loading would be varied independently, so as to optimize the performance of the HgBr laser. We have available at Westinghouse an apparatus which will enable us to make measurements over the required parameter range.

PROGRAM OBJECTIVE: TO OPTIMIZE THE LASER PERFORMANCE OF HGBR SYSTEMS

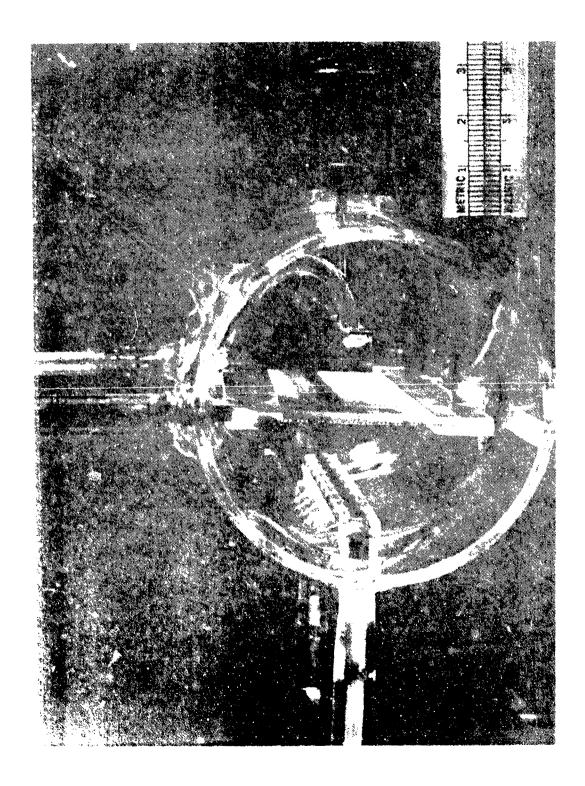
- PROGRAM TASKS: 1. OPTIMIZE THE PERFORMANCE UF A HGBR LASER
  BY VARYING THE BUFFER GAS SPECIES AND
  PRESSURE (UP TO 10 ATM)
  - 2. DEFERMINE THE OPTIMUM VAPOR DENSITY OF THE HGBR2 FOR THE BEST PERFORMANCE OF A HGBR LASER
  - 3. DETERMINE THE OPTIMUM OPERATING TEMPERATURES
    FOR HGBR LASERS (UNDER SUPER-HEAT CONDITIONS)

### LASER DISCHARGE TUBE REQUIREMENTS:

- 1. PRESSURE CAPABILITY: UP TO 10 ATM
- 2. TEMPERATURE CAPABILITY: ~300°C
- 3. CHEMICAL INERTNESS: SEALED OFF QUARTZ-MOLY TUBES









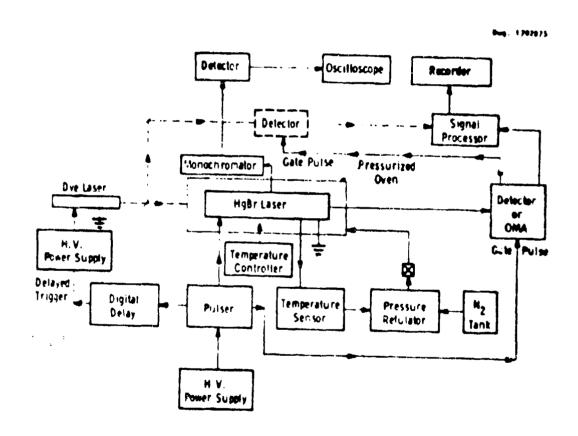


Figure 3 — Spectroscopic apparatus designed to measure the fluorescence and absorption of pulsed HgBr discharges.

### TLHG EXCIMER LASER

LASER MEDIUM: HG + TL

TEMPERATURE: ~ 900°C

PRESSURE: ~ 4 ATM

MERCURY DENSITY: 3 x 1019 cm-3

THALLIUM DENSITY: ~ 1017 cm-3

DISCHARGE VOLUME:  $0.5 \times 1.0 \times 8.0 = 4 \text{ cm}^3$ 

PEAK CURRENT: 50 A

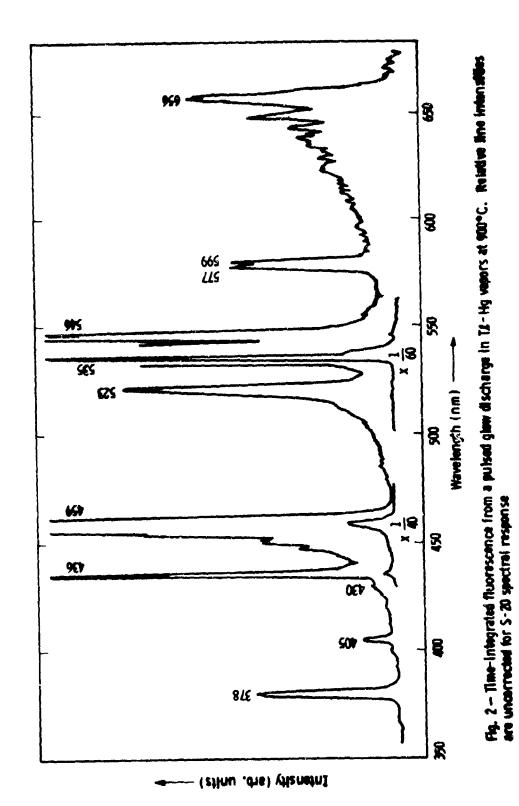
PEAK CURRENT DENSITY: 12.5 A cm⁻²

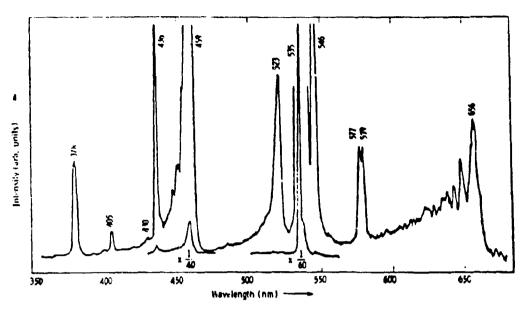
CURRENT PULSE WIDTH: ~ 100 NS FWHM

CAPACITOR CHARGE VOLTAGE: 15 KV

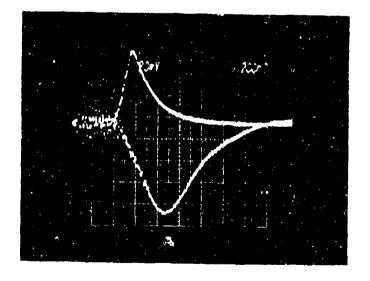
6LOW VOLTAGE: ~12 KV (EST.)

FLUORESCENCE: BLUE-GREEN EMISSION OBSERVED VISUALLY



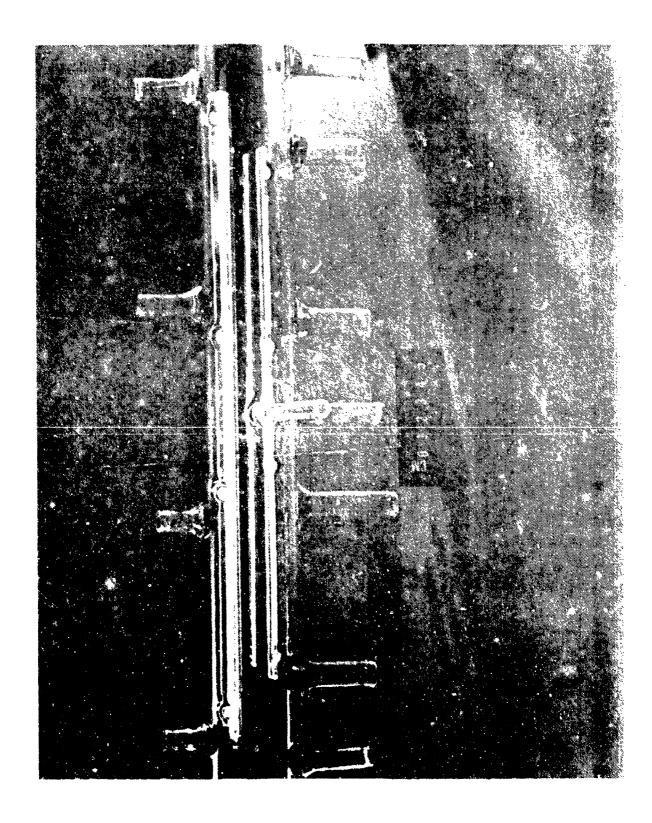


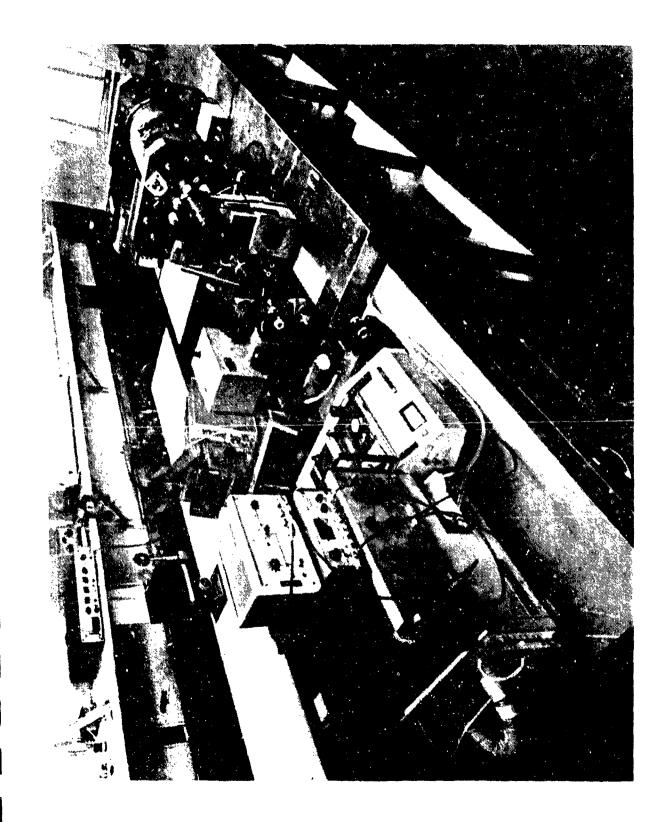
8.9  $\pm$ - Time-integrated fluorescence from a pulsad glow discharge in TZ-Hg vapors at 900°C. Relative line intensities are uncorrected for 5-20 spectral response



λ = 458 nm
920°C

Absorption





### HgBr₂/HgBr Dissociation Laser

E. Schimitschek Naval Ocean Systems Center San Diego, CA 92152

During the past six months, work was performed to increase the pulse energy, and the repetition rate and to characterize gain and extraction efficiency at wavelengths within the B-X transition region.

To date, the following results were obtained:

- 1) a 1.2 liter, UV-preionized HgBr₂/HgBr discharge laser device has been constructed, with a driver energy of up to 100 Joules. Initial testing will begin in May 1980; the goal is to extract up to 1 Joule of laser energy
- 2) a 60 cm³, UV-preionized HgBr₂/HgBr discharge laser was built with an interval cross-flow blower. This device was successfully operated up to 100 pps with no drop-off in pulse energy. The pulse energy measured so far is 30 mJ. Optimization now performed should bring the pulse energy up to 50 mJ. At that point, self-heated operation will begin.
- 3) gain has been measured as function of wavelength and  $N_2$  partial pressure. Narrow-band extraction between 490-505 nm will be undertaken by injection-locking with a tunable dye laser.

Work Performed By:

D. ALTMAN

R. KRAUTWALD J. CELTO

E. SCHIMITSCHEK

T. SHAY

ON-GOING EFFORTS:

*MEASUREMENT OF GAIN, ABSORPTION, NARROW-LINE EXTRACTION EFFICIENCY

*REP. RATE UP-SCALING

*DISCHARGE VOLUME UP-SCALING

HgBrz/HgBr CRITICAL ISSUES

•EFFICIENCY --- 1%

*REPETITION RATE --- 100 PPS

*ENERGY/PULSE

*LIFETIME --- 1010 SHOTS

1

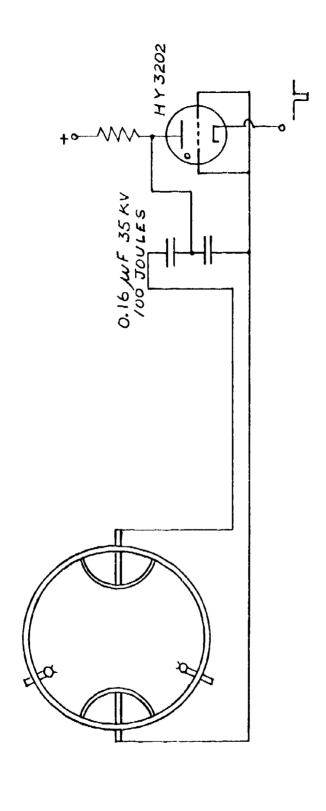
I

ENERGY /PULSE

*90 MJ DEMONSTRATED WITH 0.8J/LITER AT 1.2 AMAGAT

*PRESENTLY UNDER CONSTRUCTION 1.2 LITER DEVICE WITH ENERGY STORAGE OF 100 JOULES

*PLANNED TO OPERATE MAY 80



ONE LITER HyBrd/HyBr DISSOCIATION LASER

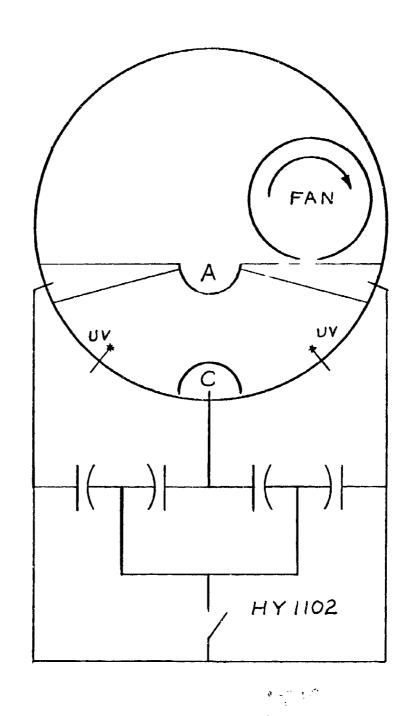
### REPETITION RATE

 ullet 60 cm 3  device with internal cross-flow blower has been constructed

*SUCCESSFULLY OPERATED AT UP TO 100 PPS WITH AVERAGE POWER OF ABOUT 1 WATT

*OPTIMIZATION (ENERGY/PULSE, EFFICIENCY) NOW IN PROGRESS

*FUTURE PLANS INCLUDE SELF-HEATED OPERATION



100 Hz Hg Bx LASER

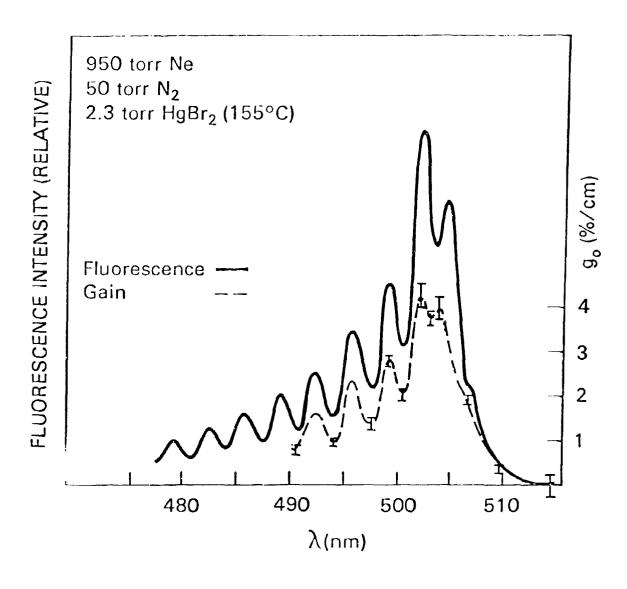
**EFFICIENCY** 

*0.95% LASER EFFICIENCY AT 50 MJ DEMONSTRATED

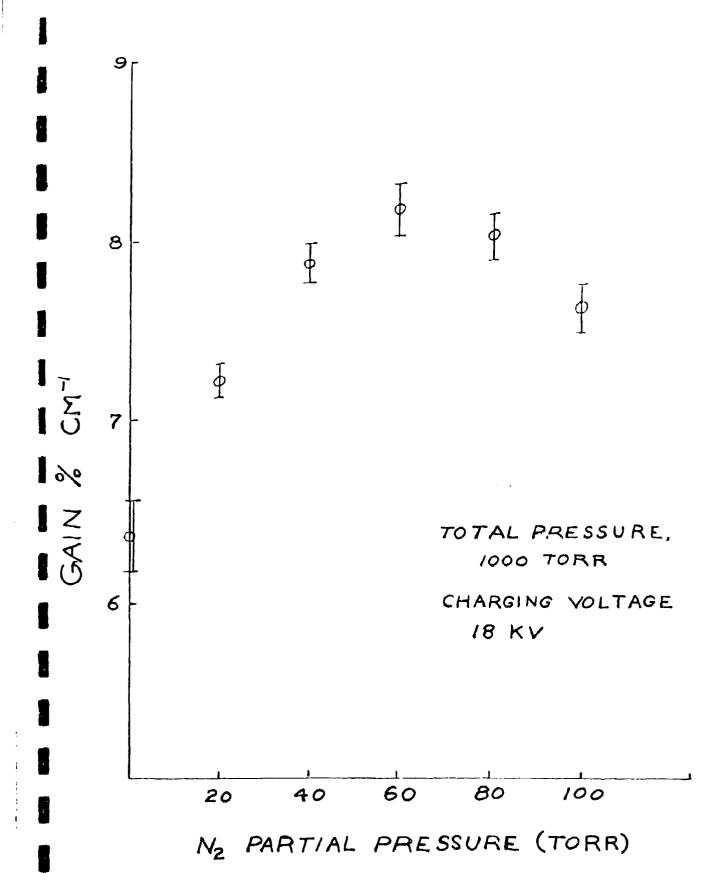
*EFFICIENCY IS COMPLICATED FUNCTION OF TOTAL GAS PRESSURE, BUFFER GAS COMPOSITION, TEMPERATURE (HgBrz PRESSURE), PREIONIZATION, IMPEDANCE MATCH OF DRIVER/PLASMA

*EFFICIENCY HAS TO BE DEMONSTRATED UNDER CONDITION OF NARROW-BAND EXTRACTION

*EFFORTS UNDERWAY AT NOSC AND UNDER CONTRACT



Gain and fluorescence profile of the HgBr B  $\rightarrow$  X transition. Conditions as indicated.

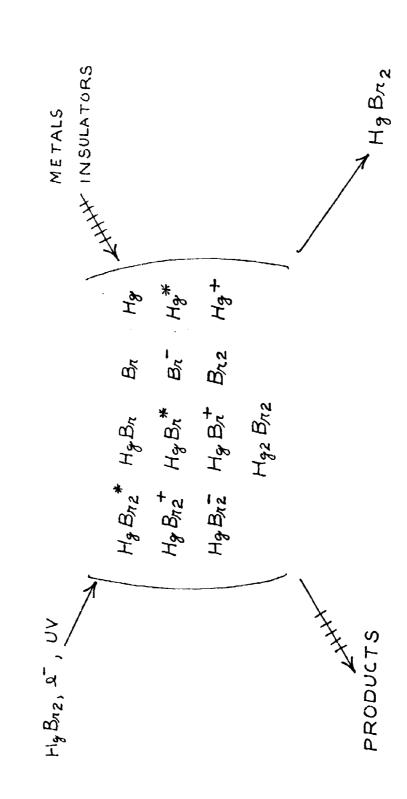


LIFETIME

*LIFETIME OF COMPONENTS OTHER THAN LASER MEDIUM: COMMON TO ALL FAST DISCHARGE LASERS

*LIFETIME OF LASER MEDIUM AND ITS EXCITED DISSOCIATION PRODUCTS IN CONTACT WITH METALS AND INSULATORS *IN-DEPTH CONTRACTUAL STUDY BEING NEGOTIATED UNDER JOINT DARPA/NAVY FUNDING

*MOST CRITICAL ISSUE



### BLUE-GREEN OPTICAL CONVERSION OF XeF* ( DARPA / ONR )

RICHARD HEINRICHS *
HOWARD HYMAN
IRVING ITZKAN
DANIEL TRAINOR

† SUPPORTED BY AERL IRAD UNDER AERL/MIT
COOPERATIVE PROGRAM

J3961

AVCO Everett Research Laboratory Inc 2385 Revere Beach Parkway Everett MA 02149

ZOAVCO EVERETT

### TO THE BLUE-GREEN THROUGH SRS*

This presentation discussed the generation of blue-green laser radiation ( $\lambda \sim 470\,\mathrm{nm}$ ) utilizing the technique of Stimulated Raman Scattering (SRS) of XeF* laser photons in molecular gases. Our specific approach involves sequential 1st Stokes conversion through two separate steps in  $H_2$  and  $D_2$ .

The short pulse, low energy experiments were performed with a Lumonic Exciplex Laser (model TE-261). To achieve high laser flux, it was necessary to alter the supplied optics to include Brewster windows and an unstable cavity. In this modified configuration, typical output for XeF* was 10-20 mj in 6 nsec which, when focussed by a 50 cm f.L. plano convex lens, provided -3 x 10⁹ watts/cm².

Our high pressure hydrogen cells are constructed from two-inch diameter steel shock tube sections of approximately 40 cm path length. These cells are fitted with high grade optical quality UV quartz windows to allow the pump beam to enter and the resulting stimulated Raman emission to exit.

To date, we have performed stimulated Raman scattering experiments whereby XeF* laser photons (351 and 353 nm) have been efficiently converted to longer wavelengths using molecular hydrogen. For example, we have observed 1st Stokes energy conversion in a simple one pass configuration of ~44%, with peak power efficiencies of near 66%. This single pass one-step conversion to 411 and 414 nm

in hydrogen has been characterized with respect to gas pressure, laser intensity, and active cell length. These quantitative experimental observations are in reasonable agreement with theoretical expectations.

Experiments on the second step of the two-step Raman conversion processes showed us to be intensity limited. Experiments to test the approach were, therefore, performed with KrF and showed >70% pump depletion. Recently, experiments were performed with a 0.6J, 400 nsec laser in single step conversion utilizing H₂. These results showed ~35% conversion of XeF* radiation to 1st Stokes at 413nm in good agreement with our expectations. This work is in progress.

### BLUE - GREEN OPTICAL CONVERSION OF XeF*

### MOTIVATION

• PROVIDE ≥ 1% EFFICIENT BLUE — GREEN LASER FOR GROUND BASED SUBMARINE COMMUNICATION MISSION

### GOAL

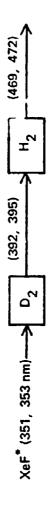
- DETERMINE FEASIBILITY OF UNIQUE TWO STEP MOLECULAR
  RAMAN APPROACH TO MEET EFFICIENCY REQUIREMENT
- DEMONSTRATE RAMAN CONVERSION TO THE BLUE -- GREEN UTILIZING A 1 TO 10 J ONE METER Xef* LASER AS A PUMP

J3962

ZAVCO EVERETT

### AERL APPROACH

TWO STEP (SEQUENTIAL 1ST STOKES) MOLECULAR RAMAN CONVERSION



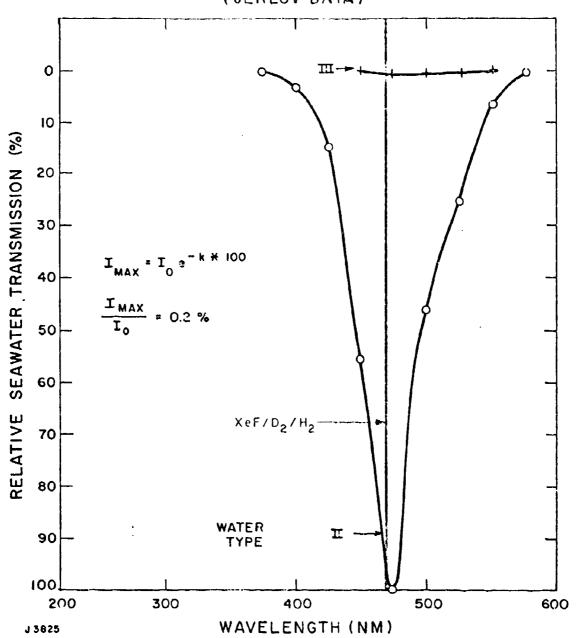
KEY-FEATURES

TWO DIFFERENT MOLECULAR SPECIES -> WAVELENGTH FLEXIBILITY

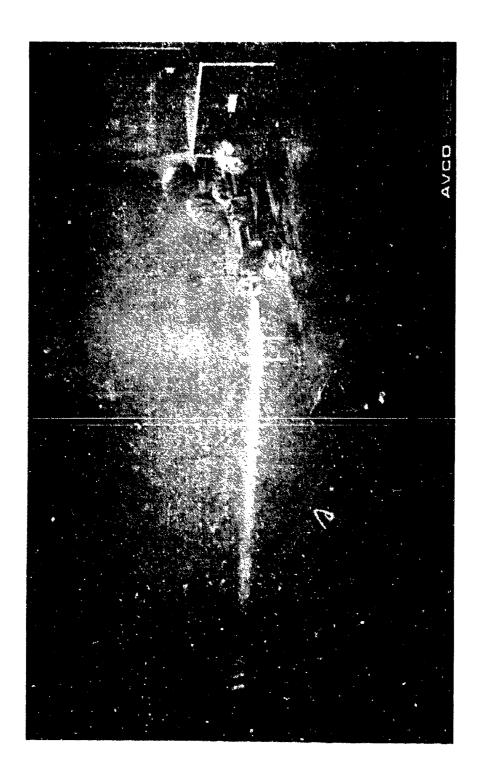
(HIGHER-ORDER STOKES, 4-WAVE) OPTIMIZATION ON 1ST STOKES - MINIMIZE COMPETITIVE PROCESSES

13964

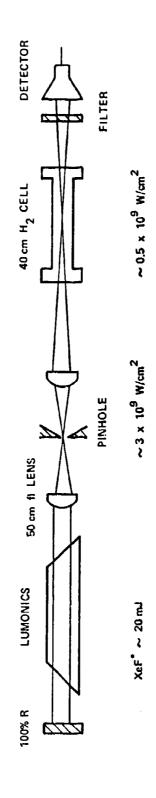
### OCEAN WATER TRANSMISSION TO 100 METERS (JERLOV DATA)



**MAVCO** EVERETT

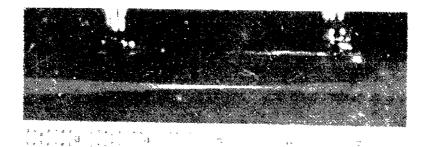


# SCHEMATIC OF EXPERIMENTAL TECHNIQUE (SINGLE STEP EXPERIMENTS)

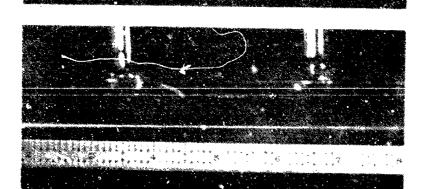


13859

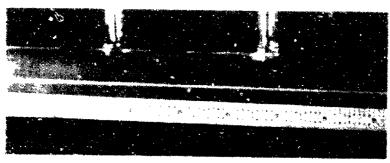
### FOCAL LENGTH VARIATION



20 cm FOCUS



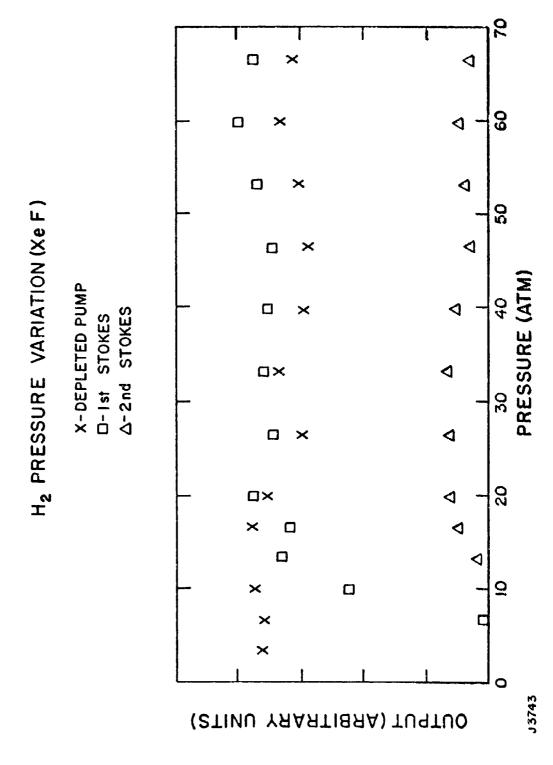
50 cm FOCUS



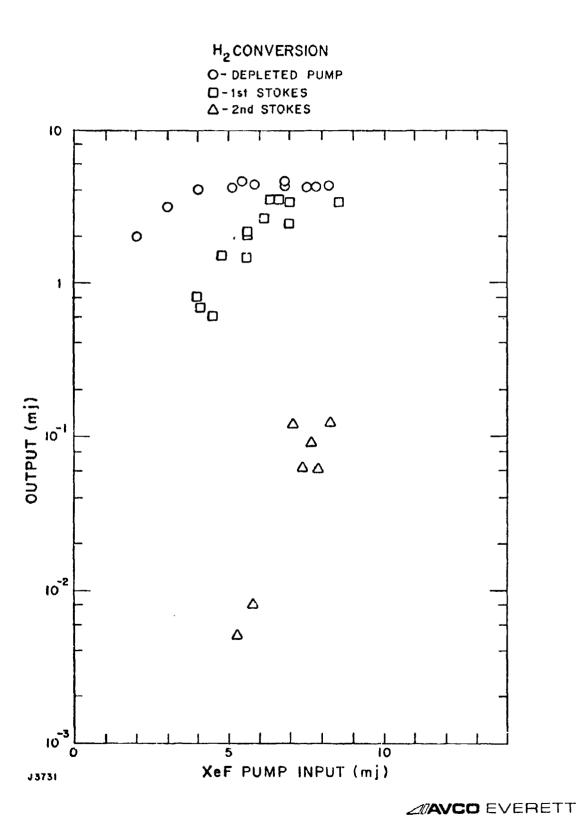
135 cm FOCUS

33747

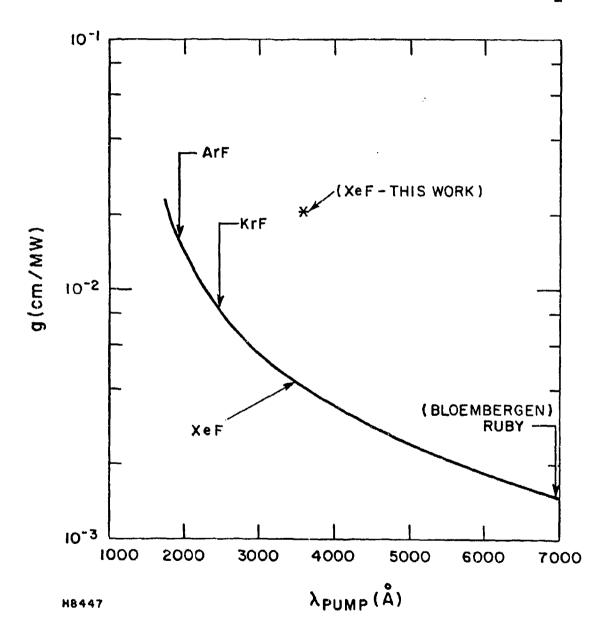
ZEAVCO EVERETT



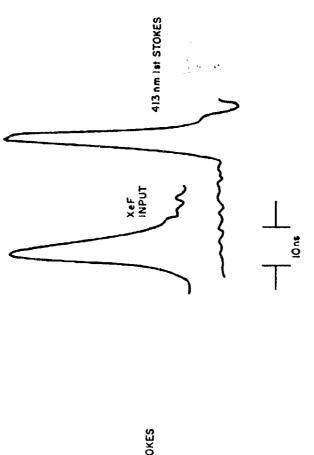
227

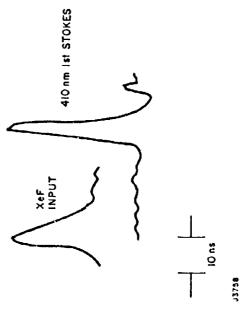


### FIRST STOKES GAIN FOR FORWARD SRS IN H2



**MAVCO EVERETT** 





### ONE STEP XeF/H2 CONVERSION EFFICIENCIES

E_{IN} (mJ) 9.6

 $E_{OUT}$  (mJ) 4.2 (S₁), ~ 0 (S₂)

ENERGY EFF (%) 44

POWER EFF (%) 66

POWER PHOTON EFF (%) 76

J3960

**MAYCO EVERETT** 

### PROGRAM STATUS (MARCH 1980)

SMALL SCALE EXPERIMENTS (≤ 40 mJ, ~ 6 nsec)

- ONE STEP
  - EFFICIENT 1ST STOKES CONVERSION IN  ${
    m H_2}$  (66%)
- TWO STEP
  - $XeF/H_2/H_2$  (EFF  $\simeq 29\%$  PUMP POWER LIMITED)
  - KrF/D $_2$ /H $_2$  ( > 70% DEPLETION OF S $_1$ (D $_2$ ) IN H $_2$  CELL)

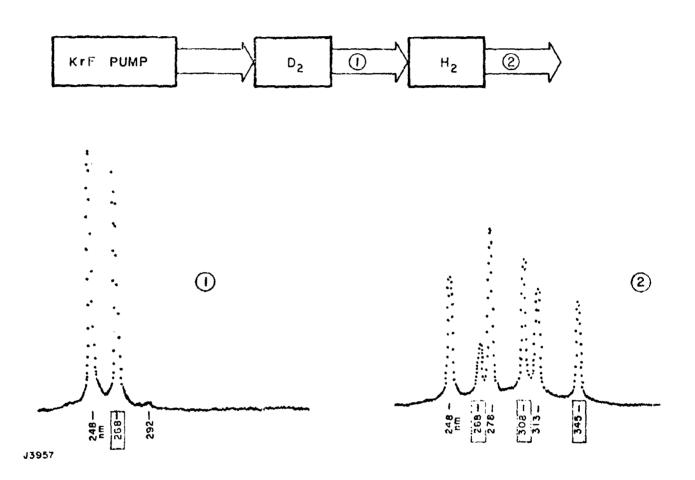
ONE METER DEVICE EXPERIMENTS (  $\geq$  1 J, 0.4  $\mu$  sec)

- ONE STEP
  - XeF/H₂ (IN PROGRESS)

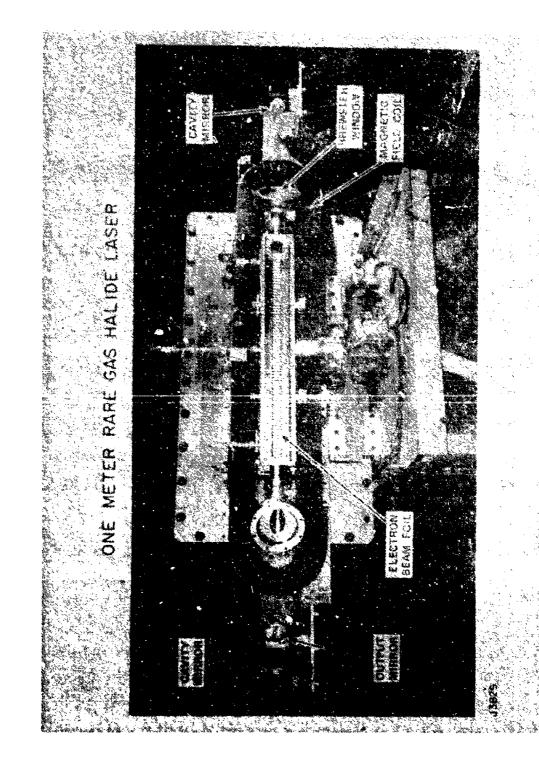
**J3963** 

**MAYCO** EVERETT

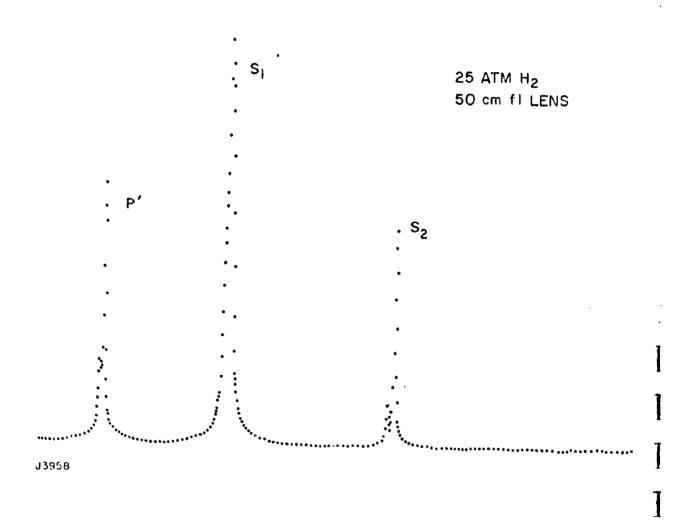
### TWO STEP KrF/D2/H2 RAMAN CONVERSION



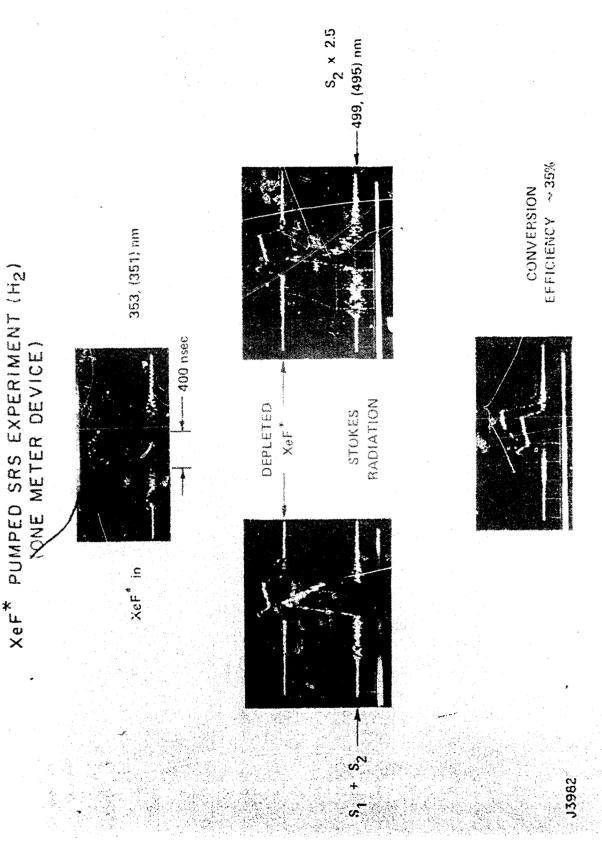
ZNAVCO EVERETI



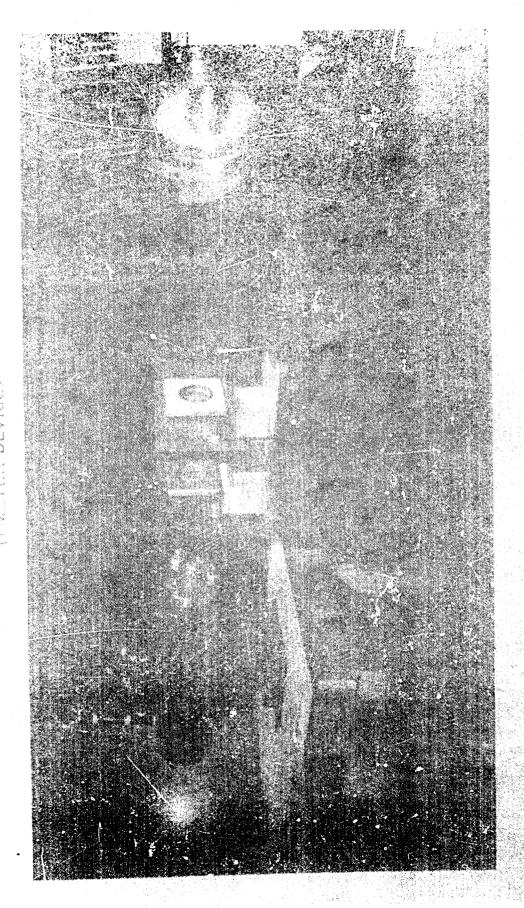
### LONG PULSE LENGTH XeF * SRS EXPERIMENT (H2)



ZOAVCO EVERETT



BLUE-OREEN OPTION CONVERSION OF Xer-X



### SCALING STUDIES OF EFFICIENT RAMAN CONVERTERS

E. A. STAPPAERTS, H. KOMINE, J. B. WEST, W. H. LONG, JR.

### NORTHROP CORPORATION NORTHROP RESEARCH AND TECHNOLOGY CENTER One Research Park Palos Verdes Peninsula CA 90274

### ABSTRACT

A program of analytical and experimental investigations has been initiated recently with DARPA sponsorship to study the scalability of molecular Raman converters for the ground-based blue-green source. Based on existing data, preliminary design parameters are obtained for a Raman oscillator-amplifier system which converts the XeF laser wavelengths into blue-green. Thermal effects in Raman amplifiers are discussed together with gas flow characteristics needed for good beam quality.

The primary laser optical requirements with respect to Raman converter design are discussed in terms of spatial and temporal uniformity, beam divergence, and spectral characteristics. A series of experiments at an intermediate energy range (20-50J) will address various scaling issues including spectral narrowing of the primary laser and Raman conversion efficiency.

# SCALING STUDIES OF EFFICIENT RAMAN CONVERTERS

March 1980

E. A. Stappaerts
H. Komine
J. B. West
W. H. Long, Jr.

Northrop Corporation
Northrop Research and Technology Center
One Research Park
Palos Verdes Peninsula, California 90274

1

### **OBJECTIVE:**

:

INVESTIGATE THE SCALABILITY OF EFFICIENT RAMAN

CONVERSION OF XeF (XeCI) LASER WAVELENGTH INTO

THE BLUE-GREEN REGION

APPROACH:

NOVEL RAMAN OSCILLATOR-AMPLIFIER SYSTEM BASED

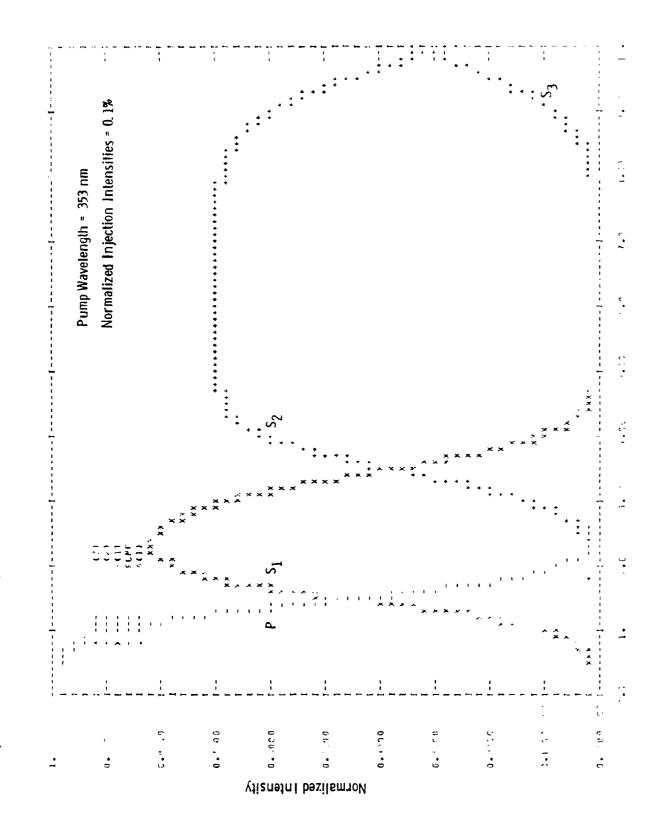
ON SELECTIVE MULTIPLE-STOKES-ORDER CONVERSION

IN MOLECULAR GASES



TABLE OF RAMAN SHIFTED XeF/XeCI LASER WAVELENGTH IN THE BLUE-GREEN REGION

	WAVELENGTH (nm)	H (nm)
PUMP RAMAN SHIFT	XeF 351 / 353	XeCI 308
2 H ₂	496 / 500	
H ₂ + D ₂	468 / 472	
2 D ₂	444 1 447	
3 Н2		009
2 H ₂ + D ₂		472
$H_2 + 2D_2$		447



### **PROGRAM ELEMENTS**

## RAMAN CONVERTER SYSTEM ANALYSIS

- **DESIGN CONSTRAINTS**
- NOM INAL OPERATING PARAMETERS
- THERMAL EFFECTS

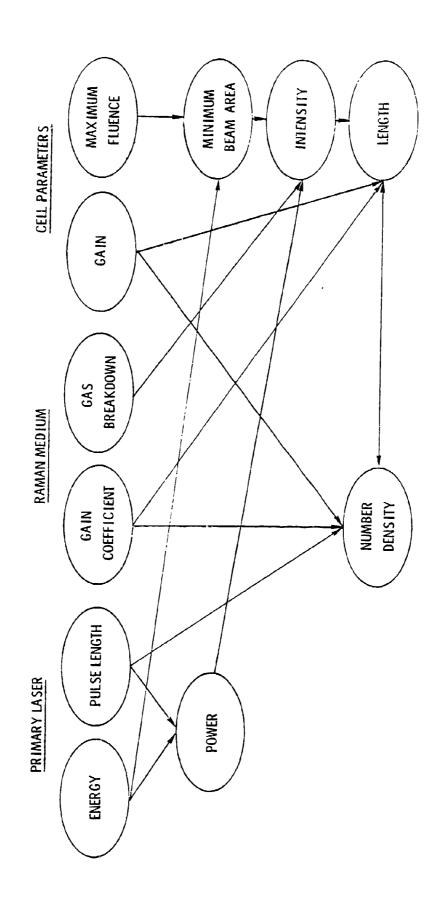
## PRIMARY LASER SYSTEM REQUIREMENTS

- **BEAM QUALITY AND PULSE SHAPE**
- SPECTRAL WIDTH CONTROL

# INTERMEDIATE ENERGY SCALING EXPERIMENTS

FY 80-81





RAMAN OSCILLATOR-AMPLIFIER SYSTEM DESIGN CONSTRAINTS

WOLVERING CONT.

SUMMARY OF DESIGN PARAMETERS

	H ₂	
	0SC	АМР
PUMP ENERGY (J)	2.	1000
INJECTED ENERGY (J)	:	*050*
LENGTH (m)	2	4
BEAM AREA (cm ² )	1.7 * 10-4	200
TEMPERATURE (K)	300	300
PRESSURE (atm)	10	က
GAIN g (cm/W)	2 * 10-8	2 * 10-8
WINDOW FLUENCE (J/cm ² )	Ŋ	S

*PER STOKES ORDER

## THERMAL EFFECTS IN RAMAN AMPLIFIERS

## MOLECULAR VIBRATION RELAXATION

QUENCHING RATE [F. DeMartini and J. Ducing, Phys. Rev. Lett., 17, 117 (1966)]:

$$p\tau = (1060 \pm 100) \times 10^{-6} atm-sec @ T = 300 K$$

$$p = 3 \text{ atm} \rightarrow \tau = 0.35 \text{ ms} \ll 1/PRF (100 \text{ Hz})$$

## TEMPERATURE RISE/DENSITY GRADIENT

- UP TO  $\sim 40\%$  Average power deposition in Raman Medium
- THERMAL LENS/BEAM DISTORTION EFFECTS WITHOUT FLOW



# RAMAN AMPLIFIER FLOW SYSTEM CHARACTERISTICS

GAS TEMPERATURE RISE PER PULSE  $\sim 2$  K OVER 0.35 m s

NEGLIGIBLE PRESSURE (SHOCK) WAVES → FLUSH FACTOR ~

NO CHEMICAL CLEANUP PROBLEMS

LOWER HEAT LOADING COMPARED TO FIIMARY LASER SYSTEM

SIMPLER FLOW SYSTEM COMPARED TO PRIMARY LASER SYSTEM

COMPRESSOR POWER ≤ 10% OF PRIMARY LASER POWER SUPPLY



## PRIMARY LASER OPTICAL REQUIREMENTS

BEAM DIVERGENCE: NEAR DIFFRACTION LIMIT

SPATIAL BEAM UNIFORMITY: < ± 20% VARIATION

TEMPORAL PULSE UNIFORMITY: NEARLY RECTANGULAR PULSE < ± 20% DISTORTION

WAVELENGTH: SINGLE LINE

 $\leq 0.2 \text{ Å } (\Delta v \leq 0.8 \text{ cm}^{-1} \text{ @ } \lambda = 500 \text{ nm})$ SPECTRAL WIDTH:



# INTERMEDIATE ENERGY SCALING EXPERIMENTAL PROGRAM

### PRIMARY LASER

DARPA/NRTC SHORT WAVELENGTH ADVANCED TEST BED (SWAT) LASER

ELECTRON BEAM PUMPING/MAGNETIC GUIDE FIELD

XeF (XeCI) OPERATION AT 20-50 J

### SPECTRAL CONTROL

SINGLE LINE OUTPUT VIA INJECTION-LOCKING

NARROW LINEWIDTH

### RAMAN CONVERSION

SECOND-ORDER RAMAN OSCILLATOR-AMPLIFIER SYSTEM

H₂ GAS



## SWAT LASER CHARACTERISTICS

### **ELECTRON GUN**

TYPE: COLD CATHODE FIELD EMISSION DIODE

CIRCUIT: THREE-STAGE MARX BANK WITH PEAKING

CAPACITOR

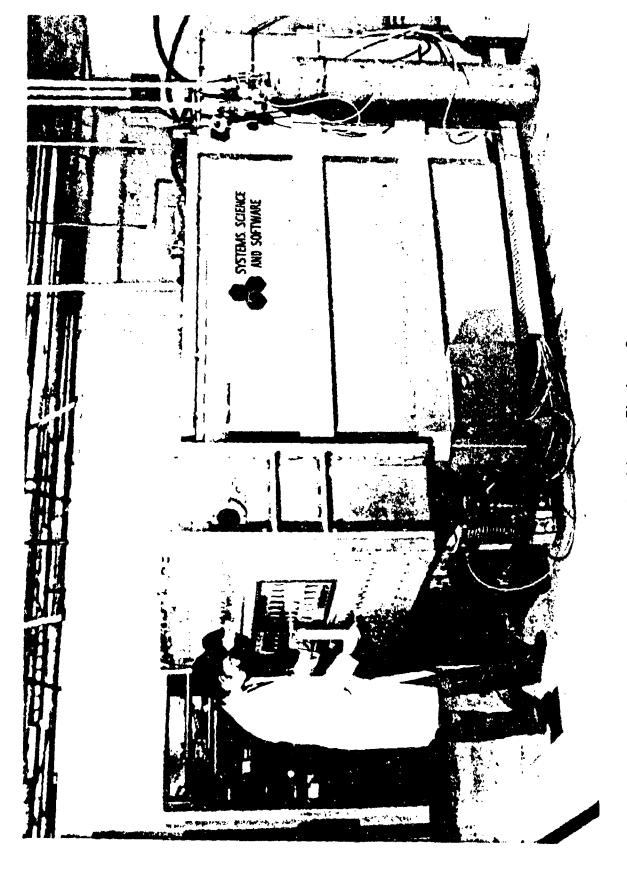
BEF. A VOLTAGE: 360 KV NOMINAL

BEAM CURRENT: 22 A FOR 400 ns PULSE

12 A FOR 800 ns PULSE

8 A FOR 1.2 µs PULSE





Swat Laser Electron Gun

## SWAT LASER CHARACTERISTICS

### LASER PERFORMANCE

ACTIVE VOLUME: 10 LITERS

KrF (50 J; 800 ns) WITH [1290 Ar, 100 Kr,  $2 \, \mathrm{F_2}$ ] MIXTURE @  $10 \, \mathrm{A/cm^2}$ 

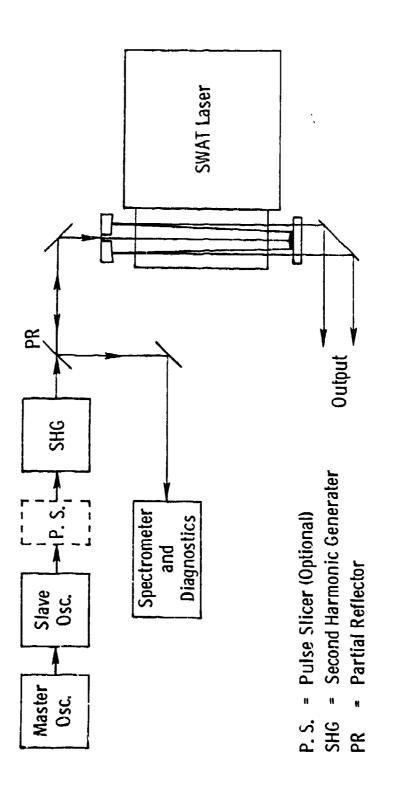
XeF (1. 7 J/  $\varrho$ ; 700 ns) WITH (2280 Ne, 7.5 Xe, 2.5 NF $_{\rm 3}$ ] MIXTURE @ 15 A/cm²

### **OPTICAL SYSTEM**

POSITIVE BRANCH CONFOCAL UNSTABLE RESONATOR

NARROW LINEWIDTH INJECTION-LOCKING





1

Ground Based Xe C1-Pb Blue Green Source

N. Djeu

Naval Research Laboratory Washington, D. C. 20375

### **ABSTRACT**

The Pb vapor Raman converted XeCl laser is a potential candidate for a ground based blue-green strategic communications system. In addition to having an intrinsic efficiency of 6%, the e-beam pumped Xe Cl laser can deliver high energy pulses in a narrow bandwidth. Coupled with high efficiency for Raman conversion, the overall system should be capable of producing the required power at the specified efficiency and output bandwidth.

In earlier experiments high conversion efficiency ( $\sim 50\%$ ) was observed with short ( $\sim 20 \text{nsec}$ ) Xe Cl laser pump pulses. Here we report the efficient conversion of 400 nsec long XeCl pump pulses. With an oscillatoramplifier configuration, an initial XeCl pulse of 200 mJ produced 80 mJ in the blue-green, giving an energy conversion efficiency of 40%. Scale-up demonstrations at the 10 J level will be pursued jointly by NRL and Maxwell Laboratories in the near future.

The question concerning the acoustic waves set up by the de-excitation of metastable Pb atoms has been examined through some order of magnitude calculations. The results show that the amplitude of the initial pressure waves has a quadratic dependency on the rate of heat release. To obtain a realistic assessment of the magnitude of the acoustic waves in the Pb vapor cell, one must know the rate of electronic quenching in Pb as well as the mechanical impedance of the wall material.

### **GROUND BASED**

## XEC1-PB BLUE-GREEN SOURCE

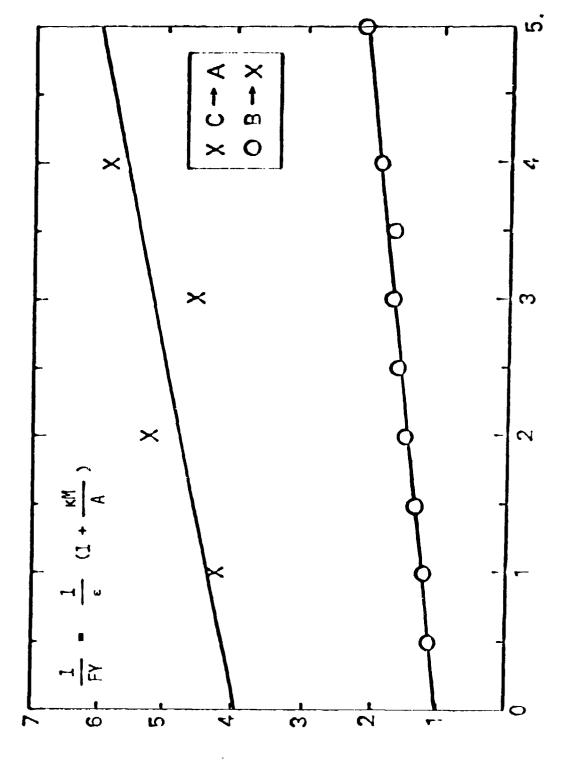
- SUMMARY OF STATUS OF E-BEAM PUMPED XECL LASER
- RESULTS ON CONVERSION OF 400 NSEC XECT PUMP PULSE
- PLANS FOR CONVERSION OF 10 J XECL PUMP PULSE
- ESTIMATES OF MAGNITUDE OF ACOUSTIC WAVES IN PB YAPOR CELL



June 1 June 10 July 1

7

Same of the same of the same of the same of the same of the same of the same of the same of the same of the same of the same of the same of the same of the same of the same of the same of the same of the same of the same of the same of the same of the same of the same of the same of the same of the same of the same of the same of the same of the same of the same of the same of the same of the same of the same of the same of the same of the same of the same of the same of the same of the same of the same of the same of the same of the same of the same of the same of the same of the same of the same of the same of the same of the same of the same of the same of the same of the same of the same of the same of the same of the same of the same of the same of the same of the same of the same of the same of the same of the same of the same of the same of the same of the same of the same of the same of the same of the same of the same of the same of the same of the same of the same of the same of the same of the same of the same of the same of the same of the same of the same of the same of the same of the same of the same of the same of the same of the same of the same of the same of the same of the same of the same of the same of the same of the same of the same of the same of the same of the same of the same of the same of the same of the same of the same of the same of the same of the same of the same of the same of the same of the same of the same of the same of the same of the same of the same of the same of the same of the same of the same of the same of the same of the same of the same of the same of the same of the same of the same of the same of the same of the same of the same of the same of the same of the same of the same of the same of the same of the same of the same of the same of the same of the same of the same of the same of the same of the same of the same of the same of the same of the same of the same of the same of the same of the same of the same of the same of the same of the same of the same o



NEON PRESSURE (atm)

INACHZE OF FLUORESCENCE YIELD

## TEMPERATURE MODIFICATION

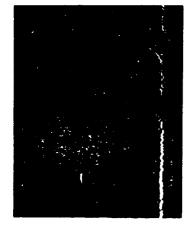
## OF E-BEAM PUMPED XEC1 LASER

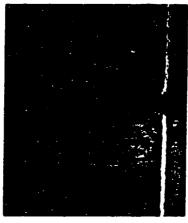
- PERFORMANCE OF THE XEC1 LASER IN THE RANGE OF -20°C TO 160°C HAS BEEN INVESTIGATED,
- WITHIN EXPERIMENTAL ERROR, NO CHANGE IN THE OUTPUT OF THE XECI LASER WAS OBSERVED.
- THE USE OF DCI GIVES 15% IMPROVEMENT OVER HC1 THROUGHOUT THE TEMPERATURE RANGE.



Ä









### E-BEAM PUMPED XECI LASER

- FORMATION INTO B AND C STATES TAKES PLACE AT AN EFFICIENCY OF 17%
- BEST INTRINSIC LASER EFFICIENCY OBSERVED TO DATE IS 6% MAINLY BECAUSE OF TRANSIENT ABSORPTION ( $\sim 0.1~{\rm Gain}$ )
- LASER OPTIMIZES AT ROOM TEMPERATURE AT A TOTAL PRESSURE OF 4 ATM (NE:XE:HCl = 98,9:1.0:0.067)
- POSSIBLE IN A LARGE PORTION OF 307.8-308.4 NM



- Trainer

-

N R L

### PB VAPOR RAMAN CONVERTER

XEC1 AT 308 NM	459 NM	1200° C	10 ¹⁷ cm ⁻³	3 x 10 ⁻⁸ cm W ⁻¹
PUMP	Оитрит	TEMPERATURE	DENSITY	GAIN

NRL

-

### PHOTON TRANSPORT IN SRS

$$\frac{3N_{s}}{3z} + \frac{1}{c} \frac{3N_{s}}{3t} = g_{0} (N_{1} - N_{r}) N_{p}N_{s}$$

$$\frac{1}{c} \frac{3N_{1}}{3t} = -g_{0} (N_{1} - N_{r}) N_{p}N_{s}$$

$$\frac{N_{s} + N_{p}}{N_{s} + N_{p}} = N_{so} + N_{po}$$

### NRI

### APPROXIMATE SCALING

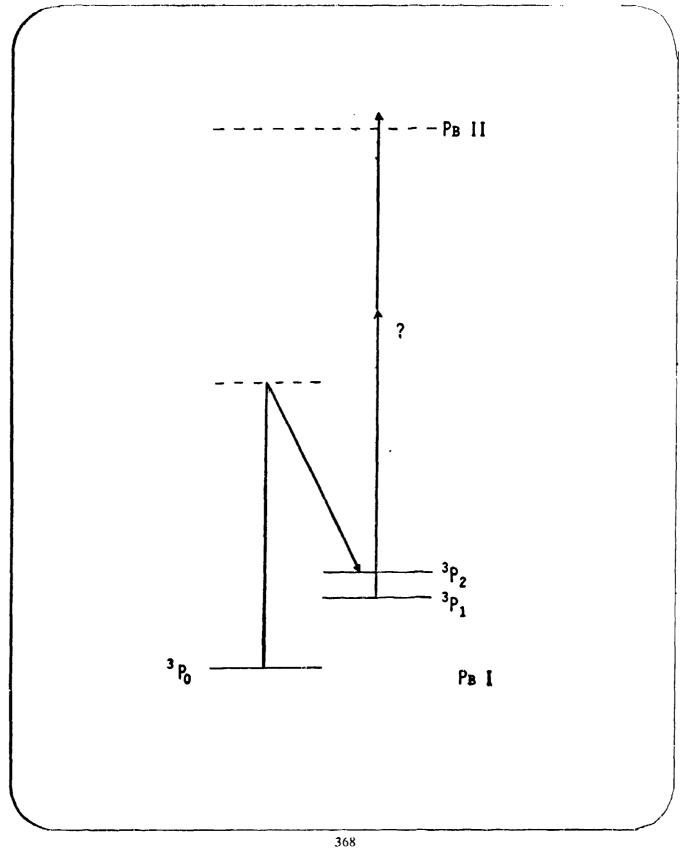
# OF SATURABLE RAMAN CONVERTER

- ASSUME CONSTANT PUMP ENERGY AND CONSTANT RAMAN MEDIUM NUMBER DENSITY
- LENGTH REQUIRED FOR EFFICIENT CONVERSION SCALES WITH PULSE DURATION APPROXIMATELY AS FOLLOWS

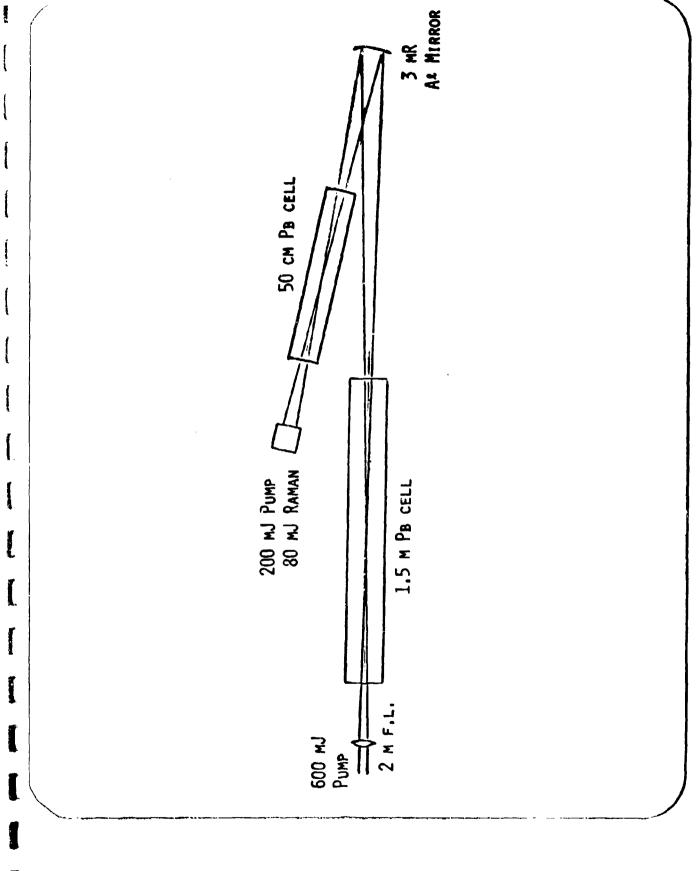
GAIN CONSIDERATION: t-1 A-12 ~ CONST.

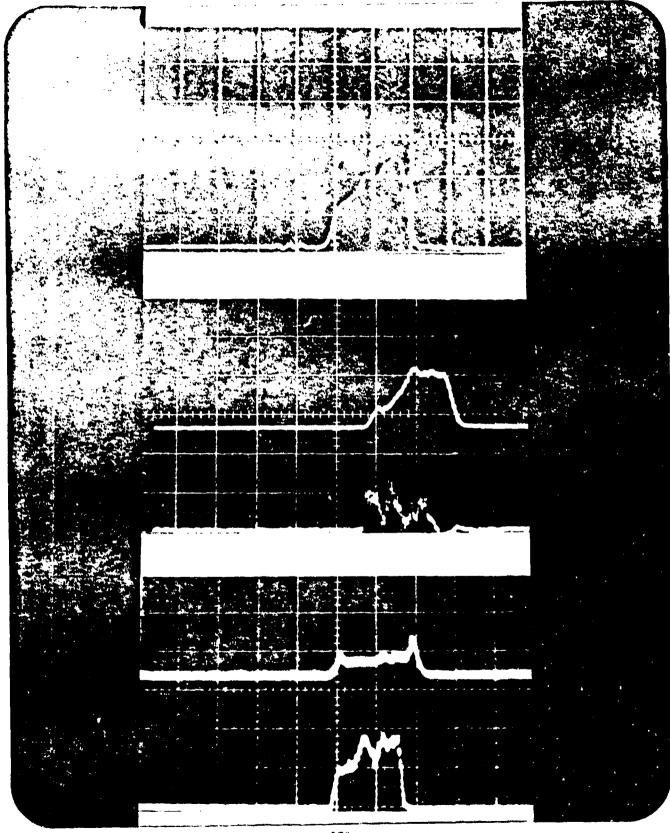
VOLUME CONSIDERATION: AL ~ CONST.

THEREFORE: 1 ~ th



The second second





### NRL

## CONCLUSIONS FROM LONG PULSE

### CONVERSION EXPERIMENT

- ENERGY CONVERSION EFFICIENCY OF 40% DEMONSTRATED FOR 400 NSEC PUMP PULSE
- NO ANAOMALOUS BEHAVIOR OBSERVED
- PB VAPOR CELLS OF REASONABLE LENGTH ARE ADEQUATE FOR CONVERTING LONG XECT PUMP PULSE

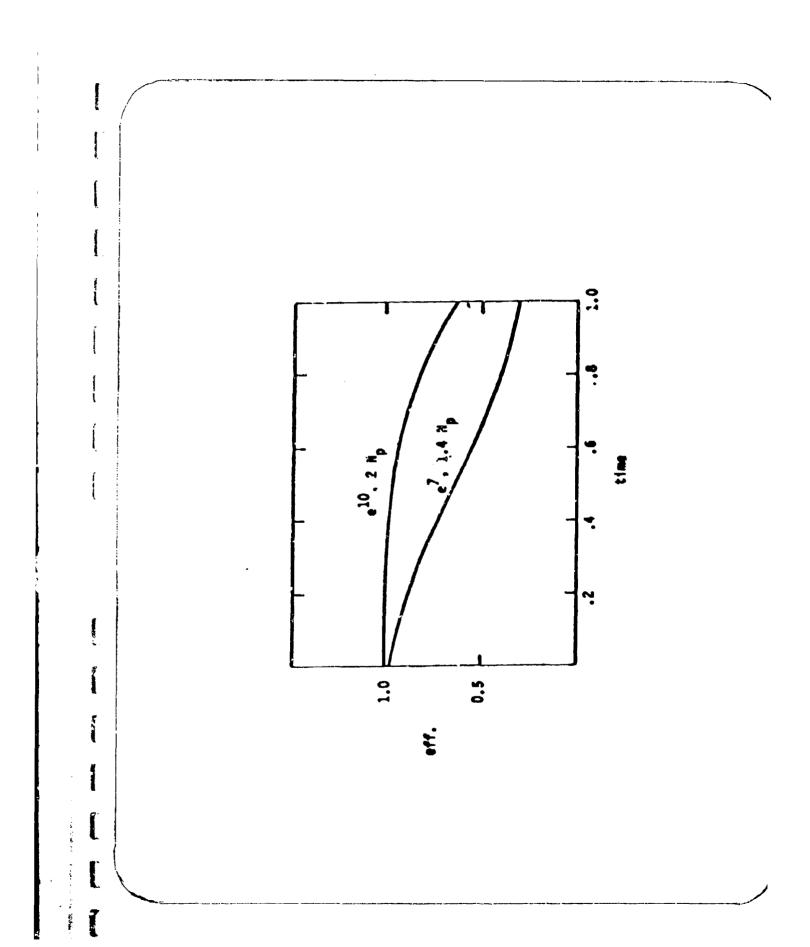
### NRL

The second

Mensa.

### SCALING TO 10 J XECI PUMP

- JOINT NRL/MAXWELL EXPERIMENT TO BE CARRIED GUT
  WITH MLI'S 40 1 DEVICE
- TWO 3 M PB VAPOR CELLS AND A COLLIMATED BEAM OF 1.5-2 CM DIAMETER WILL BE USED
- RESULTS WILL BE COMPARED WITH PREDICTIONS TO CHECK ADEQUACY OF UNDERSTANDING



## ESTIMATES OF PRESSURE WAVES

• ACOUSTIC PRESSURE PROPAGATION EQUATION:

$$r^{2} p - \frac{1}{c^{2}} \frac{3^{2} p}{3 t^{2}} = \frac{8}{c_{p}} \frac{3 H}{3 t}$$

IN UNBOUNDED SPACE

$$p(\vec{r},t) = \frac{\beta}{l_1 \pi} C_p \int dV_o \frac{H'(\vec{r}_0,t-R/C)}{R}$$

- Conversion of 1 kJ pulse in 10 m x 20 cm dia. Cell deposits approximately 1 mJ cm $^{-3}$  in medium.
- IN MIXTURE OF (HE: PB = 10:1) AND FOR H (t) =  $H_o$  (e^{-kt} e^{-2kt}), .TUDE OF PRESSURE WAVE SCALES WITH & AS

$$\Delta p \text{ (torr)} \sim 10^{-8} \text{ k}^2 \text{ (sec}^{-2})$$

IN 10 MSEC, PRESSURE WAVE HITS WALL ~ 30 TIMES



### CONCLUSIONS FROM

これになって、大の一の大のはないというできないとなっていることはないないとのできないとなっているというないというできないというないというないというないというないというないというというないというという

## PB VAPOR MEDIUM QUALITY ANALYSIS

- FOR N (PB) =  $10^{17}$  cm⁻³ And N (He) = 2 x  $10^{18}$  cm⁻³, 1.3 D.L. BEAN IMPLIES  $\Delta \rho / \rho = 10^{-3}$  (RANDOM) TO  $10^{-4}$  (ORDERED) FOR 10 M LENGTH.
- PRELIMINARY AMALYSIS INDICATES THAT MEDIUM UNIFORMITY IN PB VAPOR CELL SHOULD BE ADEQUATE AT  $\sim 100$  Hz,
- DETAILED MODELING OF ACOUSTIC MAYES WOULD REQUIRE KNOWLEDGE OF RATE OF HEAT DEPOSITION AND BOUNDARY CONDITIONS.





### TUNABLE BLUE-GREEN LASER DEVELOPMENT

Αt

### SRI INTERNATIONAL

### Research Staff

W. K. Bischel

G. Black

D. J. Eckstrom

D. L. Huestis

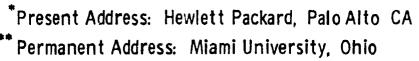
D. C. Lorents

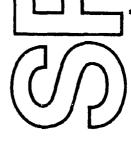
H. H. Nakano

K. Y. Tang

R. A. Tilton

H. C. Walker, Jr.





MP 80-36

Presented at the Fourth Strategic Blue-Green Laser Communication Meeting, San Diego, CA March, 1980



### PHOTOLYTICALLY PUMPED XeF(C-A) BLUE-GREEN LASER DEVELOPMENT

Presented by D. J. Eckstrom

Background and Review

Summary of Supporting Kinetics Experiments

New Measurements

Fluorescence Spectrum and Intensities

Gain/Absorption Results

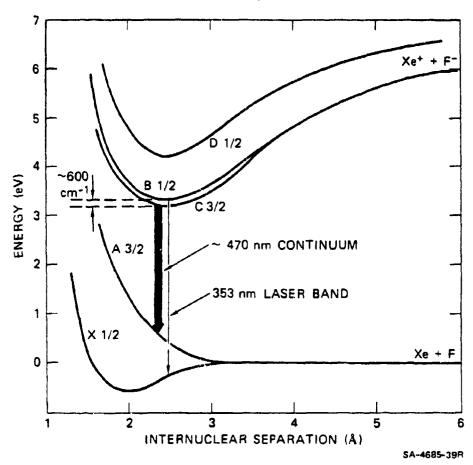
New Laser Experiments

Conclusions and Status

Scale-up Design

Open Discharge Photolytic Pumping Concept

### SCHEMATIC XeF POTENTIAL CURVES SHOWING B 1/2 - C 3/2 SPLITTING



11、11、11、日本教育は大学の場所でいて、これの日本の日本のはないはないのである。

### XeF(C-A) LASER DEMONSTRATIONS

**Photolytic** 

Bischel, et al.

SRI

A. P. L. 34, 565 (1979)

Zuev, et al.

Lebedev Inst.

Powell, et al.

Ш

Discharge

Burnham

**NRL** 

A. P. L. 35, 48 (1978)

Fisher, et al.

**MSNW** 

A. P.L. 35, 26 (1979)

E-Beam

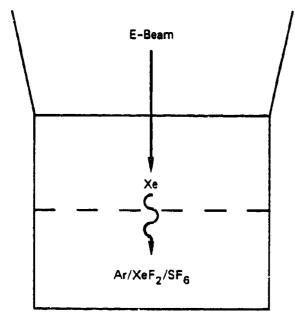
Ernst and Tittel

Rice U.

A. P. L. 35, 36 (1979)

### Why Photolytic?

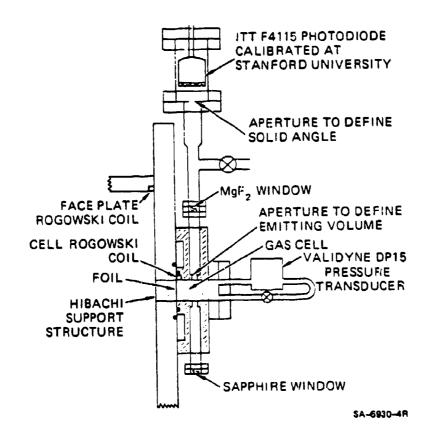
- No electrons
  - Favorable C/B population ratio
  - No ionic absorbers
- Clean excitation, simplified kinetics

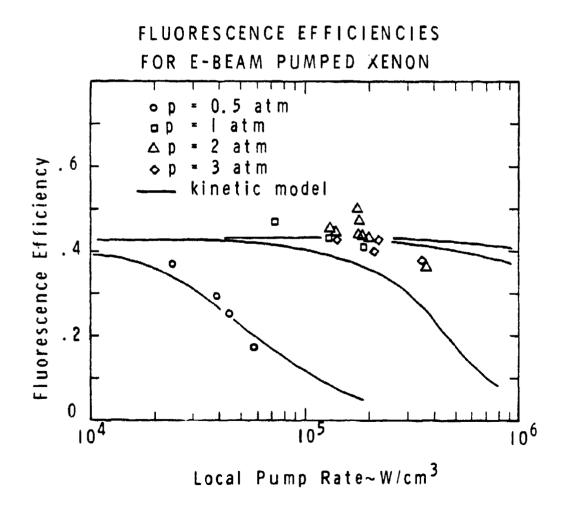


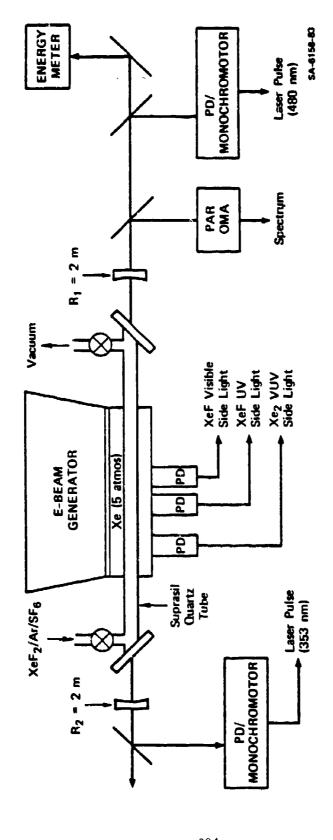
SA-6158-122

### FLUORESCENCE PUMPING

e-BEAM + Xe 
$$\rightarrow$$
 Xe⁺  $\rightarrow$  Xe⁺  $\rightarrow$  h $\nu$ (172 nm)  
h $\nu$ (172 nm) + XeF₂  $\rightarrow$  XeF⁺ + F  
XeF⁺ + M  $\rightarrow$  XeF(C) + M  
XeF(C) + h $\nu$ (483 nm)  $\rightarrow$  Xe + F + 2h $\nu$ 







•

......

المسا المنشأ

1

L'Approprie

4

ALES.

### XeF(C-A) LASER ISSUES - 1979

### KINETICS ISSUES

XeF₂ Absorption Cross Sections Excited State Quantum Yield XeF(C) Lifetime, Quenching, Mixing

### LASER CHARACTERIZATION

Fluorescence Intensities (B and C) and Spectrum

B/C Laser Competition

Quenching (XeF₂, F)

Gain Cross-sections, Calculated

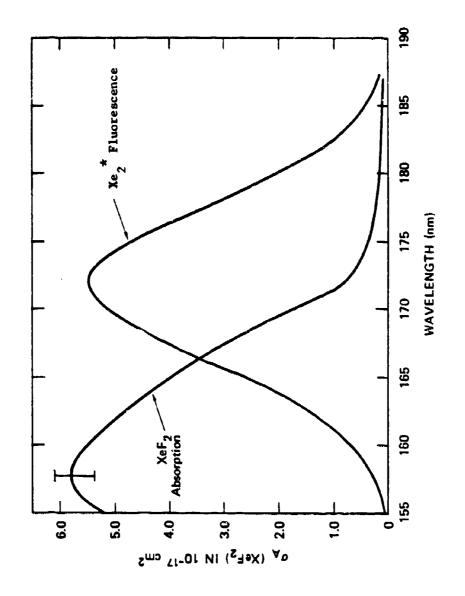
Electron mixing effects (photoionization)

Gain / Absorption

Background Absorptions (extraction efficiency)

Laser Demonstrations
Time Histories
B/C Competition
Absorptions
Tunability

OVERLAP BETWEEN XeF, ABSORPTION AND Xe2* FLUORESCENCE



### QUANTUM YIELDS

Measurements normalized to  $O(^{I}S)$  from  $N_2O^*$  (in presence of Xe)

B state QY = 0.9 +0.1

Constant 145 nm  $< \lambda < 175$  nm

### C state

QY =  $0.08 \pm 0.02$  at 157.5 nm Decreases by  $\sim 40\%$  between 146 and 172 nm [Previous work QY(C) < 0.1 QY(B)]

### D state

QY = 0.028 ± 0.005 at 155 nm

Decreases by factor of at least 2 between 155 and 165 nm

*G. Black, R. L. Sharpless, T. G. Slanger, and D. C. Lorents, J. Chem. Phys. <u>62</u>, 4266 (1975)

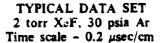
### SUMMARY OF MEASURED RATES FOR Xef*

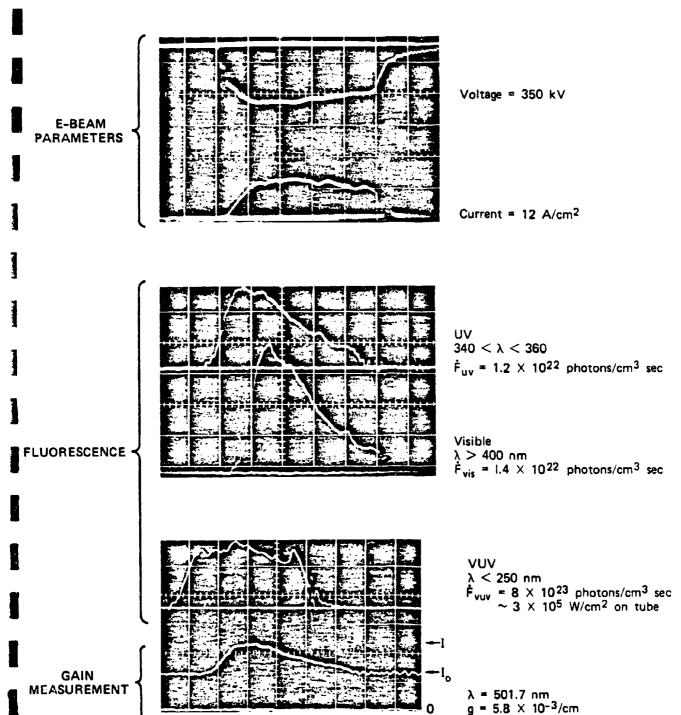
### Radiative Lifetimes

C state:  $\tau_C = 101 \pm 5 \text{ sec}$ B state:  $\tau_B = 13.3 \pm 0.2 \text{ sec}$ 

### Quenching / B-C Mixing

	Quenching		Mixing	
Rate	B State (cm ³ /sec)	C State (cm ³ /sec)	B→C (cm ³ /sec)	
XeF ₂	7.4x10 ⁻¹⁰	4.75x10 ⁻¹⁰		
Ar		7±7x10 ⁻¹⁵	1.4±0.2x10 ⁻¹¹	
N ₂		≤2.5x10 ⁻¹⁴	5.7±0.3x10 ⁻¹¹	
SF ₆		≤9x10 ⁻¹⁴	8 <u>+</u> 1x10 ⁻	
Хe	1.9x10 ⁻¹⁰		1.5×10 ⁻¹⁰	





SA-6158-116

### BIC STATE FLUORESCENCE INTENSITY RATIOS

Intensity ratio from kinetic theory

$$\frac{I(B)}{I(C)} = \frac{A_B}{A_C} \frac{k_{CB}}{k_{BC}} + \frac{A_B}{k_{BC}} \frac{I}{[R_g]} \left( I + \frac{k_C}{A_C} [XeF_2] \right)$$

$$A_B = 7.5 \times 10^7 / \text{sec}, A_C = 9.9 \times 10^6$$
  
 $k_C = 4.75 \times 10^{-10} \text{cm}^3 / \text{sec}$   
 $k_{BC} / k_{CB} = 22.8$ 

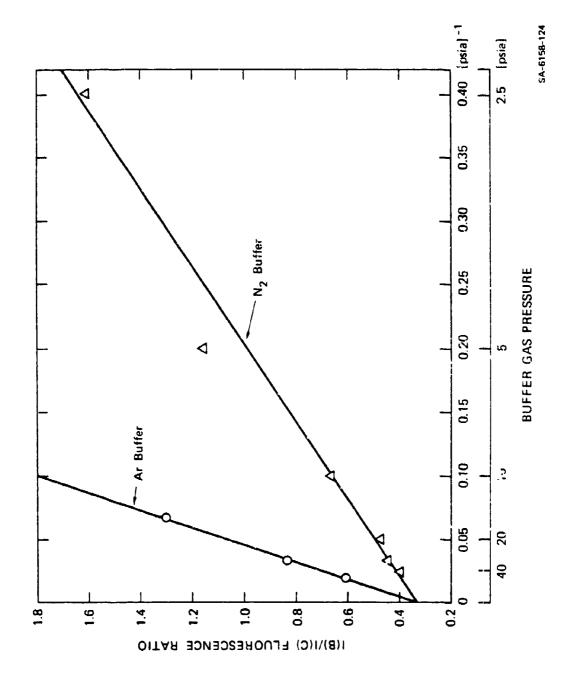
• Argon Buffer  $K_{BC} = 1.3 \times 10^{-11} \text{ cm}^3/\text{sec}$ 

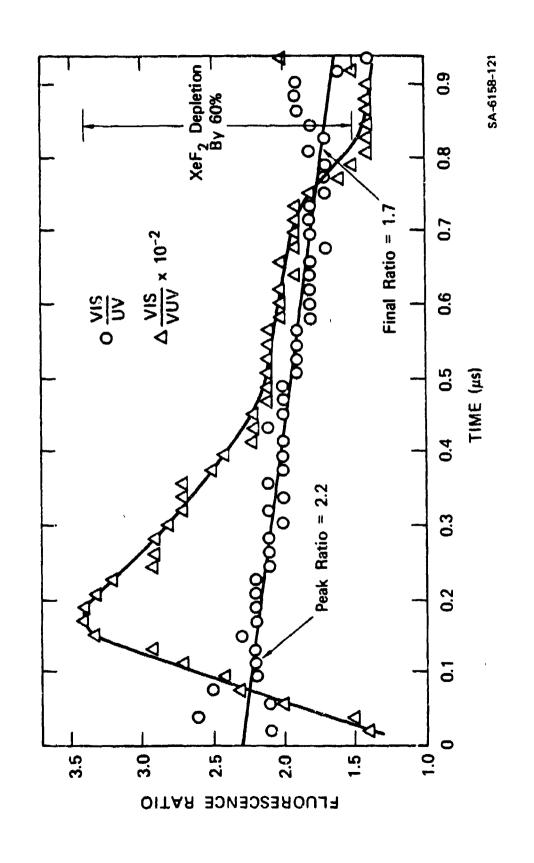
$$\frac{I(B)}{I(C)} = 0.333 + \frac{14.5}{[R_g]}$$

• N₂ Buffer 
$$K_{BC} = 5.7 \times 10^{-11} \text{ cm}^3/\text{sec}$$

$$\frac{I(B)}{I(C)} = 0.333 + \frac{3.3}{[R_g]}$$

- $[R_g]$  in units of PSIA-





7

No.

n

### EXPERIMENTAL APPROACH

### ■ Gain cross section

$$\sigma_{\rm q}$$
 =  $\ell$ n (1/1_o)/L N^{*}

where

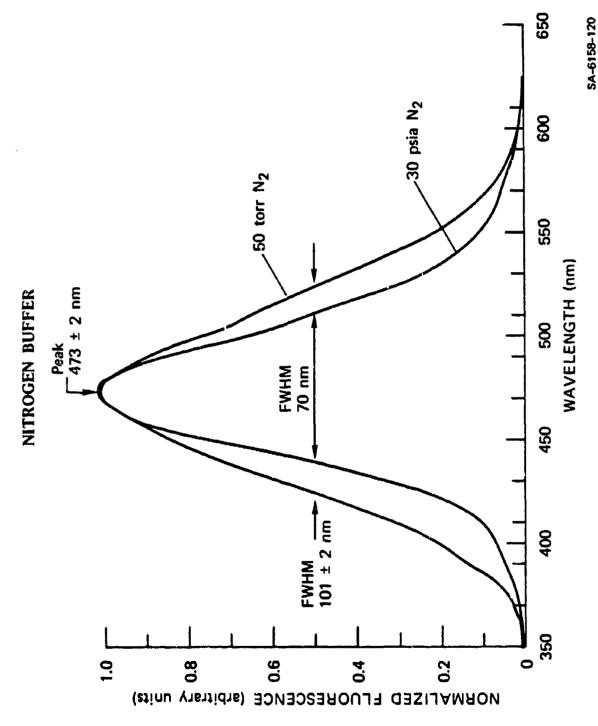
$$N^* = F_{vis} (\#/cm^3 - sec)/A$$

$$A = 10^7/\text{sec}$$

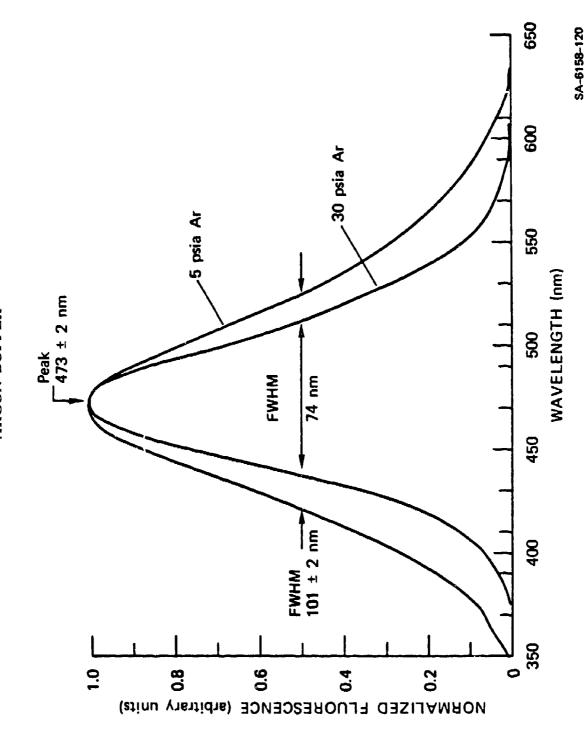
### Calculated gain cross section

$$\sigma_g = \frac{A}{8\pi c} \lambda^4 = \frac{f(\lambda)}{\int f(\lambda) d\lambda}$$

FLUORESCENCE SPECTRUM WITH ARGON AND

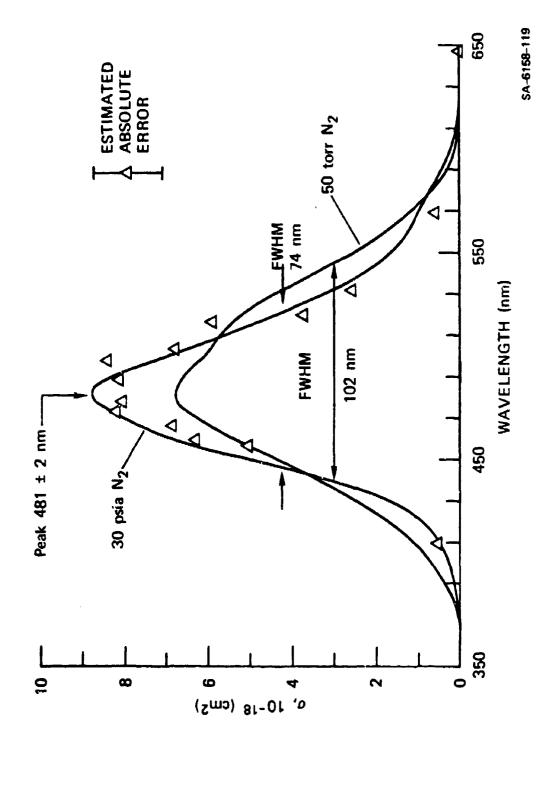


FLUORESCENCE SPECTRUM WITH ARGON AND ARGON BUFFER

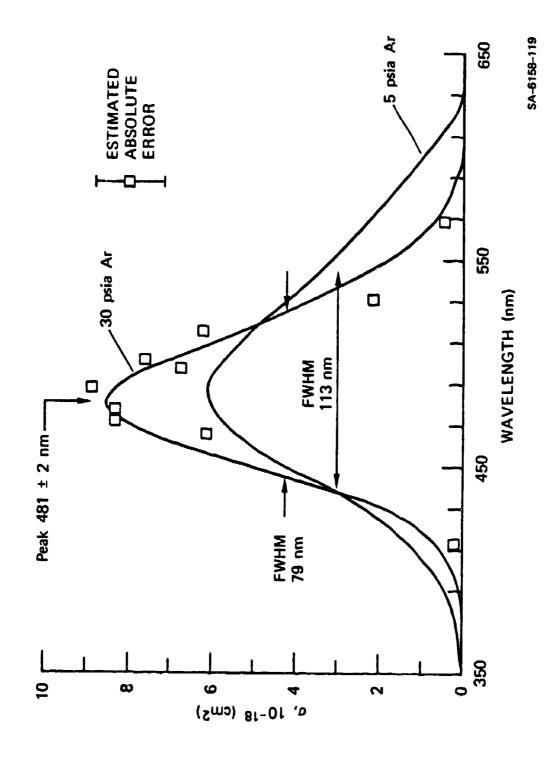


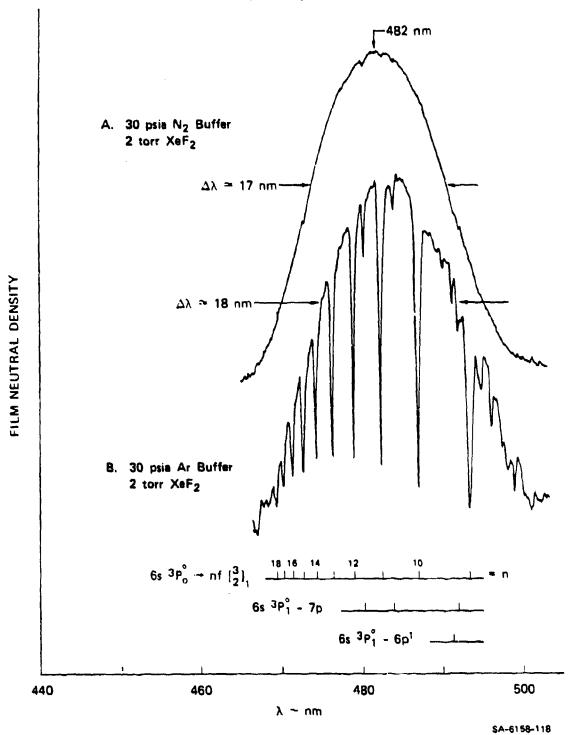
# CALCULATED AND MEASURED CROSS SECTION

NITROGEN BUFFER

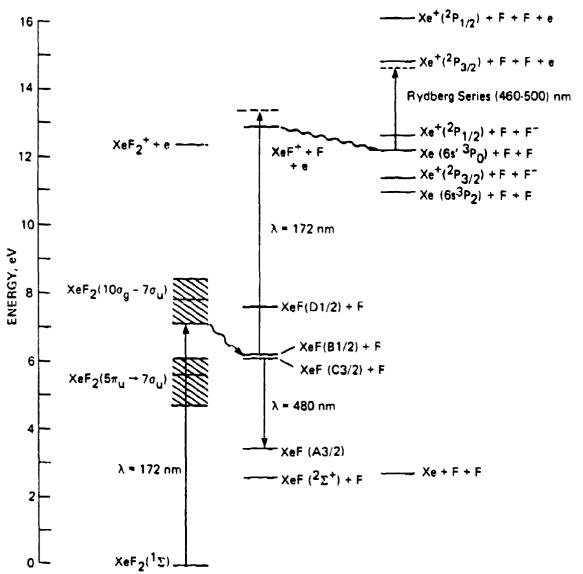


CALCULATED AND MEASURED CROSS SECTION ARGON BUFFER



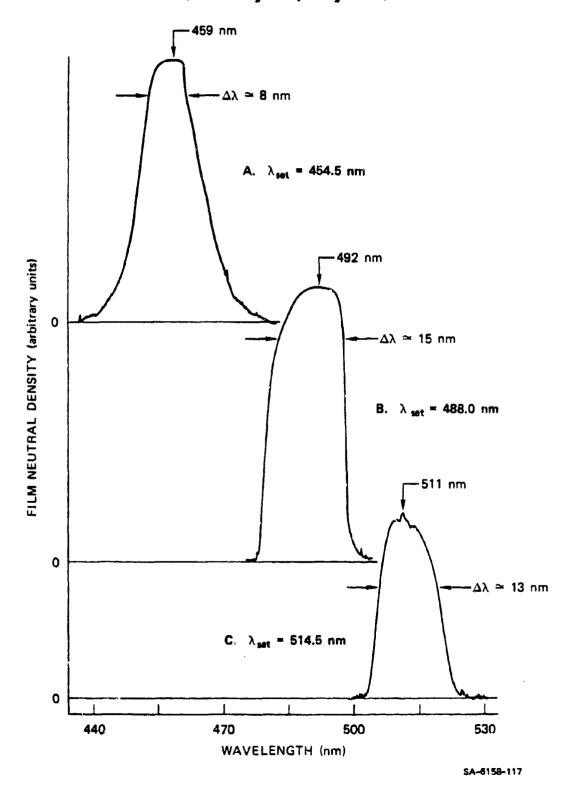


### PARTIAL ENERGY LEVEL DIAGRAM FOR XeF₂, XeF, AND Xe



SA-6158-94R1

XeF(C-A) LASER SPECTRA-TUNED (2 torr XeF₂, 30 psia N₂ Buffer)



### CONCLUSIONS

Gain/Absorption

May be weak background continuum absorption with Ar buffer

No background continuum absorption with  $\rm N_2$  buffer Discrete line absorptions suppressed with  $\rm N_2$  buffer

Photoionization

Does not affect intensity ratios at low pump rates Discrete line absorptions suppressed with  $N_2$  buffer

Quenching

Some evidence that F-atom quenching is important

B/C Competition

No B-X lasing observed in these experiments

Tunability

Demonstrated lasing from 454 to 525 nm

### STATUS

### Kinetics Issues

Quenching of XeF* by F atoms and electrons

Photoionization cross sections for XeF* near 170 nm

### Laser Issues

Coupling of VUV to laser medium (spatial and spectral)

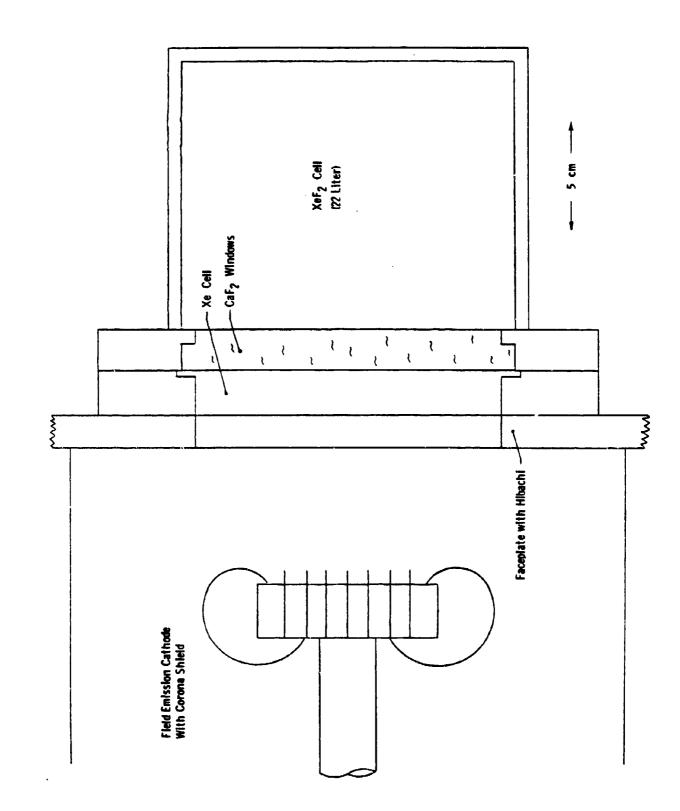
Energy extraction from medium with spatial and temporal nonuniformities

Competition from B-X superfluorescence

### Systems Issues

Recycling of XeF₂/N₂ mixture

Laser tuning and frequency narrowing to match detector characteristics



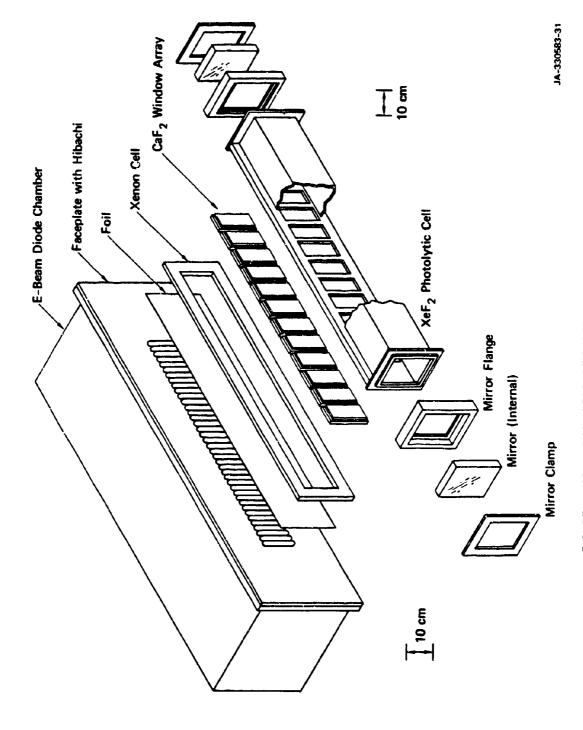


FIGURE SRI LARGE APERTURE PHOTOLYTICALLY PUMPED LASER

The Xe₂Cl Blue-Green Laser the first of a new class of lasers based on the triatomic rare gas halides

K. Y. Tang and D. L. Huestis Molecular Physics Laboratory SRI International Menlo Park, CA 94025

### DISCOVERY OF THE TRIATOMIC RARE GAS HALIDES, Rg₂X

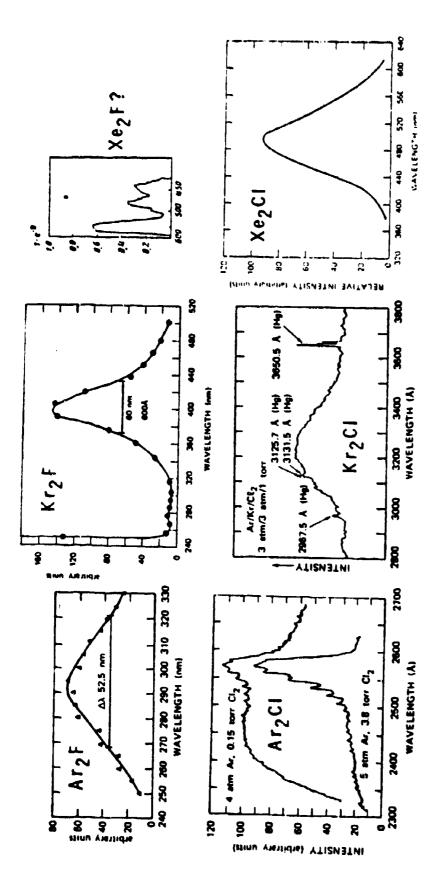
Companion Emission in RgX Laser Media

ArF (193 nm) - Ar₂F (290 nm) KrF (248 nm) - Kr₂F (400 nm) XeCl (308 nn) - Xe₂Cl (490 nm)

• Products of Interception and Quenching

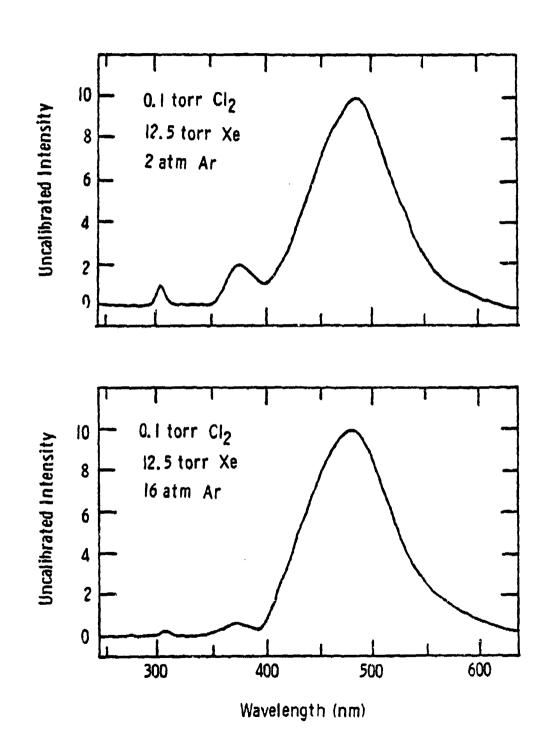
$$Rg_2^{\bullet} + X_2 \longrightarrow Rg_2X^{\bullet} + X$$
  
 $RgX^{\bullet} + 2Rg \longrightarrow Rg_2X^{\bullet} + Rg$ 

A NEW CLASS OF LASER CANDIDATES: THE TRIATOMIC RARE GAS HALIDES, R ₉₂ X	Laser Implication	Choice of Excitation Methods Potential High Efficiency No Bottle-necking	Wide Frequency Tunability	Potential High Power Interference by Absorption • Rg2X • Background
A NEW CLASS THE TRIATOMIC I	Laboratory Observation	<ul> <li>Selective Formation Pathway</li> <li>High Production Yield</li> <li>(\$\Phi\$\$\sim 0.9)</li> <li>Dissociative Lower State</li> </ul>	<ul> <li>Broad-band Emission</li> <li>(Δλ &gt; 50 nm)</li> </ul>	Cross-section ( $\sigma \le 10^{-17}  \text{cm}^2$ )



X B 2 I

EMISSION SPECTRA OF THE TRIATOMIC RARE GAS HALIDES



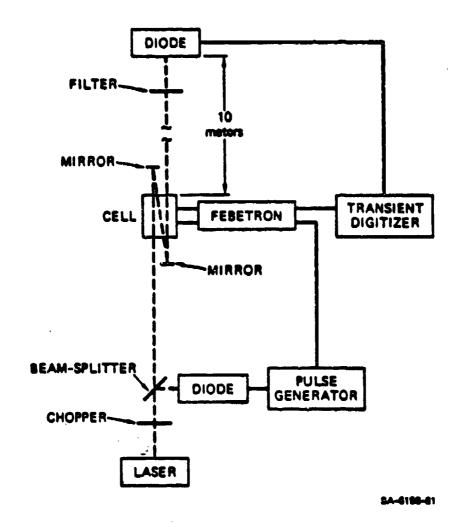
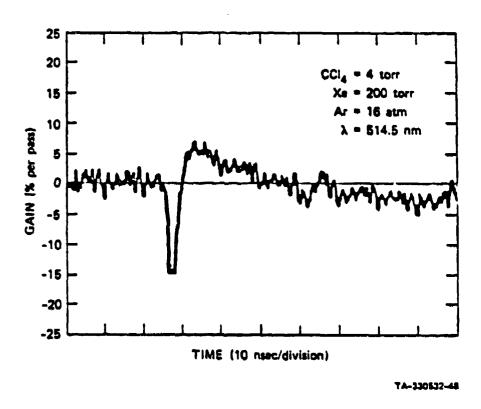
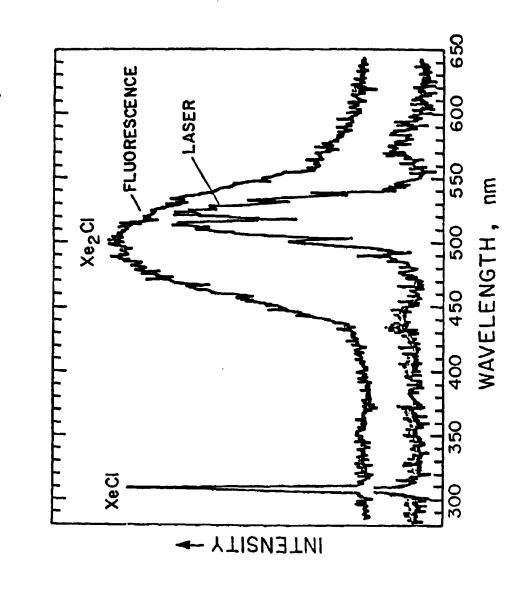


Figure 1



Weaker gain also observed at 488 and 498 nm.

By F. K. Tittel, W. L. Wilson, R. E. Stickel, G. Marowsky and W. E. Ernst



### Summary of Rg₂X Laser Study

### Status

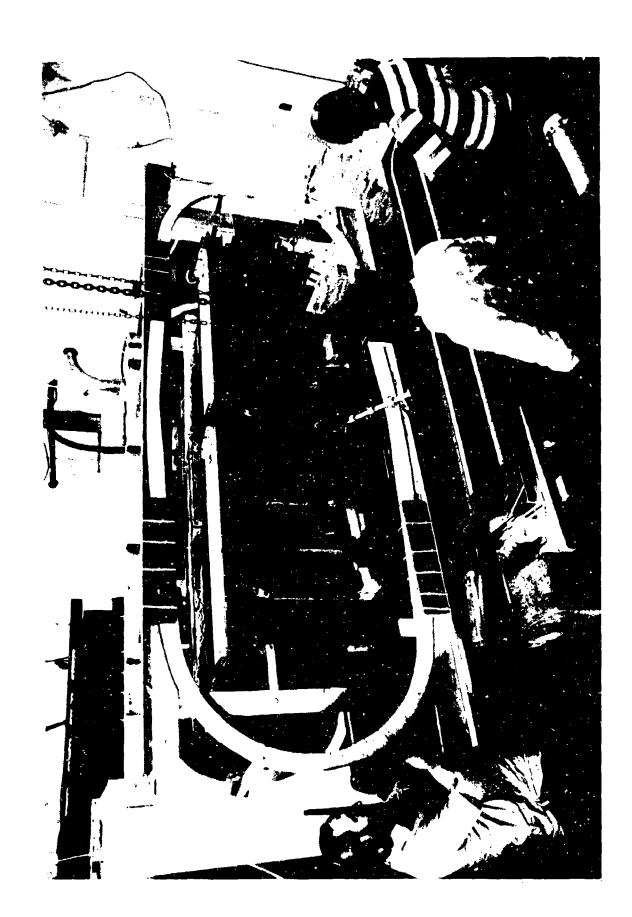
- Spectroscopy Most Rg₂X* Emission Observed
   Electronic Structure Understood
- Kinetics High Production Efficiency Verified
- Laser Gain Observed in Xe₂Cl
   Self-absorption not Important
   Laser Action of Xe₂Cl Achieved via
   Direct e-beam Excitation

### Current Xe2CI Laser Work at SRI

- Small Scale Laser Demonstration via Incoherent vuv Photolytic Pumping
- Detailed Understanding of the Kinetics

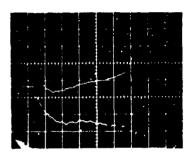
### XeC1 LASERS FOR BLUE-GREEN CONVERSION J Asmus

Maxwell Labs 8835 Balboa Avenue San Diego CA 92123



UPPER TRACE ELECTRON BEAM VOLTAGE, 88 KV/DIV, 200 NS/DIV

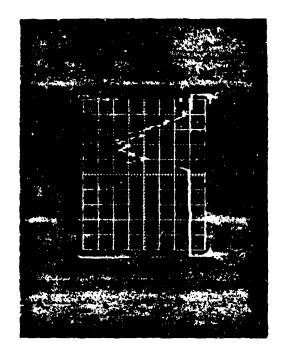
LOWER TRACE ELECTRON BEAM CURRENT, 27.4 KA/DIV, 200 NS/DIV

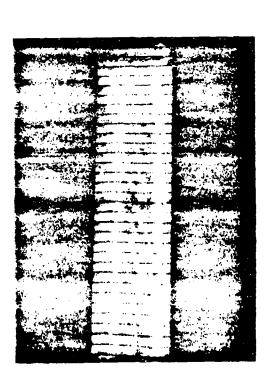




LASER LOADED FLUORESCENCE, 200 NS/DIV

## 2 METER LASER E-BEAM PERFORMANCE



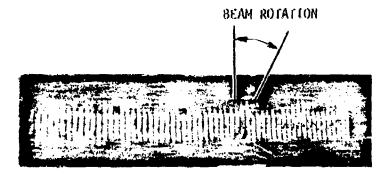


### **EMAXWELL**

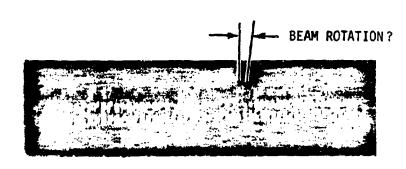
### BEAM PATTERNS VS GUIDE FIELD STRENGTHS



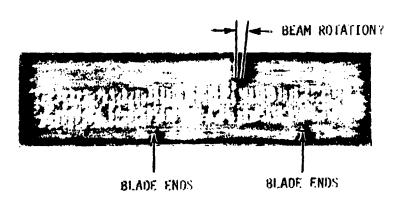
4/13-3 NO FIELD 5-BLADE CATHODE 45kV



4/4-7 278 GAUSS GUIDE FIELD 5-BLADE CATHODE 45kV



4/13-4 436 GAUSS GUIDE FIELD 5-BLADE CATHODE 45kV



4/17-2 436 GAUSS GUIDE FIELD SKEWED CATHODE 45kV

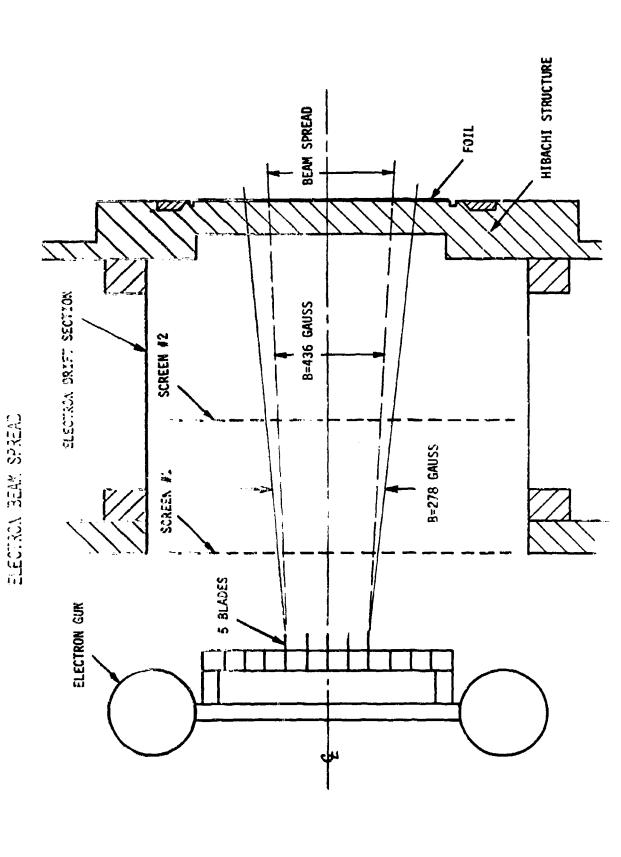
# CATHODE BLADE ARRANGEMENTS--COMPARISON

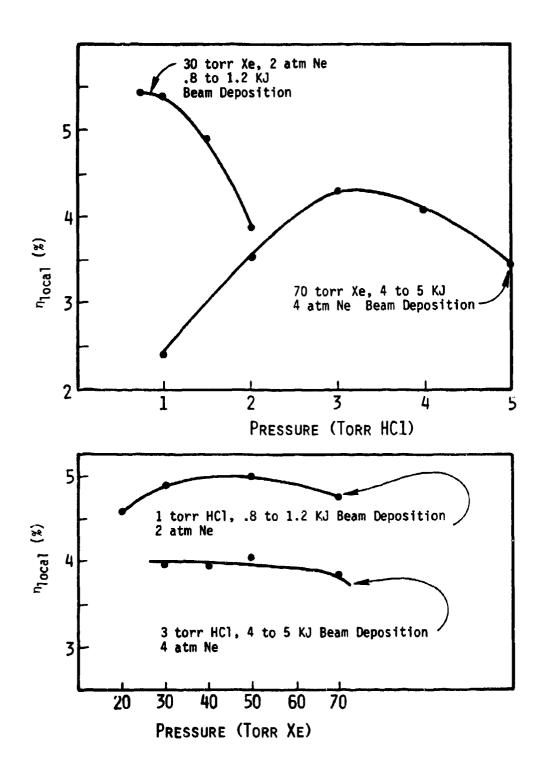


NOPMAL CATHODE ARRAY, 11 FULL BLADES



SKEW CATHODE ARRAY, 7 FULL BLADES AND 4 STEPPED BLADES







## 40 L LASER OPERATION (JUNE-AUG)

### XeF

	3.50	2.5 AMMSAT		NEAR FIELD DISTRIBUTION±10% (APERTURE)	COATING DAMAGE TESTS (6 J)±5% (APERTURE/4)	650
ENERGY/PULSE,	TEMPERATURE,	DENSITY.	ELECTRICAL EXCITATION75%	NEAR FIELD DISTRIBUTION	COATING DAMAGE TESTS (E	NUMBER OF TEST SHOTS

	LASER VOLUME (LITERS)	E BEAM Deposition (KJ)	Laser Output (J)	LOCAL ¹ Efficiency	SPECIFIC LASER GUTPUT (J/L)
KRF	09	9	300	5%	5
XeF	09	9	200	3,3%	3
XeC1	04	ħ	200	5%	5

1 LOCAL EFFICIENCY = LASER OUTPUT/DEPOSITED BEAM ENERGY

-

## **MAXWELL**

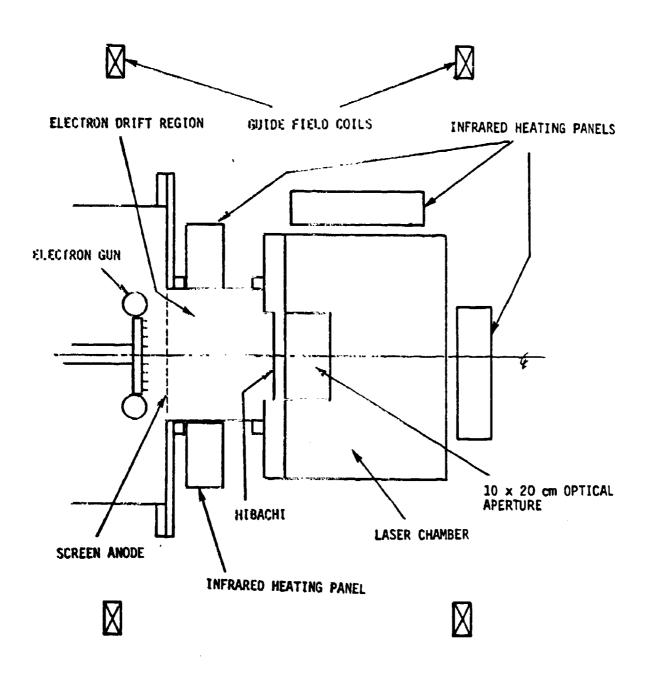
and the second of the second of the second of the second of the second of the second of the second of the second of the second of the second of the second of the second of the second of the second of the second of the second of the second of the second of the second of the second of the second of the second of the second of the second of the second of the second of the second of the second of the second of the second of the second of the second of the second of the second of the second of the second of the second of the second of the second of the second of the second of the second of the second of the second of the second of the second of the second of the second of the second of the second of the second of the second of the second of the second of the second of the second of the second of the second of the second of the second of the second of the second of the second of the second of the second of the second of the second of the second of the second of the second of the second of the second of the second of the second of the second of the second of the second of the second of the second of the second of the second of the second of the second of the second of the second of the second of the second of the second of the second of the second of the second of the second of the second of the second of the second of the second of the second of the second of the second of the second of the second of the second of the second of the second of the second of the second of the second of the second of the second of the second of the second of the second of the second of the second of the second of the second of the second of the second of the second of the second of the second of the second of the second of the second of the second of the second of the second of the second of the second of the second of the second of the second of the second of the second of the second of the second of the second of the second of the second of the second of the second of the second of the second of the second of the second of the second o

## COATING DAMAGE TESTS

### XeF, N ON ONE

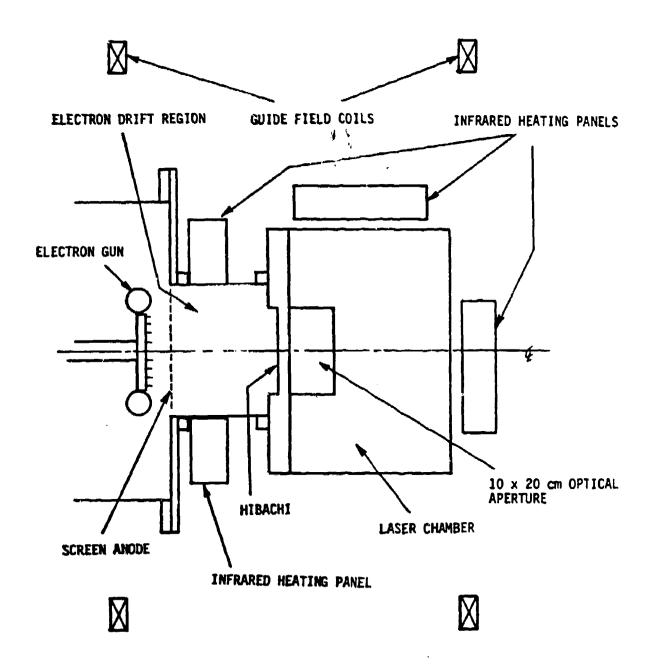
SHOTS TO Damage >50	>50	24-40	8-10	1-2	>50	×50	>50	28	20
FLUX . (J/CM ² ) 0.6	1.2	2.5	2.9	9.6	9.6	1.2	2.5	4.2	2.3
TM 2 (6 INCH MOLY, 99.5%)					FM 1 (6 INCH MOLY, 98.5%)				
9)					(6 1				
TM 2					Ξ.				

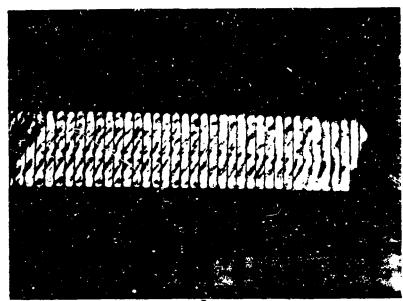
### E-BEAM TO 40 LITER LASER INTERFACE



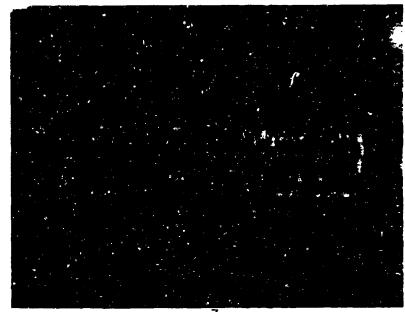
45KY, 4 AVAGAT NEON. CU LINER (DATA TAKEN DURING NAVY MIRROR RUNS) AVERAGE OF FOUR 15-SHOT RUNS 2 LASER GAS DEGRADATION SHOT NUMBER (n) 60 kV, 5 AMAGAT NEON 55kV, 4 AMEAT NEON. 1.0-8 (SYITAJSA) TUTTUO RELATIVE)

### E-BEAM TO 40 LITER LASER INTERFACE





CARBON FELT CATHODE WITH 2 DIMENSIONAL E-BEAM NEUTRALIZATION (ONE-HALF OF 20CM x 2 METER E-BEAM)



CARBON FELT CATHODE WITH 3 DIMENSIONAL E-BEAM NEUTRALIZATION (ONE-HALF OF 20CM X 2 METER E-BEAM)



ELECTRON BEAM EXCITED BLUE-GREEN XEF

4. 4. 4. 4.

J.D. CAMPBELL

C.H. FISHER

R.E. CENTER

A.L. PINDROH

(SUPPORTED BY DARPA)

Mathematical Sciences Northwest PO Box 1887 Bellevue WA 98009

# ELECTRON BEAM EXCITED BLUE-GREEN XEF

OBJECTIVE: INVESTIGATE FEASIBILITY OF A BLUE-GREEN

Xef LASER USING ELECTRON BEAM PUMPING

PROGRAM: DETERMINE GAIN OR ABSORPTION ON XeF 460 nm

BAND AS FUNCTION OF

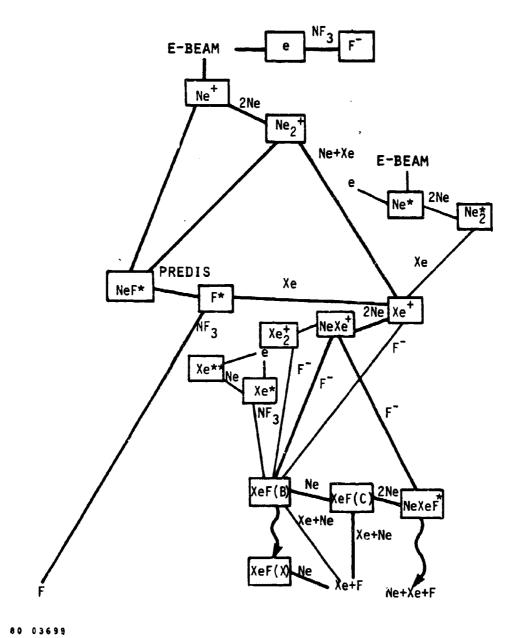
-- GAS PRESSURE

-- GAS MIXTURE

-- GAS TEMPERATURE

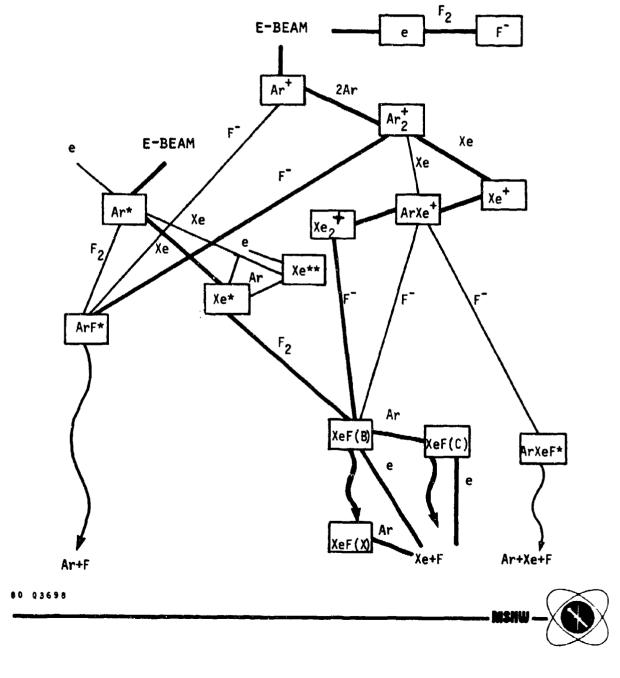
DEVELOP KINETIC MODEL TO PREDICT LASER PERFORMANCE

PERFORM OSCILLATOR EXPERIMENTS FOR HIGHEST GAIN CONDITIONS

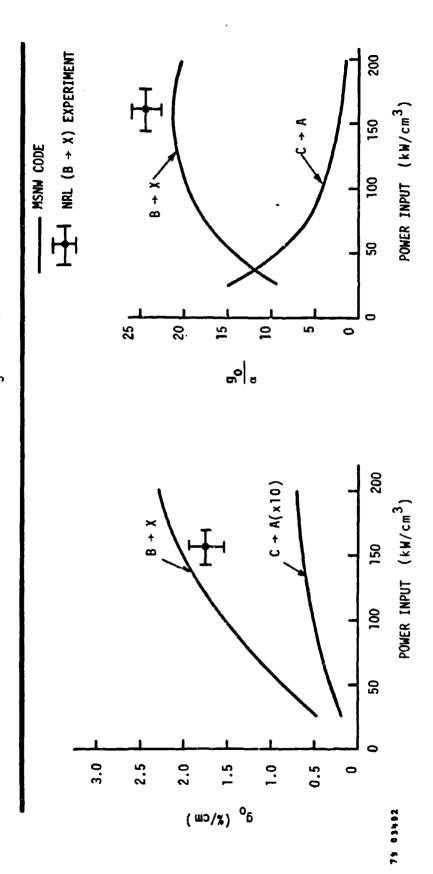


MSRW —

### XEF FORMATION KINETICS



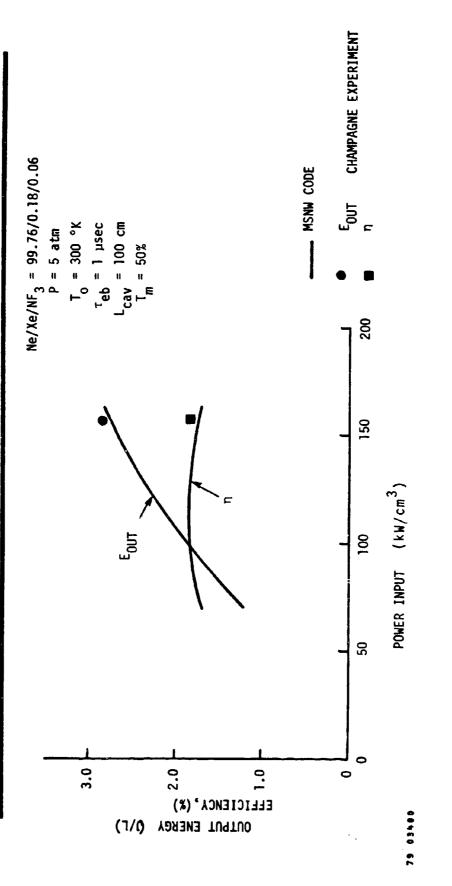
CODE PREDICTIONS FOR Ne/Xe/NF3 MIXTURES







XeF* (B+X) POWER EXTRACTION



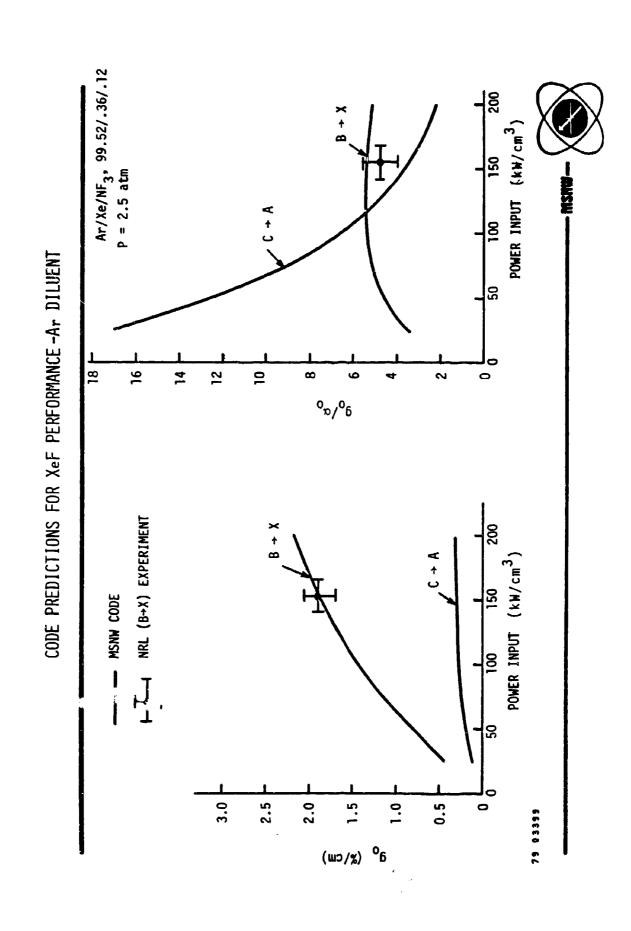


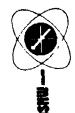
-

the second

200

1



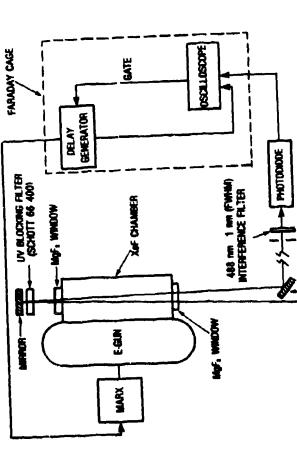


PROBE LASER

CHOPPER 16

APERTURE 1

MEMOR



EXPERIMENTAL SETUP FOR XEF(C+A) GAIN MEASUREMENTS

80 03696

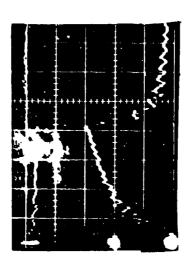


# ROOM TEMPERATURE GAIN/ABSORPTION DATA OBTAINED USING A CW AT LASER PROBE

MIXTURE COMPOSITION: 0.12% NF3, 0.24% Xe, Neon

- PROBE LASER INTENSITY 3
- E-GUN CURRENT PROFILE (B)

200 ns/div



5 ATM MIXTURE

2 ATM MIXTURE

488 nm PROBE

488 nm PROBE

5 ATM MIXTURE

514.5 nm PROBE



**(B)** 

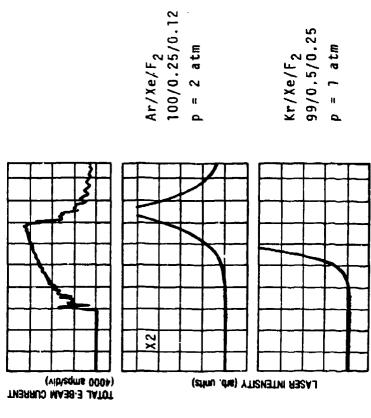
3



### SUMMARY OF XEF (C+A) GAIN/ABSORPTION DATA

Xe	NF ₃	F ₂	DILUENT	P(atm)	t(°C)	λ(nm)	NET GAIN (cm-1)	NET ABS
0.25%	0.12%		¥	4-5	20	488.0	5×10 ⁻⁴	
						514.5		5×10 ⁻⁴
0.5%	0.12%		₹	2	20	488.0	<5×10 ⁻⁴	
Ī						514.5		5×10 ⁻⁴
0,25%		0,12	₹	4	20	488.0	~3×10 ⁻⁴	
0.25%		0.12	Æ	4	-20	488.0	~6×10 ⁻⁴	
0.25%		0.12	Ar	1.5	20	488.0	<5×10 <b>-4</b>	
0.25%		0.12		1.5	-24	488.0		5×10 ⁻⁴





Kr/Xe/F₂ 99/0,5/0,25 p = 1 atm

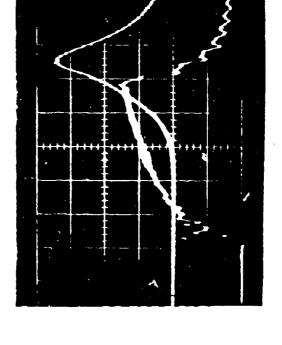
TME (200 neeckliv)

80 03697



# TEMPORAL DEPENDENCE OF XEF(C+A) STIMULATED EMISSION

$$Kr = 1$$
 atm  $Xe = 4$  torr  $F_2 = 2$  torr



480 nm STIMULATED EMISSION

TIME (200 nsec/div)

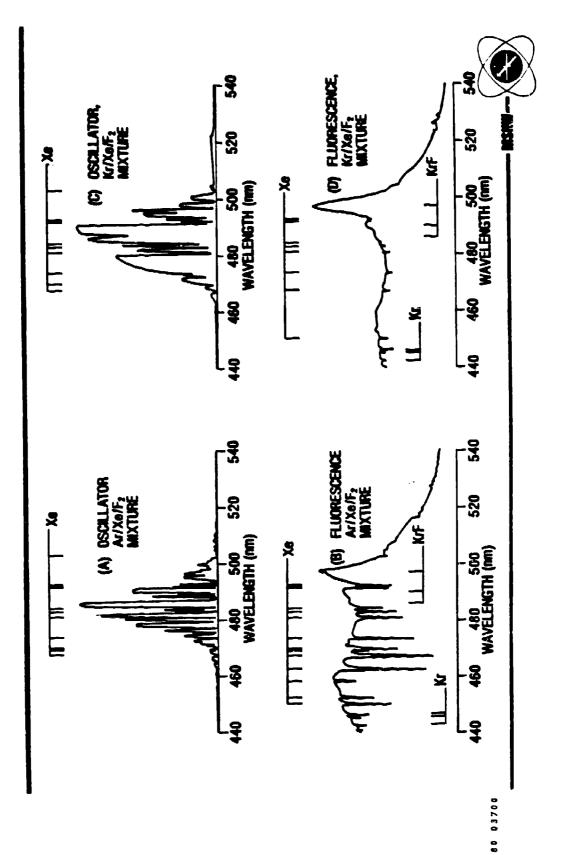
E-BEAM CURRENT (4 kA/div)

80 03695

.

1)

E-BEATI EXCITED XEF(C+A) LASER AND FLUORESCENCE SPECTRA





### BLUE GREEN XEF STATUS

LASING DEMONSTRATED USING SCALABLE E-BEAM EXCITATION

TUNABILITY DEMONSTRATED USING INJECTED DYE LASER PULSE

Kr DILUENT GIVES BEST PERFORMANCE

EXPERIMENTAL NET GAINS ARE SMALL (~5×10-4 cm-1)

### THE CURRENT STATUS OF COPPER LASER DEVELOPMENT RE Grove

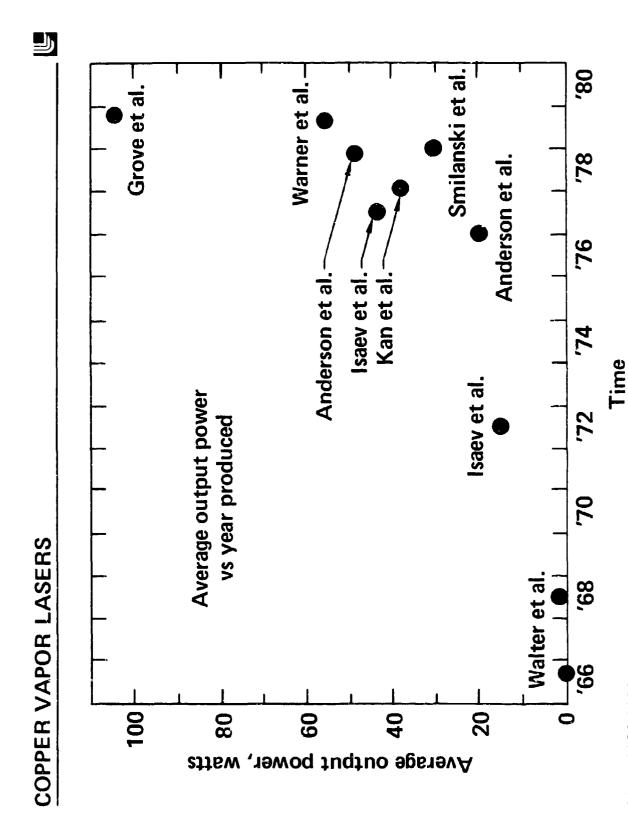
### Summary

The applicability of copper vapor lasers to many military and industrial problems has been limited in the past due to a lack of engineering development, demonstration of high average power operation, or scaling capability. Recent work at the Lawrence Livermore Laboratory has changed considerably the outlook for copper vapor lasers. A copper laser system is presently nearing completion which will have a total power capability of 400 - 500 W at a prf of 6 kHz. The laser system has already demonstrated single aperture powers from individual master oscillator-power amplifier chains of over 100 W with efficiencies of  $\sim 0.7$  percent. The individual MOPA chains are made up of an oscillator and five amplifiers, and produce about 16 mj/pulse at 6 kHz. Both the laser heads and their associated electronics have been engineered to achieve a high degree of maintainability and reproducibility.

In addition to this successful demonstration of the use of copper lasers in a MOPA configuration, recent experiments at LLL have confirmed that under certain operating conditions, volumetric deactivation of the lower laser level in copper can be achieved. This permits simple bore diameter scaling of the active volume of a copper laser and thus allows substantial increases in both the pulse energy and average power. A large bore copper laser with a 7.3 cm I.D. has recently been operated at output average powers of 55 W at 5 kHz (11 mj per pulse). Based on earlier experiments at General Electric Company at low repetition rates, the pulse energy for this bore diameter is expected to increase by about a factor of three as the prf is reduced to  $\sim$ 1 kHz.

Finally, recent work in the Soviet Union over the past two years has resulted in the achievement of energy densities of about 500  $\mu j/cm^3$  using transverse discharges and extremely high copper densities ( $\sim\!\!10^{17}$  to  $10^{18}$  per  $cm^3$ ). Attainment of specific energies around this value would, of course, result in extremely large pulse energies in small active volumes. However, the specific energies achieved at LLL to date in engineered, scalable copper laser designs, when considered in the context of simple bore diameter scaling and efficient MOPA operation, could result in copper lasers of reasonable size which have the pulse energies and other performance parameters required for many military and industrial applications.

PO Box 5508
Livermore CA 94550



30-17-0280-0636

### METHODS FOR INCREASING SINGLE APERTURE POWER



Increase hot zone

Use master oscillator-power amplifier (MOPA) configuration

Increase bore diameter

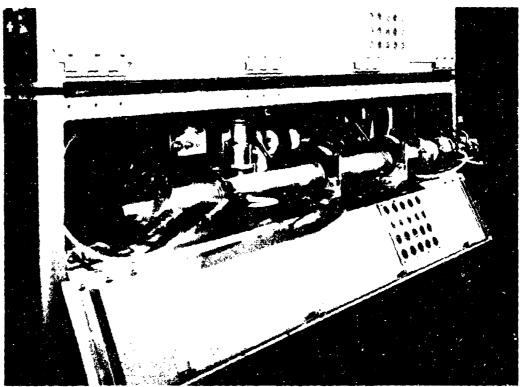
Not thought possible until recently

- Preliminary results very promising

Increase output energy density

30-05-0380-1030

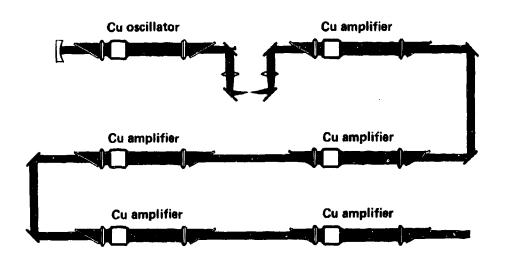




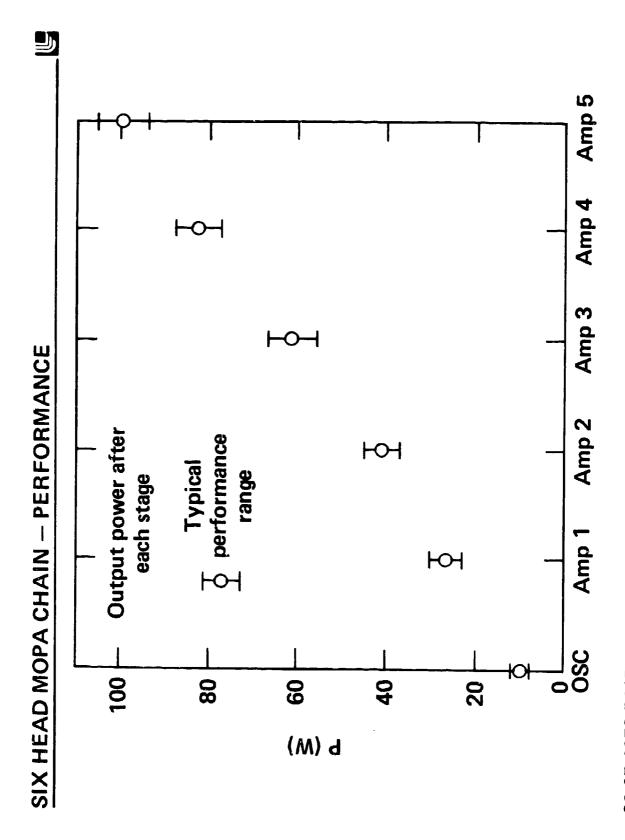


### SIX HEAD MOPA CONFIGURATION





30-01-1279-5092



30-05-1279-5115

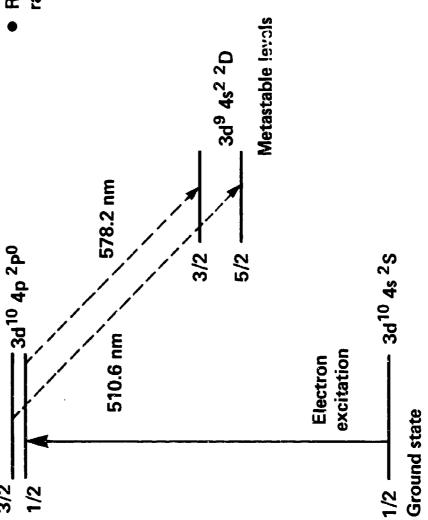
į

## LARGE BORE COPPER VAPOR LASER





rate of deactivation of metastable Repetition rate dependent on



30-17-0280-0434

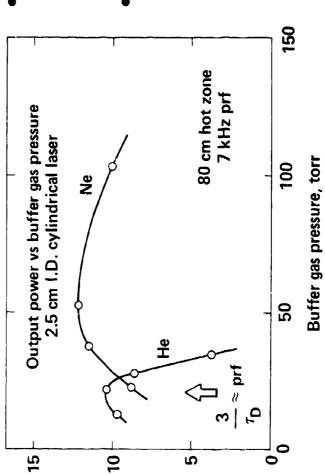
# CVL - OPERATION IN HELIUM AND NEON





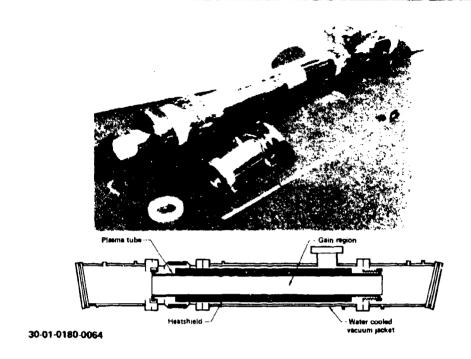
- PRF 
$$\approx 3/\tau_D$$
  
-  $\tau_D \propto P \cdot r^2$ 

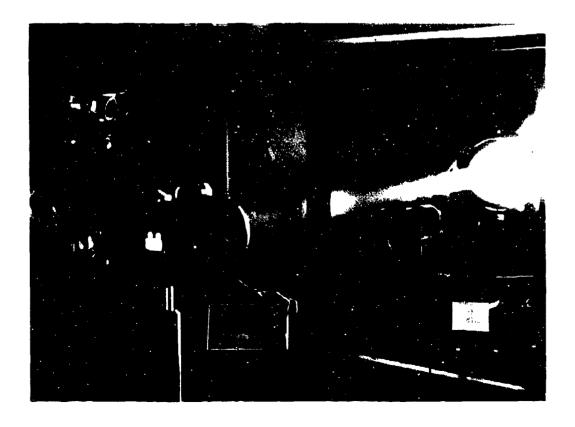
 Deactivation of Cu metastable in Cu-neon laser has characteristics of a volumetric process



30-05-0280-0439

Output power, watts





### **OSCILLATOR PERFORMANCE**

7.3 cm (2.9 in.) Discharge tube I.D. Neon pressure Tube length Hot zone

122 cm (48 in.) 60 cm (23 in.) 4 – 5 kHz 33 torr

**%9.0** 

Efficiency (as osc)

osc output power vs elec input power 20 9 40 Output power, watts

> **55 W** Output power

Input power, kW

30-05-0180-0056

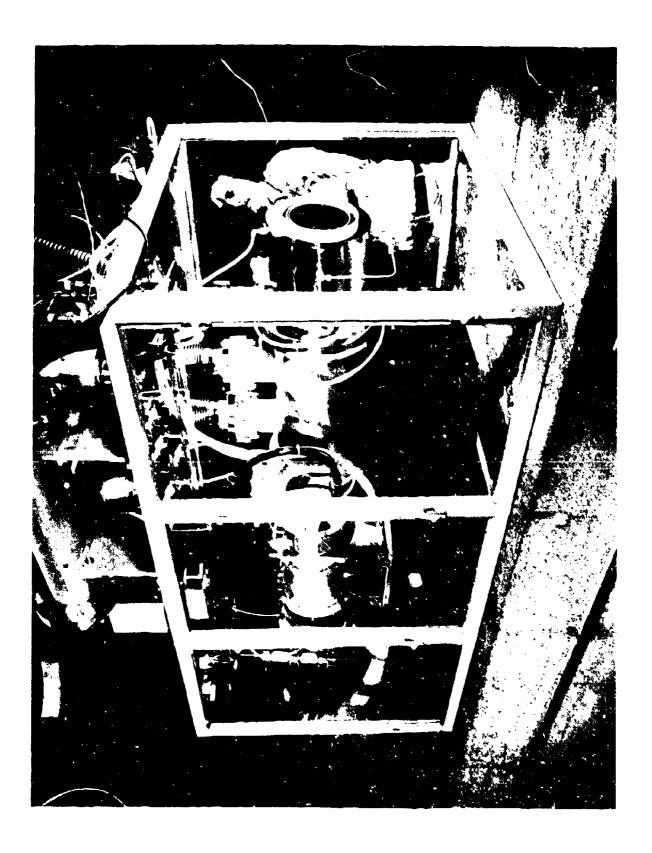
Year.

J

### **OUTPUT ENERGY DENSITY**

Location	Date	Discharge	PRF	Output Energy Density	Estored Eosc	Stored Energy Density
ns-rrr	1977	Longitid (2.5 cm)	6 kHz	11 µJ/cm ³	1.5	17 μJ/cm ³
US-GE	1977	Longitud (2.5 – 4 cm)	1 – 2 kHz	30 µJ/cm ³	1.5*	45 μJ/cm ^{3*}
US-LLL	1979	Longitud (7.3 cm)	5 kHz	6 μJ/cm ³	1.8	10 µJ/cm ^{3*}
USSR	1976	Transv	Single shot	400 µJ/cm ³	1	ı
USSR	1977	Transv	Single shot	$640  \mu \mathrm{J/cm^3}$	1	ı

* Estimated



### DEVELOPMENT - SUMMARY COPPER VAPOR LASER

- Copper lasers in 15-100 W (2-16 mJ) range are now well into engineering phase
- Effective use of MOPA configuration demonstrated
- Large bore (7.3 cm) Cu laser operated at 55 W
- Volumetric deactivation permits simple bore diameter scaling



Applicability of copper vapor lasers to many strategic and tactical problems should be reevaluated

30-17-0380-1032

### CHANNEL CHARACTERIZATION SESSION

### DOWNLINK LASER CLOUD PROPAGATION EXPERIMENTS

G. R. Hostetter

GTE Sylvania PO Box 188 Mountain View, CA 94042

During the months of August-September 1979 the Downlink Lase Cloud Experiment was conducted by GTE for DARPA and the Navy. It was designed to obtain the first data on the stretching of a lase pulse resulting from vertical propagation through a cloud layer. The pulse stretching data is needed to design systems that can communicate between satellites and submarines using high intensit short pulse lasers.

# DOWNLINK LASER CLOUD EXPERIMENT

### SPONSORS-DARPA/NAVY

CLOUD EXPERIMENT

Systems

ORJECTIVE

OSTATE FLAST BEAL WORLD DATA FOR LASER PURSES PROPAGATING VERTICALLY TABOUGH OF A PS

### GLE SYLVANIA

## DOWNLINK LASER CLOUD EXPERIMENT

• - KEY ISSUES

•- OPTICAL TRANSMISSION

•- PULSE STRETCHING AND SHAPE

CLOUD AND RECORDING EQUIPMENT LASER RECEIVER LASER TRANSMITTER (DOWNLINK LASER CLOUD EXPERIMENT) CLOUD PROBE COMMUNICATIONS **BARKING SANDS** R.ADAR +

**GLE SYLVANIA** 

TEST SET-UP

Z
TIC
2
RED
Ω
A
Ž
) II
) EC
o
U
AT/
Ω

Systems

COORD INATION FOR TESTS	SOURCE FOR DATA	BASIC DATA	REDUCED DATA	DATA EVALUATION
GTE	GTE	RECEIVED LASER SIGNAL AMPLITUDE	<ul><li>TRANSMISSION</li><li>PULSEWIDTH</li><li>PULSE SHAPE</li></ul>	
GTE	BARK ING SANDS	AIRCRAFT POSITION	۸S	GTE
GTE	NOSC	PARTICLE SIZE AND DENSITY OF CLOUDS (EXTINCTION COEFFI- CIENT) BASE AND HEIGHT OF CLOUDS	OPTICAL THICKNESS OF CLOUD	
GTE	HSS/NOSC	PATH LENGTH DATA FROM MOONLIGHT	<ul><li>PULSEWIDTH</li><li>PULSE SHAPE</li></ul>	HSS/NOSC
			۸S	
			OPTICAL THICKNESS OF CLOUD	

### PULSE SHAPE DATA: RUN NO. 182; SEPT 9, 0:55 AM (LOCAL TIME) (DOWNLINK LASER CLOUD EXPERIMENT)

System

AMPLITUDE (LINEAR)

(VOLTS)

(VOLTS)

0.1

0.1

11ME ( #SEC)

I'SZ DINIDECADE

(LOG SCALE)

TIME 10 µSEC/DIV

PULSEWIDTH (1/2 POWER)--6 MICROSECONDS

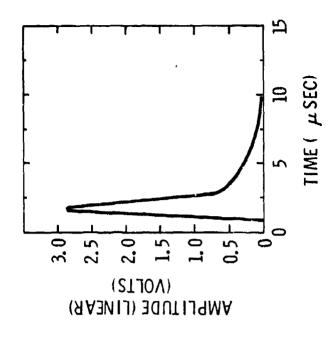
TIME TO PEAK--2 MICROSECONDS

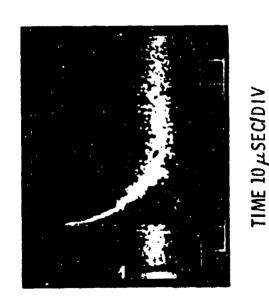
CLOUD GEOMETRIC THICKNESS--≈ 4000 FT

OPTICAL THICKNESS--TBD

### PULSE SHAPE DATA: RUN #082; AUG 30, 21:16 (PM) (LOCAL TIME) (DOWNLINK LASER CLOUD EXPERIMENT)

Systems





J'S2 DINIDECADE (LOG SCALE) **AMPLITUDE** 

PULSE WIDTH (1/2 POWER)--1 MI CROSECOND CLOUD GEOMTRIC THICKNESS-- ≈ 1500 TIME TO PEAK -- 1 MICROSECOND **OPTICAL THICKNESS--TBS** 

### PULSE SHAPE DATA: RUN #352; SEPT 21, 22:28 PM (LOCAL TIME) (DOWNLINK LASER CLOUD EXPERIMENT)

The second second second second second second second second second second second second second second second second second second second second second second second second second second second second second second second second second second second second second second second second second second second second second second second second second second second second second second second second second second second second second second second second second second second second second second second second second second second second second second second second second second second second second second second second second second second second second second second second second second second second second second second second second second second second second second second second second second second second second second second second second second second second second second second second second second second second second second second second second second second second second second second second second second second second second second second second second second second second second second second second second second second second second second second second second second second second second second second second second second second second second second second second second second second second second second second second second second second second second second second second second second second second second second second second second second second second second second second second second second second second second second second second second second second second second second second second second second second second second second second second second second second second second second second second second second second second second second second second second second second second second second second second second second second second second second second second second second second second second second second second second second second second second second second second second second second secon



Systems

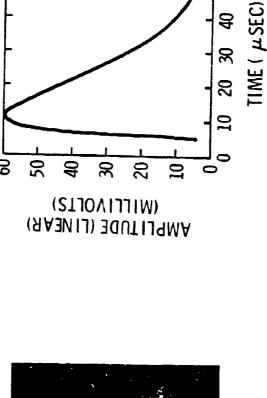
8 (MILLIVOLTS) AMPLITUDE (LINEAR)

TIME 10 ASECIDIV

8

40 50

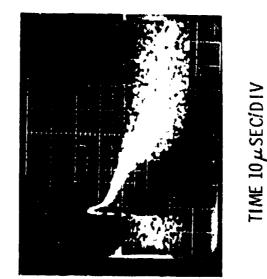
PULSEWIDTH (1/2 POWER)--22 MICROSECONDS CLOUD GEOMETRIC THICKNESS-- ≈8000 FT TIME TO PEAK -- 5 MICROSECONDS **OPTI CAL THI CKNESS--TBD** 



J. 25 DIVIDECADE (FOG SCALE) **AMPLITUDE** 

### PULSE SHAPE DATA: RUN #129; SEPT 7, 1:53 AM (LOCAL TIME) (DOWNLINK LASER CLOUD EXPERIMENT)





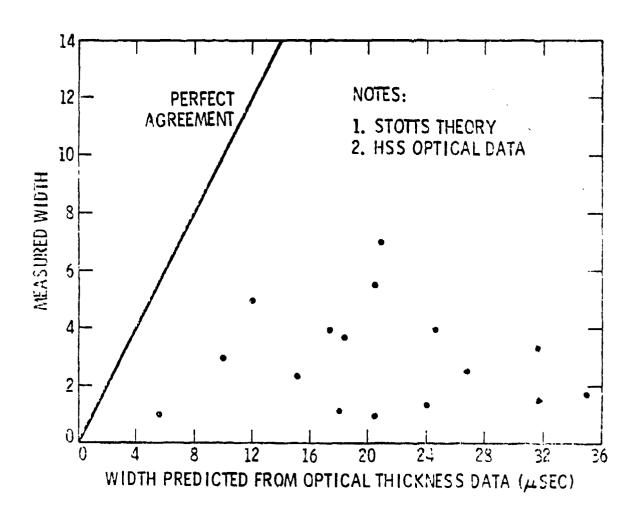
AMPLITUDE (LOG SCALE) 1.25 DIVIDECADE

PULSEWIDTH (1/2 POWER)--3 MICROSECONDS

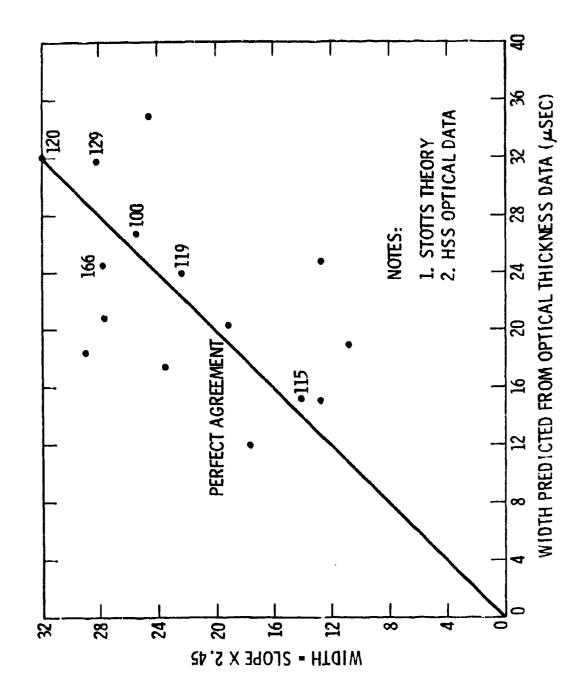
TIME TO PEAK--2 MICROSECONDS

CLOUD CEOMETRIC THICKNESS--≈5000 FT

OPTICAL THICKNESS--TBD



Data Analysis: Pulse Width-Predicted Vs Measured



Data Analysis: Pulse Width-Predicted VS Inferred From Slope

I would

1

### CONCLUSIONS

### (DOWNLINK CLOUD EXPERIMENT)

Systems

PULSE WIDTH LESS THAN PREDICTED

■ ANALYTICAL MODELS SHOULD BE IMPROVED TO INCLUDE REAL WORLD CLOUD GEOMETRIES

■ DO MORE EXPERIMENTATION

TEST DESCRIPTION

EQUIPMENT

• TEST SITE

TEST SCHEDULE

DATA REDUCTION

DATA AND SOURCES

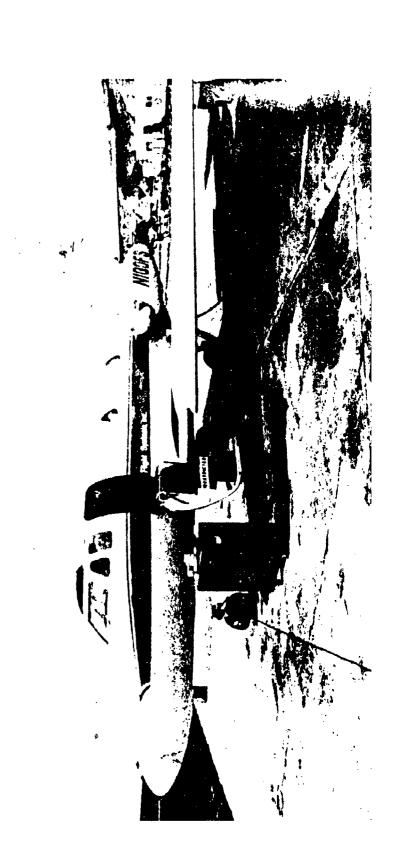
ANÁLYSIS STEPS

CLOUD DATA

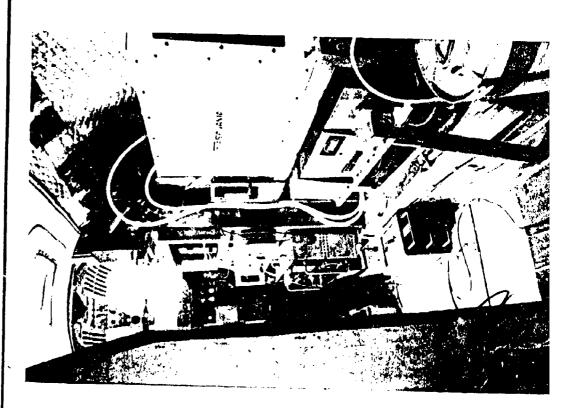
ADDITIONAL ANALYSIS



## HIGH ALTITUDE AIRCRAFT (DOWNLINK LASER CLOUD EXPERIMENT)



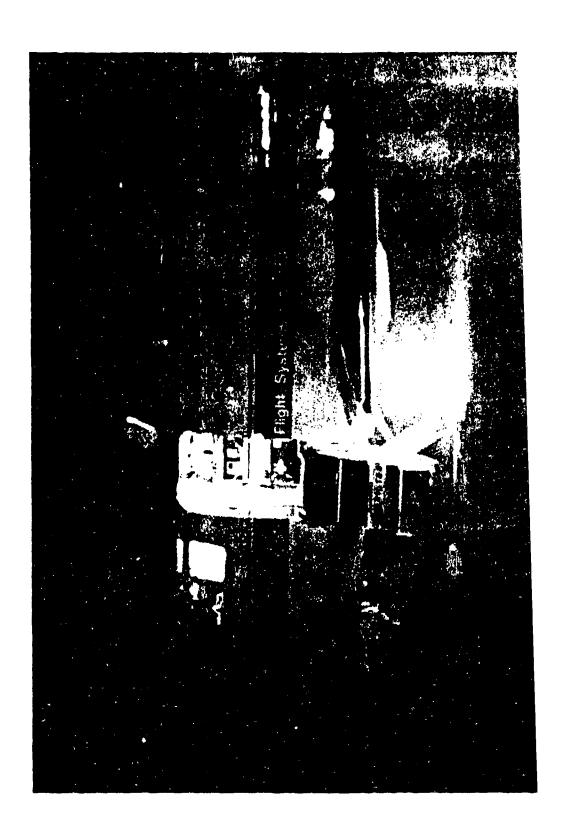
# LASER MOUNTED IN AIRCRAFT (DOWNLINK LASER CLOUD EXPERIMENT)

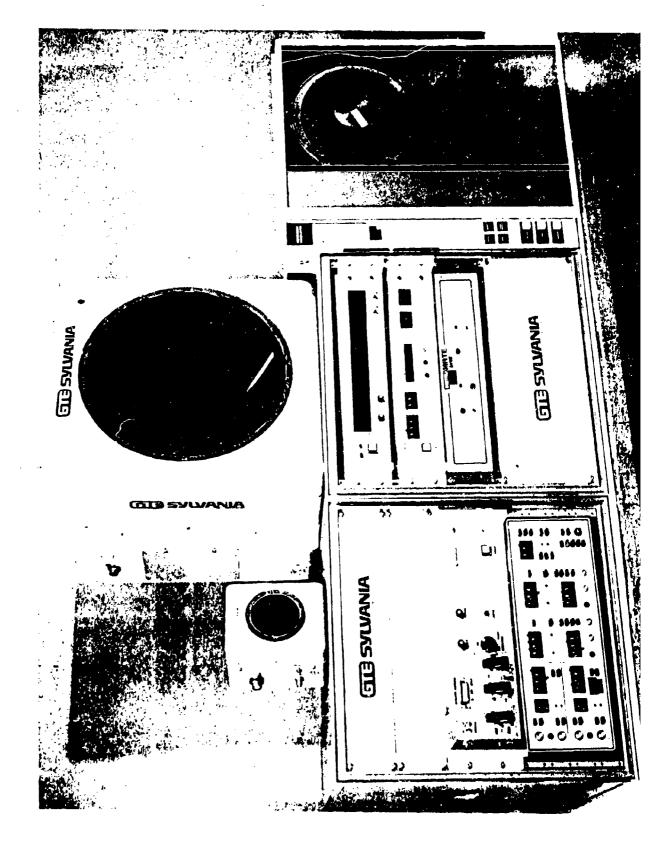






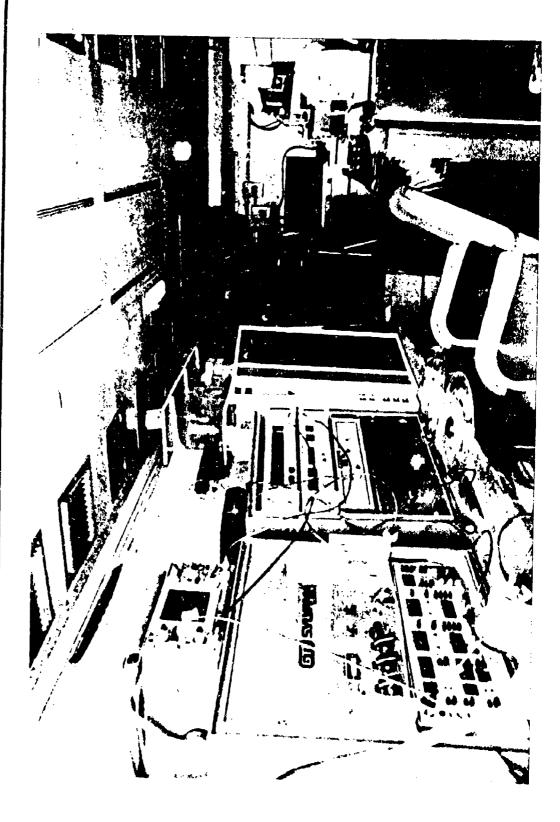
# PREFLIGHT LASER TEST (DOWNLINK LASER CLOUD EXPERIMENT)

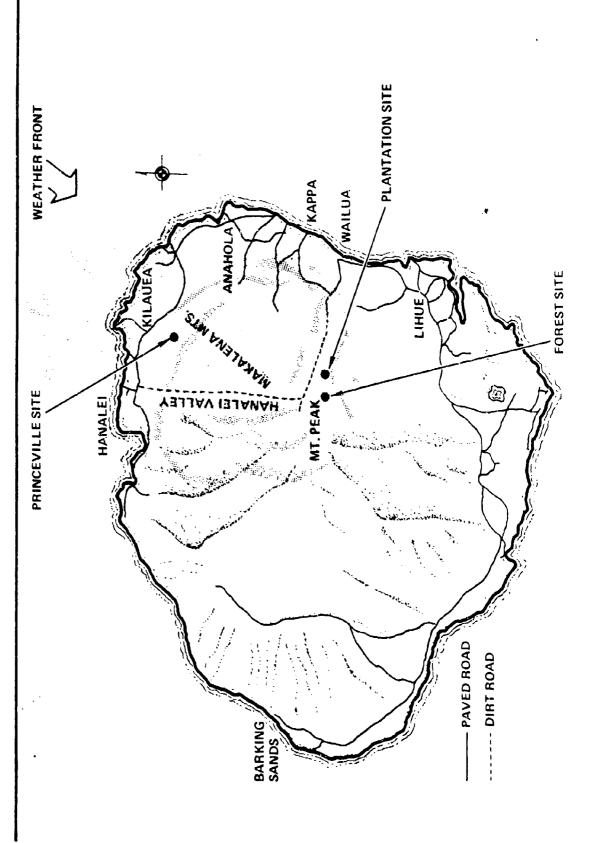






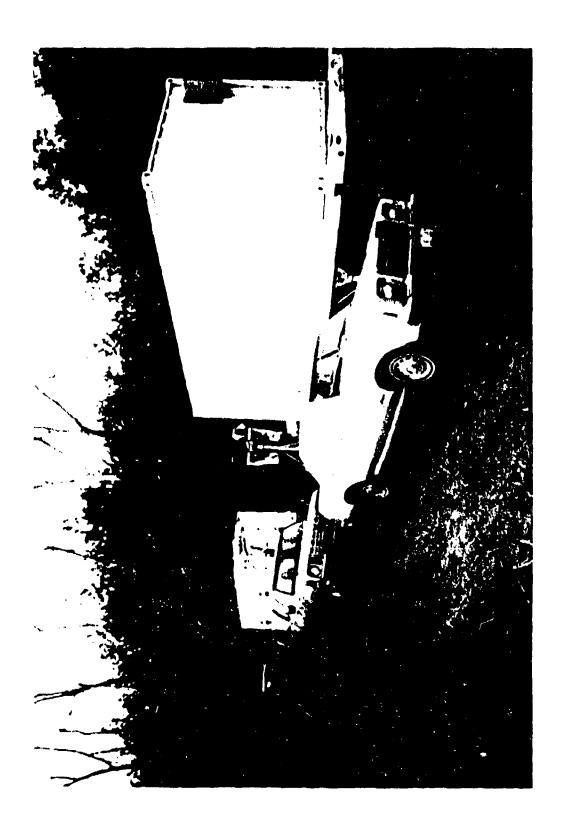






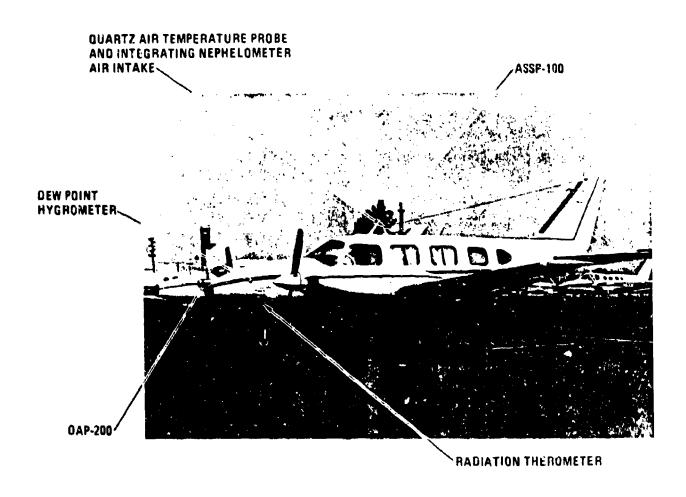
TEST SITE: AERIAL VIEW (DOWNLINK LASER CLOUD EXPERIMENT)





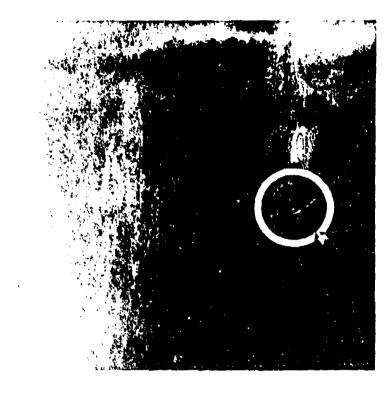
# TEST SITE LAYOUT (DOWNLINK LASER CLOUD EXPERIMENT)

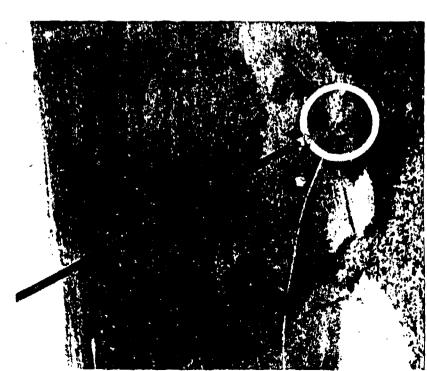


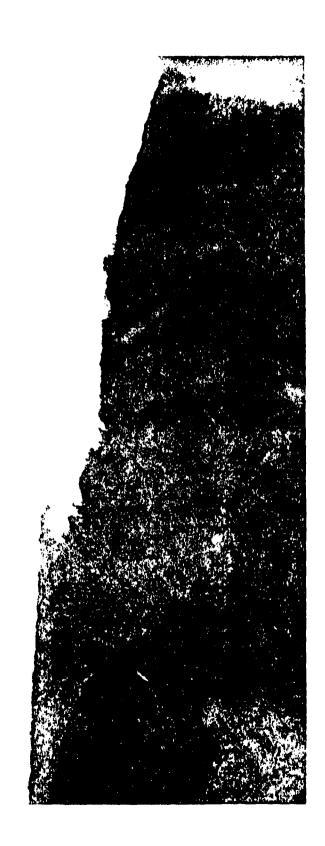


Instrumented Cloud Probe Aircraft

# FLIGHT PATH OF CLOUD PROBE AIRCRAFT (DOWNLINK LASER CLOUD EXPERIMENT)







-

To the second

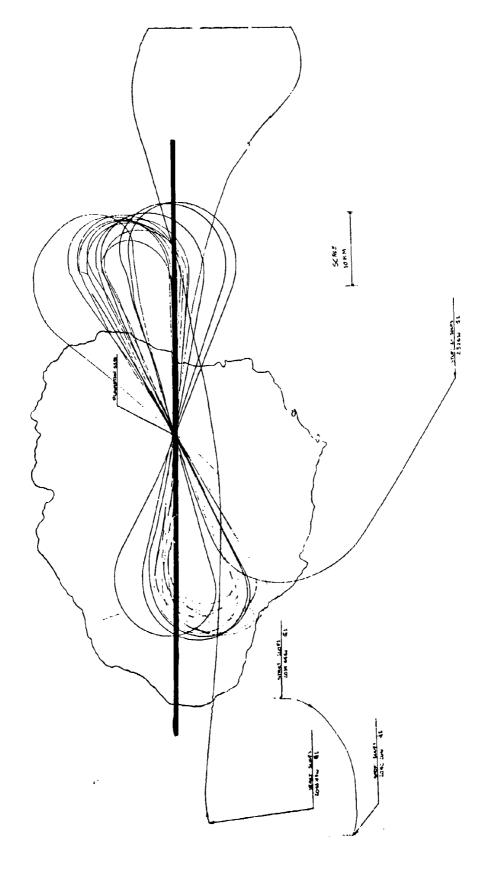
IJ

## CLOUD PATTERNS (DOWNLINK LASER CLOUD EXPERIMENT)





## PLOT BOARD PLOT, LARGE SCALE (DOWNLINK CLOUD EXPERIMENT)



Sylvania Systems Group Western Division

Paris Service

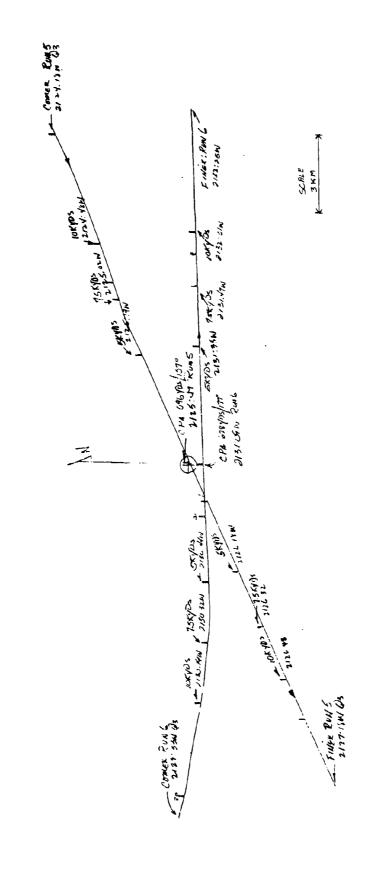
State of the same of

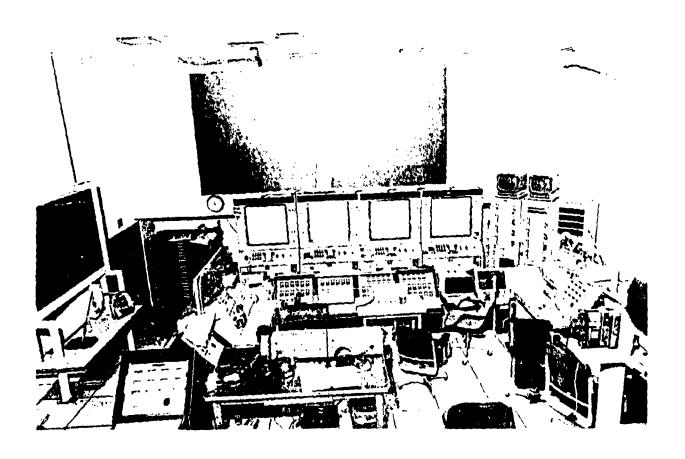
-

THE PARTY OF

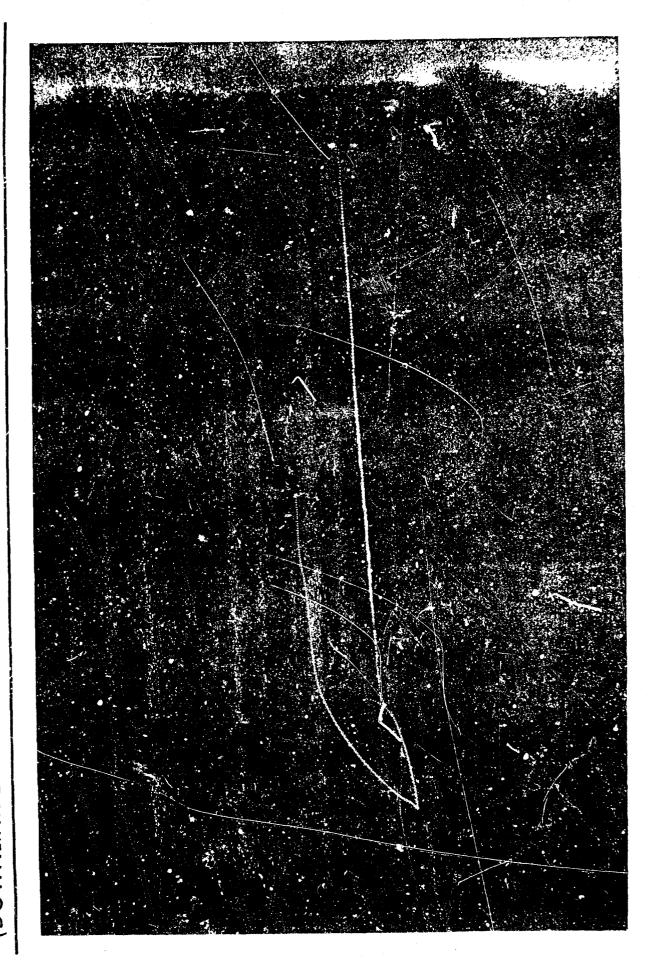
Systems

### (DOWNLINKCLOUD EXPERIMENT) PLOT BOARD PLOT, FINE SCALE





Control Room "BRAVO" at PMRF



Systems

	1	707		AUGUST 1979			
L	NOS	MOIN	IUES	WED	IHURS	FRI	SAT
				1	2	3	4
2		9	7	∞	9 FLIGHT TEST	10	
15	12 GTE/HSS 13 ARRIVE		14 PMRF INTERFACE	15	16	17	18
19	A I R CRAFT ARRIVE			52	23	<b>(2)</b>	25
<b>5</b> 0		22		29	30	31	

FR! SAT	-	8	15	20 LAST 22	29	
9 THURS		(BEST TWO NIGHTS FOR HSS)	(I)	(Z) (Zi)	27 28	
SEPTEMBER 1979 WED		(S) (BEST TWO NIG	(Z)	60	26	1
TUES		4		(18)	25	
MON		3	10	<b>(1)</b>	24	
SUN		2	6	16	23 RETURN TO CONIIS	

Sylvaria Systems Group Western Division

-

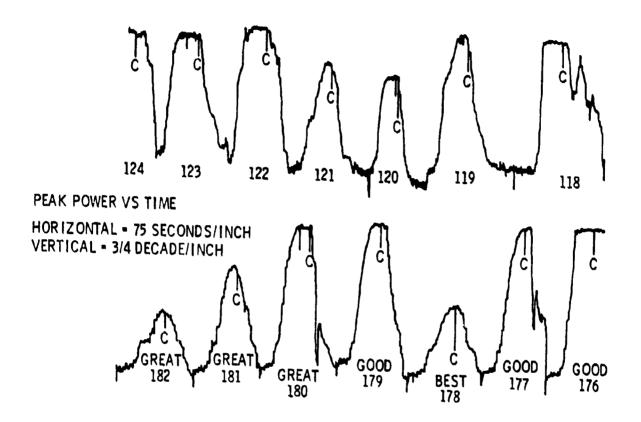
bases in the

### **OVERVIEW** (DOWNLINK CLOUD EXPERIMENT) **DATA TAKING**

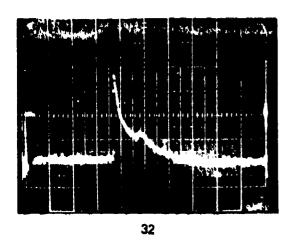
- 19 TOTAL FLIGHTS, TEST OR DATA
- 13 FLIGHTS WITH GOOD DATA, 3 WITH ONLY MARGINAL DATA
- 360 DATA RUNS (200, 000 DATA PULSES X 4, 000 BITS/PULSE = 800 MILLION BITS INFO)
- 80 RUNS, HIGHEST PRIORITY (GOOD DATA)
- 84 RUNS, SECOND PRIORITY (MARGINAL DATA)

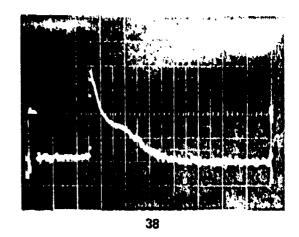
- DATA AVERAGING
- PULSE PARAMETER EVALUATION
- SLOPE EVALUATION

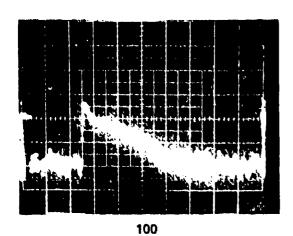
į

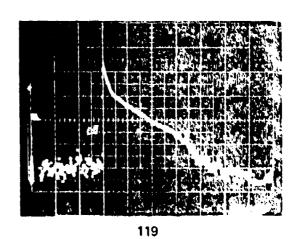


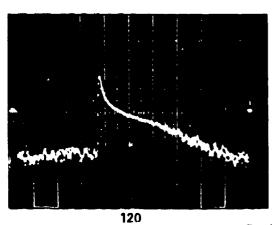
Data Survey, Typical Plot

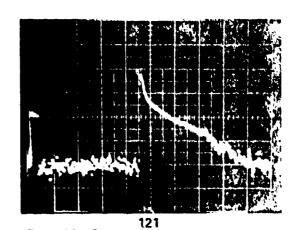




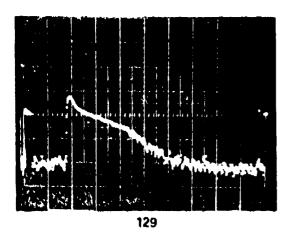


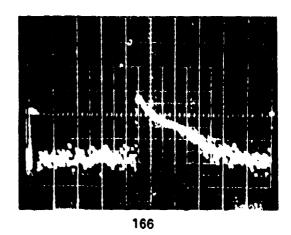


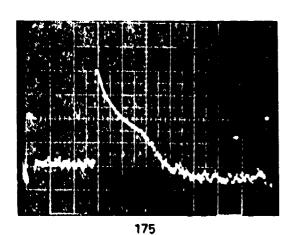


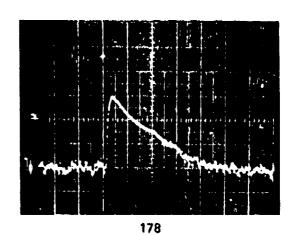


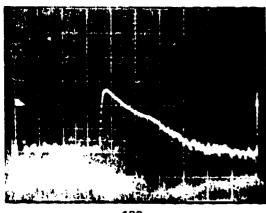
Typical Data From Six Runs

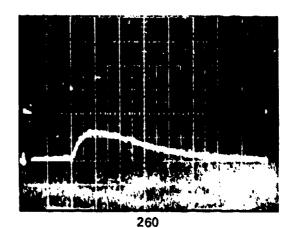












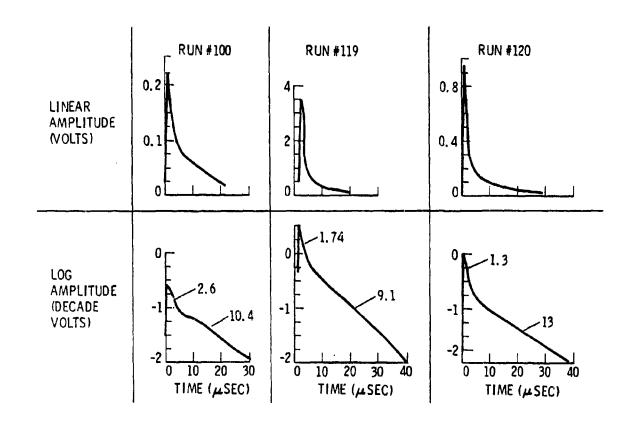
182

Typical Data From Six Runs

Ivania Systems Group estern Division

### PULSE SHAPE PARAMETERS

GTE RUN UMBER	(µsec) WIDTH	TIME TO PEAK	MEAN DELAY	10 ⁻⁶ W PEAK POWER	10 ⁻¹² WS ENERGY	ATTENU- ATION	usec/1/e  SLOPE 1	μsec/l SLOPE 2
190	Bomb							
191	2.2	1.4	1.4	1.12	2.63	.033	1	6
192	1.8	.8	1.34	2.4	5.9	.039	1	6
193	2.0	1.0	4.5	1.19	4.67	.058	1,5	9
200		ļ		.209				
225				.209		,		
						ŕ		
231	.8	.4		11.9	11.5	.14		
232	1.0	.4		6.5	8.81	.11		
233	1.0	.6		4.9	6.56	.082		
234	2.2	1.0	3.9	.94	3.95	.049	2	6
235	.8	.4		12.8	13.9	.17		
236	1.8	1.0		2.47	6.89	.086		
237	2.0	1.2	.8	11.2	35.6	.45	1	5
238	.6	.4		14.6	10.7	.133		
249	1.0	.6		11.9	20.6	.26		
250								
252				.178				



Reduced Data Plots

### (DOWNLINK CLOUD EXPERIMENT) SLOPE EVALUATION

- FOR DIAGNOSTIC PURPOSES, CALCULATE SLOPE OF LOG PLOTS TIME CONSTANT
- MANY CURVES WITH TWO DISTANT TIME CONSTANTS

Systems

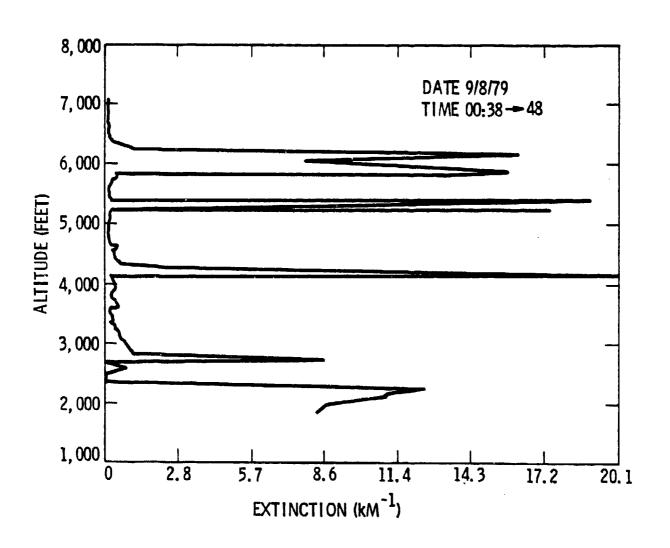
CLOUDY TIMES CYCLIC

8 - 8:30 PM

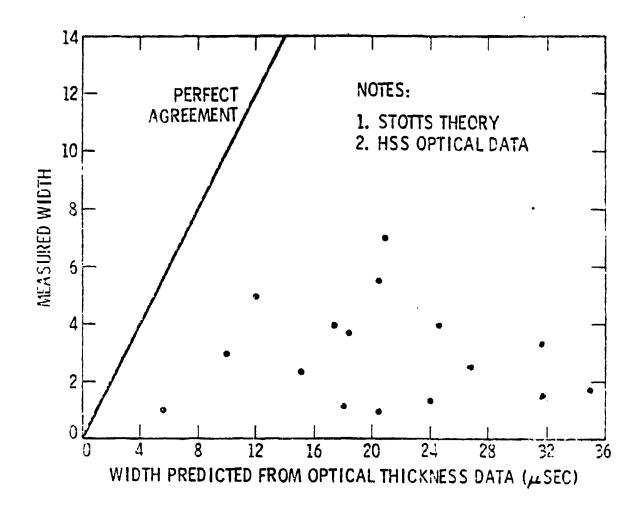
10 - 10:30 PM

12:30 - 1:00 AM

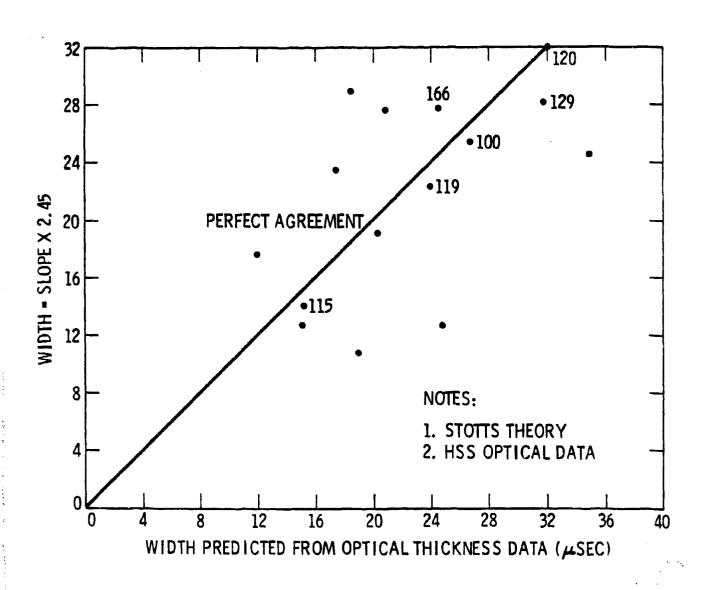
- TYPICAL OPTICAL THICKNESS CALCULATED BY HSS = 15 - 80
- CLOUD PROBE DATA CALCULATE OPTICAL THICKNESS = 1 - 10



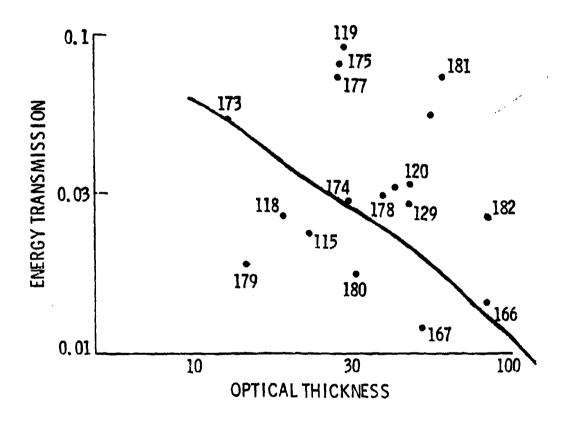
Typical Extinction Coefficient Vs Altitude Plot



Data Analysis: Pulse Width-Predicted Vs Measured



Data Analysis: Pulse Width-Predicted VS Inferred From Slope



Data Analysis: Transmission As Optical Thickness

### REPORT OUTLINE (DOWNLINK CLOUD EXPERIMENT)

### FINAL REPORT

- INTRODUCTION AND SUMMARY
- EXPERIMENT DESCRIPTION
- DATA REDUCTION AND ANALYSIS

### APPENDICES

- PULSE SHAPE RAW DATA OVERVIEW
- RAW CLOUD DATA AND RUN PRIORITIES
- LASER AND LASER PLATFORM
- **PULSE SHAPE PARAMETERS**
- CLOUD CHARACTERISTICS
- TYPICAL RAW DATA PHOTOGRAPHS
- REDUCED DATA PLOTS

1

Frankriger ( ) 1 maß ( ) 1 maß ( ) 1 man og ( ) 1 man og ( ) 1 man og ( ) 1 man og ( ) 1 man og ( ) 1 man og ( ) 1 man og ( ) 1 man og ( ) 1 man og ( ) 1 man og ( ) 1 man og ( ) 1 man og ( ) 1 man og ( ) 1 man og ( ) 1 man og ( ) 1 man og ( ) 1 man og ( ) 1 man og ( ) 1 man og ( ) 1 man og ( ) 1 man og ( ) 1 man og ( ) 1 man og ( ) 1 man og ( ) 1 man og ( ) 1 man og ( ) 1 man og ( ) 1 man og ( ) 1 man og ( ) 1 man og ( ) 1 man og ( ) 1 man og ( ) 1 man og ( ) 1 man og ( ) 1 man og ( ) 1 man og ( ) 1 man og ( ) 1 man og ( ) 1 man og ( ) 1 man og ( ) 1 man og ( ) 1 man og ( ) 1 man og ( ) 1 man og ( ) 1 man og ( ) 1 man og ( ) 1 man og ( ) 1 man og ( ) 1 man og ( ) 1 man og ( ) 1 man og ( ) 1 man og ( ) 1 man og ( ) 1 man og ( ) 1 man og ( ) 1 man og ( ) 1 man og ( ) 1 man og ( ) 1 man og ( ) 1 man og ( ) 1 man og ( ) 1 man og ( ) 1 man og ( ) 1 man og ( ) 1 man og ( ) 1 man og ( ) 1 man og ( ) 1 man og ( ) 1 man og ( ) 1 man og ( ) 1 man og ( ) 1 man og ( ) 1 man og ( ) 1 man og ( ) 1 man og ( ) 1 man og ( ) 1 man og ( ) 1 man og ( ) 1 man og ( ) 1 man og ( ) 1 man og ( ) 1 man og ( ) 1 man og ( ) 1 man og ( ) 1 man og ( ) 1 man og ( ) 1 man og ( ) 1 man og ( ) 1 man og ( ) 1 man og ( ) 1 man og ( ) 1 man og ( ) 1 man og ( ) 1 man og ( ) 1 man og ( ) 1 man og ( ) 1 man og ( ) 1 man og ( ) 1 man og ( ) 1 man og ( ) 1 man og ( ) 1 man og ( ) 1 man og ( ) 1 man og ( ) 1 man og ( ) 1 man og ( ) 1 man og ( ) 1 man og ( ) 1 man og ( ) 1 man og ( ) 1 man og ( ) 1 man og ( ) 1 man og ( ) 1 man og ( ) 1 man og ( ) 1 man og ( ) 1 man og ( ) 1 man og ( ) 1 man og ( ) 1 man og ( ) 1 man og ( ) 1 man og ( ) 1 man og ( ) 1 man og ( ) 1 man og ( ) 1 man og ( ) 1 man og ( ) 1 man og ( ) 1 man og ( ) 1 man og ( ) 1 man og ( ) 1 man og ( ) 1 man og ( ) 1 man og ( ) 1 man og ( ) 1 man og ( ) 1 man og ( ) 1 man og ( ) 1 man og ( ) 1 man og ( ) 1 man og ( ) 1 man og ( ) 1 man og ( ) 1 man og ( ) 1 man og ( ) 1 man og ( ) 1 man og ( ) 1 man og ( ) 1 man og ( ) 1 man og ( ) 1 man og ( ) 1 man og ( ) 1 man og ( ) 1 man og ( ) 1 man og

l-seggand

## DATA ANALYSIS SUMMARY (DOWNLINK CLOUD EXPERIMENT)

Systems



- STABLE PULSE SHAPES
- ► ATTENUATION LESS THAN WHAT PREDICTED
- DUAL MODE OF PROPAGATION THROUGH CLOUDS INDICATED BY DATA

- - -

the same of the same of

-

Participation (

Total State of the last of the last of the last of the last of the last of the last of the last of the last of the last of the last of the last of the last of the last of the last of the last of the last of the last of the last of the last of the last of the last of the last of the last of the last of the last of the last of the last of the last of the last of the last of the last of the last of the last of the last of the last of the last of the last of the last of the last of the last of the last of the last of the last of the last of the last of the last of the last of the last of the last of the last of the last of the last of the last of the last of the last of the last of the last of the last of the last of the last of the last of the last of the last of the last of the last of the last of the last of the last of the last of the last of the last of the last of the last of the last of the last of the last of the last of the last of the last of the last of the last of the last of the last of the last of the last of the last of the last of the last of the last of the last of the last of the last of the last of the last of the last of the last of the last of the last of the last of the last of the last of the last of the last of the last of the last of the last of the last of the last of the last of the last of the last of the last of the last of the last of the last of the last of the last of the last of the last of the last of the last of the last of the last of the last of the last of the last of the last of the last of the last of the last of the last of the last of the last of the last of the last of the last of the last of the last of the last of the last of the last of the last of the last of the last of the last of the last of the last of the last of the last of the last of the last of the last of the last of the last of the last of the last of the last of the last of the last of the last of the last of the last of the last of the last of the last of the last of the last of the last of the last of the

## RECOMMENDATIONS (DOWNLINK CLOUD EXPERIMENT)

- IMPROVE ANALYTICAL MODELS TO INCLUDE REAL WORLD CLOUD GEOMETRIES
- CONDUCT ADDITIONAL EXPERIMENTS IN REAL WORLD ENVIRONMENT

### THE TEMPORAL AND SPATIAL SMEARING OF BLUE-GREEN PULSES IN CLOUDS

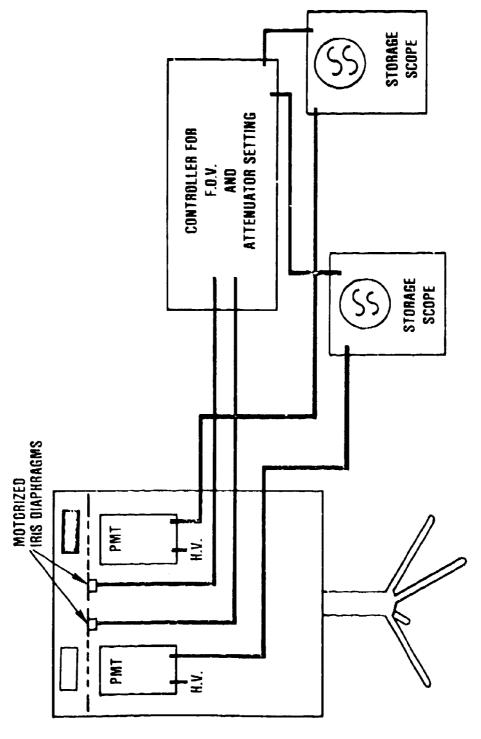
G. C. Mooradian and M. Geller NOSC

The time history of large diameter (approximately 6 km) blue-green laser pulses propagating through clouds in Kauai was measured as function of receiver field of view (FOV). Analyses of the data showed that the transmitted power of each pulse could be represented by a linear combination of two modified Gamma functions:  $P(t) = C_1 \exp(-k_1 t) + C_2 (\exp-k_2 t)$ . One term is the diffusion component, and the other term is a lower order multiple scattering part, which may even be a direct, non-scattered portion of the transmitted beam. Some data showed that for wide FOV, the received pulse consisted of a large diffusion component, and that as the FOV decreased, the pulse energy in the diffusion component decreased and the non-diffusion part increased. In the limit of the smallest FOV, only the non-diffusion component was obtained. Other examples show that for very dense clouds, the only component received was the diffusion type. Data was presented for the power received as a function of FOV of the receiver for various values of optical thickness, and for the case where the transmitting aircraft was not directly overhead, but 5000 yards distant, and for the cases where the receiver was intentionally directed 5 and 10 degrees from the vertical. The measured pulse widths were consistently smaller than the theoretical values derived from Stotts** using the value of optical thickness as inferred by the HSS moon radiometric data. This discrepancy may be explained by the overestimation in the values of cloud physical thickness measurements made by the meteorological aircraft.

**Stotts: Applied Optics, 17, 504 (1978)

## NOSTR

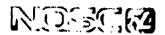
# VARIABLE FIELD OF VIEW RECEIVERS AND DATA RECORDING SETUP



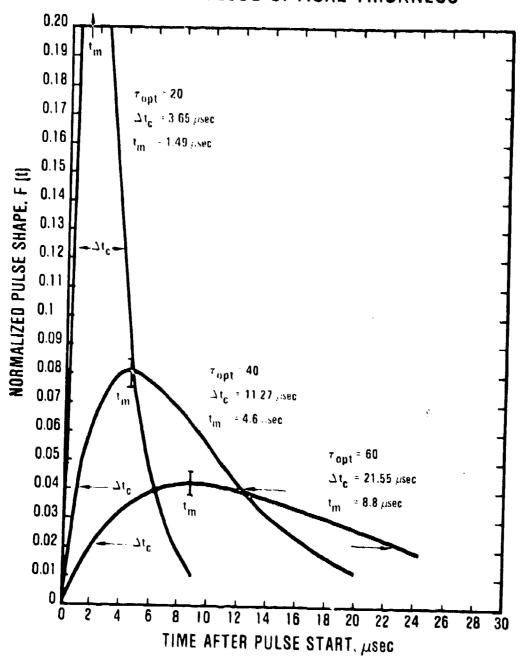
100

F. radio 44

7

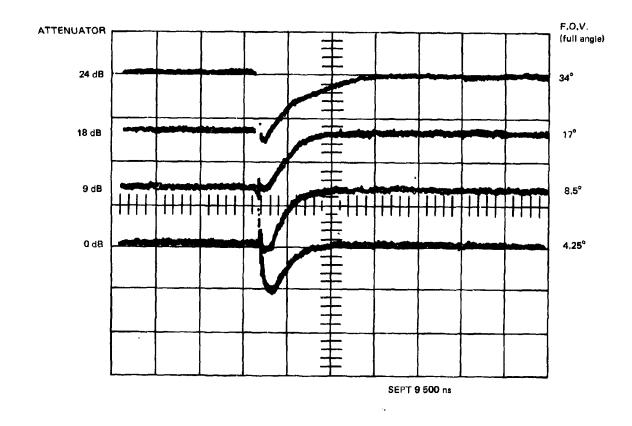


#### REPRESENTATIVE NORMALIZED PULSE SHAPES AS A FUNCTION OF CLOUD OPTICAL THICKNESS



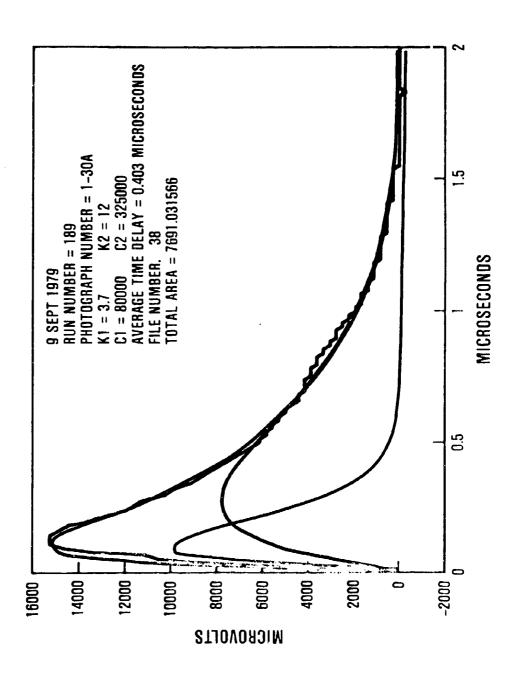


ENERGY PER PULSE (AREA UNDER CURVE) =  $\frac{C}{K^2}$ DIFFUSION COMPONENT f(t) = Cte-K PEAK POWER (t = 1/K) = 0.368 C/K PULSE WIDTH (FWHM) =  $\frac{2.45}{K}$ AVERAGE TIME DELAY =  $\frac{2}{K}$ 



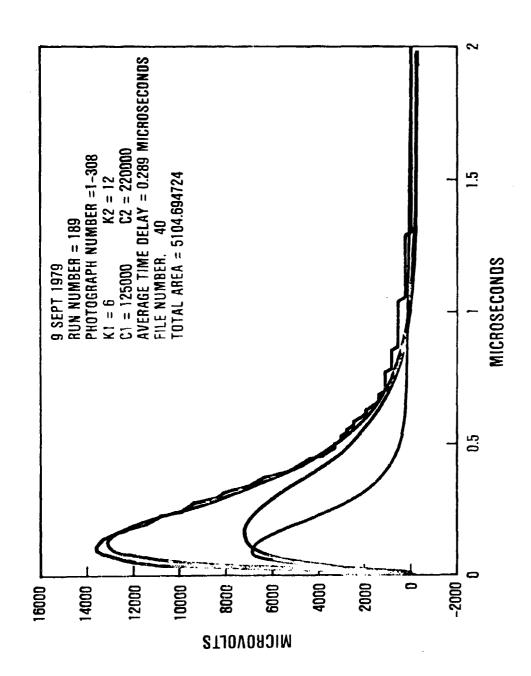


記録を開発を記されています。

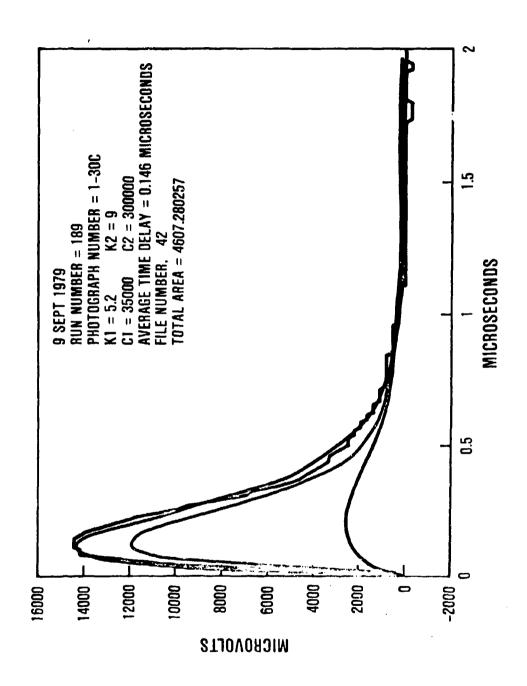




こうこうにはから、これのということはできるとはいいというまではいます。大きないないのは、からいはないないないないないないできないないないないないできないないできないというということがあっています。

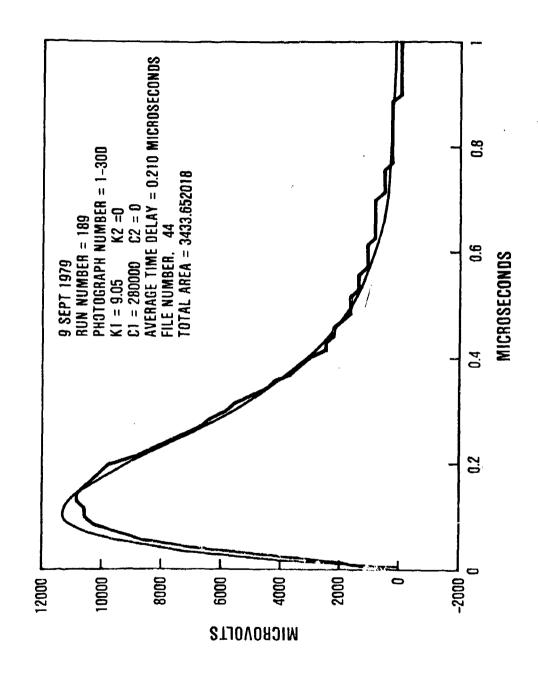


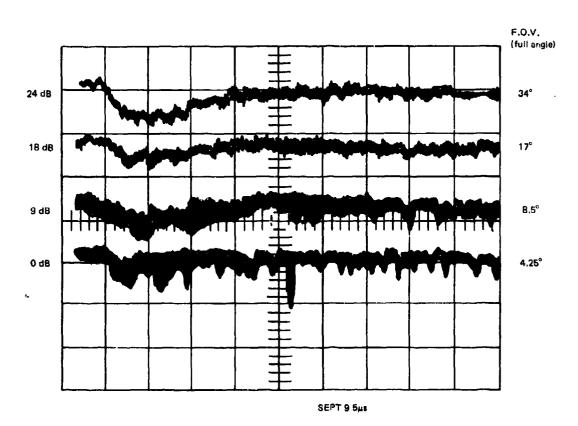




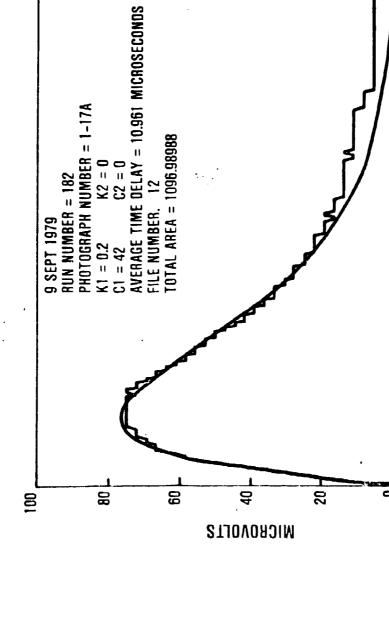


The second second second second second second second second second second second second second second second second second second second second second second second second second second second second second second second second second second second second second second second second second second second second second second second second second second second second second second second second second second second second second second second second second second second second second second second second second second second second second second second second second second second second second second second second second second second second second second second second second second second second second second second second second second second second second second second second second second second second second second second second second second second second second second second second second second second second second second second second second second second second second second second second second second second second second second second second second second second second second second second second second second second second second second second second second second second second second second second second second second second second second second second second second second second second second second second second second second second second second second second second second second second second second second second second second second second second second second second second second second second second second second second second second second second second second second second second second second second second second second second second second second second second second second second second second second second second second second second second second second second second second second second second second second second second second second second second second second second second second second second second second second second second second second second second second second second secon



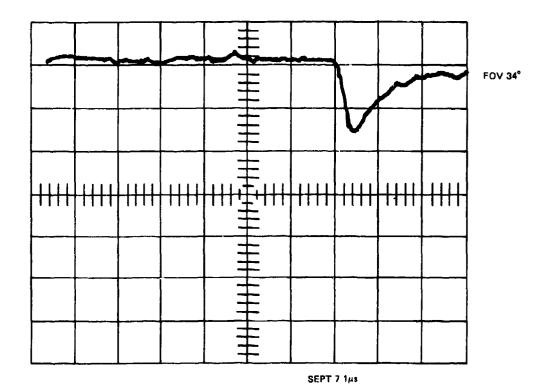


f

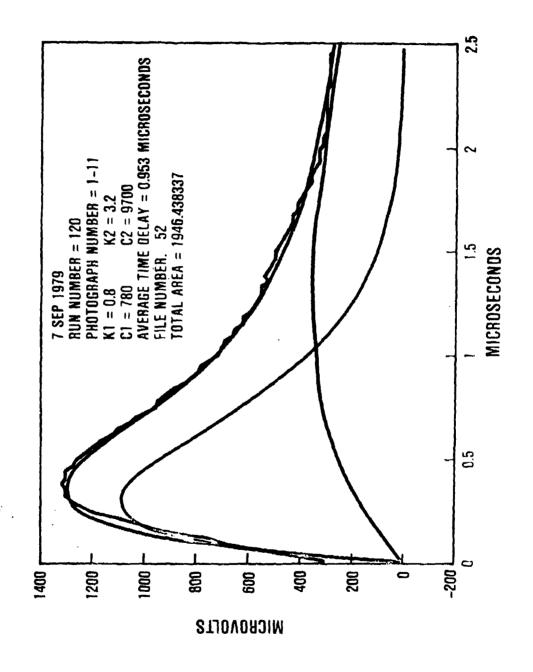


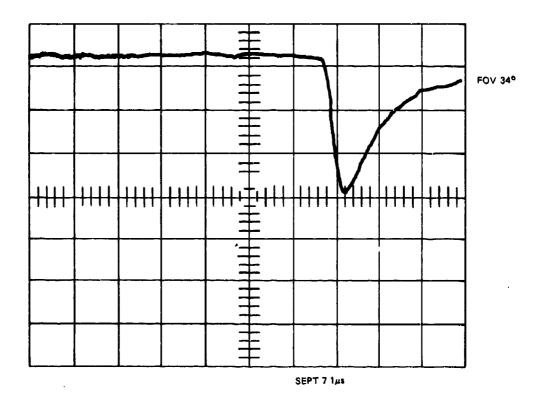
MICROSECONDS

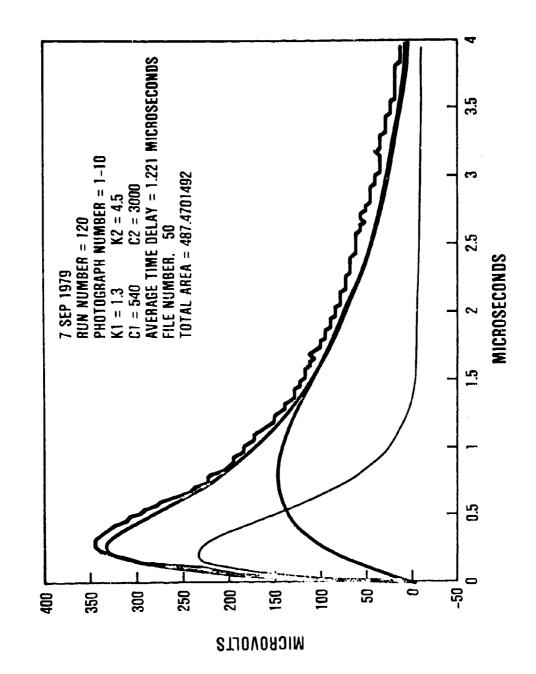
വ

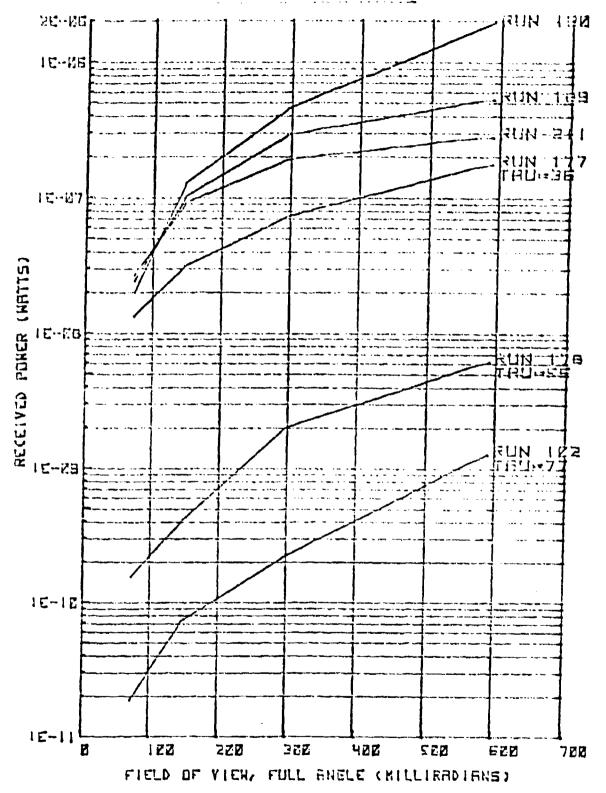


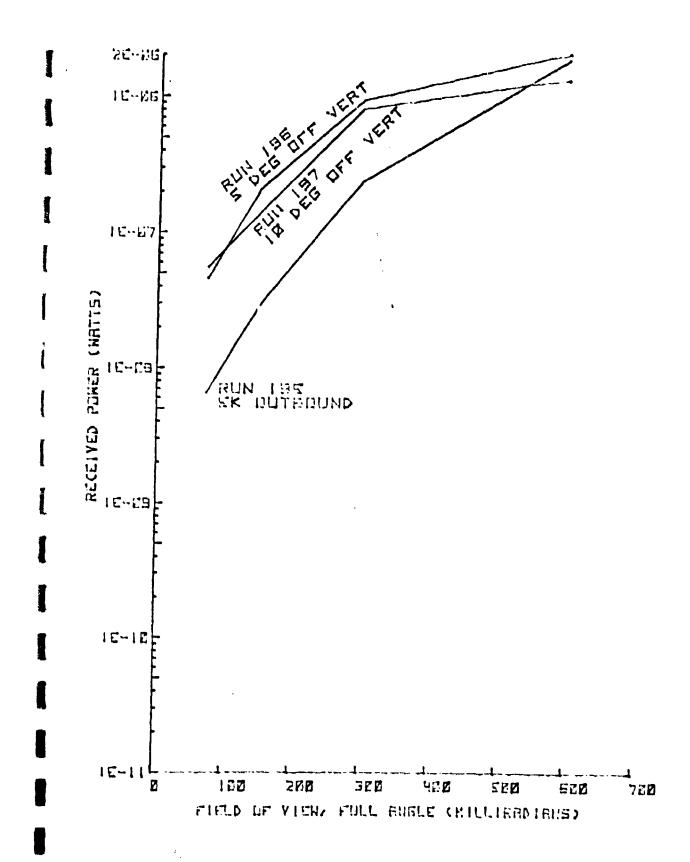














## totts: Multipath time spread

$$= \frac{Z}{C} \left\{ \frac{0.30}{\omega_0 \tau \gamma_0^2} \left[ \left[ \left( 1 + 2.25 \, \omega_0 \tau \gamma_D^2 \right)^{3/2} - 1 \right] - 1 \right] \right\}$$

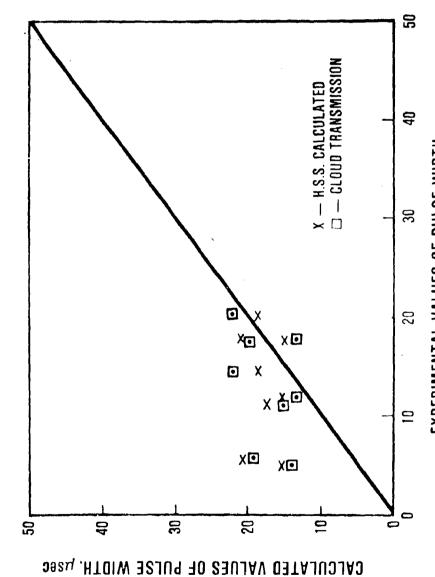
$$\gamma_0$$
 = RMS SCATTER ANGLE

$$\tau$$
 = OPTICAL THICKNESS

$$\omega_0 = 1$$



# COMPARISON OF EXPERIMENTAL AND THEORETICAL PULSE WIDTHS



#### KAUAI CLOUD EXPERIMENT MEASUREMENTS: O₂ ABSORPTION TECHNIQUES

#### H.S. Stewart and D. F. Hansen

A. Discussion of Basic Technique and Pre-Kauai Experimental Measureme by H.S. Stewart.

Slide 2. States the basic concept of the technique

Slide 3. States the method of concept implementation

Slide 4. Lower half of slide shows how resolution spectrum of sunlight as transmitted by one, two and three air masses. The selected wavelength for measuring O₂ absorption, 0.7606μ is shown as "on" and the wavelength for O₂ free observation, 0.7530μ, is marked as "off". Top of slide shows zenith angles for one, two and three air mass observations.

Slide 5. Illustrates concept of diffuse transmission as compared to specular transmission, IoS(Z)/Io.

Slide 6. The 0.5° field-of-view teleradiometer and its on and off band filters used for measurements of O₂ absorption in clouds.

Slide 7.

San Nicolas Island, CA. Observations of O₂ absorption in overcasts were made at NW corner near the NRL Tower Site.

Slide 8. Calibration of the teleradiometer made against setting sun. In this plot log (on-band reading) -log (off-band reading) is plotted against (path through atmospheric O₂)^{1/2} and gives a straight line.

Reduced data for May 3, 1979 overcast. Readings are made at zenith angles 30°, 45°, and 60° and azimuth values north, east, south and west. On the figure for each direction the time delay in the overcast in microseconds is printed above the transmission of the overcast.

Slide 10. The same as Slide 9 but for May 4.

Slide 11. The left hand side of the slide shows a camera system for recording the on-band/off-band ratio simultaneously for many lines-of-sight. The camera views the whole hemisphere of the sky via the reflecting sphere. Separate

HSS Inc 2 Alfred Circle Bedford MA 01730

- Slide 11 (cont.) pictures are taken through the on-band and the off-band filters. Data is reduced separately for each of 125000 lines-of-sight giving time delay in O₂ and cloud and overcast transmission.
- Slide 12. From data taken as in Slide 11 a curve of probability of geometric plus diffusion delay as a function of delay time is generated. Slide 12 shows such a curve for 0937 3 August 1977.
- Slide 13.

  It is possible that future observations may involve multiple lines-of-sight but not as many as 125,000. The slide shows a possible subdivision of the hemisphere of the sky into 25 elements giving equal signals from a uniform overcast. Some radiometric gadget might be used for such observations.
  - B. KAUAI EXPERIMENT; by D. F. Hansen.
  - This is a photograph of the two-channel teleradiometer used during Kauai experiment. Use of the moon, instead of the sun as the source of illumination required the instrument to have high sensitivity. This sensitivity was provided by use of thermoelectrically cooled photomultiplier tubes and six-inch diameter collecting apertures. Each channel was equipped with a six-inch diameter interference filter; the center wavelength of the on-band channel was 7608 A, with a half-peak bandwidth of 15 A; the center wavelength of the off-band channel was 7530 Å with a bandwidth of 30 Å. A circulating fluid heat-exchanger unit, also shown in the photograph was used to extract the heat from the thermoelectric coolers.
  - Slide 15. Photograph of the electronic controls and PAR photon counting systems used in conjunction with the two-channel teleradiometer.
  - Slide 16. Summary of data-run participation using the two-channel teleradiometer during the KAUAI Experiment.

Slide 17.	Calibration curve for the two-channel teleradiometer generated prior-to the experiment, with cloud-free lines of sight at Barking Sands, Kauai using sunlight (greatly attenuated) as the source of illumination; and also using cloud-free lines of sight and the moon as the source, during the evenings when the experiments were
	conducted.
Slide 18.	Visual observations of overcast and precipitation which were present during each of the data runs for two evenings when the teleradiometer participated in the KAUAI experiment.
Slide 19.	Typical Data-Results. Table summarizing the measurements made with the two-channel teleradiometer on each data run and the data derived from the measurements.
Slide 20.	Comparison of mean-time-delays measured by GTE-Sylvania with mean-time delays measured with the two-channel teleradiometer for Aircraft Run No. 120. The zenith angle changes for the Sylvania data as the aircraft passes overhead whereas for any given run the zenith angle to the moon is fixed for the teleradiometer measurement.
Slide 21.	Comparison of mean-time-delays measured by GTE-Sylvania with mean-time-delays measured with the two-channel teleradiometer for Aircraft Run No. 119.
Slide 22.	Comparison of mean-time-delays measured by GTE-Sylvania with mean time delays measured with the two channel teleradiometer for Aircraft Run No. 100. Note the large change in mean-time-delays which occured in the Sylvania data when the rain shower commenced over the site.
	The major differences between the Sylvania and HSS Inc measurements of mean-time-delay are attributed to the fact that the zenith angle to the moon was quite different than the zenith angle to the aircraft for all data runs.

Slide 23.

Slide 24.

Scatter diagram of correlation between NOSC and HSS Inc. Values of Optical Thickness--obtained on eighteen data runs,

Plot of mean-time-delay vs product of optical thickness and

geometric thickness of the clouds for 23 data runs.

#### PURPOSE

TO DEDUCE THE DELAY AND SMEARING OF A LIGHT

PULSE IN ITS TRANSIT OF A CLOUD OF OVERCAST

USING STEADY STATE OBSERVATIONS OF SUNLIT CLOUDS,

### BASIC CONCEPT

一年の後、一年の大田

THE LONGER A PHOTON TAKES IN CETTING THROUGH

A SCATTERING AND ABSORBING CLOUD THE GREATER

THE PROBABILITY THAT IT WILL BE ABSORBED.

# CONCEPT IMPLEMENTATION

Entition and design in the second of the second of the second of the second of the second of the second of the second of the second of the second of the second of the second of the second of the second of the second of the second of the second of the second of the second of the second of the second of the second of the second of the second of the second of the second of the second of the second of the second of the second of the second of the second of the second of the second of the second of the second of the second of the second of the second of the second of the second of the second of the second of the second of the second of the second of the second of the second of the second of the second of the second of the second of the second of the second of the second of the second of the second of the second of the second of the second of the second of the second of the second of the second of the second of the second of the second of the second of the second of the second of the second of the second of the second of the second of the second of the second of the second of the second of the second of the second of the second of the second of the second of the second of the second of the second of the second of the second of the second of the second of the second of the second of the second of the second of the second of the second of the second of the second of the second of the second of the second of the second of the second of the second of the second of the second of the second of the second of the second of the second of the second of the second of the second of the second of the second of the second of the second of the second of the second of the second of the second of the second of the second of the second of the second of the second of the second of the second of the second of the second of the second of the second of the second of the second of the second of the second of the second of the second of the second of the second of the second of the second of the second of the second of the second of the sec

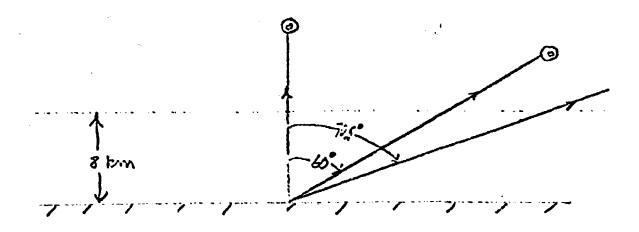
THE STRENGTH OF OXYGEN ABSORPTION AT ABOUT

= 0.7606 µ IS MEASURED FOR THE SUNLIGHT

TRANSMITTED BY AN OVERCAST AND THIS IS CORRELATED

TO THE MEAN PATH LENGTH IN THE OVERCAST AND

THE MEAN TIME OF THANSIT.



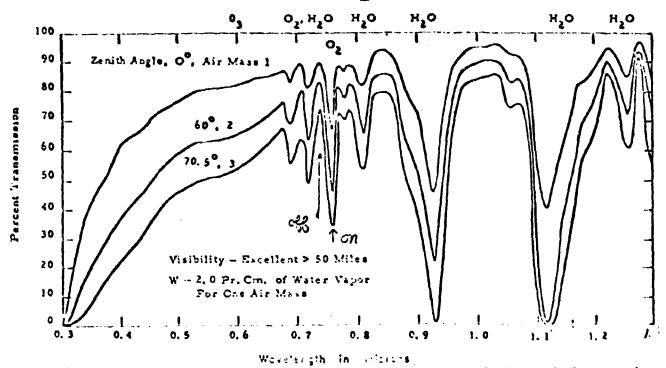
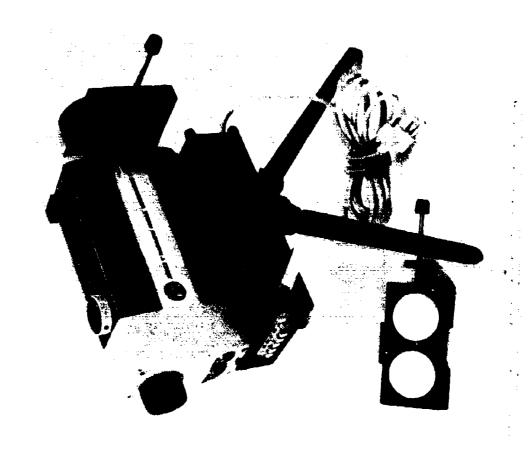


Fig. 6. Transmission of the atmosphere in the near ultraviolet, visible, and near infrared. (From R. O'B. Carpenter and R. M. Chapman, in "Effects of Night Sky Backgrounds on Optical Measurements," p. 25. Geophysics Corp. of America, March 6, 1959.)

Figure 7. Diffuse and specular transmission.

Slide 5.



Slide 7.

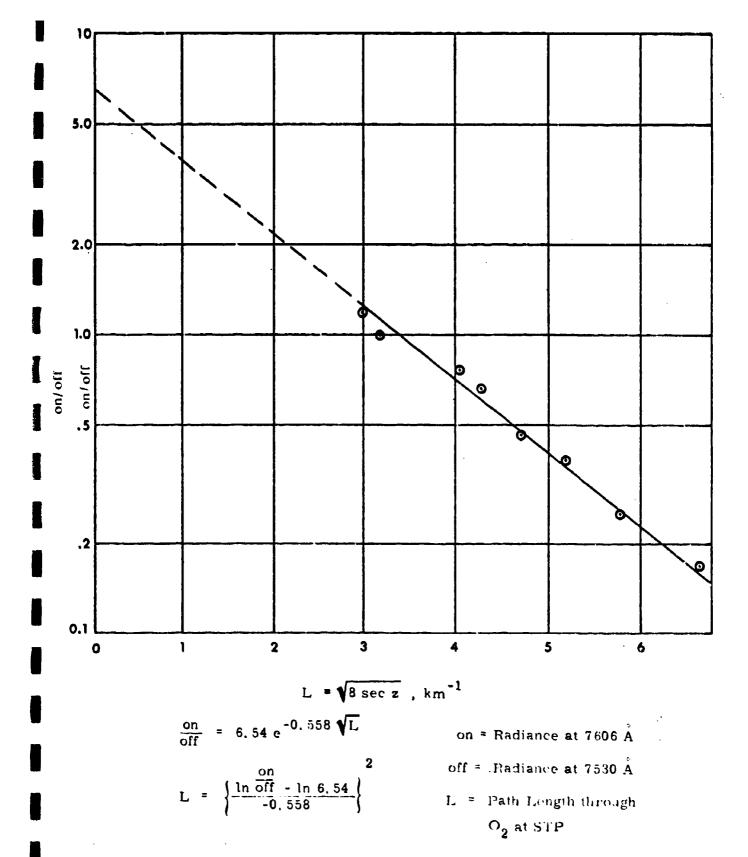
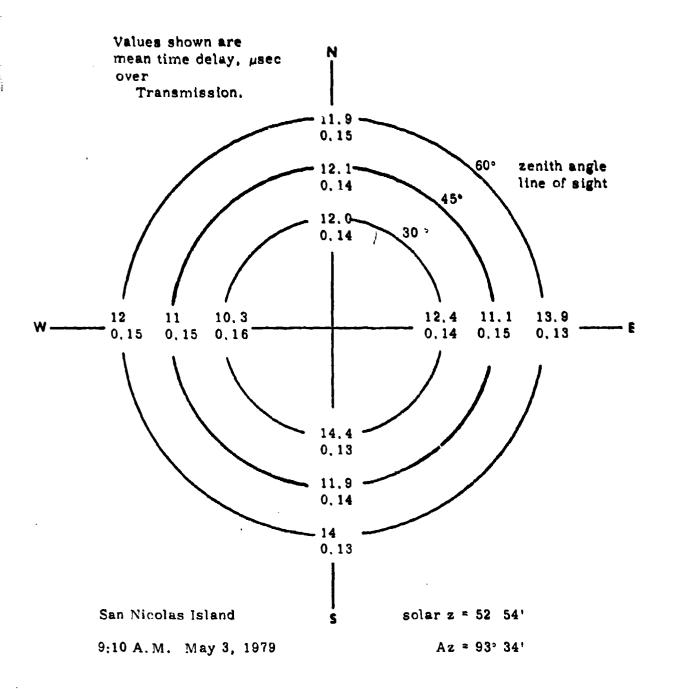


Figure 5. Calibration of two wavelength televadiometer, 18 March 1979.



: 1

1

:

. .

Figure 8. OVERCAST TIME DELAY AND TRANSMISSION

Slide 9.

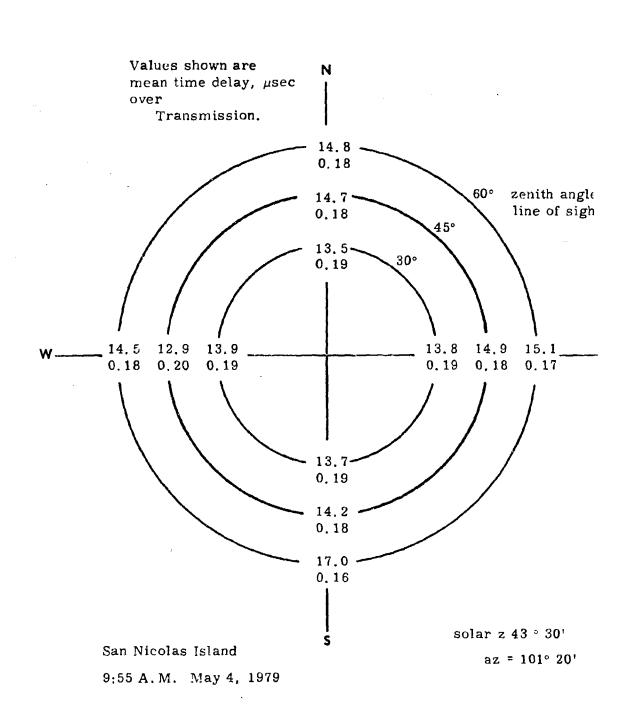


Figure 9. OVERCAST TIME DELAY AND TRANSMISSION

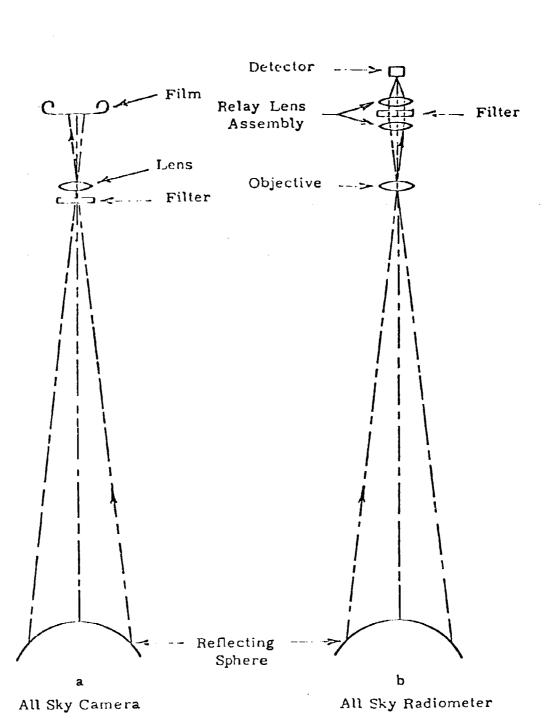
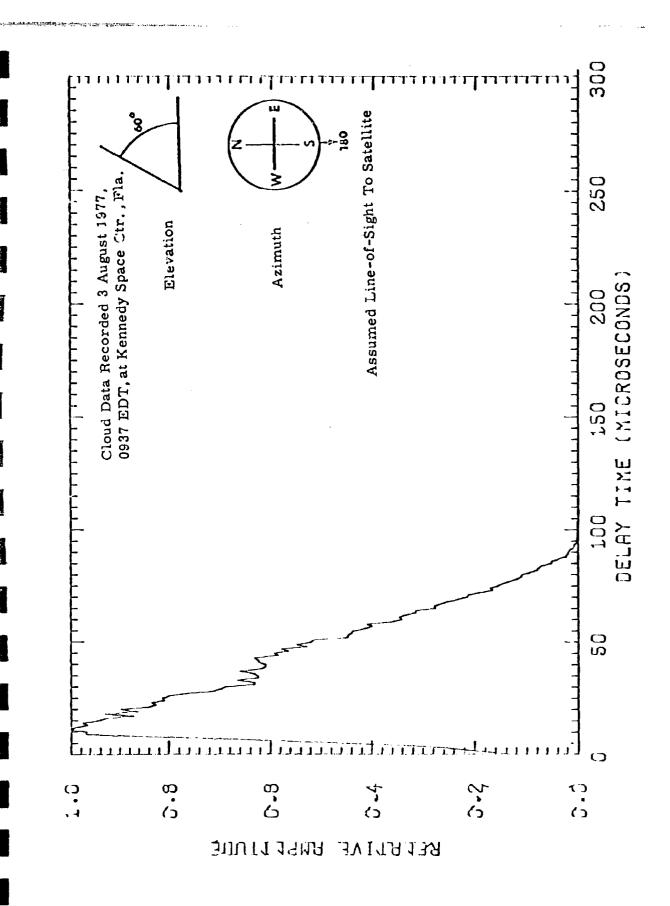


Figure 4.6. All sky detectors using reflections from a spheric surface.

Slide 11.



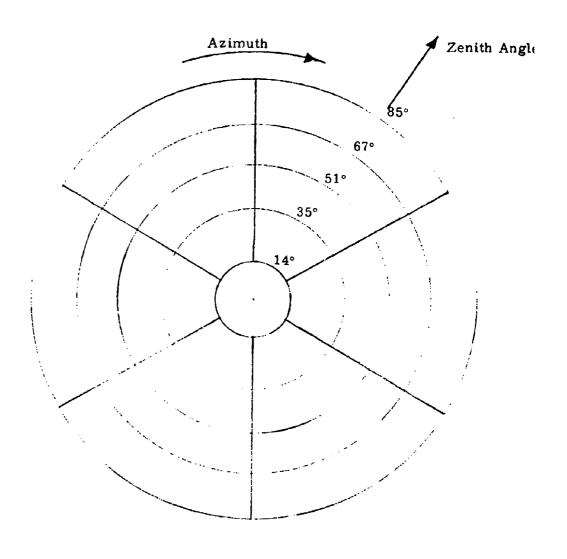
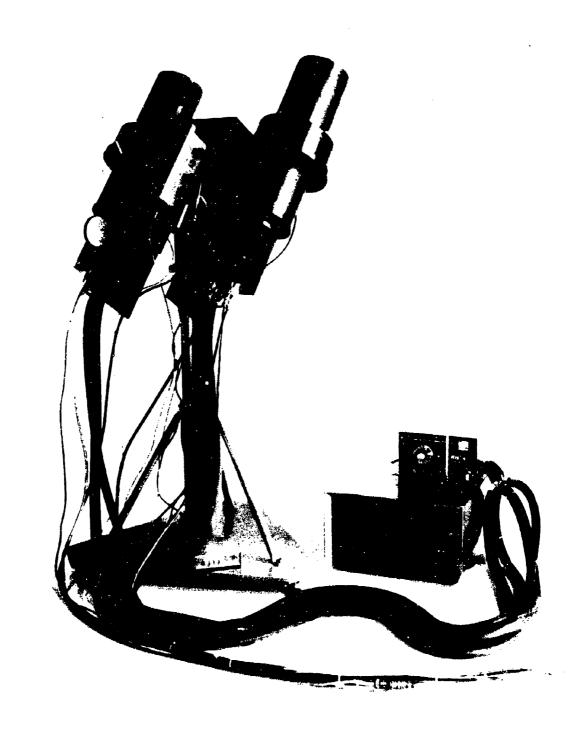
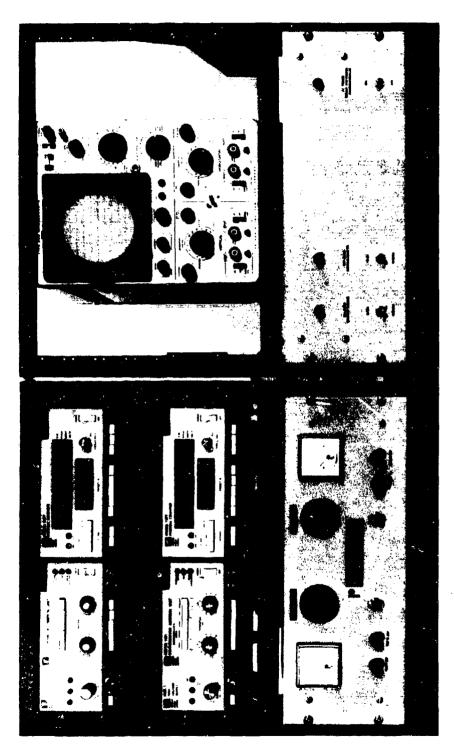


Figure 3. Solid angles receiving equal power from uniform overcast.

Slide 13,





Slide 1.

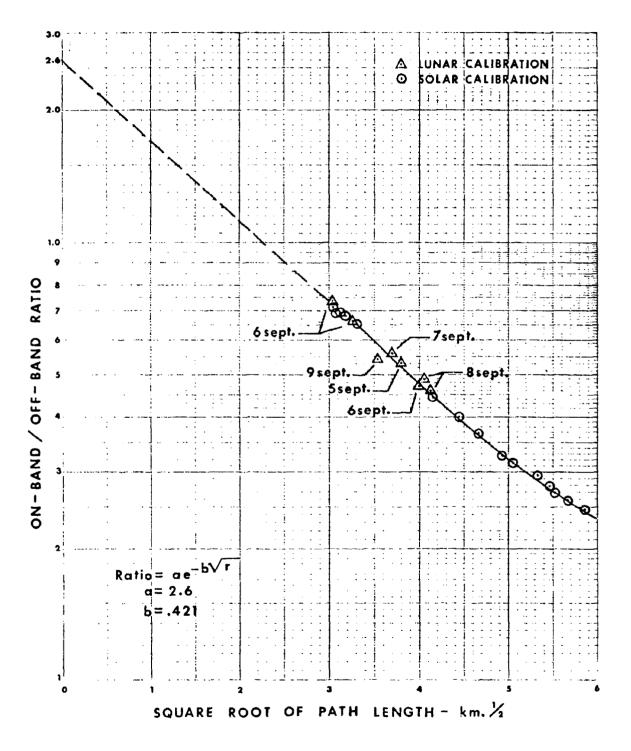
## KAUAI LASER - CLOUD EXPERIMENT TELERADIOMETER PARTICIPATION

- - **- - - ~ 3**36

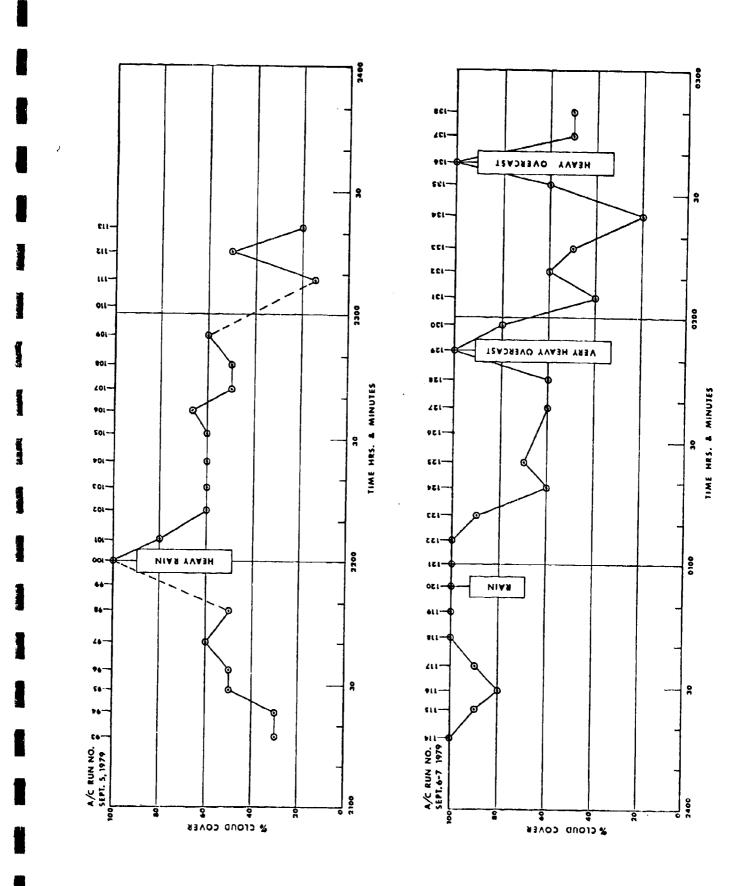
TELERADIOMETER PARTICIPATION	117
A/C RUNS SELECTED FOR ANALYSIS **	28
A/C RUNS WITH SIGNIFICANT MEAN-TIME-DELAY	12
***BASIS OF SELECTION	
(1) CLOUDS IN OVERHEAD DIRECTION	
(2) CLOUDS IN LOS TO MOON	
(3) GTE-SYLVANIA DATA SHOWS PULSE STRETCHING	
(4) TELERADIOMETER DATA SHOWS MEAN-PATH-DELAY	

NUMBER OF AIRCRAFT RUNS - - - - -

Slide 16.

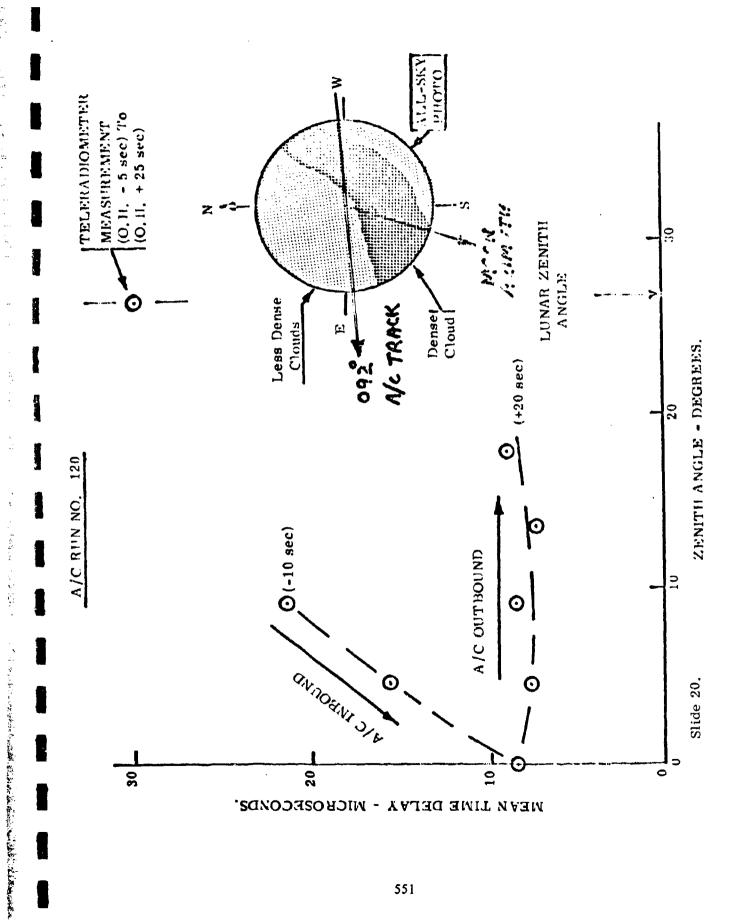


Slide 17.



KAUAI CLOUD EXPERIMENT - 1979 TELERADIOMETER MEASUREMENTS

RUN NO: 166	AIRCRAFT	EKADIO	PARAMETERS	RAFT PARAMETERS CLOUD STAT	EMEN IS	JS	LUNAR	AR INFO	
Date: 7/8 Sept	Altitude:	41,869	ft.	Bottom 1	Bottom Heights: 2200	ſt.	Elevation Angle	1	61.8 deg.
Time: 0104	Direction:	. 057 °		Tops (Max):		6500 ft.	Zenith Angle		28.2 deg.
Site: Plantation Site Elev: 600 ft.	Speed:	452	mph.	Tops (Mean):	ean):	ft.	Azimuth Angle	Angle 131	
				Distance	From	O.H. Pos	Position (Yds)	(8)	
PARAMETER		Units	-10,000	-7, 500	-5,000	О.Н.	+5,000	+10,000	+15,000
MEASURED OR DERIVED	ć								
On-Band/Off-Band Ratio	-	1	. 489	. 469	.461	. 438	.435	. 425	.415
Total Pathlength in ${\rm O_2}$		km	15.76	16.56	16,89	17.91	18.05	18.52	19.01
Cloud Free Pathlength in	02	km	9.08	80.6	9.08	9.08	9.08	9.08	9.08
Mean Path Delay		km	6, 68	7.48	7.81	8.83	8.97	9.44	9,93
Mean Time Delay (uncorrected)	ected)	твес	22.3	24.9	26.1	29.4	29.9	31.5	33.1
CALCULATED (Cloud Model)	del)								
Mean Time Delay (Corrected)	cted)	рави	26.2	29.3	30.5	34.4	35.0	36.8	38.7
Cloud Transmission		PE	11.5	10.3	6.6	8.8	8.7	8.2	7.8
Mean Free Path (Transport)	rt)	meter	118	106	101	89	88	83	46
Mean Free Path (Optical)		meter	20	18	17	15	15	14	13
Optical Thickness		;	65.1	73.0	76.4	86.5	87.9	92.8	97.7
Time A/C At Position		min:sec							
	ľ								



2. 2. 2.

ra .

10 to 10 to 10 to 10 to 10 to 10 to 10 to 10 to 10 to 10 to 10 to 10 to 10 to 10 to 10 to 10 to 10 to 10 to 10 to 10 to 10 to 10 to 10 to 10 to 10 to 10 to 10 to 10 to 10 to 10 to 10 to 10 to 10 to 10 to 10 to 10 to 10 to 10 to 10 to 10 to 10 to 10 to 10 to 10 to 10 to 10 to 10 to 10 to 10 to 10 to 10 to 10 to 10 to 10 to 10 to 10 to 10 to 10 to 10 to 10 to 10 to 10 to 10 to 10 to 10 to 10 to 10 to 10 to 10 to 10 to 10 to 10 to 10 to 10 to 10 to 10 to 10 to 10 to 10 to 10 to 10 to 10 to 10 to 10 to 10 to 10 to 10 to 10 to 10 to 10 to 10 to 10 to 10 to 10 to 10 to 10 to 10 to 10 to 10 to 10 to 10 to 10 to 10 to 10 to 10 to 10 to 10 to 10 to 10 to 10 to 10 to 10 to 10 to 10 to 10 to 10 to 10 to 10 to 10 to 10 to 10 to 10 to 10 to 10 to 10 to 10 to 10 to 10 to 10 to 10 to 10 to 10 to 10 to 10 to 10 to 10 to 10 to 10 to 10 to 10 to 10 to 10 to 10 to 10 to 10 to 10 to 10 to 10 to 10 to 10 to 10 to 10 to 10 to 10 to 10 to 10 to 10 to 10 to 10 to 10 to 10 to 10 to 10 to 10 to 10 to 10 to 10 to 10 to 10 to 10 to 10 to 10 to 10 to 10 to 10 to 10 to 10 to 10 to 10 to 10 to 10 to 10 to 10 to 10 to 10 to 10 to 10 to 10 to 10 to 10 to 10 to 10 to 10 to 10 to 10 to 10 to 10 to 10 to 10 to 10 to 10 to 10 to 10 to 10 to 10 to 10 to 10 to 10 to 10 to 10 to 10 to 10 to 10 to 10 to 10 to 10 to 10 to 10 to 10 to 10 to 10 to 10 to 10 to 10 to 10 to 10 to 10 to 10 to 10 to 10 to 10 to 10 to 10 to 10 to 10 to 10 to 10 to 10 to 10 to 10 to 10 to 10 to 10 to 10 to 10 to 10 to 10 to 10 to 10 to 10 to 10 to 10 to 10 to 10 to 10 to 10 to 10 to 10 to 10 to 10 to 10 to 10 to 10 to 10 to 10 to 10 to 10 to 10 to 10 to 10 to 10 to 10 to 10 to 10 to 10 to 10 to 10 to 10 to 10 to 10 to 10 to 10 to 10 to 10 to 10 to 10 to 10 to 10 to 10 to 10 to 10 to 10 to 10 to 10 to 10 to 10 to 10 to 10 to 10 to 10 to 10 to 10 to 10 to 10 to 10 to 10 to 10 to 10 to 10 to 10 to 10 to 10 to 10 to 10 to 10 to 10 to 10 to 10 to 10 to 10 to 10 to 10 to 10 to 10 to 10 to 10 to 10 to 10 to 10 to 10 to 10 to 10 to 10 to 10 to 10 to 10 to 10 to 10 to 10 to 10 to 10 to

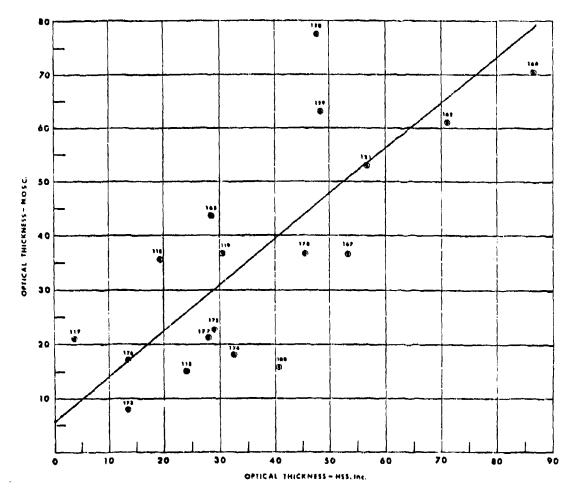
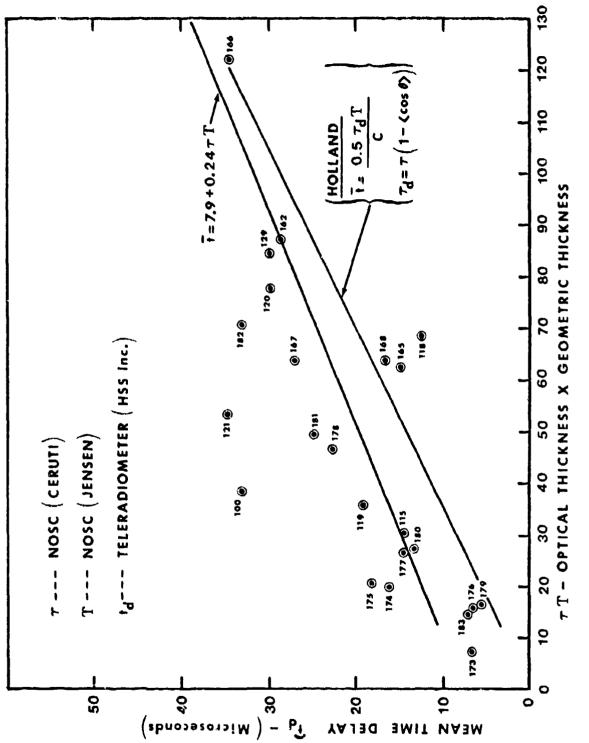


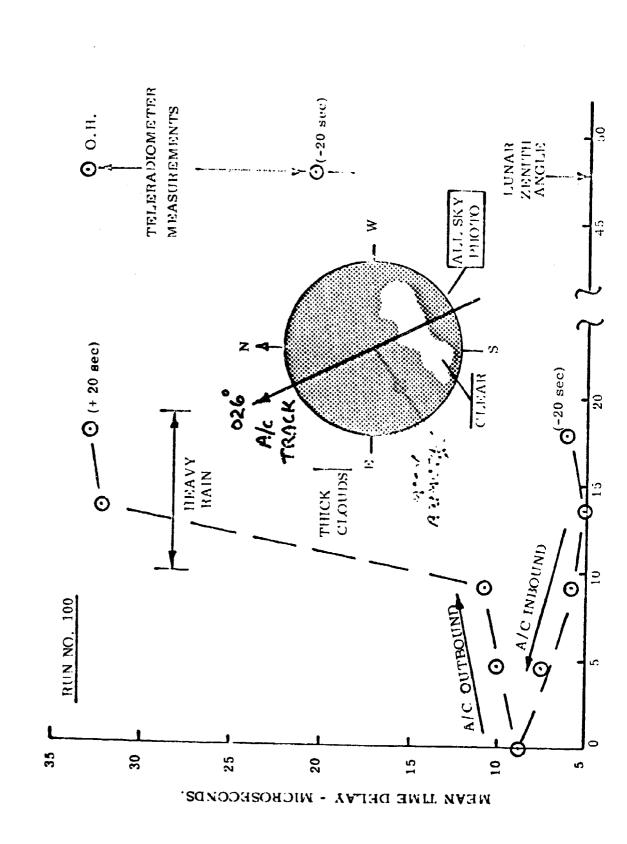
Figure . Scatter diagram of correlation between NOSC and HSS Inc Values of Optical Thickness for eighteen data runs; the Coefficient of Determination  $r^2 = 0.89$  and the Correlation Coefficient r = 0.94.

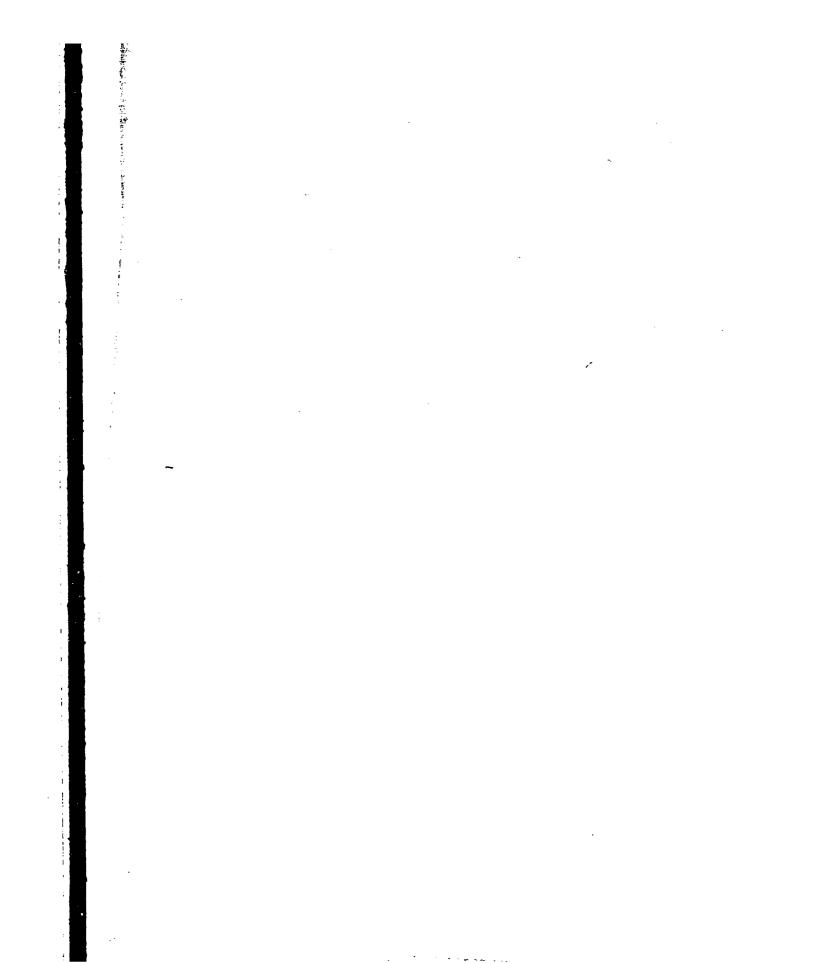
Slide 23.



Slide 24.

:.





#### UPLINK PROPAGATION AND ADAPTIVE OPTICS*

D.P. Greenwood

27 March 1980

Massachusetts Institute of Technology Lincoln Laboratory P.O. Box 73 Lexington, Massachusetts 02173

#### **ABSTRACT**

The basic limitation to propagating a laser beam from ground to space for the Blue Green communication application is atmospheric turbulence. Also, thermal blooming is beginning to be significant for laser power levels above approximately 100 kWatt, average power, for a wavelength of 0.48  $\mu m$ . We have addressed the degree to which the beam is spread by these aberrating effects, and also the effectiveness of adaptive optics in correcting for the induced phase errors. Adaptive optics appear feasible in reducing the beam spread to near diffraction-limited performance, however, there are a number of residual errors: amplitude, fitting, isoplanatism, bandwidth and signal-to-noise. With reasonable care in reducing these errors, the up-link loss can be reduced to approximately 5 - 10 dB (depending on zenith angle), of which 2 - 5 dB can be attributed to atmospheric extinction.

"The views and conclusions contained in this document are those of the contractor and should not be interpreted as necessarily representing the offical policies, either expressed or implied, of the United States Government."

^{*} This work is sponsored by the Advanced Research Projects Agency.

SLC PRESENTATION

San Diego, CA

D.P. Greenwood

27 March 80

#### **UP-LINK PROPAGATION AND ADAPTIVE OPTICS**

#### PROBLEM STATEMENT

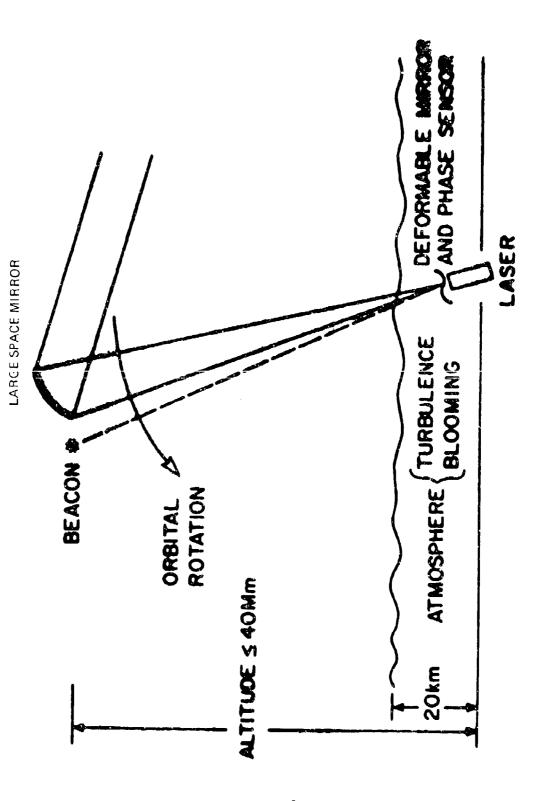
**OBJECTIVE:** 

• To efficiently transfer power from a ground-based high power laser to a spaceborne target.

APPROACH:

• Estimate the aberrating effects of atmospheric turbulence and thermal blooming.

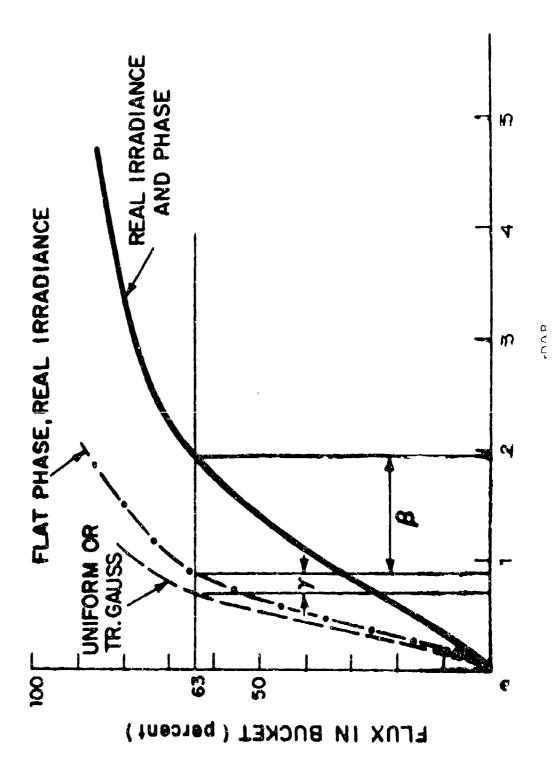
•For sufficiently large atmospheric aberrations with respect to jitter and device quality, consider the effectiveness of wavefront correction by adaptive optics, including fast tracking.



COMPENSATION FOR TURBULENCE AND BLOOMING ON AN UP-LINK

#### OUTLINE

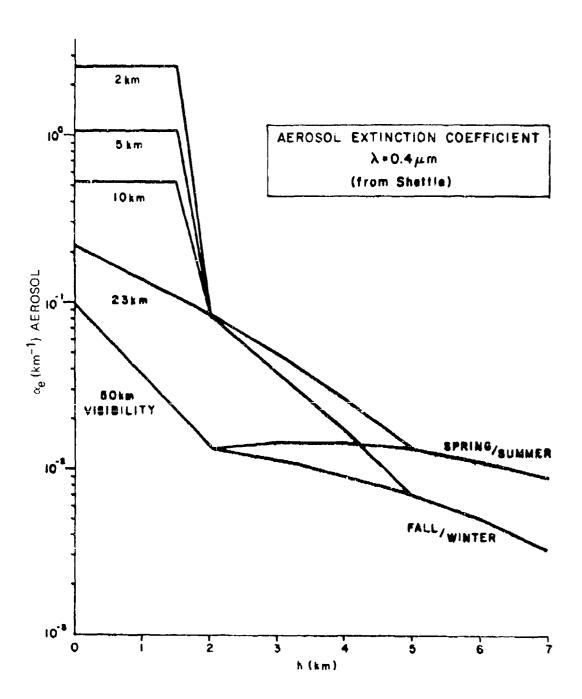
- I. Methodology
  - Identifies sources of aberration causing beam spread
- 2. Discussion on extinction, beam quality, jitter
- 3. Turbulence
  - Uncorrected beam spread
  - Effectiveness of correction using adaptive optics
- 4. Thermal Blooming
  - Magnitude of error
  - Correction using adaptive optics
- 5. Combination of effects computation of link loss
- 6. Summary



ATMOSPHERIC EXTINCTION (at 0.43  $\mu\text{m}$ , Zenith, Sea Level to  $\infty)$ 

exb(-N _e )	0, 73° 0, 71 0, 54 0, 33 0, 15 0, 15 0, 11	tm (varies
N Total	0.35 0.35 0.58 0.62 1.12 1.18 1.98 1.98 1.98	neight of 0.35 c
Ne Rayleigh ⁴	0.17	^I rw = fattwinter ² s/s = spring/summer ³ For an equivalent column height of 0.35 cm (varies from 0.25 - 0.42 cm over US)
Ne Ozone ³	0.01	f/w = fa   2s/s = s    3For an   from 0.2
N _e Aerosois	0.14 0.17 0.44 0.94 1.8 1.8	neter used
Horizontal Visibility	50 km fw ¹ 23 km fw  10 km fw  5 km fw  5 km fw  2 km fw  5 s/5	*Sample system parameter **Conservative value used

4Based on US Std. Atmosphere 1962



18-00-17067

# SAOT AREA AND IRRADIANCE

. AREA ON TARGET

$$A = A_{\infty} \left[ \gamma^2 \beta^2 + \frac{\Delta A_T}{A_{\infty}} + \frac{\Delta A_B}{A_{\infty}} + \frac{\Delta A_J}{A_{\infty}} \right]$$

WHERE

A = DIFFRACTION LIMITED AREA

B,7 = DEFINE DEVICE QUALITY

DAT = INCREASE IN AREA DUE TO TURBULENCE

DAB = INCREASE IN AREA DUE TO THERMAL BLOOMING

 $\Delta A_{J} = INCREASE$  IN AREA DUE TO JITTER (= $2\pi\sigma_{J}^{2}$ )

• IRRADIANCE (Average)

$$I = 0.65 \text{ PA}^{-1} \exp(-N_e)$$

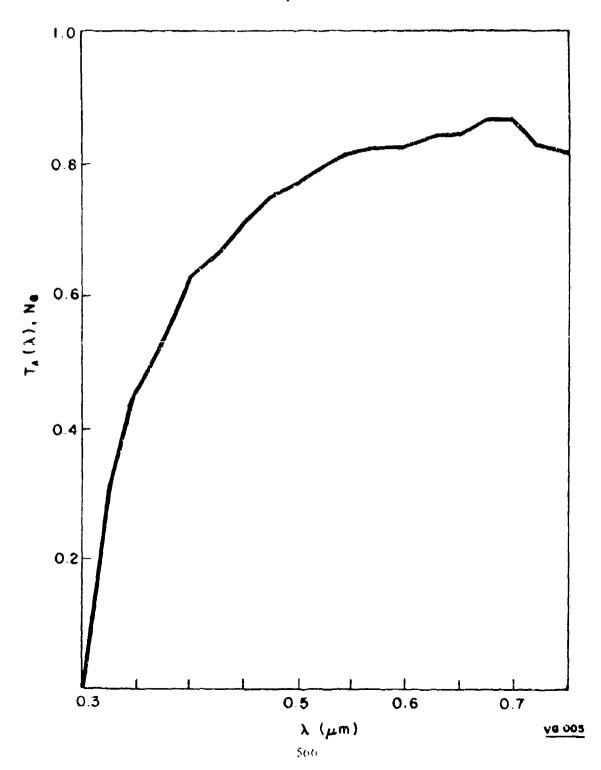
WHERE

P * LASER POWER

N = EXTINCTION NUMBER

# ATMOSPHERIC TRANSMISSION TO ZENITH FROM SEA LEVEL, BASED ON EXCELLENT VISIBILITY (50 miles)

(from ref. 2 or 4, same curve)



#### SAMPLE SYSTEM PARAMETERS USED IN COMPUTATIONS

#### Laser:

Power  $P_{AV} = 120 \text{ kW or less*}$ Wavelength  $\lambda = 0.48 \mu\text{m}$ 

#### System:

Ground-based Beam Quality  $\beta$  = 1.2 Amplitude Factor  $\gamma$  = 1.1 Output Aperture Diameter  $\rho$  = 4m

#### Atmosphere: (Values at Zenith)

Turbulence coherence length  $r_0 = 10 \text{ cm}$  Conservative  $r_0 = 10 \text{ cm}$  4 cm

Isoplanatic angle  $\theta_0 = 25 \text{ rad}$  15 $\mu$ rad

Log-amplitude mean square  $\sigma_x^2 = 0.05 \text{ neper}^2$  0. I neper²

#### Satellite:

Synchronous  $h_{\uparrow}$  = 40 Mm Zenith angle  $\theta_{z}$  = 0-720 Aperture diameter  $\theta_{z}$  = 10m

^{*120} kW corresponds 4 kJ/pulse, 30 pps

#### DIFFRACTION AND DEVICE LIMITED AREA

$$A_{00} = \pi (0.65 \, \lambda L/D)^2$$

Diffraction

$$A_0 = \gamma^2 \beta^2 A_{00}$$

Device

Sample System:

$$A_{00} = 30.6 \text{ m}^2$$

$$A_0 = 53.3 \text{ m}^2$$

(Beam diameter 8.2 m)

#### JITTER CONTRIBUTION

$$\Delta A_J = 2\pi \sigma_J^2 L^2$$

Criterian: Have jitter contribution < device limited area

$$2\pi\sigma_{\mathrm{J}}^{2}L^{2}<\mathrm{A_{0}}$$

Sample System:  $\sigma_{\rm J} < 70~{
m nrad}$ 

(Beyond current state of the art, but an even smaller jitter is desirable

#### UNCORRECTED TURBULENCE

$$\Delta A_T/A_{00} \approx (D/r_0)^2$$

where  $r_0$  = atmospheric coherence length (Fried)

$$r_0^{-5/3} = 0.423 \text{ k}^2 \int_0^L c_n^2 (z) dz$$

$$r_0 \sim (\sec \theta_z)^{-3/5}$$

Sample System:

$$\Delta A_{T}/A_{00} = 1600$$

$$\Delta A_{T} = 4.9 \times 10^{4} \text{ m}^{2}$$

$$\Delta A_{T}/A_{00} = 6.6 \times 10^{3}$$

$$\Delta A_{T} = 2.0 \times 10^{5} \text{ m}^{2}$$

$$at \theta_{Z} = 72^{0}$$

Clearly, turbulence must be corrected, and the correction must be very good, such that only  $\leq 1\%$  remains.

#### TURBULENCE

#### MULTI-ELEMENT ADAPTIVE OPTICS CORRECTION

$$\frac{\Delta A_T}{A_{00}} \approx -1 + \exp \left[c_{FIT}^2 + \sigma_{AMPL}^2 + \sigma_{ISO}^2 + \sigma_{BW}^2 + \sigma_{SN}^2\right]$$

where FIT ~ Fitting Error

AMPL ~ Amplitude Error

ISO  $\sim$  Isoplanatic Error

BW ~ Bandwidth Error

SN ~ Signal-To-Noise Error

**CAUTION:** 

The above model is very simplistic and not rigorous.

There are complex interactions between all terms listed.

#### FITTING ERROR

$$\sigma_{FIT}^2 = 0.35 \, (d/r_0)^{5/3}$$
 (rad²)

where d = interactuator spacing

The number of actuators is

$$N_a = \pi (D/2d)^2$$

For a fitting error (minimum) of 1/10 wave:

$$\sigma_{FIT}^2 = 0.395$$
 (rad²)  
d/r₀ = 1.1

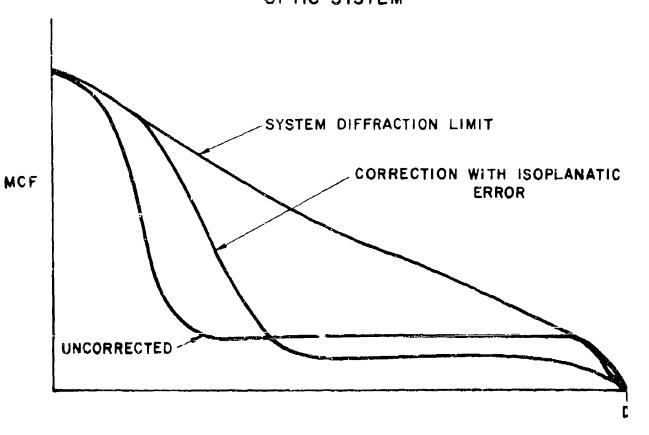
Sample system:

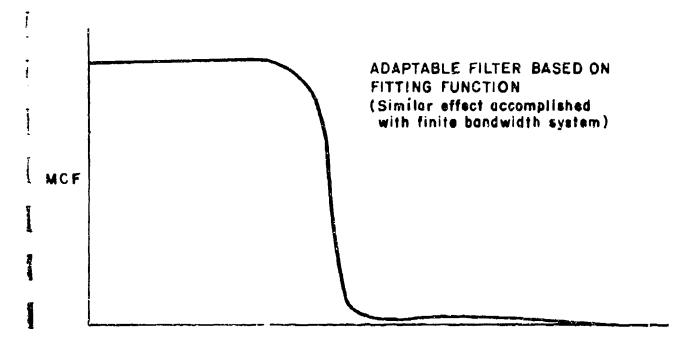
$$N_a = 1040$$
  $\theta_z = 0$   $\theta_z = 72^0$ 

Conservative system:

$$N_a = 6500$$
  $\theta_z = 0^0$   
 $N_a = 26600$   $\theta_z = 72^0$ 

### MATCHED FILTER ADAPTURE OPTIC SYSTEM





#### AMPLITUDE ERROR

 $\sigma_{\text{AMPL}}^2 = \sigma_{\text{X}}^2$  , the log-amplitude mean-square value

J. J. Burke, J. Opt. Soc. Am., <u>60</u>, p. 1262-3. has an average

$$\sigma_{\mathbf{X}}^2 = 0.05$$

Sample System:

$$\sigma_{\rm X}^2 = 0.05 (\sec \theta_{\rm Z})^{11/6}$$

Conservative System:

$$\sigma_{\rm X}^2 = 0.1 (\sec \theta_{\rm Z})^{11/6}$$

(Note  $\sigma_{\rm X}^2$  saturates at about 0.5 hence second value too high at large  $\theta_{\rm Z}$ )

#### ISOPLANATIC ERROR

(For synchronous altitude satellite)

$$\sigma_{150}^{2} \approx 6.88 6\theta_{e}/\theta_{o})^{5/3}$$

(Fried's 1st Definition)

where  $\delta\theta_e$  = accuracy with which beacon is positioned relative to  $2V_1$  /c point ahead angle

and

 $\theta_0$  = isoplanatic angle

$$\theta_0^{-5/3} = 0.423 \text{ k}^2 \int_0^\infty C_n^2 (z) z^{5/3} dz$$

Sample System:

$$\theta_0 = 25 (\sec \theta_z)^{-8/5}$$

(urad)

Conservative System

$$\theta_0 = 15 (\sec \theta_z)^{-8/5}$$

#### ISOPLANATIC ERROR (cont.)

Set 
$$\sigma_{150}^2 = (2\pi/10)^2 \text{ rad}^2$$

Find 
$$\delta \theta_{e} = 0.18 \theta_{o}$$

#### Sample System

$$\begin{cases} \delta\theta_{\rm e} = 4.5 \mu \text{rad} \\ L\delta\theta_{\rm e} = 180 \text{m} \end{cases} \begin{cases} \theta_{\rm z} = 0 \end{cases}$$

$$\begin{cases} \delta \theta_e = 0.69 \mu \text{rad} \\ L \delta \theta_e = 28 \text{ m} \end{cases} \theta_z = 72^0$$

(relative to an offset of 760 m)

Conservative System

$$\delta\theta_e = 2.7 \, \mu \text{rad}, \quad \theta_z = 0$$

$$\delta\theta_e$$
 = 0.41 $\mu$ rad,  $\theta_z$  = 720

Note that for dynamic tracking, the offset will vary, as these numbers are a function of Zenith angle.

#### **BANDWIDTH ERROR**

$$\sigma_{BW}^2 = (2.69 \, f_0 / f_c)^{5/3}$$

(assumes a closed loop response equivalent to an RC filter)

$$f_0^{5/3} = 0.0196 \text{ k}^2 \int_0^L c_n^2(z) v^{5/3}(z) dz$$

$$f_0$$
 = atmospheric frequency (depending on wind direction)  
 $f_C$  = system cutoff frequency (3 dB point of RC filter) 
$$\begin{cases} (\sec \theta_z)^{3/5} \\ (\sec \theta_z)^{-2/5} \end{cases}$$

AMOS Model  $f_0 = 45 \text{ Hz} \quad (\theta_z = 0)$ (Conservative for  $\approx 100 \text{ Hz}$ )

Sample System:

Assume 
$$\sigma_{BW}^2 = (2\pi/10)^2 \text{ rad}^2$$

$$f_C = 211 \text{ Hz}$$

$$\tau_C = 0.75 \text{ sec}$$

Conservative System:

#### SIGNAL-TO-NOISE ERROR

$$\sigma_{SN}^2 = a/S_D^2$$
 rad²

where a = constant on the order of unity, dependent on sensor wavelength and type. (Shearing interferometer at  $\lambda$  has a = 1.2)

and S_n = signal-to-noise ratio

For a desired 
$$\sigma_{SN}^2 = (2\pi/10)^2 \text{ rad}^2$$
  
 $S_n = 2$ 

A beacon of 0.1 mWatt, diameter 0.1 m in visible gives  $S_n = 2$ , when interactuator spacing = 0.1 m

#### TURBULENCE SUMMARY

- Turbulence degradation is severe but in part correctable with adaptive o
- Adaptive optics residual errors to be considered are: isoplanatic, amplitude, bandwidth, fitting and signal-to-noise. All are important
- A more careful theoretical analysis is required to properly combine effects
- With a cooperative source, the beam spread can be restricted to probably no more than a few times device limited

#### THERMAL BLOOMING

Posults from absorption of laser radiation in atmosphere, thus creating "thermal lens" due to temperature gradient across beam.

Methodology

$$\frac{\Delta A_{B}}{A'_{O}} = (N_{D}/N_{DC}) + 0.72 (N_{D}/N_{DC})^{2}$$

where  $N_D$  = distortion number

 $N_{DC}^*$  critical distortion number (depends on  $\gamma$ )

and 
$$A_0' = \gamma^2 A_{00}$$

Wave Optics Code Runs

(Can be  $N_{DC} \approx 3$ -6 for real beams with irregular irradiance distribution)

#### INTEGRATED DISTORTION NUMBER

$$N_{D} = \frac{ckP}{\beta a} \int_{0}^{\infty} \frac{\alpha(z) \exp(-\int_{0}^{z} \alpha_{e}(z') dz')}{v(z)} dz$$

where 
$$c = 1.66 \times 10^{-9} \text{ m}^3/\text{J}$$

k = wave number  $2\pi/\lambda$ 

a = beam radius = D/(2/2)

P = laser power

a(z) - absorption coefficient

 $a_e(z)$  = extinction coefficient

V(z) • wind velocity normal to path

and z = incremental position along path

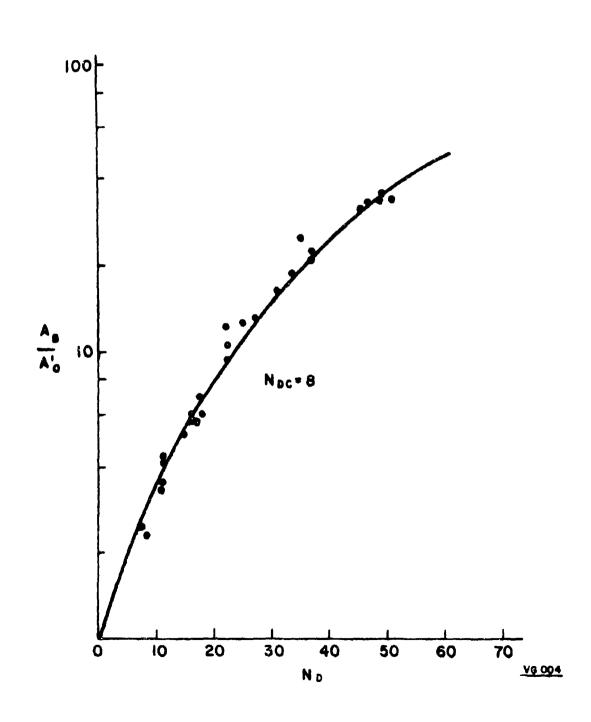
#### SIMPLIFIED DISTORTION NUMBER

$$N_D \approx \frac{ckP}{\beta a} \exp(-N_e) \sum_{i=1}^{n} (N_a/V)_i$$
  
where  $N_e = \int_0^\infty a_e(z) dz$ , extinction number

and 
$$\frac{N_a}{V} = \int_0^\infty \frac{a(z)}{V(z)} dz$$

for each absorbing constituent

# THERMAL BLOOMING FOR TRUNCATED GAUSSIAN BEAM



### ABSORBING CONSTITUENTS

(at 
$$\lambda = 0.48 \mu m$$
)

Molecular - ozone

by photo dissociation

$$h\nu + 0_3 \rightarrow 0_2 + 0 + KE$$

approximately 1/3rd of energy goes into photodissociation, the rest into kinetic energy

 $N_{aozone} = \frac{2}{3}$  0. 0063 sec  $\theta_z$  (for equivalent ozone column height of 0. 35 cm)

(Conservative  $N_a = \frac{2}{3}$  0.0095 sec  $\theta_z$ )

Aerosol - carbonaceous, naturally occurring. Each particle absorbs as black body and reradiates to surrounding molecules.

### ABSORBING CONSTITUENTS (cont.)

N_{a aerosol} ^{- (sec ⊕}z) · ≺

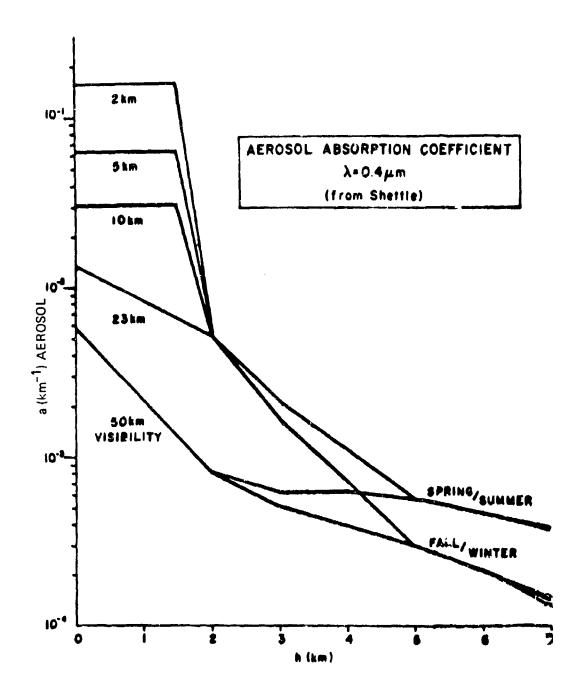
	Model:	
7. 79 x 10 ⁻³	50 km vis. f/w ^{l*}	
9. 21 x 10 ⁻³	s/s ²	
2. 29 x 10 ⁻²	23 km vis. f <i>l</i> w	
2.47 x 10 ⁻²	s/s	
5. 48 x 10 ⁻²	10 km vis. f/w	
5. 66 x 10 ⁻²	s/s**	
0. 103	5 km vis. f/w	
0. 105	s/s	
0. 256	2 km vis. f/w	
0. 258	s/s	

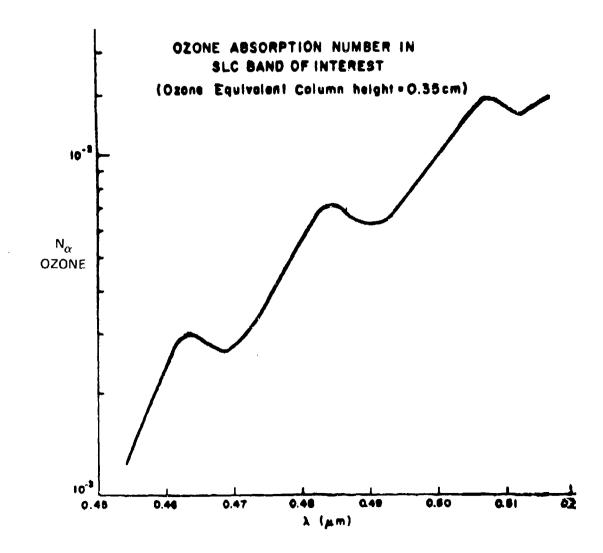
ifw = fall/winter,

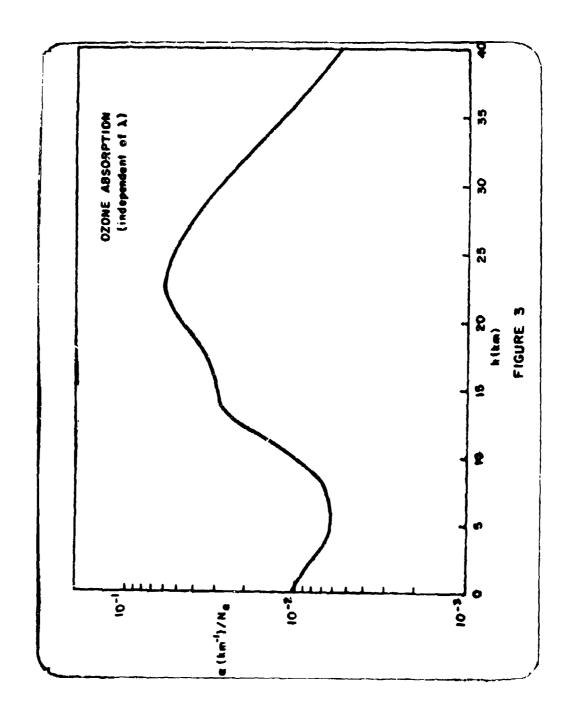
 2 s/s = spring/summer

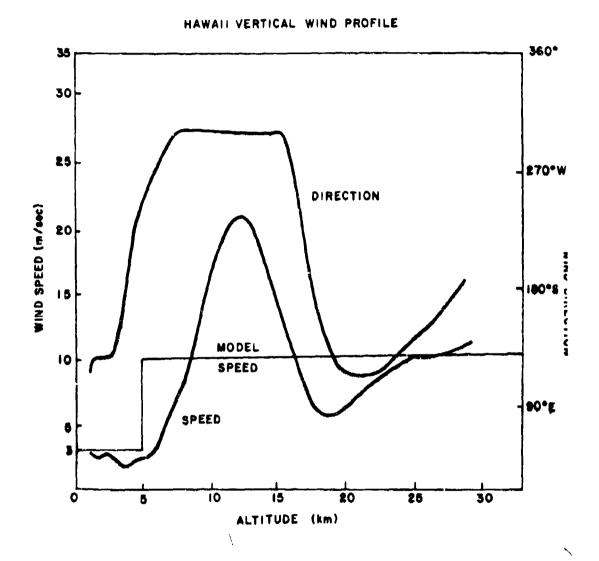
*Sample system number

**Conservative value used









### THERMAL BLOOMING CORRECTABILITY

- Absorbing constituents all in near field, hence thin lens correction possible
- Bandwidth, stroke and fitting* requirements for blooming are less stringent than turbulence requirements
- Thermal blooming correction modeled by adjusting N_{DC} in wave optics code
  - *Caution -- we assumed a fairly smooth irradiance profile and good beam quality. A higher  $\gamma$  will contribute to high spatial frequencies in blooming-induced phase error

### **UP-LINK LOSS COMPUTATIONS**

Link Loss

$$\mathcal{L} = 10 \log_{10} [A^{-1} \pi (D_2/2)^2 \exp(-N_e)]$$

where

A = far field beam spread

D₂ = receiving aperture diameter (in space)

 $N_e$  = extinction number

$$\hat{A} = A_{00} \left[ \gamma^2 \beta^2 + \frac{\Delta A_T}{A_{00}} + \frac{\Delta A_B}{A_{00}} + \frac{\Delta A_J}{A_{00}} \right]$$

### UP-LINK LOSS COMPUTATIONS (cont.)

Sample System	$\theta_{\rm z} = 0^{\rm O}$	$\theta_{\rm Z}$ = $72^{\rm O}$	
System jitter	$\sigma_{ m j}$ = 70 nrad	70 nrad	
AO Cutoff frequency	f _C = 211 Hz	211 Hz	
AO Number of actuators	N _{act} = 1040	4260	
AO Signal-to-noise	s _n - 2	2	
Beam position accuracy	δθ _e = 5 μrad	0.7 µrad	
Cnot cizo	A = 195 m ²	254 m ²	•
Spot size	A * 192 M⁻	<b>2</b> 24 m ⁻	
Extinction Loss	1. 4 dB	4.5 dB	
UP LINK Loss	L = 5, 3 dB	9. 6 dB	

### UP-LINK COMPUTATIONS (cont.)

Conservative System	$\theta_{\rm z} = 0^{\rm o}$	$\theta_z$ = $72^{\circ}$	
System jitter	$\sigma_{\rm j}$ = 70 nrad	70 nrad	
AO Cutoff frequency	f _c = 470 Hz	470 Hz	
AO Number of actuators	N _{act} = 6500	26600	
AO Signal-to-noise	s _n = 2	2	
Beacon Position Array	$\delta  heta_{ m e}$ = 2.7 $\mu$ rad	0. 4 μrad	
Spot size	A = 222 m ²	258 m ²	•
Extinction loss	5 dB	16 dB	
UP-LINK Loss	L = 9.6 dB	21.5 dB	

### **SUMMARY**

- Efficient transfer of a visible laser beam from ground to a space mirror seems possible, based on physics and extrapolated state of the art
- Adaptive optic correction for turbulence is required, and thermal blooming will be corrected as a subset of turbulence
- Critical areas where further work is required:
  - -Large number of subapertures (preferably low voltage)
  - -Accurate beacon positioning/pointing
  - Very precise jitter and boresight correction
  - -Atmospheric measurements
  - -Superb device quality (sufficient power assumed)

### LABORATORY EXPERIMENTAL EFFORT

### Approach:

Simulation, Involving Phase Screens For Turbulence And Absorption Cells For Thermal Blooming.

Simulates Full Atmosphere, And Includes Far Field Diagnostics

### Schedule:

Closed Loop Circuitry, Diagnostics

Complete

Phase Sensor Delivery

Integration

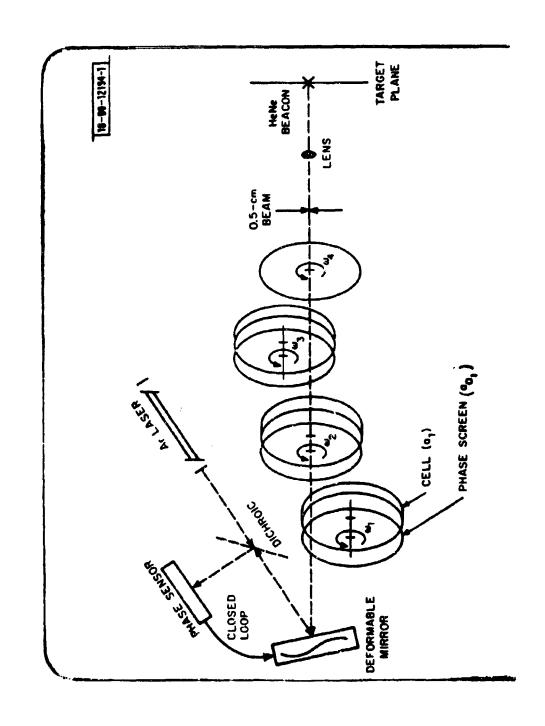
Experimentation

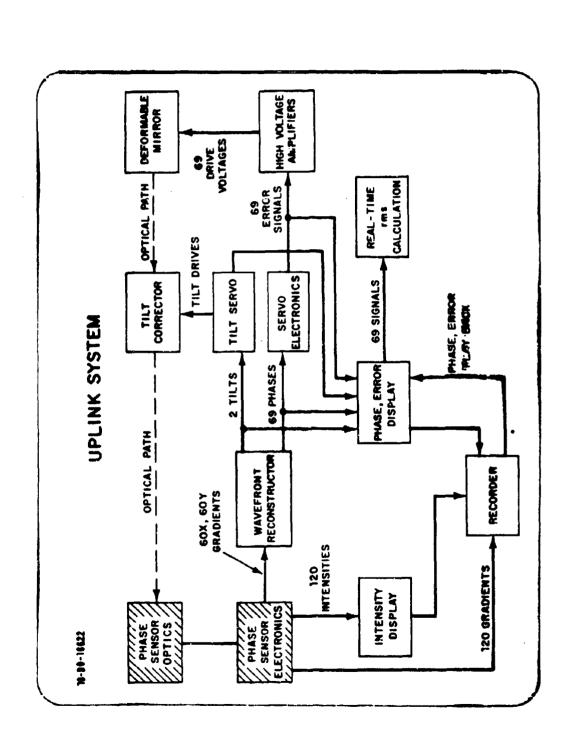
Complete

May 1980

June-August 1980

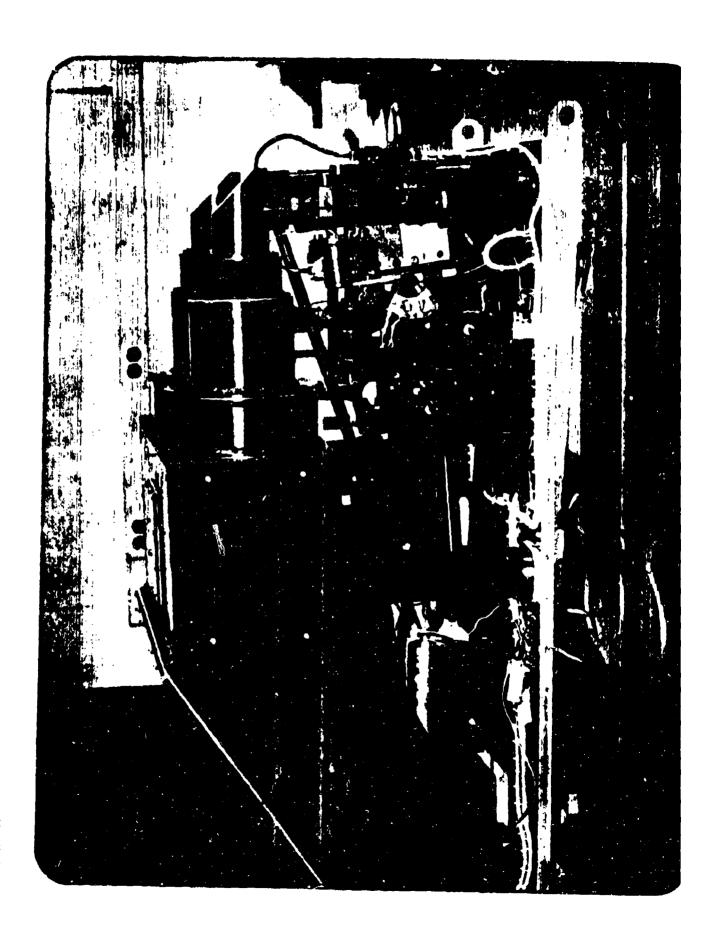
September 1980 +





Significants and a series

to the second of the second of



### LABORATORY EXPERIMENTAL GOALS

- VERIFY INTEGRATED SYSTEM OPERATION
- INVESTIGATE PROPER CLOSED LOOP STABILITY IN THESE CONDITION
  - Relatively High/Low Turbulence and Blooming
  - Presence of  $2\pi$  Ambiguities (Varying Shear)
  - Various Degrees of Anisoplanatism
  - High/Low S:N
  - Varying Wind Speed & Slew Rate
  - Overfilled/Underfilled Aperture
  - Presence of Central Obscuration
  - Tilt Control On/Off
  - •Thermal Blooming Transients

Quadi-Inherent characteristics of the diffuse attenuation coefficient for irradiance

K. S. Baker and R. C. Smith

University of California, San Diego Scripps Institution of Oceanography Visibility Laboratory San Diego, California 92152

### Abstract

The diffuse attenuation coefficient for downwelling irradiance  $(K_d)$ , the coefficient used to describe the attenuation of irradiance as a function of depth in natural waters, is an apparent optical property. As such, it is a function of the geometry of measurement and other factors which alter the radiance distribution as a function of depth. In spite of this, measurements of downwelling irradiance versus depth and sun zenith angle show that  $K_d$  is relatively insensitive to changes in sun angle, thus displaying "quasi-inherent" characteristics, except for very large sun zenith angles. Data will be shown to demonstrate this for a highly productive water type.

Introduction. The diffuse attenuation coefficient for downwelling irradiance is defined as .

$$K_d(Z) \equiv \frac{-1}{E_d(Z)} \left( \frac{dE_d(Z)}{dZ} \right). \tag{1}$$

or alternatively.

$$\frac{E_d(Z_1)}{E_d(Z_1)} = \exp\left[-K_d \cdot (Z_2 - Z_1)\right] \tag{2}$$

where  $K_d$  has units of reciprocal length, and Z is the depth at which the downwelling irradiance,  $E_d(Z)$ , is measured. Thus  $K_d$  is an optical property used for describing the attenuation with increasing depth of radiant energy in natural waters.

Preisendorfer¹ has defined inherent and apparent optical properties of the sea according to their invariance under changes in the radiance distribution about the point at which the property is measured. If the property is invariant with respect to changes in the radiance distribution, it is said to be an inherent optical property, otherwise it is an apparent optical property. The diffuse attenuation coefficient for downwelling irradiance  $(K_d)$  is an apparent optical property since it is derivable from the irradiance and radiance, both apparent optical properties.

Like other apparent optical properties irradiance  $K_d$  is so called because!: its behaviour with depth exhibits reproducible regularities in a wide range of natural water types; it is possible to formulate exact mathematical interrelationships that hold, for all practical cases, between  $K_d$  and the inherent optical properties; and the use of  $K_d$  permits practical solutions to a wide range of problems in ocean optics.

The concept of irradiance  $K_d$  is particularly useful in bio-optics^{2,3}. It not only provides a measure of natural irradiance as a function of depth, *i.e.* from Eq. (2),

$$E_d(Z) = E_d(0^-)e^{-K_d - Z}$$
 (3)

but when  $E_d(Z)$  is converted to quanta and hence photosynthetically available radiation, PAR(Z).

$$PAR(Z) = PAR(0^{\circ})e^{-K_d \cdot Z}, \tag{4}$$

it can be used to optically classify ocean water types in terms of dissolved and suspended biogenous material⁴. Also,  $K_d$  is an important parameter for describing the remote sensing of ocean color⁵, which in turn holds the possibility of synoptically determining ocean productivity.

Beyond the usefulness and regularities that have earned irradiance  $K_d$  the title of an apparent optical property, several workers have observed that  $K_d$  is relatively insensitive to changes in the solar zenith angle^{6,7,8}. Hojerslev⁷, in clear waters off Sardinia, and Aas¹, in more turbid Oslofjorden, measuring broad band irradiance or total quantum irradiance concluded that the "solar-elevation effect" in irradiance  $K_d$  was relatively small and limited to shallow depths. For some years Visibility Laboratory data has indicated the relative independence of  $K_d$  from solar zenith angle using a narrow band instrument⁶.

In the following we present a recent and comprehensive suite of spectral irradiance data that demonstrates this relative invariance to solar-elevation of  $K_d(\lambda)$  across the visible spectrum. We know of no previously published narrow bandwidth results that demonstrates this effect. To the extent that  $K_d(\lambda)$  can be shown to be independent of the geometrical distribution of the sun's input, it may be viewed as a quasi-inherent (or at least as independent of the sun zenith angle  $\theta$ ) for a wide range of practical oceanographic problems.

The results presented here are derived from a set of data taken in July 1979 at San Vicente Reservoir, east of San Diego. The reservoir is representative of the most productive ocean waters having a chlorophyll concentration of approximately 7 mg  $C/m^3$  and an attenuation length of 1/3 meter.

<u>Data.</u> To obtain a comprehensive suite of spectral irradiance data as a function of depth and solar elevation requires almost ideal environmental and experimental conditions. First, atmospheric conditions must remain uniform throughout the day. The data reported herein were obtained under clear skies through a dry "desert type" atmosphere. Second, the air-water interface must be relatively smooth. Waves increase the uncertainty in measuring depths accurately and require longer integration times to obtain average irradiance values at each depth. The latter is an important factor if complete spectral and depth data are to be obtained throughout the day as a function of  $\theta$  since long integration times are inconsistent with the need to obtain depth profiles in a time short compared to a significant change of sun angle. Our San Vicente data were obtained when the water surface was flat calm and only slightly wind rippled. Third, the water column must be relatively uniform and remain so throughout the duration of the experiment. Figure 1, shows a plot of temperature and transmittance ( $\lambda$ -550 nm) vs depth. These data indicate that the water column was nearly uniform to a depth of about 6 meters. Subsequent similar measurements indicated that the optical properties of the water column remained relatively uniform throughout our experiment. Finally, for this type of study, favorable experimental conditions are required. Our data were obtained from a moored barge equipped with adequate rigging so that shadowing effects on our irradiance measurements were negligible (except at high noon). The barge provided a platform where rapid, efficient and continuous operation of several instruments could be carried out simultaneously from sunrise to sunset.

Spectral irradiance,  $E_d(Z,\theta,\lambda)$  depth profiles were obtained throughout the day. Figure 2 shows the results of a single  $E_d(Z,\theta,\lambda)$  depth profile obtained between 1136 and 1225. Eleven of these complete spectral irradiance depth profiles were obtained throughout the day. Between each  $E_d(\lambda)$  profile a rapid monochromatic depth profile at 550 nm was obtained as an independent check on our analysis procedure for calculating  $K_d(\lambda)$  values as a function of solar zenith angle. In addition, the calibration of the instrument was checked against an internal reference lamp several times during the day.

The spectral irradiance depth profile shown in Fig. 2 is composed of nine events where an event consists of a spectral scan at a fixed depth. Each of these events took approximately three to four minutes to complete. Data was taken every 5 nm from 350 to 750 nm. The beginning and ending time of each event was accurately recorded. As a consequence, each set of  $E_d(Z,\lambda)$  data, i.e. each event, could be associated with a specific sun zenith angle (or more precisely a small range of angles associated with the specific three to four minute period). Thus it is possible to replot the  $E_d(Z,\theta,\lambda)$  data, for a given wavelength, as a function of sun zenith angle with depth as a parameter.

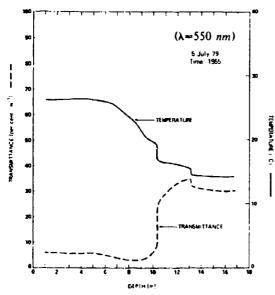


Figure 1. Temperature and transmittance vs depth for San Vicente Reservoir (32° 58'N, 116° 35'W) 5 July 1979.

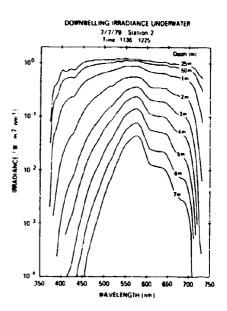


Figure 2. Downwelling spectral irradiance vs wavelength for several depths.

One half of such a plot is shown in Fig. 3. The data points, one from each event, are seen to progress with zenith angle (i.e. time) as a spectral depth profile is obtained. Our analysis procedure is, for each wavelength: to combine morning and afternoon data sets because they are virtually identical; to fit a best curve (by eye) through these  $E_d$  vs  $\theta$  data points; and to then select from these curves for each  $\lambda$  the  $E_d(Z)$  data at fixed  $\theta$  values for use in determining  $K_d(\theta, \lambda)$ .

It should be noted that this analysis procedure corrects for sun elevation changes that occur during the measurement of a spectral irradiance depth profile. This correction is generally ignored or considered to be insignificant when  $E_d$  measurements are confined to small sun zenith angles. This correction is absolutely necessary in order to accurately describe solar elevation effects on irradiance  $K_d$  and its neglect may, in part, account for earlier misconceptions regarding the behaviour of  $K_d$  vs  $\theta$ .

Analysis and Discussion. Figure 4 presents the results of this analysis, where we now show irradiance (at a fixed wavelength) vs depth for selected sun zenith angles. It can be noted immediately that these curves are almost parallel, indicating that derived  $K_d$  values will be relatively insensitive to changes in sun zenith angle.

For the present discussion we have chosen to ignore the variation of  $K_d(\theta,\lambda)$  with depth; i.e. in determining  $K_d(\theta,\lambda)$  values we have fit a straight line through the  $E_d$  vs Z data. This variation is currently being investigated and will be published elsewhere. For our current discussion it is important to recognize that, independent of how or at what optical depth  $K_d$  is determined, the slopes of the  $E_d$  vs Z curves behave in a "parallel", i.e. similar, manner for all sun angles. Thus our conclusions drawn for straight line  $K_d$  values are valid however we retermine  $K_d$ .

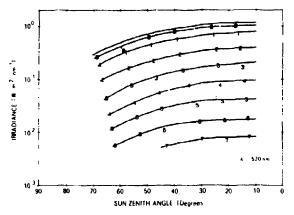


Figure 3. Downwelling irradiance, at 520 nm, versus sun zenith angle for several depths (0.25, 0.50, 1, 2, 3, 4, 5, 6 and 7 meters). Data points are indicated by the center of numerals specifying the depth in meters (except for the top two curves).

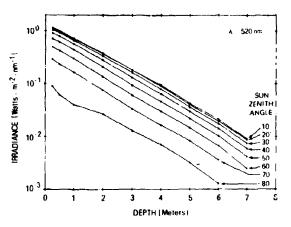


Figure 4. Downwelling irradiance, at 520 nm, vs depth for several sun zen h angles.

These data are replotted from the data

shown in Fig. 3.

From data such as that shown in Fig. 4 the diffuse attenuation coefficient for downwelling irradiance,  $K_d(\theta, \lambda)$ , can be derived. Figure 5 presents  $K_d(\theta)$  vs sun zenith angle for several selected wavelengths. Again, it can be seen that  $K_d$  is relatively insensitive to changes in sun zenith angle. Factors that may contribute to the insensitivity of  $K_d$  to sun angle include: first, that the full upper hemisphere is compressed by refraction to a half-angle 48° cone; second, that with increasing sun zenith angles the ratio of sky to total irradiance increases.

Variations of  $K_d$  with changes in sun zenith angle are shown quantitatively in Fig. 6. Here we have plotted the ratio of the diffuse attenuation coefficient at  $\theta$  degrees to that at  $\theta=10^\circ$  ( $K_d(\theta)/K_d(\theta=10^\circ)$ ) versus sun zenith angle. A solar zenith angle of ten degrees was the highest sun elevation during these experiments. These data indicate that  $K_d(\theta)/K_d(10^\circ)$  varies less than five percent for sun zenith angles of less than 40° and the variability of  $K_d$  throughout the day ( $\theta=10^\circ$  to 80°) is less than twenty percent. This is true over the full spectral range of our data. Making a first order correction, using the cosine of the refracted sun zenith angle^{7,8}, does not significantly reduce the variability of  $K_d$  with  $\theta$ .

These data indicate that the diffuse attenuation coefficient for downwelling irradiance,  $K_d(\lambda)$ , is relatively insensitive to changes in sun angle, thus displaying "quasi-inherent" characteristics. Thus, to within an estimateable accuracy,  $K_d(\lambda)$  may be considered independent of sun elevation and is useful for a wide range of practical oceanographic problems. A complete theoretical analysis and description of these results is currently under study and will be presented elsewhere.

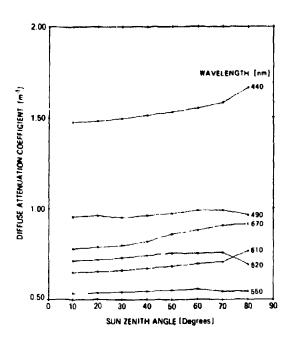


Figure 5. Diffuse attenuation coefficient for irradiance vs sun zenith angle for several wavelengths.

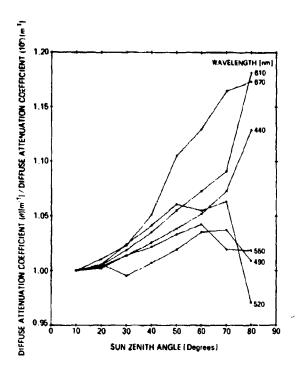


Figure 6. The ratio  $K_d(\theta)/K_d(\theta = 10^\circ)$  vs sun zenith angle for several wavelengths.

These data were derived from the data presented in Fig. 5.

### References

- 1. Preisendorfer, R. W. (1979) Hydrologic Optics
- 2. Morel, A. (1978) Available, useable, and stored radiant energy in relation to marine photosynthesis. Deep Sea Research 25, 673-688.
  - 3. Smith, R. C. (1979) Intro to Optical Oceanography. This volume.
  - 4. S. nith, R. C. and K. S. Baker (1978a) Optical Classification of natural waters. Limnol. Oceanogr. 23, 260-267.
- 5. Smith, R. C. and K. S. Baker (1978b) The bio-optical state of ocean waters and remote sensing. Limnol. Oceanogr. 23, 247-259.
  - 6. Smith, R. C. (1970) Unpublished data
- 7. Hojerslev, N. K. (1974) Daylight measurements for photosynthetic studies in the western mediterranean. Univ. of Copenhagen, Report 26, 38pp.
- 8. Nielsen, J. H. and E. Aas (1977) Relation between solar elevation and the vertical attenuation coefficient of irradiance in Oslofjorden. U, of Oslo, Report 31, 42pp.

# ASSESSMENT OF THE DIFFUSE ATTENUATION COEFFICIENT FROM REMOTE SENSED (CZCS) RADIANCE

R. W. Austin

Visibility Laboratory
of the
Scripps Institution of Oceanography
University of California, San Diego

Abstract: This program has as its goal, the accumulation and storage of ocean optical properties that can be used as a data base to assess the potential performance of optical communication systems. Available data from in-situ measurements are to be used where available but are totally inadequate in number for the large ocean areas required. A method utilizing the Coastal Zone Color Scanner (CZCS) is being tried which will permit the diffuse attenuation coefficient (K) of the surface waters to be determined synoptically over large areas. The characteristics of the CZCS are described. Examples of the spectral K's measured on surface validation cruises are shown and compared with the Jerlov, with pure sea water and with spectral K's generated using an algorithm developed by Smith and Baker.

A new algorithm for determining the K(490) and K(520) is presented which depends on the ratio of the upwelling water radiances at 443 and 520 nanometers---two of the spectral bands of the CZCS. A relationship between K(490) and plankton pigment concentration is given which may prove useful estimating K's in areas where chlorophyll concentrations have been made. The problem of the relationship between the K measured at the surface and that applying to the upper 100 meters is addressed and some examples shown. Four CZCS images where K's have been calculated over the entire scene are presented. A comparison is shown between the K's measured in-situ and calculated from the CZCS radiances for 4 stations.

# OCEAN OPTICAL PROPERTIES

REMOTE SENSING OF DIFFUSE ATTENUATION COEFFICIENT

K-algorithm Development

Surface Validation Cruises

NIMBUS 7/CZCS Data Acquisition

Digital Image Processing

DEPTH DEPENDENCE OF K

Surface K vs K to 150 meters - emperical

Relationship between K(z) and STD profiles

Emperical Model Development

AQUISITION OF ADDITIONAL DEEP WATER K'S

R/V JORDON

R/V OCEANOGRAPHER

1

-

***

1000

# ORBIT PARAMETERS USED FOR COVERAGE PLOTS

S
ERS
'n
-
쁘
AME
AR
죠.
_
_
-
0
)RBI
Ç
7
7
Ξ
Σ
ō
Z

955 KM	99.2 ₀
LTITUDE	NCLINATION

	DAY
	PFR
PERIOD	ORRITS

(RESULTS IN DAILY ASCENDING NODE SEPARATION OF 4.550)

13.82

104.15 MINUTES

SEPARATION	ORBITS
ASCENDING NODE	FOR ADJACENT

26.040 (WESTWARD MOTION)

	TIME	
2	NODE	
LAUNCH ! ARAGEIENS	ASCENDING NODE	
LAUNCH	As	

DATE

?	
Ū	
ä	
-i	

00	
<u></u>	
1978	
•	
25	
~	
_	
2	
<u>Ş</u>	

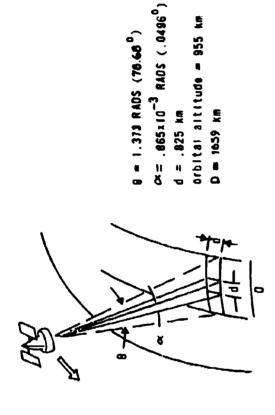


Figure 2.4-1 CZCS Scanning Arrangement

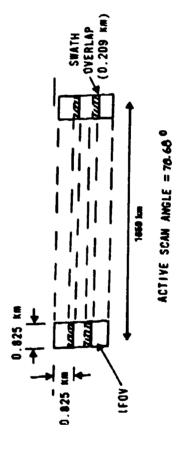
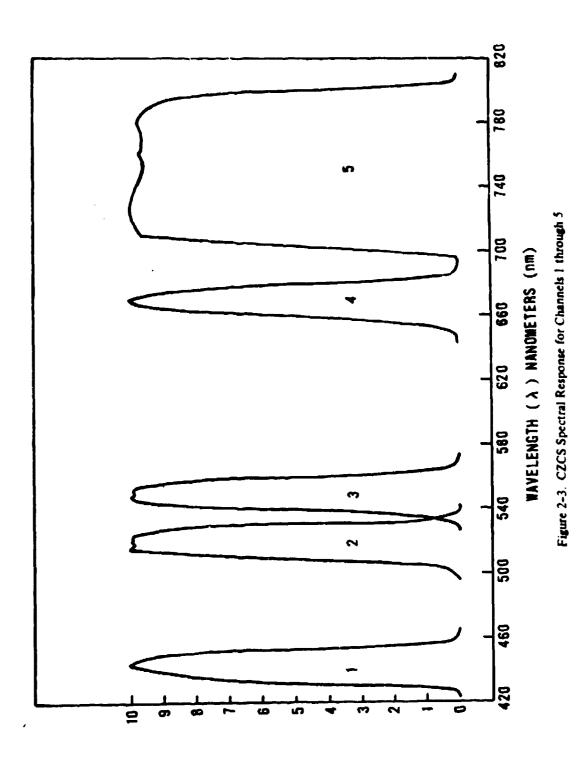
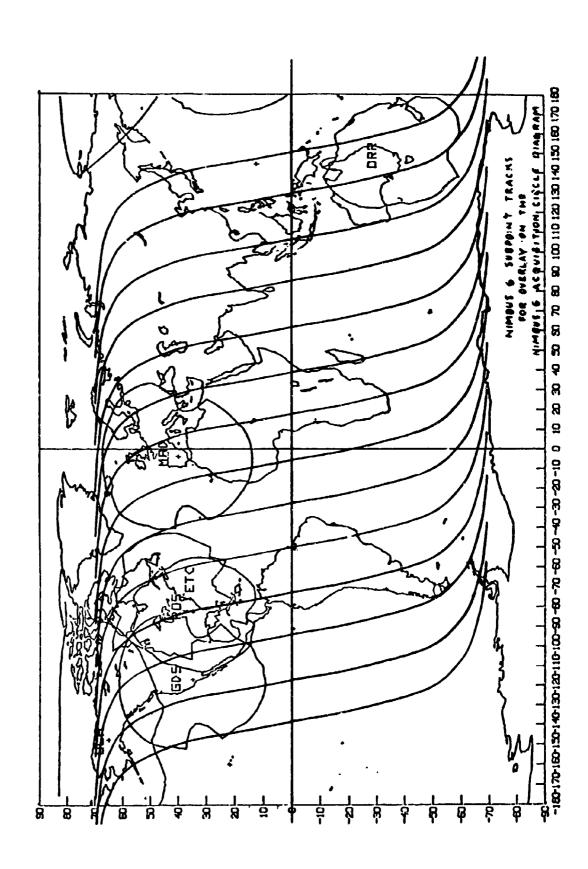
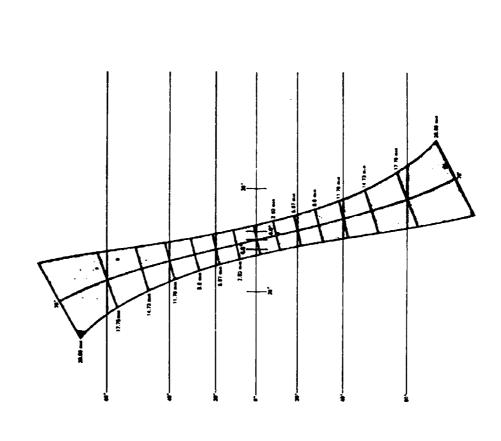


Figure 2.4-2 CZCS Earth Scan Pattern

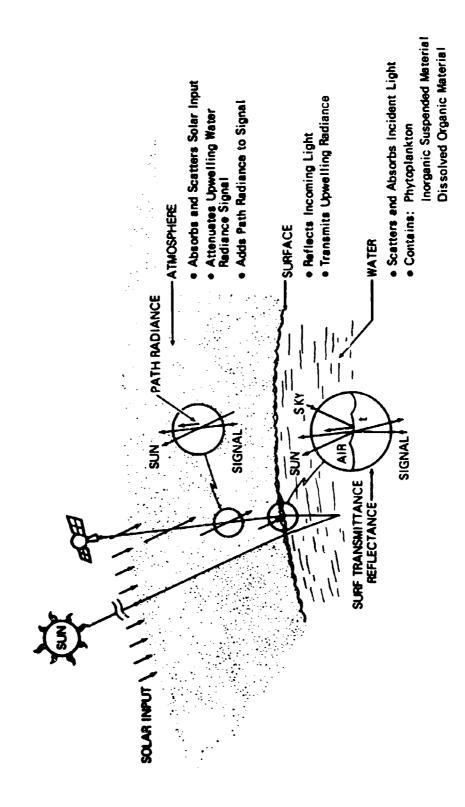
U

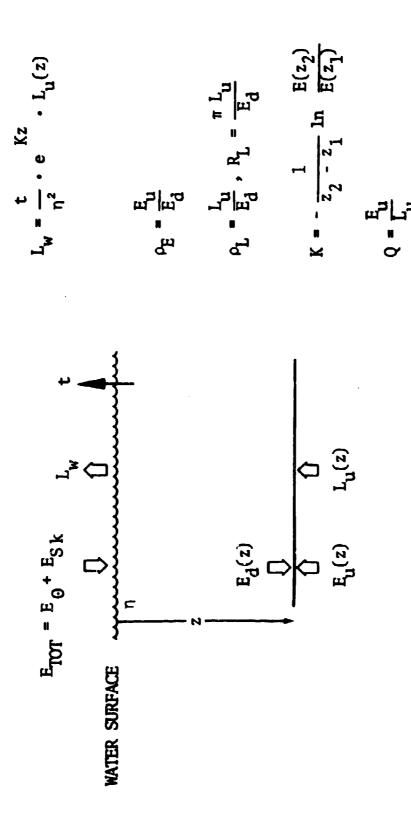




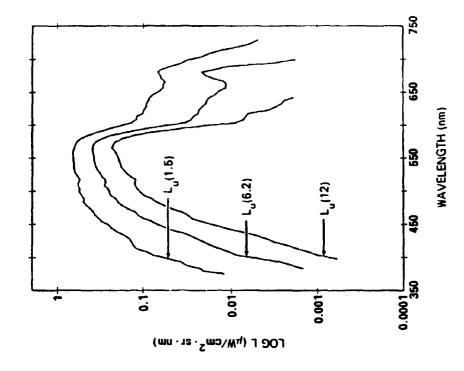


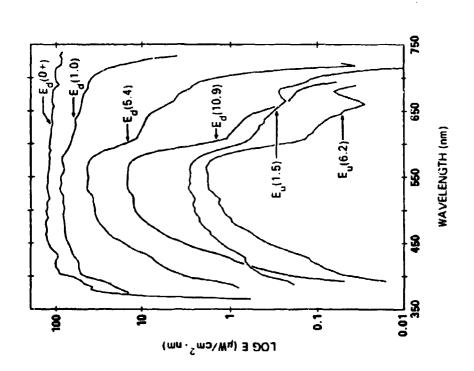
REQUESTED OCEAN COVERAGE COASTAL ZONE COLOR SCANNER





IN-WATER SPECTRO-RADIOMETRY





$$K = (a^{*2} + 2a^{*}b_{b}^{*})^{\frac{1}{2}}$$

**DUNTLEY** 

 $K \doteq a + \frac{b}{n}$  where  $n \sim 6$ 

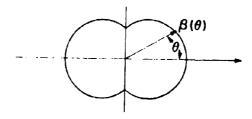
**HONEY** 

 $K_T = K_w + k_1 C_k + K_x$ 

SMITH & BAKER

Let Kw = aw + bbw

and since  $\beta_{\mathbf{w}}(\theta)$  is symmetric i.e.

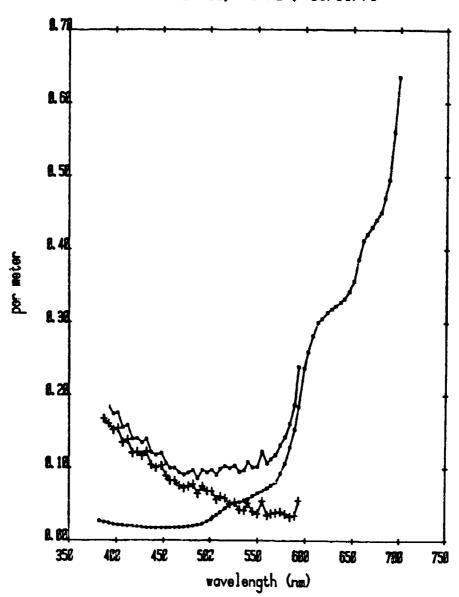


bbw = 1/2 bw,

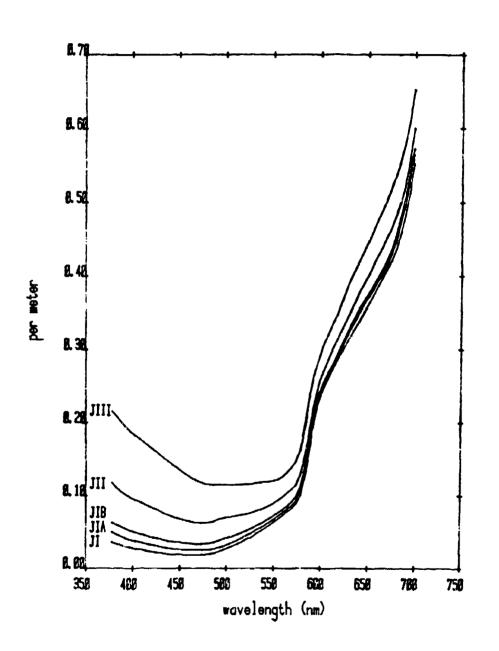
Then

Kw = aw + 1/2 bw

DIFFUSE ATTEN
Station 12, "GYRE", 11/19/78



## DIFFUSE ATTEN, Jerlov



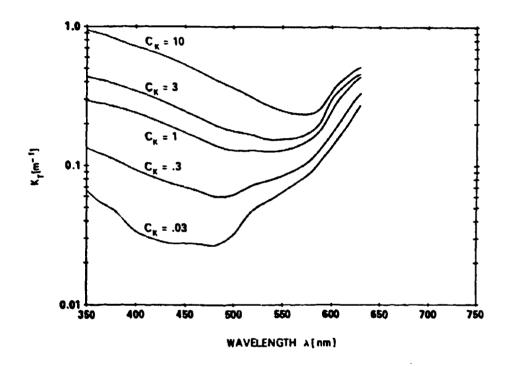
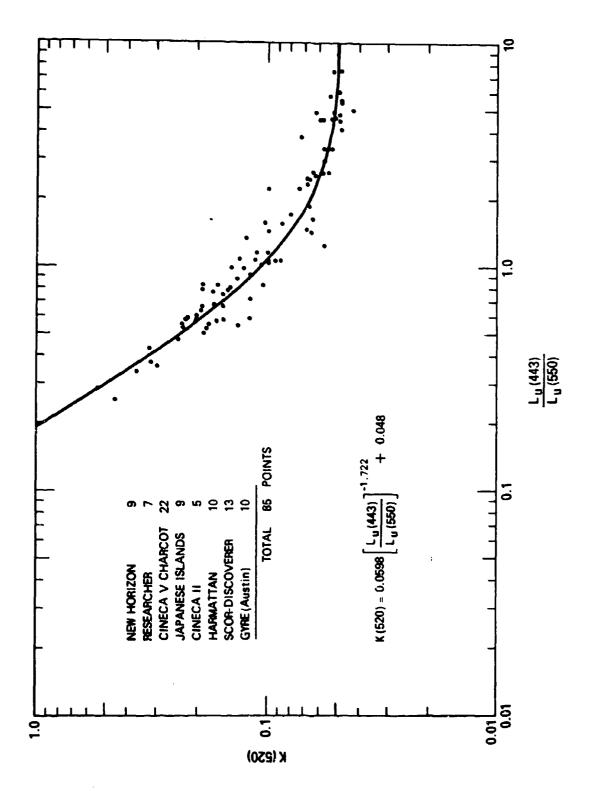
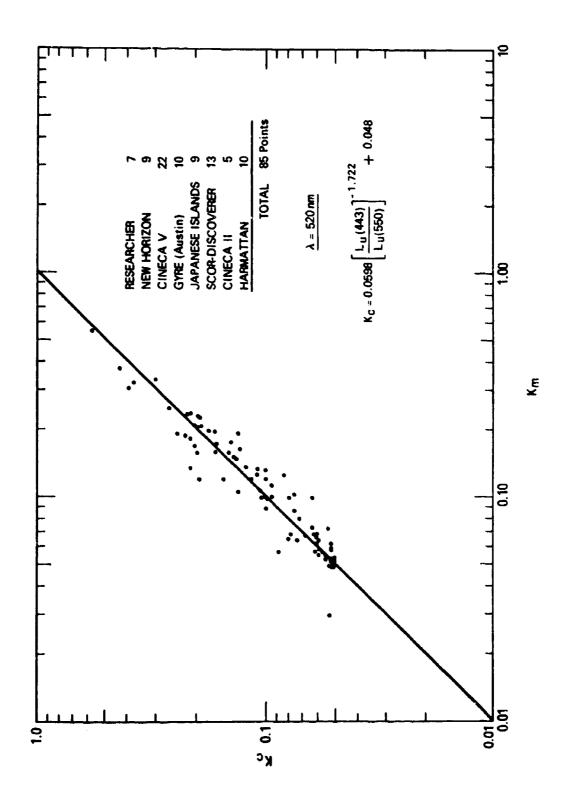
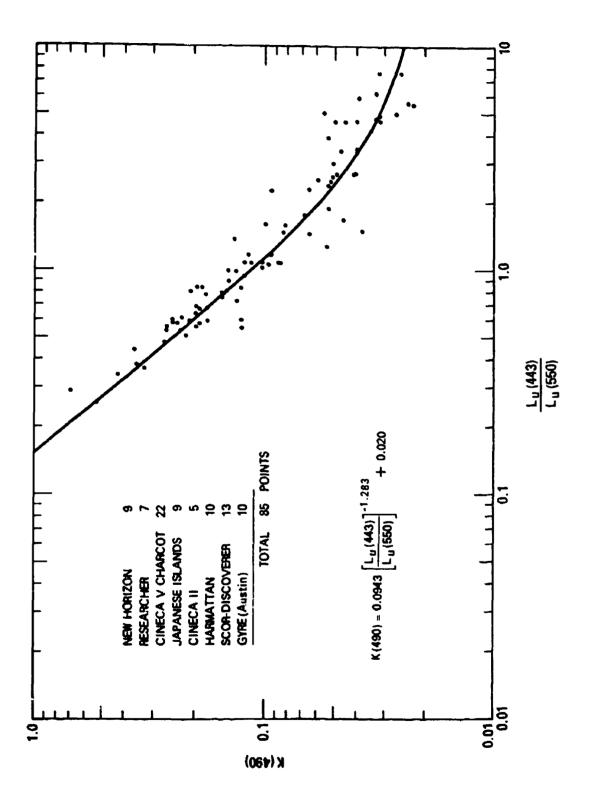


Fig. 4. Diffuse attenuation coefficient for irradiance  $K_{\chi}[m^{-1}]$  as a function of wavelength for various values of chlorophyll-like pigment concentration  $C_{\chi}[\text{(mg pigment} \cdot m^{-3})]$ . The curves were calculated using Eqs. 4 and Table 1.

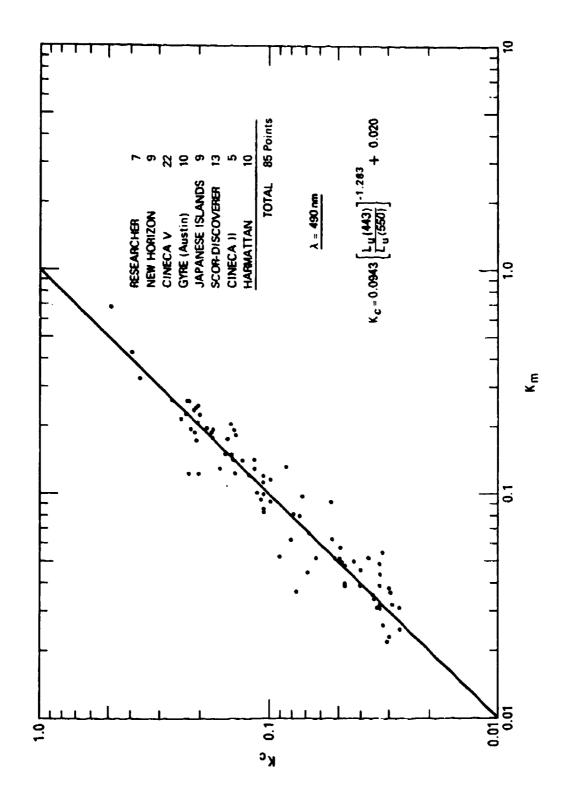




S. Str. A. Landing Manager Land



U



$$K(490) = 0.0943 \left[ \frac{L_u(550)}{L_u(443)} \right]^{1.283} + 0.02$$

### 85 STATIONS

$$K < 0.1$$
  $\overline{X} = 1.057$   $0.02$   $S = 0.275$   $0.16$ 

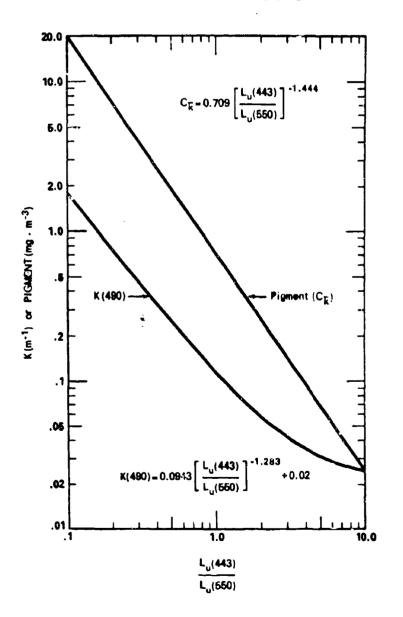
.002

$$K > 0.1$$
  $\overline{x} =$ 

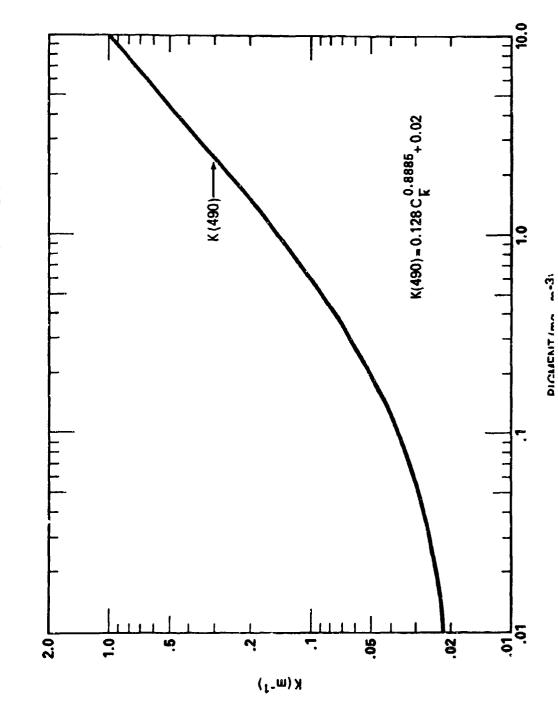
1.028

$$s = 0.185$$

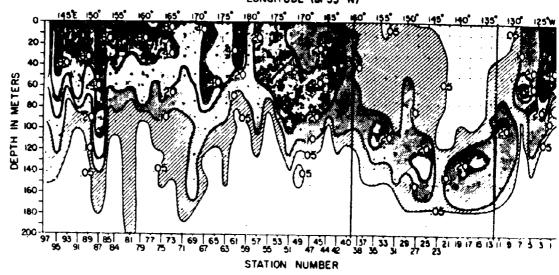
### DIFFUSE ATTENUATION COEFFICIENT AND PLANT PIGMENT CONCENTRATION VS BLUE- GREEN RADIANCE RATIO



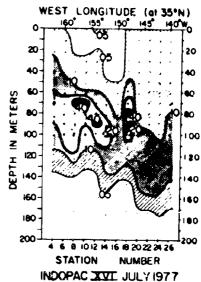
DIFFUSE ATTENUATION COEFFICIENT -K- vs CHLOROPHYLL + PHAEOPHYTIN PIGMENT CONCENTRATION

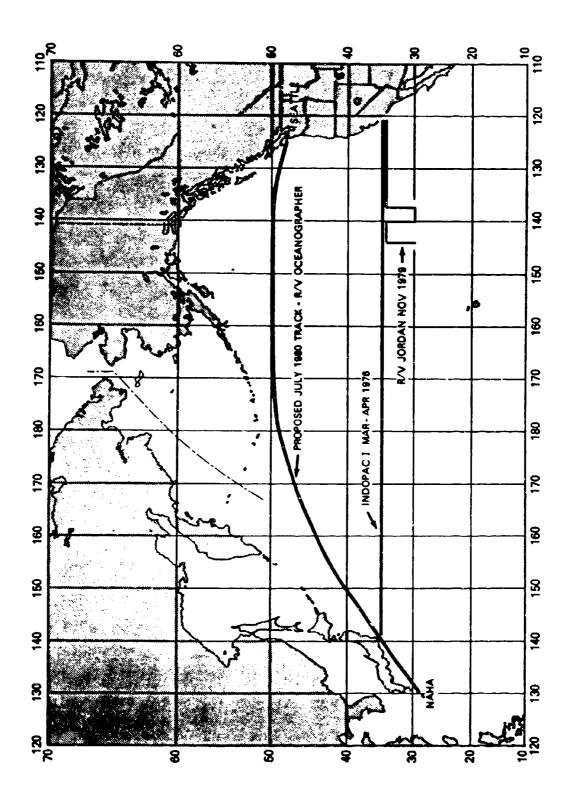


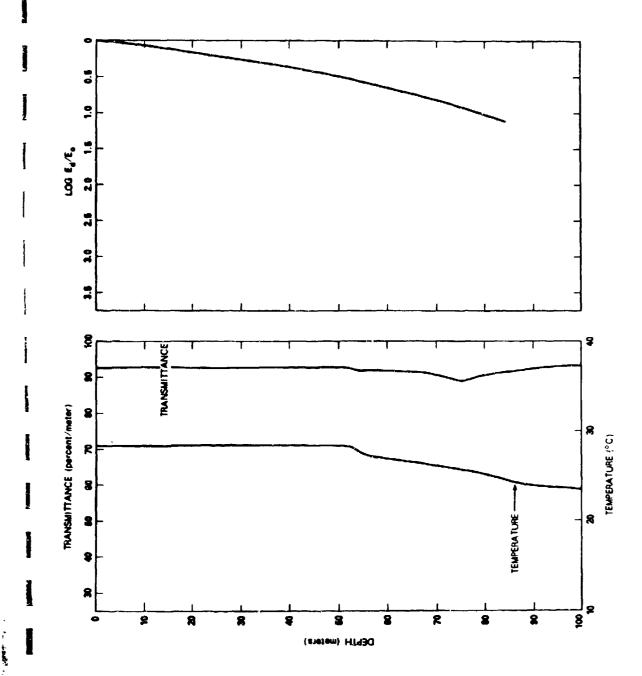
INDOPAC I MARCH-APRIL 1976 LONGITUDE (at 35° N)

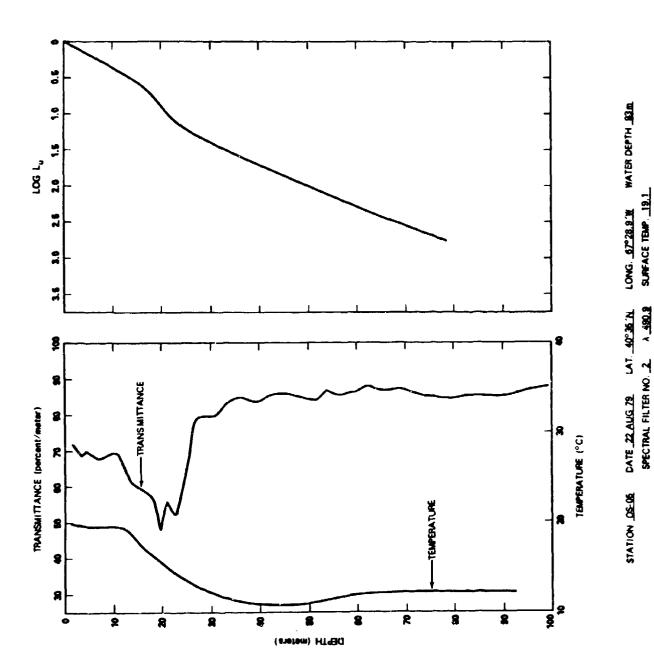


CHLOROPHYLL (mg/m3)





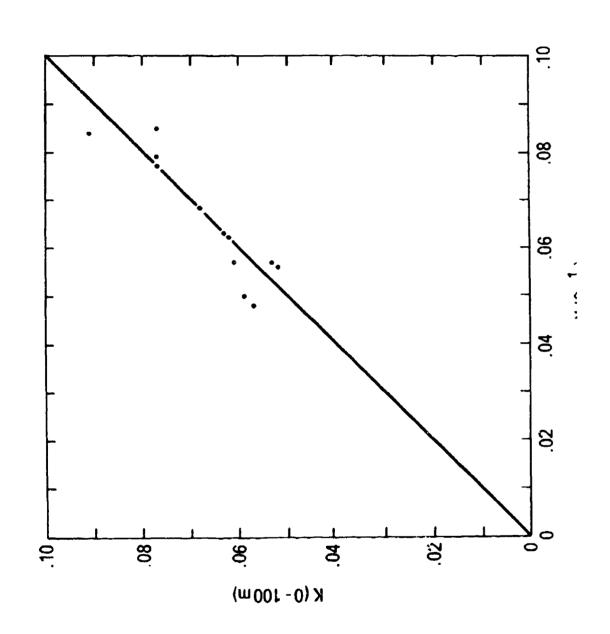


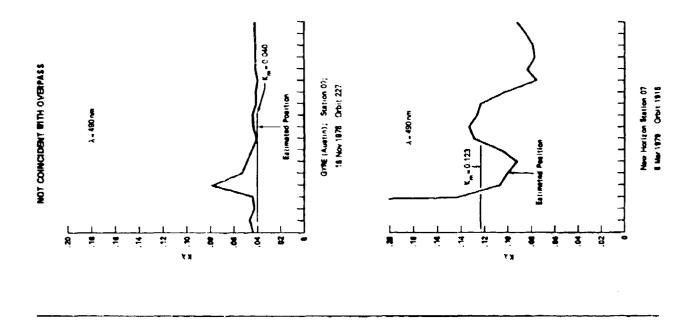


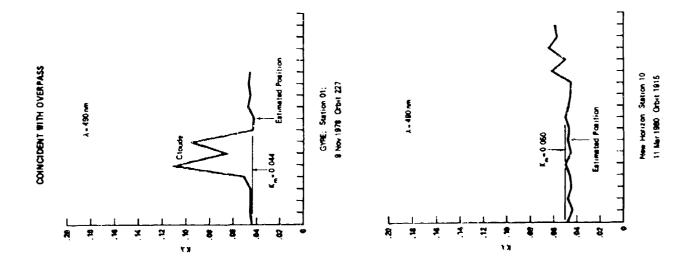
A 490.9

630

K TO 100 METERS PLOTTED AGAINST K TO FIRST ATTENUATION DEPTH







### AN ANALYTIC MODEL FOR CLOUD TROPAGATION AP Ciervo ABSTRACT

This paper presents an analytic model for the propagation of an optical pulse through a multiple scattering medium. Such a model is needed to investigate the effect of clouds on optical communications from satellite to submatine. Key results include simple expressions for the first two spatial and angular moments of the radiance distribution for a narrow delta-function source immersed in an infinite scattering medium. The moments support a diffusion approximation for the transport process in an infinite plane-parallel cloud. First the radiance is calculated at the cloud exit and on a plane an arbitrary distance below the cloud, then power collected by a finite receiver located on this plane is computed. The model is validated by comparing its results with computer simulation curve fits for optically thick clouds (i.e., 1 > 15). The model is capable of duplicating nearly all the simulation results but at significantly lower cost. Furthermore, finite receiver calculations that are impractical to simulate are readily computed.

Pacific Sierra Research 1456 Cloverfield Blvd Santa Monica CA 90404

# AN ANALYTIC MODEL. FOR PROPAGATION THROUGH CLOUDS



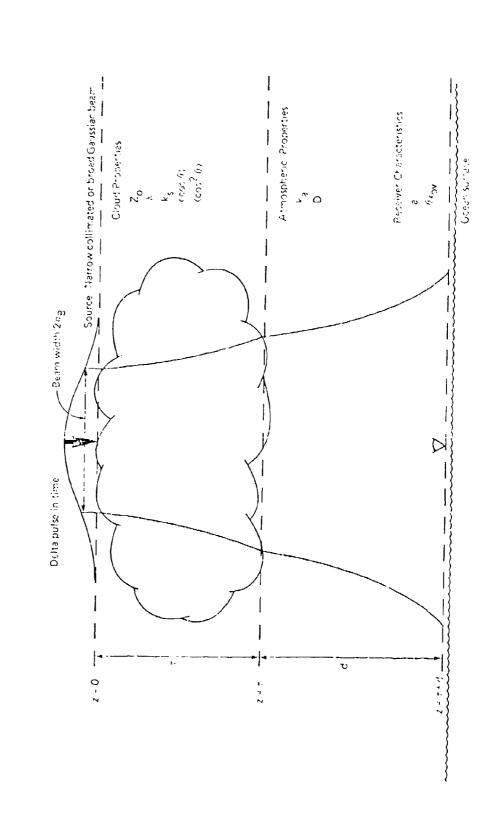
PSR

Advantages for Blue-Green Systems Analysis

efficient calculation of aperture and field of view effects on received pulse for optimization studies provides physical insight into scattering process not apparent in Monte Carlo curve fits

may help resolve anomalies in experimental vs calculated results

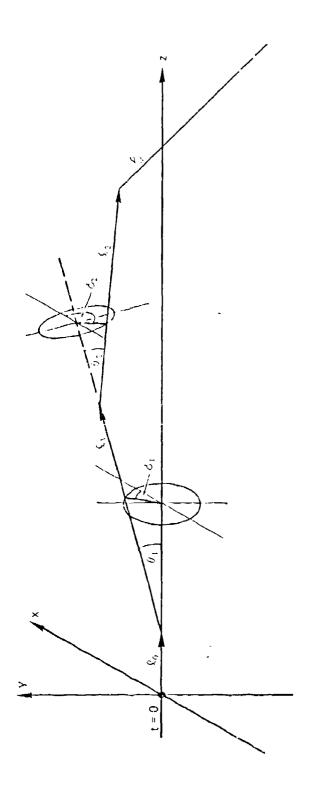
confirms or suggests alternative modular expressions for current Navy single pulse blue-green downlink propagation model



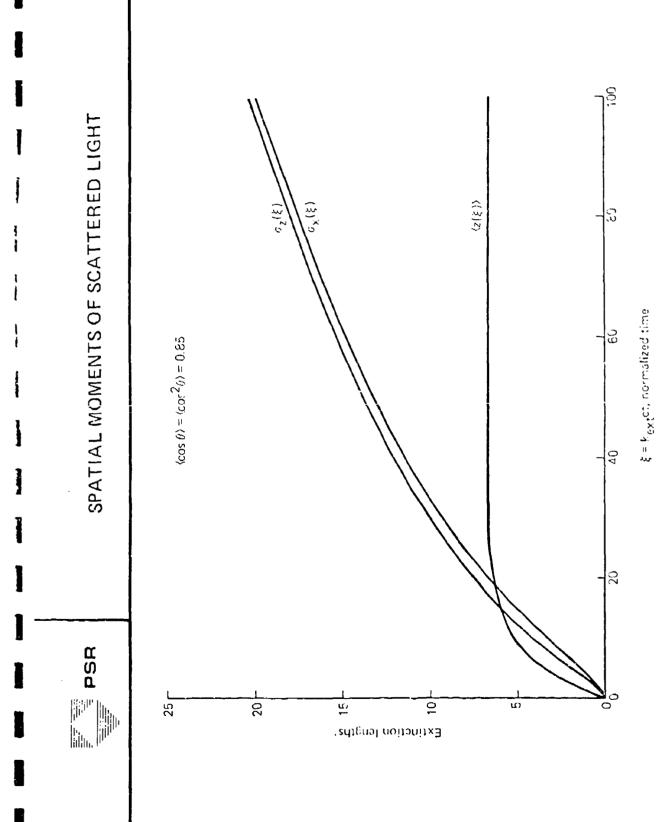
PROPAGATION PATH

PSB

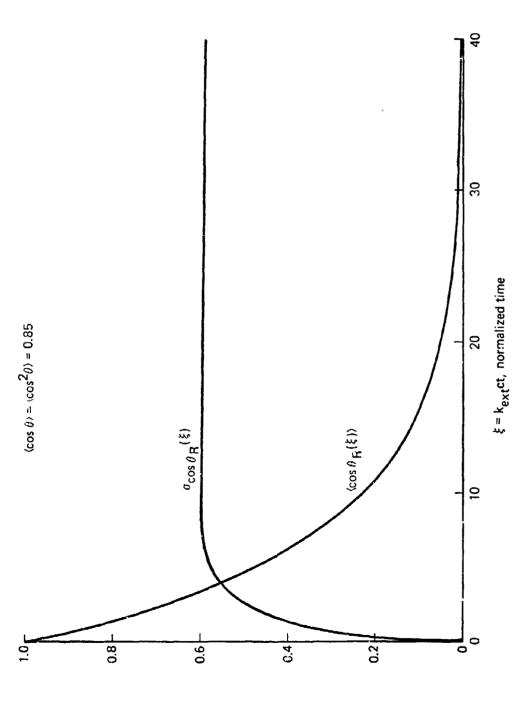
ASa 📑

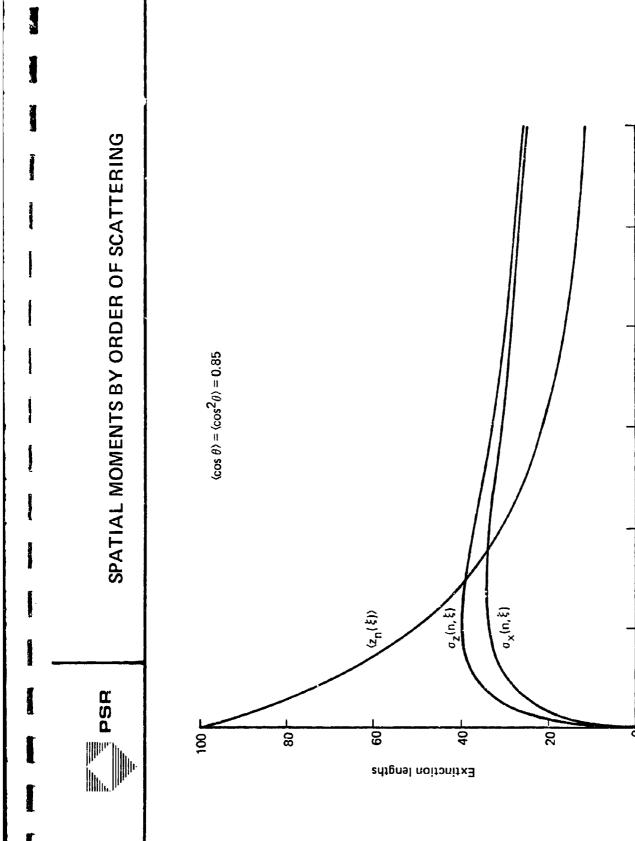


Notes: 1. Photon is at orgin directed along z-axis at t=0. 2. Leg lengths  $\ell_n$  exponentially distributed 3. Polar angles  $\ell_n$  distributed according to scalar phase function 4. Azimuthal angles  $\ell_n$  uniformly distributed





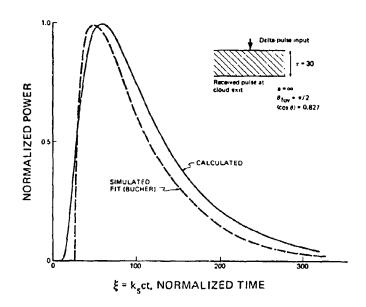


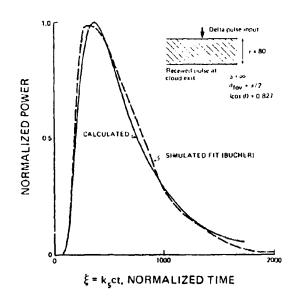


n, number of scatterings



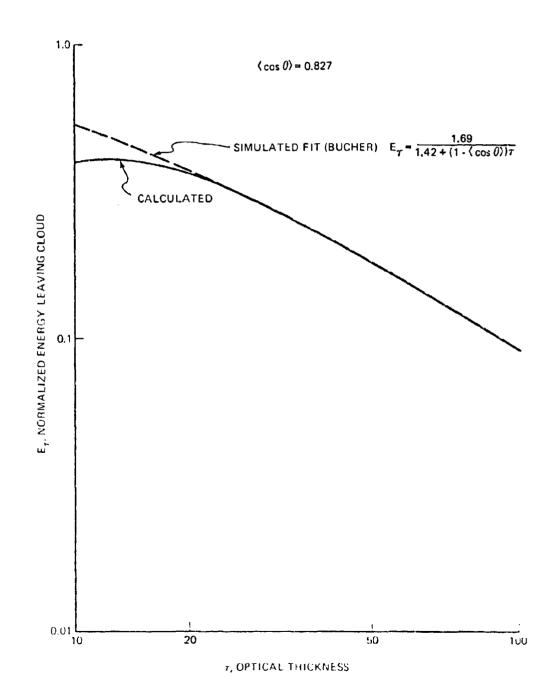
### **ANALYTIC VS SIMULATED PULSE SHAPES**



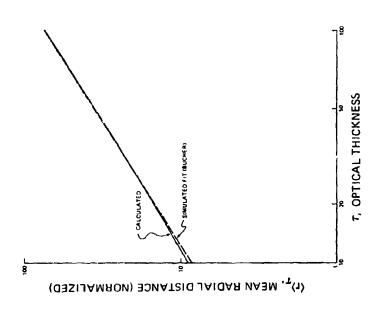


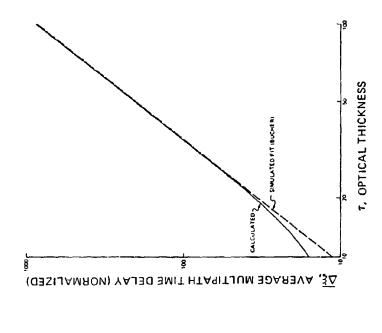


### ENERGY TRANSMISSION VS OPTICAL THICKNESS



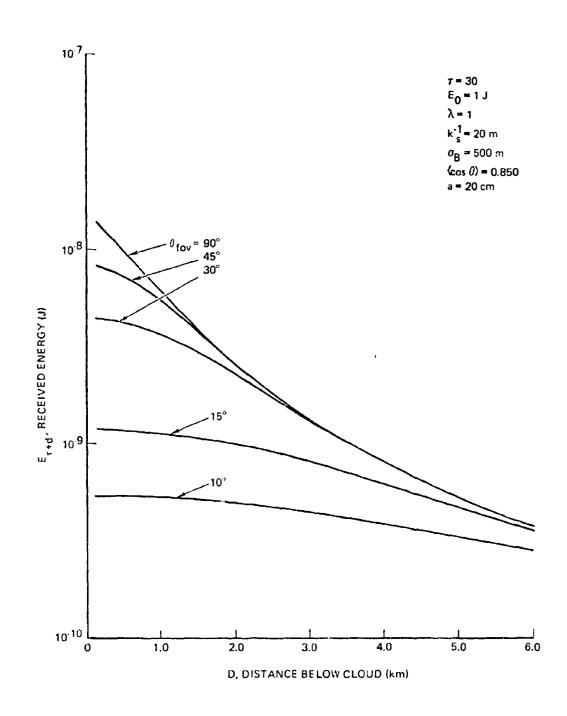
 $\langle \cos \theta \rangle = 0.827$ 





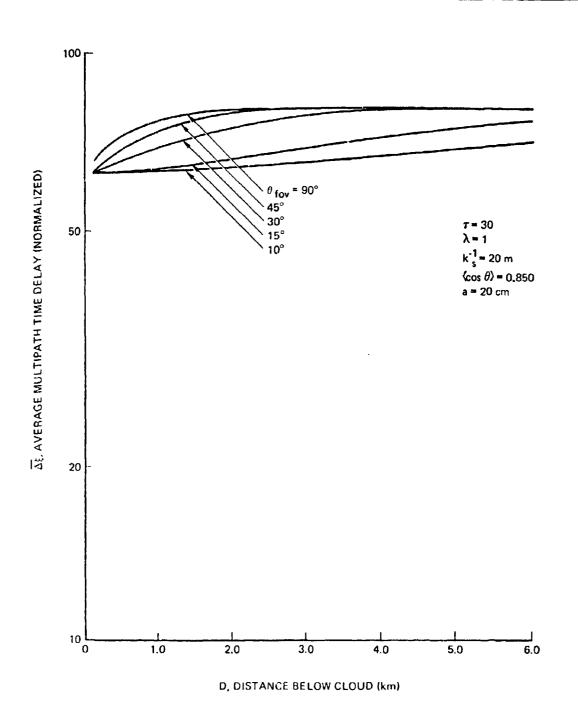


### FOV EFFECTS ON RECEIVED ENERGY BELOW CLOUD



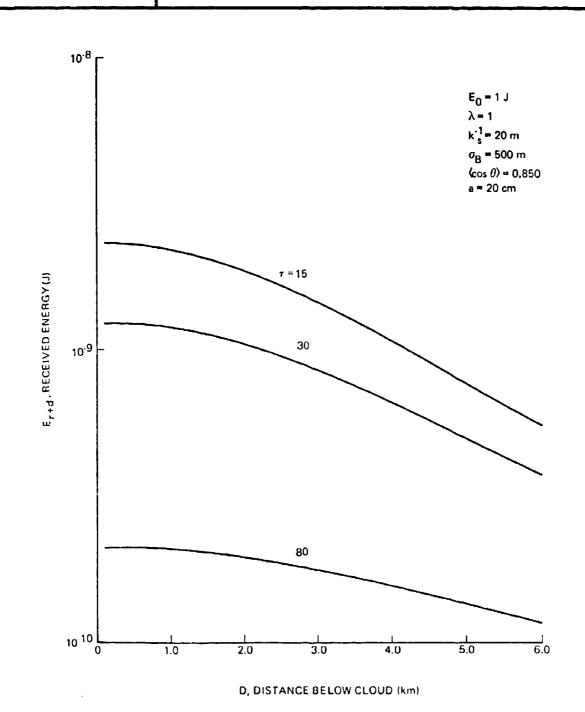


### FOV EFFECTS ON MULTIPATH DELAY





### EFFECT OF CLOUD AND ATMOSPHERIC LAYER ON RECEIVED ENERGY



## MODULAR EXPRESSIONS FOR CURRENT NAVY MODEL



PHYSICAL QUANTITY	NAVY MODEL EXPRESSION
Pulse shape	Confirmed
Pulse stretch due to clouds	Replace with Bucher expression
Energy transmission through cloud	Confirmed
Energy transmission, cloud to ocean	Compare with new expression
Angular spread of exiting photons	Replace with new expression

- 1 - 1

1